ABSTRACT

Title of Dissertation: EVALUATING THE BENEFITS, SUSTAINABILITY, AND RESILIENCE OF GREEN INFRASTRUCTURE ON A SUSTAINABLE RESIDENTIAL HOME

Rhea Thompson, Doctor of Philosophy, 2018

Dissertation Directed By: Associate Professor, Dr. David Tilley
Department of Environmental Science & Technology

With global populations becoming increasingly urbanized, green infrastructure (GI) is progressively being recognized as a sustainable approach to mitigating urban environmental problems. Unlike traditional 'hard' engineering approaches that historically viewed problems in isolation and solutions in singular terms, implementation of GI promises some deferment from the effects of urbanization by providing a multitude of benefits such as reduced stormwater runoff and flooding, decreased heat waves, and enlivened local environments and ecological habitats. These benefits are important considering many cities are projected to be more vulnerable to the effects of urbanization with climate change, especially as the vast amount of the global population lives in coastal urban environments.

However, the diversity of GI benefits has not been fully characterized, and they are

increasingly applied in residential settings. Furthermore, current research has not fully explored the beneficial role of GI in achieving sustainable and resilient communities.

Using an Integrated Water: Energy Monitoring System measuring meteorological, water, and energy fluxes over two years (July 2014-June 2016) on a sustainable home in Rockville, Maryland, U.S., the following objectives were explored:

(1) Examined how a sloped modular extensive green roof, constructed wetland and bioretention designed in-series affected site hydrology. Furthermore, we studied the effect of season, antecedent substrate water content, storm characteristics (size, intensity, frequency), and vegetation development (green roof only) on hydrological performance.

(2) Characterized the seasonal thermal performance of the green roof (to the building and surrounding environment) relative to the cool roof. Evaluated how green roof thermal performance related to evapotranspiration, solar reflectance (albedo) and thermal conductance (U-value). Additionally, the effect of substrate water content, vegetation development, and microclimate on evapotranspiration, albedo and U-values was assessed.

(3) Green roof evapotranspiration was measured and compared to values predicted with the FAO-56 Penman-Monteith model. Furthermore, the effects of substrate water content, vegetation characteristics and microclimate on evapotranspiration rates was also evaluated.

(4) Finally, using *emergy* theory, GI sustainability and resilience relative to a gray wastewater system and natural forest was explored.

EVALUATING THE BENEFITS, SUSTAINABILITY, AND RESILIENCE OF GREEN
INFRASTRUCTURE ON A SUSTAINABLE RESIDENTIAL HOME

By

Rhea Thompson

Dissertation submitted to the Faculty of the Graduate School of the
University of Maryland, College Park, in partial fulfillment
of the requirements for the degree of
Doctor of Philosophy
2018

Advisory Committee:

Dr. David Tilley, Chair
Dr. W. Braham
Dr. P. Kangas
Dr. M. Pavao-Zuckerman
Dr. A. Ristvey

Dedication

This work is dedicated to all those who paved the way for me

– and those who will come after me.

To my loving grandparents, Kenneth and Lyril Miller, parents, sister, best friend and other

loved ones,

I am forever thankful.

Acknowledgments

Table of Contents

List of Tables

List of Figures

List of Abbreviations

Albedo	Solar reflectance
CAM	Crassulacean acid metabolism
CBA	Cost-benefit analysis
CSO	Combined sewer overflow
CW	Constructed wetland
ED	Emergy diversity index
EIV	Emergy importance value
ELR	Environmental Loading Ratio
ET	Evapotranspiration
EYR	Emergy Yield Ratio
FAO-56	FAO-56 version of the Penman–Monteith model
GHG	Greenhouse gas
GI	Green infrastructure
K_C	Crop coefficient
K_S	Water stress coefficient
LAI	Leafe area index
LCA	Life cycle analysis
NFS	Natural Forest System
U-value	Thermal conductance or heat transfer coefficient
UHI	Urban heat island
VWC	Volumetric water content
WWTP	Wastewater treatment plant

Chapter 1 Introduction

In 2016, over half (54.5%) of the world's population lived in urban settlements, and it is estimated that by 2030, urban areas will house 60% of people globally (United Nations, 2016). To meet the rapid rise of populations, a new city is needed to accommodate one million new urban inhabitants around the world every week (Raji et al., 2015). However, the rapid rise and development of large urban centers in the developing world will be among the greatest challenges to ensuring human well-being and a viable global environment (Borgström et al., 2006).

First, there are tremendous consequences to constructing buildings to meet rising populations– construction practices are one of the major contributors of environmental problems, particularly due to the utilization of non-renewable materials. United States Green Building Council estimates for example, that commercial and residential construction buildings release 30% of greenhouse gases (GHG) and consume 65% of electricity in the U.S. (Bianchini and Hewage, 2012a). Furthermore, urban development frequently decreases the amount and quality of green space, which leads to fragmentation and isolation of the remaining parcels of natural ecosystems. We are increasingly understanding that human well-being and a viable global environment depend on these natural ecosystems and the services they provide (Borgström et al., 2006).

Many of these critical ecosystem services are related to energy-water balance. For example, without urban vegetation many cities are suffering from the effects of urban heat islands (UHI)– thermal energy requirements now account for 36% of primary energy use in buildings in the U.S. (Borgström et al., 2006; Ürge-Vorsatz et al., 2012). Furthermore,

an increase in area of impervious surfaces has caused stormwater runoff problems. Runoff has put heavy pressure on water resources in many semiarid regions, while in other regions, surface runoff has degraded water quality and increased flood risks (Czemiel Berndtsson, 2010; Rowe, 2011; Yang and Cui, 2012). There are also major energy requirements and GHG emissions associated with managing stormwater– a typical medium sized wastewater treatment plant in the U.S. consumes 1200 kWh of energy to treat one million gallon of wastewater (Flynn and Traver, 2013). Other ecosystem services green spaces provide include reduced air pollution, noise pollution, and enhanced health. Furthermore, urban vegetation has important recreational and cultural values for urban citizens (Borgström et al., 2006).

To meet these challenges, many urban communities have traditionally relied heavily on engineered solutions such as air conditioning systems and stormwater infrastructure. However, conventional 'hard' engineering solutions to restoring urban energy-water balance are vulnerable and failure prone, especially considering climate change projections of more intense storms and heat waves. This is because conventional infrastructure relies on a few nonrenewable energies and resources to provide cities with one or two benefits, often with unintended consequences (Figure 1-1).

For example, increasing reliance on fossil fuels to meet building thermal demands makes cities vulnerable to energy shortages, while there is the unintended consequence of further contributing to climate change as fossil fuel use results in GHGs being emitted to the atmosphere. Furthermore, in many communities there are combined sewer systems to manage raw sewage and stormwater for transport to fossil fuel dependent wastewater treatment plants. There are unintended consequences associated with this as runoff of

heavy storms frequently overwhelm gray infrastructure, resulting in combined sewers overflowing into water bodies with adverse effects (Czemiel Berndtsson, 2010; Rowe, 2011).

Non-Renewable Resources
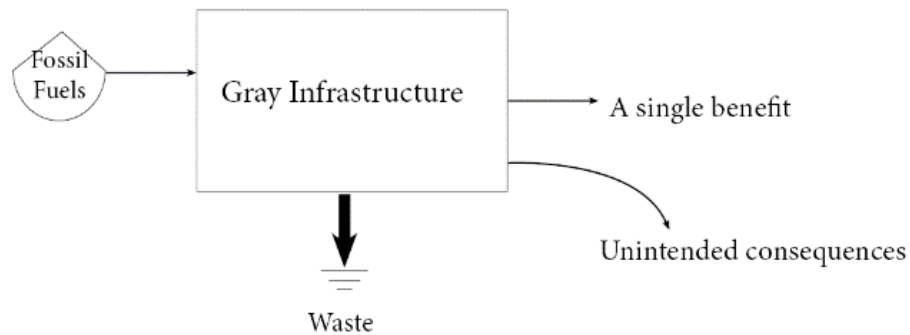
Figure 1-1 Traditional infrastructure relies on a few nonrenewable energies and resources to provide cities with one or two benefits, often with unintended consequences.

Due to these challenges the concept of sustainability has been introduced to the urban communities, with green infrastructure (GI) – such as green roofs, bioretention areas, porous pavements, rain barrels/cisterns, and green roofs– increasingly being recognized as a sustainable approach to urban environmental problems. GI is defined as natural and constructed green spaces that utilize vegetation, soil, and other components to replicate natural processes that provide benefits for human populations in the urban setting. In addition to stormwater management GI can provide multiple benefits including mitigation of the UHI effect, decreased energy use, improved air and water quality, carbon sequestration, benefits to human physical and mental health, access to recreational opportunities, and improved habitat for biota. Many of these additional benefits play a role in urban settings mitigating and adapting to the effects of changing climate, and can have

positive impacts on local economies (Law et al., 2017). As a result, GI are increasingly seen as a more sustainable alternative to traditional engineering practices because in providing these multitude of benefits, they make use of the natural abilities and functions of ecosystems (e.g., soil, plants, bacteria) – Figure 1-2.

Figure 1-2 Green infrastructure is increasingly seen as a more sustainable alternative to traditional engineering practices because in providing a multitude of benefits, they make use of the natural abilities and functions of ecosystems (e.g. stormwater reduction, thermal cooling, etc.).

Chapter 2 Literature Review

2.1 Green Roof Design and Energy-Water Benefits

The shortage of greenery in cities can be partially solved by altering buildings' rooftop properties with plant and soil especially in areas where ground space is limited. Green (vegetated, eco or living) roofs are basically roofs planted with vegetation on top of a growing medium (substrate or soil layer). The concept was designed and developed to promote the growth of various forms of vegetation on the top of buildings and thereby provide aesthetical as well as environmental and economic benefits (Vijayaraghavan, 2016). In terms of energy-water related benefits, green roofs remedy the heat island effect due to their use of watered vegetation, reduce indoor temperature fluctuations and decrease the level of building energy consumption in heating and cooling, as well as reduce or delay the runoff of excess stormwater (Hashemi et al., 2015). Green roofs can present numerous other economic and social benefits in addition to more obvious environmental advantages such as improved water and air quality, decreased noise pollution, extended roof life, and increased green space in urban environments (Vijayaraghavan, 2016)

Green roofs are generally comprised of several components from top to bottom; vegetation, growing medium, filter fabric, drainage material (moisture retention), root barrier, waterproofing membrane, insulation layer and structural layer. Besides that, there are some additional components depending on the climatic conditions like irrigation systems (Besir and Cuce, 2018). The role played by each component is well defined, and the type of each green roof component depends on the geographic location (Vijayaraghavan, 2016). Furthermore, although green roofs layers and materials are

similar among manufacturers; each manufacturer has developed its own system (Bianchini and Hewage, 2012a).

The development of a green roof can use versatile construction techniques such as a complete system, a modular system or pre-cultivated blankets. The complete system encompasses the entire roof while the other two are planted before being integrated above the rooftop (Berardi et al., 2014). Furthermore, green roofs are broadly classified into extensive or intensive, though some authors include a semi-intensive classification. Classifications into extensive and intensive roofs are based on depth, vegetation type, construction material, management and allocated usage. An intensive green roof is generally a roof garden characterized with a thick substrate layer, allowing for a wide variety of plants such as trees and shrubs that can be implemented to create an appealing natural environment with improved biodiversity, while also providing recreation space. They are typically characterized with greater weight, require higher maintenance in the form of fertilizing, weeding and watering, and incur high capital cost. Extensive green roofs require less depth of soil and are thought to support only limited types of vegetation including grasses, moss and few succulents. They are generally characterized with lower weight, minimal maintenance and less water needs, and low capital cost. Semi-intensive green roofs accommodate small herbaceous plants, ground covers, grasses and small shrubs due to moderately thick substrate layer. These roofs require frequent maintenance as well as sustain high capital costs (Berardi et al., 2014; Vijayaraghavan, 2016).

Differences in green roof classification also impact the benefits they provide. The reduction, diversion or treatment of stormwater runoff are some of the most extensively researched benefits of green roofs. Additionally, green roofs have been introduced as one

of the most efficient mediums of energy savings in the building sector, with the energy-related performance of green roofs having become one of the most common benefit for which they are promoted and adopted (Berardi et al., 2014; Besir and Cuce, 2018; Saadatian et al., 2013). Owing to the thick substrate layer, intensive roofs encompass comparatively better potential for improved insulation, enhanced stormwater management and energy performances, whereas energy performance and stormwater management potential is relatively low for extensive systems. However, of the three types, extensive green roofs are most common around the world due to building weight restrictions, costs and maintenance. Furthermore, their construction process is technically simple and allows for implementation on sloped roofs (Berardi et al., 2014; Vijayaraghavan, 2016).

One of the important drivers of energy and hydrological performance of green roofs is thought to be evapotranspiration (ET), which is a combined process of soil evaporation and plant transpiration (Tan et al., 2017). The physical process in which water transfers from soil into the atmosphere is called evaporation. Transpiration is a *physiological* process in plants through which water uptaken by the root system escapes through the stomata on leaves or the pores of the skin, where it is vaporized (Poë et al., 2015; Raji et al., 2015).

Evapotranspiration is thought to be one of the biggest drivers of green roof hydrological performance. More specifically, during dry periods between storm events ET plays a role in reducing substrate water content, which increases the retention capacity, or soil moisture deficit of green roofs (Poë et al., 2015). At the same time, ET plays a significant role in green roof cooling. When solar radiation is absorbed by a green roof, energy/latent heat is absorbed and dissipated to turn water into vapor. The latent energy associated with transpiration is typically a large part of the energy balance, and a major

pathway for removing heat created by solar and longwave absorption. The effect entails active cooling of the air immediately above the roof surface while reducing the overall heat transmission to the building (He and Jim, 2010; Ouldboukhitine et al., 2014; Poë et al., 2015; Tjaden, 2014).

Evapotranspiration can be obtained by direct measurement (Ouldboukhitine et al., 2014). Forces inducing ET losses are a function of the microclimate (i.e. solar radiation, air temperature, wind, relative humidity) and plant physiology. However, the rate at which these forces induce ET depends upon the substrate–water characteristics (i.e. field capacity, permanent wilting point, permeability), any additional moisture storage capacity within the vegetation layer, and the plant's physiological response at the prevailing moisture content (Poë et al., 2015). Moreover, there are several factors related to green roof design (selection of substrate and vegetation) that affect ET. In order of importance, prior studies have identified substrate water content as the most critical factor for ET. If there is sufficient soil moisture available, then plant characteristics, and weather would affect ET most significantly (Tan et al., 2017). Although ET is important to the energy and water balance of green roofs, it has not been well studied, especially in real conditions and there is little experimental data examining ET rates and attributing factors.

There are also several approaches with models that achieve ET in a time step by taking into account a number of physical parameters (radiation, pressure, wind, etc.) and characteristics of the plants (Ouldboukhitine et al., 2014). These models are important since direct measurements of ET are rarely available, and it is difficult to quantify in real-time because of changing environmental fluxes (Starry, 2013; Sumner and Jacobs, 2005). In terms of evaluated models, the FAO-56 version of the Penman–Monteith model has been

shown to provide a better prediction amongst other methods for green roofs (Berretta et al., 2014).

The FAO-56 equation is derived from the Penman-Monteith equation (Equation 2-1) which combines two approaches– a mass balance approach and an energy balance approach– to calculate ET. The mass balance approach assumes water will diffuse away from the leaf surface in direct proportion to the vapor pressure deficit of the surrounding air and the velocity of the wind at any given time. The energy balance approach infers ET from the difference between energy going into and out of the leaf, assuming no storage component (Starry, 2013).

$$\textbf{Equation 2-1} \qquad ET = \frac{\Delta(Rn\text{-}G)\text{-}\,\rho_a c_p\,\frac{(e_s\text{-}e_a)}{r_a}}{\Delta + \gamma\left(1 + \frac{r_s}{r_a}\right)}$$

Described by Allen et al. (1998), the FAO-56 Penman–Monteith model (Equation 2-2) is the updated equation recommended by FAO (Food and Agricultural Organization of the UN) and the World Meteorological Organization to estimate reference potential ET from a grass surface (Allen et al., 1998; Berretta et al., 2014). The FAO-56 equation basically simplifies the standard Penman-Monteith equation used to predict ET by assuming the stomatal conductance and albedo of a reference grass crop. It is assumed that the definition for the reference crop is a hypothetical reference crop with crop height of 0.12 m, a fixed surface resistance of 70 s m^{-1}, and an albedo value (i.e., portion of light reflected by the leaf surface) of 0.23 (Starry, 2013; Zotarelli and Dukes, 2010). The reference surface most closely resembles an extensive surface of well-watered, actively growing green grass of uniform height that completely shades the surface (Hilten, 2005).

Using the assumptions mentioned, the Penman-Monteith method reduces to the following equation:

Equation 2-2 $$ET_o = \frac{0.408\Delta(R_n\text{-}G)+\gamma\frac{c_n}{T+273}(e_s\text{-}e_a)u_2}{\Delta+\gamma(1+c_du_2)}$$

Where, ET_o = reference evapotranspiration from a well-watered crop (mm/day)

Δ = slope of saturation vapor pressure curve (kPa/ °C)

R_n = net radiation at crop surface (MJ/m^2 day)

G = heat flux density to the soil (MJ/m^2 day)

γ = psychrometric constant (kPa/°C)

T = mean daily temperature 2 m above the ground (°C)

u_2= mean daily wind speed 2 m above the soil surface (m/s)

e_s = mean saturation vapor pressure (kPa)

e_a = mean actual vapor pressure (kPa)

C_n = numerator constant that depends on reference crop

C_d = denominator constant that depends on reference crop

A major limitation of many methods of estimating ET is that they assume that moisture is in abundant supply (Poë et al., 2015). Several ET equations, including the FAO-56 version, have been found to overestimate ET for *Sedum* species common on green roof systems, even after correcting for water limited conditions (Starry, 2013; Tjaden, 2014). Thus, it has been suggested that agricultural models are not appropriate for estimating

green roof ET when water is limited and one should limit the use of models to the well-watered condition, a condition that may not be applicable on a green roof (Voyde, 2011).

2.2   Constructed Wetland Design and Hydrological Benefits

Constructed wetlands (CWs), constructed stormwater wetlands, or reed beds, are man-made wetlands specially designed to store and filter stormwater runoff (Droguett, 2011). Because wetlands are viewed as natural wastewater treatment systems, CWs provide an efficient, low-cost, easily operated alternative to conventional treatment systems (Scholes et al., 1998). They are particularly beneficial in urban settings where the built environment has drastically altered the natural hydrological cycle, and are able to treat wastewater in a more controlled environment than in natural wetlands (Droguett, 2011).

In terms of design, stormwater wetlands usually incorporate both zones of dense vegetation (shallow macrophytes zones) and deeper open water, and they are often combined with a pre-treatment sedimentation pond or forebay worldwide for urban stormwater management (Al-Rubaei et al., 2016; Greenway, 2015). Furthermore, CWs are generally classified into two types— free water surface wetlands (FWS) and subsurface flow wetlands. Free water surface wetlands are defined as wetland systems where the water surface is exposed to the atmosphere (most natural wetlands are FWS systems), while subsurface wetlands are characterized by stormwater flowing and filtering horizontally through sediment. Each type exhibits different advantages and disadvantages that must be properly evaluated in the context of the collection system. Although the technology is apparently simple, understanding the proper role of each type of wetland is a challenging process requiring experienced designers to properly evaluate the most appropriate system (Droguett, 2011).

There have been numerous studies demonstrating that CWs have the ability to effectively remove pollutants from urban stormwater runoff (Al-Rubaei et al., 2016). They are capable of modifying, removing or transforming a variety of water pollutants by a combination of biological, chemical and physical processes, whilst, depending on their area, are also able to provide the wildlife and recreational benefits commonly associated with natural wetland systems (Scholes et al., 1998). However, while their role in water quality improvement has been well studied, there is debate as to whether CWs can reduce runoff. Some studies state CWs are generally suitable best management practices for both water storage and water quality improvement (Greenway, 2015). Other studies state that they are more effective for pollutant removal as it is believed they have a limited ability to reduce overall runoff volumes since their only losses are due to ET (Fletcher et al., 2013). Relevant to this study, to our knowledge there are no published studies of CWs integrated with a residential home, which would make their overall design unique to meet site constraints.

2.3 Bioretention Design and Hydrological Benefits

Bioretention, often referred to as rain gardens or biofilters, is increasingly being adopted in urban and suburban areas to reduce stormwater flow rate, flow volume, pollutant concentrations and to facilitate groundwater recharge. Rapid implementation of bioretention areas is also due to their flexibility in size and location, aesthetic value, and cost-effectiveness compared to traditional treatment methods. While several possible design configurations exist, bioretention are generally depressional areas constructed by placing a porous soil medium in shallow trenches or basins and planting various types of vegetation (Yang et al., 2013).

Bioretention operate by filtering diverted runoff through dense vegetation, followed by vertical filtration through soil filter media. Treatment is achieved through a number of different processes including sedimentation, infiltration, sorption, and biological transformation/decomposition. Water is often times then collected in underdrains at the base of the filter media for discharge to sewer systems, receiving waters, or storage for reuse (Hatt et al., 2009; Yang et al., 2013). Despite the plethora of published studies to date, performance data for bioretention have generally been limited to the laboratory-scale, with few studies reporting on field-scale testing. Furthermore, research to date has generally focused on the pollutant removal performance of bioretention, with less attention given to its hydrologic performance. Bioretention areas have previously been thought to have little water quantity control benefit and provide only minor flood control benefits. However, there has been little empirical data or even modelling to support this notion (Hatt et al., 2009).

2.4   Green Infrastructure Sustainability and Resilience

Green infrastructure, by relying on natural processes and energies to provide urban communities with ecosystem services like UHI mitigation and stormwater management, is thought to increase the sustainability of cities as they adapt to climate change. However, although GI has been touted as a sustainable technology, it is currently designed to manage downstream impacts of urbanization without consideration of broader, "up-stream" environmental, economic, and social impacts associated with its implementation and operation. This gap in knowledge incites unanswered questions such as: Do GI benefits outweigh these "up-stream" environmental impacts? What and where are the non-monetary costs and benefits throughout the life of a practice? Are some GI practices "greener" than

others (Flynn and Traver, 2013)? This final question is pertinent as there are many types of GI, and there has been limited comparison of sustainability between types (Law et al., 2017). Finally, GI sustainability relative to gray infrastructure or natural ecosystems in which they are designed to mimic have not been fully explored.

The most prominent environmental accounting methods currently used to explore GI sustainability are cost-benefit analysis (CBA) and life-cycle assessment (LCA), however each model has its limitation. One of the most controversial criticisms of CBA is that it evaluates environmental impacts and ecosystem services to humans using economic analysis when many environmental impacts such as human life and some irreversible effects on ecology are not convertible into monetary values (Reza, 2013). Furthermore, LCA has been criticized as a utilitarian user-side approach to sustainability, only focusing on environmental impacts due to resource consumption and emissions while ignoring the work of ecosystems to provide 'freely available' services and products (e.g. rainfall, soil organic matter, etc.) (Reza, 2013). Thus, it has been proposed that sustainability cannot be assessed simply by counting mass and energy flows, but by accounting for the direct and *indirect* energy supporting flows. *Emergy* is proposed as a more holistic ecological accounting method for determining if the direct and indirect energy requirements of GI are less than produced benefits over each system's life-span.

Emergy synthesis is the process of determining the sorts of energies and resources used up directly or indirectly in the biosphere to produce a specific product or service (i.e., joules of electricity used or produced by a system). Emergy accounting is unique because it is possible to tangibly evaluate the contribution of environmental, economic, and social

impacts in a single energy-based unit known as solar energy joules (sej, or solar emjoules), and to determine an overall unbiased value for sustainability objectives (Reza et al., 2014).

A key concept in the emergy evaluation process is *solar transformity* or *unit emergy value* (UEV). Solar transformity values convert flows (e.g., grams, joules, dollars) to solar energy joules – in other words, it represents the amount of emergy required to produce one unit of an output or benefit (Equation 2-3) (Reza et al., 2014). The transformity of solar radiation equals one by definition (1.0 sej/J), while the transformities of all other flows and storages (including those related to human societies) are calculated based on their convergence patterns through the biosphere hierarchy (Ulgiati et al., 2011). Ultimately, this principle differentiates emergy synthesis from other sustainability appraisal tools as emergy implies that 'with resource use comes responsibility'— high-emergy resources are valuable because of the amount of physical and thermodynamic work that went into producing them and should not be squandered (Raugei et al., 2014).

Equation 2-3 $\quad UEV = \dfrac{\text{Solar energy joules (seJ)}}{\text{Available energy flow (Joule, grams, dollars)}}$

Equation 2-4 $\quad \text{Emergy} = UEV \times \text{Available energy flow}$

The following example shows how one would convert a value to emergy terms. If 12E+04 sejs of coal and 4E+04 sejs of labor are required to generate 1 J of electricity, the UEV of electricity is 16E+04 sej/J (Reza et al., 2014). Where, solar energy joules account for the amount of "free" environmental work done by nature to generate flows. To determine total emergy if 2 J of electricity is used to produce a green roof, one would apply Equation 2-4 and total emergy would be 32E+04 sej. Once inputs and benefits are

converted to emergy values, sustainability can be assessed with several ratios that evaluate total emergy of inputs (e.g. manufacturing, installation and maintenance) and benefits produced over a system's lifetime. In this study we focused on the Emergy Yield Ratio (EYR) and Environmental Loading Ratio (ELR) which are fully described in section (Assessing Sustainability with Emergy).

In addition to sustainability, resilience has become an important goal of many communities as global populations have become increasingly urbanized and as climate change progresses— with many communities viewing GI as a means of improving urban resilience due the multifaceted benefits they provide. Resilience, as applied to integrated systems of people and the natural environment, has three interrelated characteristics, one of them being the amount of change a system can undergo and still retain the same controls on function and structure. In the resilience discourse, management of diversity per se is considered to be a key attribute for building resilience in complex adaptive systems (Colding and Barthel, 2013). This is because diversity functions as insurance– it spreads risks, creates buffers, and opens up for multiple strategies from which humans can learn in situations when uncertainty is high. Diversity also plays an important role in the reorganization and renewal processes of disturbed systems (Colding and Barthel, 2013), and makes systems less vulnerable to natural and human-induced changes such as resource availability fluctuations.

In ecology, the Shannon diversity index (*H*), has been used often to assess ecosystem diversity. Derived from information theory, *H* evaluates species richness (*S*), the abundance of species in the community, and species evenness (*E*), how similar the abundance of different species are in an area (Ulgiati et al., 2011). *H* is calculated using

Equation 2-5, where p_i is the proportion of the number individuals in a species to the total number of individuals in ith species sampled (N_i) (Equation 2-6). A large H value indicates a diverse community.

$$\text{Equation 2-5} \qquad H = -\sum P_i \log[P_i]$$

$$\text{Equation 2-6} \qquad P_i = N_i / \sum N_i$$

Since GI benefits are diverse and not easily 'additive', it has been proposed that the environmental accounting technique of *emergy* evaluation could be extended using information theory— the basis of the Shannon Index— to enumerate the energetic diversity of GI and provide a new metric of resilience. Previously, this system-level *emergy diversity index* (derived from the Shannon diversity index) was used to quantify the diversity of species in ecological systems, and diversity of energy and resources in economic systems (Brown et al., 2006; Ulgiati et al., 2011). The new emergy based indicator differs from the typical way of estimating *H—* which is based on simply counting individuals, biomass or other stocks— because it uses the flows of energy and materials in *emergy* terms. Resilient systems are supported by a variety of emergy flows that make it more likely to develop complex structures, while systems that only rely on a small set of sources out of a large number of potentially available ones possess a built-in fragility that may determine their collapse in times of shrinking or changing resource basis (Ulgiati et al., 2011). The system-level emergy diversity index is described in section 6.2.5 (Extending Emergy to Enumerate Resilience).

2.5   Research Justification

Despite the success of GI during the last decade, the diversity of their benefits has not been fully characterized, or appreciated by the building industry and municipal regulators, particularly in residential settings. Furthermore, their role in improving urban sustainability and resilience has not been fully explored. A green roof, constructed wetland, and bioretention designed in-series on a sustainable home were studied to better understand their energy-water benefits, as well as their role in improving sustainability and resilience.

We believe these findings are relevant to the building industry and municipal regulators because in many communities, GI has been incentivized or mandated without having a full understanding of how they perform over time. For example, many municipalities have started to implement or even mandate green roofs on buildings. Consequently, more and more green roofs are being established and commercial green roof products have started to appear in the market doing brisk business. This is concerning as the focus of green roof developers has often been limited to achieving basic aesthetical benefits. Many other benefits, such as stormwater management and thermal cooling are just as achievable, but thus far many green roofs are generally not optimized to provide these benefits. This is generally due to lack of research on different aspects of green roofs and premature introduction of products into the market (Vijayaraghavan, 2016).

Thus, there is a great need for green roof– and green infrastructure as a whole research, especially of systems in residential systems where they are increasingly applied. With many homes possessing sloped roofs with weight load restrictions, many new green roofs could likely be sloped, extensive and modular like the system in this study.

Furthermore, due to space constraints, many CWs and bioretention areas applied to residential communities may likely be similar in design to the systems in this study.

2.6   Research Objectives and Hypotheses

Objective 1: 1) Determine and compare the hydrological performance of the green roof, constructed wetland, and bioretention designed in-series. 2) Evaluate the effect of season, antecedent substrate water content, storm characteristics (size, intensity, frequency), and vegetation development (green roof leaf area index and percent cover) on retention.

The need to develop a practical and sustainable approach to stormwater management is rapidly becoming a priority as human development and climate change alters urban hydrologic cycles. In recent decades, GI has been viewed as a sustainable alternative to stormwater management, with the reduction, diversion or treatment of storm water runoff being one of its most extensively researched benefits. However, hydrological studies are largely limited to green roofs. Furthermore, rarely have multiple GI practices in-series been monitored (most study individual practices), even though most stormwater regulations require them to be installed in-series to receive permits (Brown et al., 2012). Finally, studies on the effectiveness of GI in residential settings is lacking– most studies are laboratory based or of systems larger in scale such as GI in the public right-of-way.

The purpose of this objective was to examine how an extensive green roof, constructed wetland and bioretention integrated in-series on a sustainable home affected site hydrology. Furthermore, the effect of season, antecedent substrate water content, storm characteristics (size, intensity, frequency), and vegetation development (green roof leaf area index and percent cover) on retention were studied. We hope findings provide insight

on the benefit of designing GI in-series for stormwater management in residential settings, especially as we expect many future residential systems to be similar in design to the ones in this study. It was predicted that the GI would have an impact on site hydrology. Furthermore, that antecedent substrate water content, event size, intensity and frequency, as well as low vegetation development of the green roof would impair retention.

Objective 2: 1) Characterize the seasonal thermal performance of *WaterShed's* sloped extensive green roof (to the building and surrounding environment) relative to its cool roof. 2) Determine the effect of green roof properties (ET, solar reflectance and thermal conductance) on thermal performance. 3) Evaluate the effect of substrate water content, vegetation development (leaf area index and percent cover), and microclimate (net radiation and air temperature, etc.) on ET, albedo and thermal conductance values.

In recent years many policy makers and governments have taken decisive measures to systematically reduce carbon emissions and energy use in buildings (Besir and Cuce, 2018). These include advanced eco-technologies, energy efficient systems and renewable energy sources. In this context, green roofs are often identified as a valuable strategy for making buildings more sustainable (Berardi et al., 2014). Cool roof strategies (high albedo and emissivity) are also progressively drawing the attention of the scientific community and the market due to their effective role in reducing building energy requirements and also mitigating urban heat island effects (Ganguly et al., 2015).

However, there are several knowledge gaps in green roof thermal performance research. One of them being that despite widespread application, green roof systems are not standardized (Tan et al., 2017) and there is much uncertainty regarding their thermal performance in real conditions, especially in regional climates characterized by winters,

or in comparison to alternatives technologies like cool roofs (Berardi et al., 2014; Bevilacqua et al., 2017; Saadatian et al., 2013). Furthermore, there is much unknown regarding the processes that affect green roof thermal performance in real conditions.

Thus, this study is unique in that we simultaneously researched the thermal performance of a green and cool roof across seasons. Findings are relevant to the scientific community in helping us better understand how green roofs operate, which has implications to how we design and maintain them locally to reduce building energy demand. This is increasingly important as global nonrenewable energy sources diminish, and has implications to reducing the contribution of buildings to climate change. Altogether it was hypothesized that cool roof thermal performance would be optimal in warmer months, while the green roof would be preferable during colder months. Furthermore, evapotranspiration, albedo and thermal conductance properties would significantly impact thermal performance.

Objective 3: 1) Characterize the evapotranspirative nature of *WaterShed's* sloped extensive green roof. 2) Evaluate the effect of substrate water content, vegetation characteristics (leaf area index and percent cover) and microclimate characteristics (net radiation, air temperature, relative humidity, wind speed) on ET rates. 3) Compare measured evapotranspiration to rates predicted with the FAO-56 Penman–Monteith model.

Although ET is important to the energy and water balance of green roofs, it has not been well studied, especially in real conditions and there is little experimental data examining ET rates and attributing factors. Additionally, although the FAO-56 version of the Penman–Monteith model has been shown to provide a better prediction amongst other methods for green roofs (Berretta et al., 2014), the model has been found to overestimate

ET for the *Sedum* species common on green roof systems, especially under water-limited conditions and even after correction (Starry, 2013; Tjaden, 2014).

By evaluating the evapotranspirative nature of the green roof and comparing measured values to rates predicted with the FAO-56 Penman–Monteith model, we hope to better quantify ET on a sloped extensive green roof and determine the applicability of the model to the system. It was hypothesized that <u>with a thin depth and sloped configuration, moisture may be limiting factor to ET, resulting in ET overestimations during dry periods with the FAO-56 Penman-Monteith model.</u>

Objective 4: Using emergy theory, explore green roof, constructed wetland and bioretention sustainability and resilience relative to a wastewater system and natural forest.

By relying on natural processes and energies to provide urban communities with ecosystem services, GI has the ability to increase the sustainability and resilience of cities as they adapt to climate change. However, GI sustainability and resilience have not been fully explored. Several environmental accounting methods such as cost-benefit analysis and life-cycle assessment have been used to explore GI sustainability, however these models have limitations. One of the most controversial criticisms of CBA is that it evaluates environmental impacts and ecosystem services to humans using economic analysis when many environmental impacts such as human life and some irreversible effects on ecology are not convertible into monetary values (Reza, 2013). Furthermore, LCA has been criticized as a utilitarian user-side approach to sustainability, only focusing on environmental impacts due to resource consumption and emissions while ignoring the work of ecosystems to provide 'freely available' services and products (e.g. rainfall, soil organic matter, etc.) (Reza, 2013). Thus, it has been proposed that sustainability cannot be

assessed simply by counting mass and energy flows, but by accounting for the direct and *indirect* energy supporting flows. *Emergy* is proposed as a more holistic ecological accounting method for determining if the direct and indirect energy requirements of *WaterShed's* GI are less than produced benefits over each system's life-span.

Furthermore, as global populations have become increasingly urbanized and as climate change progresses, urban resilience may greatly depend on the implementation of GI. In the resilience discourse, management of diversity per se is considered to be a key attribute for building resilience in complex adaptive systems (Colding and Barthel, 2013). Diversity functions as insurance– it spreads risks, creates buffers, and opens up for multiple strategies from which humans can learn in situations when uncertainty is high. Diversity also plays an important role in the reorganization and renewal processes of disturbed systems (Colding and Barthel, 2013), and makes systems less vulnerable to natural and human-induced changes such as resource availability fluctuations.

In ecology, the Shannon diversity index, has been used often to assess ecosystem diversity. Since GI benefits are diverse and not easily 'additive', we proposed that the environmental accounting technique of *emergy* evaluation could be extended using information theory— the basis of the Shannon Index— to enumerate the energetic diversity of GI and provide a new metric of resilience. Previously, this system-level *emergy diversity index* (derived from the Shannon diversity index) was used to quantify the diversity of species in ecological systems, and diversity of energy and resources in economic systems (Brown et al., 2006; Ulgiati et al., 2011). The new emergy based indicator differs from the typical way of estimating diversity— which is based on simply counting individuals, biomass or other stocks— because it uses the flows of energy and materials in *emergy*

terms. Resilient systems are supported by a variety of emergy flows that make it more likely to develop complex structures, while systems that only rely on a small set of sources out of a large number of potentially available ones possess a built-in fragility that may determine their collapse in times of shrinking or changing resource basis (Ulgiati et al., 2011).

By integrating information theory with emergy evaluation, were able to quantify how much the green roof, CW and bioretention increase the flow of information at the ecological, environmental, social and economic levels compared to a typical wastewater treatment plant and natural forest. It was hypothesized that GI should be more sustainable and resilient than gray infrastructure since it relies on a host of natural energies (i.e., sun, water, atmospheric deposition) to produce an excess of benefits.

2.7   Site Description: *WaterShed's* Green Infrastructure
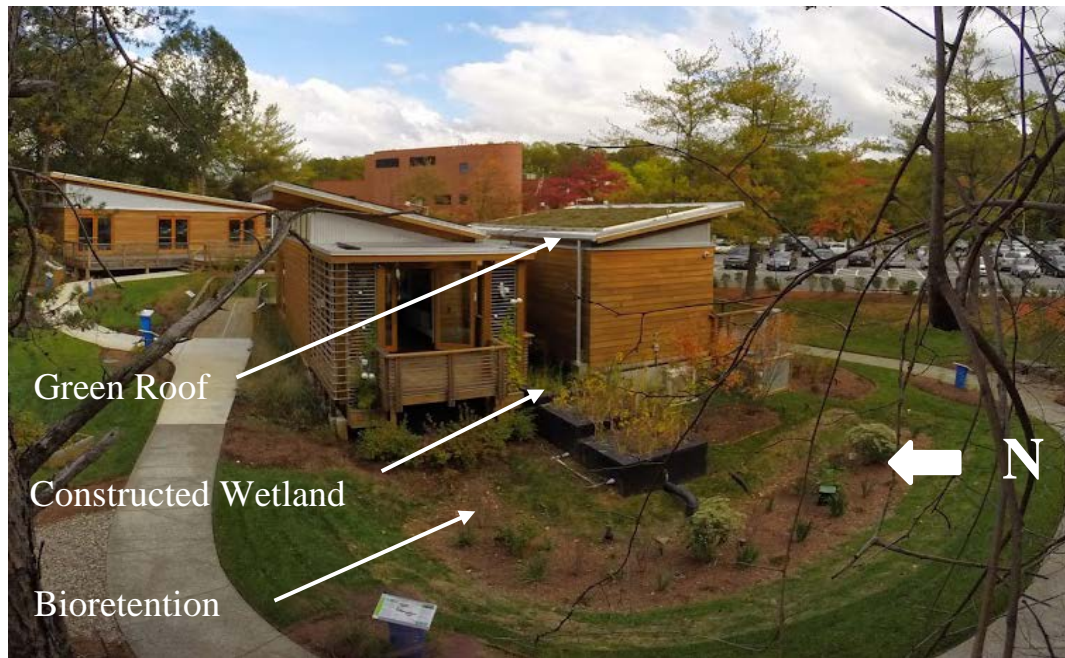
Figure 2-1 *WaterShed's* butterfly roof design allows for stormwater runoff from the 29 m^2 green roof to drain into a three-chamber constructed wetland (8.68 m^2). Finally, surface runoff, and stormwater flowing from the constructed wetland flow into a 32.6 m^2 bioretention.

Residential integration of a green infrastructure in-series (green roof, constructed wetland, bioretention) was researched on *WaterShed*, the University of Maryland's 2011 winning sustainable solar house built for the US Department of Energy Solar Decathlon competition (Figure 2-1). Since the competition, *WaterShed* was acquired by one of Maryland's regional energy companies, Pepco Holdings, Inc., and is now permanently housed in Rockville, MD.

An Integrated Water: Energy Monitoring System of 241 sensors (Campbell Scientific Dataloggers and instrumentation) were installed throughout *WaterShed* to help validate the performance of the various interior and exterior systems. Supplementary

information on the exterior sensors installed and their respective location can be found in Appendix A. Overall data was collected from dataloggers every 15 minutes, with varying sub-scan intervals. These sub-scans are averaged or totaled within the 15-minute window to provide the collected data. Once data was wirelessly transmitted to centralized dataloggers, it was downloaded as Microsoft Excel spreadsheets for analyzation.

As described in Figure 2-2, the green roof is a LiveRoof Lite extensive modular system (6.35 cm or 2.5 in deep, 10° sloped, 29 m^2 or 312 ft^2, north-facing) and is waterproofed with a white thermoplastic polyolefin (TPO) membrane which has a border ranging from 38.1-50.8 cm (15–20 in) between the vegetation and edge of the roof. A modular green roof is defined as system that has removable trays that contain all the normal green roof components, that can be added to the roof surface (Gregoire and Clausen, 2011).

Substrate composition by weight is approximately 84.4% engineered shale (19 lb/ft^2), 11.1% compost (2.5 lb/ft^2), 4.4% sand (1 lb/ft^2). The original plant selection included *Sedum album* 'Coral Carpet,' *Sedum spurium* 'Dragon's Blood,' *Sedum spurium* 'Tricolor,' *Sedum reflexum* 'Blue Spruce,' and *Sedum sexangular* 'Utah.' These *Sedum* species are a type of perennial stonecrop within the Crassulaceae family ranging in shape, color, and growing preferences. Generally, succulents such as *Sedum*, have been the most studied and used plants for green roofs. One of the main reasons *Sedum* seem ideally suited to green roof cultivation is the fact that it grows by natural moisture even if there is a little soil and does very well in rocky areas. Furthermore, many *Sedum* possess crassulacean acid metabolism (CAM). During periods of soil moisture deficit, CAM plants keep their stomata closed during the day when transpiration rates are normally high and open them at night when transpiration rates are lower. This is in contrast to C3 and C4 plants, which do

not keep their stomata closed during the day and have higher water use rates than CAM plants (Al-Busaidi et al., 2013).
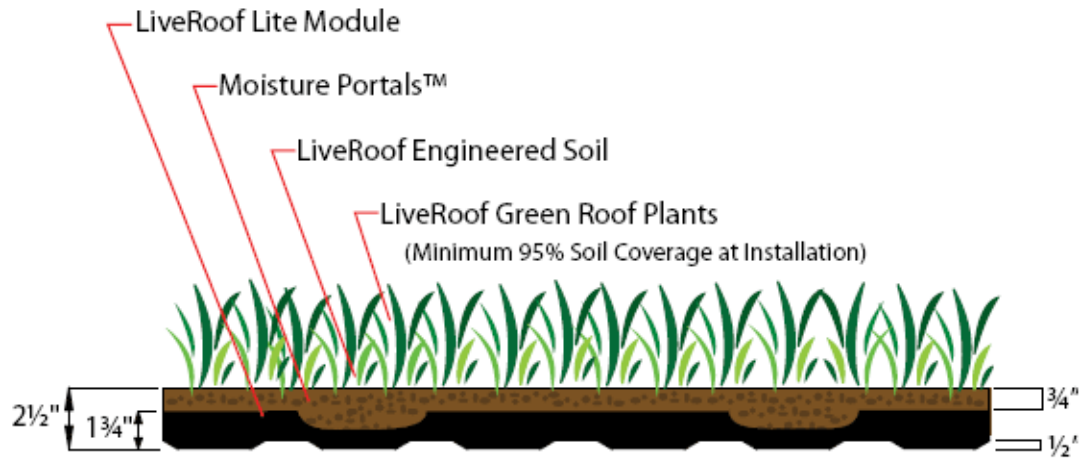
Figure 2-2 Rendering of the LiveRoof Lite Module installed on *WaterShed*. Soil is approximately 6.35 cm deep, and the module size is 30.48 cm x 60.96 cm x 4.58 cm. Saturated weight is approximately 73.2-83.0 kg/m^2 and the dry weight is 58.6 kg/m^2. The system is ideal for retrofit projects where load limitations exist (Image Credit: LiveRoof).

Stormwater runoff from the green roof, drains into a three-chamber constructed wetland (8.68 m^2 or 93.4 ft^2) running east to west through the central axis of the house (Figure 2-3). The first chamber is a free-standing wetland designed to receive direct input of stormwater runoff from the green roof. The final two chambers are horizontal subsurface flow wetlands receiving stormwater from the first chamber. The system has the potential to treat graywater from the house, however Maryland legislation currently prohibits graywater treatment with CWs. The wetland is comprised of plant species: *Nymphaea odorata, Iris versicolor*, *Peltandra virginica*, *Typha latifolia*, *Pontederia cordata*, *Schoenoplectus pungens*, and *Hibiscus coccineus*.

27
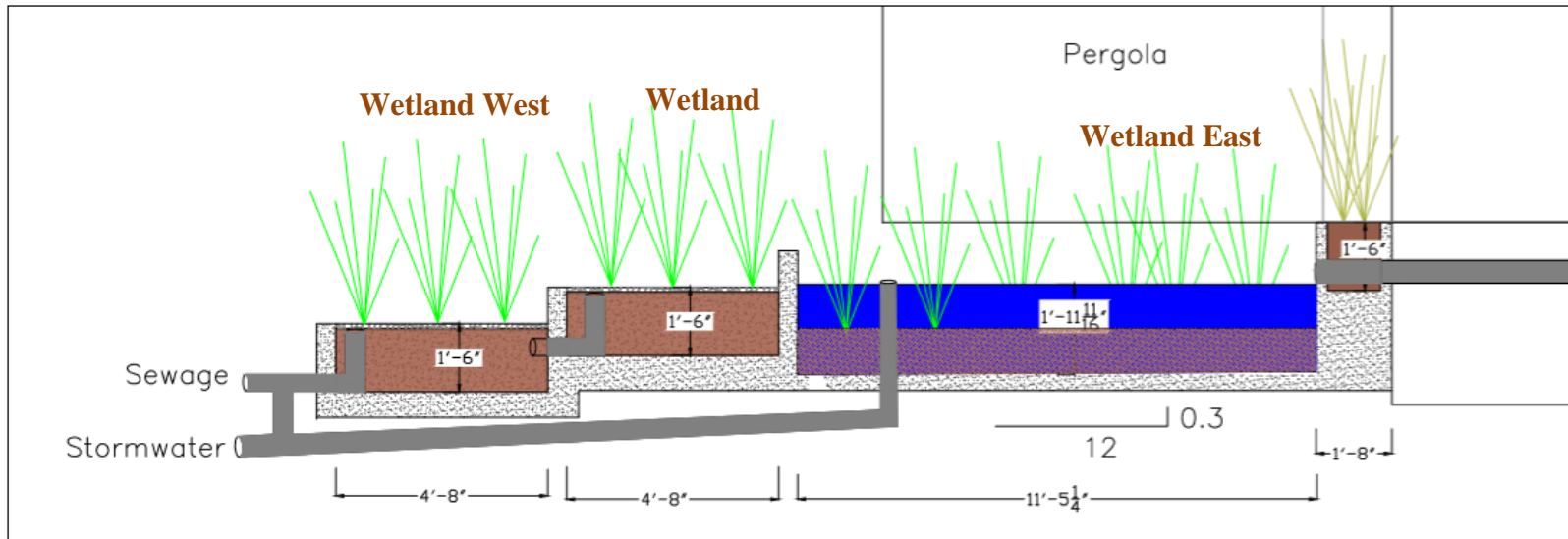
Figure 2-3 Stormwater runoff from the green roof, drains into a three-chamber constructed wetland (8.68 m^2) running east to west through the central axis of the house. The first chamber (wetland east) is a free-standing wetland designed to receive direct input of stormwater runoff from the green roof. The final two chambers (wetland center and wetland west) are horizontal subsurface flow wetlands receiving stormwater from the first chamber. The system has the potential to treat graywater from the house. Finally, stormwater flowing from the constructed wetland flows into a 32.6 m^2 bioretention (Image credit: Scott Tjaden).

Figure 2-4 Surface runoff and stormwater runoff flowing from the constructed wetland flows into a 32.6 m² bioretention (7.62 cm mulch layer, 70.0 cm planting media, 15.2 cm sand layer, 15.2 cm stone layer above the underdrain, and 7.62 cm stone layer below the underdrain) with groundwater outlet. Plant list and media specifications were not accessible.

Finally, surface runoff, and stormwater runoff flowing from the constructed wetland flow into a 32.6 m² (350.9 ft²) bioretention (7.62 cm or 3 in mulch layer, 70.0 cm or 27.6 in planting media, 15.2 cm or 6 in sand layer, 15.2 cm or 6 in stone layer above the underdrain, and 7.62 cm or 3 in stone layer below the underdrain) with groundwater outlet (Figure 2-4). Media specifications and a plant list were not provided, however current design guidance from the state of Maryland recommends bioretention planting soil be a sandy loam, loamy sand, loam (USDA), or a loam/sand mix (should contain a minimum

35 to 60% sand, by volume). The clay content for these soils should be less than 25% by volume. Plant material selection should be based on the goal of simulating a terrestrial forested community of native species. The community should be dominated by trees, but have a distinct community of understory trees, shrubs and herbaceous materials. Commonly used species for bioretention areas are provided in Table A.4 of *Maryland's Stormwater Design Manual* (MDE, 2009).

Chapter 3 Green Infrastructure Hydrological Performance

3.1   Objective

The need to develop a practical and sustainable approach to stormwater management is rapidly becoming a priority as human development and climate change alters urban hydrologic cycles. In recent decades, green infrastructure (GI) has been viewed as a sustainable alternative to stormwater management, with the reduction, diversion or treatment of storm water runoff being one of its most extensively researched benefits. However, water retention studies are largely limited to green roofs. Furthermore, rarely have multiple GI practices in-series been monitored, even though most stormwater regulations require these practices to be installed in-series to receive permits. Most studies typically only evaluate individual practices (Brown et al., 2012). Finally, studies on the effectiveness of GI in residential settings is lacking– most studies are laboratory based, or of systems larger in scale such as GI in the public right-of-way.

The purpose of this objective was to examine how an extensive green roof, constructed wetland and bioretention integrated in-series on a sustainable home in Rockville, Maryland (USA) affected site hydrology over 116 storm events that occurred between July 2014 and June 2016. Furthermore, the effect of season, antecedent substrate water content, storm characteristics (size, intensity, frequency), and vegetation development (green roof leaf area index and percent cover) on retention were evaluated.

We hope findings provide insight on the benefit of designing GI in-series on residential properties, especially as we expect many future systems to be similar in design to the ones in this study. For example, with many homes possessing sloped roofs with

weight load restrictions, many new green roofs could likely be sloped, extensive, and modular. Furthermore, due to space constraints, many constructed wetlands and bioretention areas applied to residential communities may likely be similar in design to the systems in this study.

3.2 Introduction

One effect of urbanization is an increase in area of impervious surfaces, which has many consequences for urban communities and the surrounding environment. Impervious surfaces cause infiltration of stormwater to decrease, and instead runoff urban landscapes. One effect of increased runoff is a reduction of groundwater replenishment, which has put heavy pressure on water resources in semiarid regions. While in other regions, surface runoff has degraded water quality by depositing polluted runoff into nearby waterbodies and/or causing combined sewer overflows (CSOs), while increasing flood risks (Czemiel Berndtsson, 2010; Rowe, 2011; Yang and Cui, 2012).

More specifically, in communities where there are combined sewer systems to manage raw sewage and stormwater, heavy storm events can stress stormwater infrastructure and result in a CSOs when the volume of runoff exceeds the capacity of the stormwater system. This results in raw untreated sewage and stormwater flowing out of relief points into waterbodies, which has adverse effects on water quality (Rowe, 2011). Even in communities with separate stormwater managements systems, impervious surfaces still degrade waterways by collecting pollutants such as oil, heavy metals, salts, pesticides, and animal wastes that wash into waterbodies (Rowe, 2011). Other known adverse effects of traditional stormwater infrastructure are erosion of waterways and localized flooding (Pennino et al., 2016). All together these issues are increasingly concerning as studies

indicate that in certain regions where climate change is projected to increase the frequency of intense precipitation events (Czemiel Berndtsson, 2010), these problems are expected to worsen. Because of these risks, traditional 'hard' engineering approaches to restoring urban water balance using gray infrastructure are viewed as vulnerable and failure-prone.

Green infrastructure– such as green roofs, bioretention areas, porous pavements, rain barrels/cisterns, and green roofs– is increasingly being recognized as a sustainable approach to urban environmental problems. GI is defined as natural and constructed green spaces that utilize vegetation, soil, and other components to replicate natural processes that provide benefits for human populations in the urban setting (Law et al., 2017). Though GI provide a variety of environmental, social and economic benefits, GI are largely being implemented throughout major cities across the US to help recharge groundwater, reduce flooding, improve water quality, and reduce CSOs (Pennino et al., 2016). Furthermore, the reduction, diversion or treatment of stormwater runoff are some of its most extensively researched benefits.

3.2.1   Extensive Green Roof Hydrological Performance

The hydrological performance of green roofs is well studied, with previous published studies showing the ability of green roofs to retain and detain stormwater (Zhang et al., 2015). However, research on extensive green roofs particularly on residential buildings is lacking. In terms of extensive green roofs, Gregoire and Clausen (2011) performed a meta-analysis of green roof studies and found that extensive green roofs constructed to reduce stormwater runoff were able to intercept, retain, and evapotranspire between 34–69% of precipitation, with an average retention rate of 56% (Gregoire and

Clausen, 2011). Another meta-analysis in 2015 reported retention values between 15.5-68% from various studies undertaken on extensive green roofs (Nawaz et al., 2015).

However, with all these studies it is important to note that direct comparisons between findings are difficult to make given a whole range of conditions unique to each study (Nawaz et al., 2015). The following factors are largely known to influence green roof water retention capacity and runoff dynamics (Carson et al., 2013; Czemiel Berndtsson, 2010):

Green roof characteristics: number of layers and type of materials, instillation type, substrate thickness, substrate type, vegetation cover, type of vegetation, roof geometry (slope/length of slope), roof position (e.g. shadowed or not, faced direction), roof age, monitored drainage area, substrate water holding capacity and saturated hydraulic conductivity

Season/ Climate conditions: length of proceeding dry period, characteristics of storm event (size, duration, and intensity), and meteorological parameters like air temperature, wind conditions, humidity

The green roof in this study is modular, extensive and sloped. It is well known that decreasing the slope and increasing the depth of a green roof's growing layer is more likely to reduce runoff (Berardi et al., 2014). Other relevant variables such as substrate water content, storm event characteristics, season and vegetation characteristics are also known to play an important role in retention capacity (Czemiel Berndtsson, 2010). For example, when the effect of event size, substrate volumetric water content and vegetation on stormwater retention efficiency was studied on an un-irrigated extensive green roof in

Central Texas, event size explained 55.4% of the retention rate in trays with substrate only and 70.6% of the variation observed in vegetated trays. Furthermore, researchers found rainfall frequency to strongly affect substrate volumetric water content, where greater time between events was imperative to substrate drying out, thus improving the ability of the green roof to retain additional water (Volder and Dvorak, 2014). It is important to note however that some researchers have suggested that substrate drying time can have a negative impact on stormwater retention. More specifically, one study suggested that at certain volumetric water contents (below 8%) substrates are likely to become hydrophobic, reducing initial capacity to retain water (Griffin, 2014). In addition to the frequency of storms, the reduction of antecedent soil moisture in between storm events via plant water uptake has also been found to be essential to retention (Jim and Peng, 2012).

3.2.2   Constructed Wetland Hydrological Performance

Constructed wetlands (CWs), constructed stormwater wetlands, or reed beds, are man-made wetlands specially designed to store and filter storm water runoff (Droguett, 2011). Because wetlands are viewed as natural wastewater treatment systems, CWs provide an efficient, low-cost, easily operated alternative to conventional treatment systems (Scholes et al., 1998). There are numerous studies demonstrating that the ability of CWs to effectively remove pollutants from urban stormwater runoff (Al-Rubaei et al., 2016). However, there is debate as to whether CWs can reduce runoff. Some studies state CWs are generally suitable best management practices for both water storage and water quality improvement (Greenway, 2015). Other studies state that they are more effective for pollutant removal as it is believed they have a limited ability to reduce overall runoff volumes since their only losses are due to evapotranspiration (Fletcher et al., 2013).

A review of existing literature found that while CWs have been used extensively for many years, they have only more recently been applied to residential settings. To our knowledge there are no studies on the hydrological performance of CWs integrated with residential buildings.

In terms of comparable studies, Lenhart and Hunt (2011) found that a 0.14 ha stormwater treatment wetland in River Bend, North Carolina, reduced peak flows and runoff volumes by 80% and 54%, respectively, and they suggested that stormwater wetlands should be considered a viable GI option, especially where there are sandy soils (Lenhart and Hunt, 2011). In another study where the long-term hydraulic and treatment performance of a 19-year old CW treating stormwater from a 320-ha urban catchment was evaluated, the were significant peak flow reductions achieved by the constructed stormwater wetland for all storm events (65–89%), and the flow volume reductions for the thirteen events ranged between 12-67% (average flow volume reduction was 22%). Researchers also noted that the hydraulic performance of the CW in reducing runoff volumes varied from positive to negative reduction for some events, especially with storm events preceded by short dry periods and/or high rainfall intensities (Al-Rubaei et al., 2016).

3.2.3 Bioretention Hydrological Performance

Bioretention has increasingly become popular over the past decade as a stormwater best management practice in urban and suburban areas because it facilitates groundwater recharge, while reducing stormwater flow rate, volume, and pollutants. Rapid implementation of bioretention areas is also due to their flexibility in size and location, aesthetic value, and cost-effectiveness compared to traditional treatment methods (Yang et

al., 2013). However, to date performance data for bioretention have generally been limited to the laboratory-scale, with few studies reporting on field-scale testing. Furthermore, research to date has generally focused on the pollutant removal performance of bioretention, with less attention given to its hydrologic performance. Bioretention areas have previously been thought to have little water quantity control benefit and provide only minor flood control benefits. However, there has been little empirical data or even modelling to support this notion (Hatt et al., 2009).

In terms of studies that have evaluated the hydrological performance of bioretention, Ahiablame et al. (2012) summarized several findings and reported that bioretention reduce runoff by 48-97%. Liu et al. reviewed several studies and found bioretention to reduce peak flow by 44-99%, and reduce runoff volumes by 50-100% (Liu et al., 2014). Furthermore, a review of existing literature found the following factors to affect hydrological performance:

Event Size, Inflow Volume and Rate

- The reduction of bioretention runoff volumes and rates depends on the magnitude of rainfall events. During small events, researchers found bioretention facilities can readily capture the entire inflow volume within the media (Davis, 2008).

- Hatt et al. showed bioretention to be effective in on average, retaining 33% of the inflow volume (range: 15–83%) and attenuating peak runoff by at least 80% (range: 37–96%). Of the five predictor variables, retention of water was found to be most influenced by peak inflow rate and inflow volumes (Hatt et al., 2009).

- Yang et al. (2013) studied a biphasic rain garden that consisted of a saturated zone to enhance nitrogen removal followed by an unsaturated zone. The peak flow and volume reduction between influent and the unsaturated zone effluent were 67% and 28%, respectively. When studying the effect of rainfall size on the average cumulative volumes and the flow rates of influent and effluent (unsaturated zone effluent), no measurable effluent was observed during light rainfall events (<6 mm) due to the storage capacity of the saturated zone, while during the representative medium (6–12 mm) and heavy (>12 mm) rainfall events, runoff volume reduction percentages decreased (59% for medium rainfall events and 54% for the heavy rainfall events) (Yang et al., 2013).

Length of Proceeding Dry Period, Substrate Water Content, Vegetation and Evapotranspiration

- Researchers found that in general, the hydraulic performance of biphasic rain gardens was affected by initial water conditions in the saturated zone. A greater reduction in both peak flow and volume was observed when the saturated zone was less water saturated because of longer rainfall intervals and/or high ambient temperatures with high ET rates, increasing water storage capacity in the saturated zone that was used to retain runoff during the next event (Yang et al., 2013).
- A study evaluating the pollutant removal and hydrologic performance of five, 10-year old street-side bioretention systems subjected to a series of simulated rainfall events using synthetic stormwater found that all the basins were able to attenuate the system flows and significantly reduce peak outflow rates compared to inflow rates. The percentage reductions in outflow volumes varied from 32.7% and 84.3%.

Furthermore, the change in measured moisture content during tests was found to be highly variable. In accordance with expectation, the drier the pre-basin, the higher the volume of water was stored within the basin during testing, and consequently lower volumes of water were discharged (Lucke and Nichols, 2015).

- Richards et al. (2015) compared the performance variance between a vegetable raingarden that was lined, and an unlined raingarden in which runoff water was allowed to infiltrate into the ground. The ability of the two raingardens to reduce runoff was evaluated based on both the frequency (days) and volume of flow. The infiltration-type raingarden, sized 7.5% of its catchment area, reduced both the volume and frequency of runoff by >90%. In comparison, the lined raingarden reduced the volume of runoff by 63% and the frequency by 34%. The unlined raingarden's performance was found to be more variable over time, particularly in response to variation in rainfall and ET rates. Also, it was most effective in reducing runoff from rainfall events that were preceded by dry periods (Richards et al., 2015).

- Researchers attributed a 48-74% reduction of runoff that flowed through bioretention systems to infiltration and ET (Chapman and Horner, 2010).

- A study of the hydrologic performance of field scale biofiltration systems showed vegetation to be important for maintaining hydraulic capacity because root growth and senescence countered compaction and clogging (Hatt et al., 2009).

Season/Climate

- Hunt et al. studied three bioretention systems in North Carolina. Results indicated that efficiencies of runoff volume reduction changed significantly seasonally,

partially due to lower ET rates in the winter compared to other seasons (Hunt et al., 2006).

- Paus et al. examined the seasonal hydrological effectiveness of bioretention cells in cold climates and found that saturated hydraulic conductivity values during winter/early spring were only 25 to 43% of those during summer (Paus et al., 2015).

Internal Water Storage

- Three bioretention cells constructed in low permeability soils in northeast Ohio were monitored. In this study, between 31 and 68% of observed rainfall events were completely captured (i.e., no drainage or overflow) by the bioretention cells. The inclusion of an internal water storage (IWS) zone allowed the three cells to reduce runoff by 59%, 42%, and 36% over the monitoring period despite the tight underlying soils. The two cells with lesser runoff reductions were noted to have lower drawdown rates and smaller IWS zone thicknesses (Winston et al., 2016).

3.2.4   Green Infrastructure In-series Hydrological Analysis

Although GI is being implemented in cities across the world to manage stormwater, rarely have multiple practices in-series been studied even though most stormwater regulations require them to be installed in-series to receive permits– most studies typically only monitor individual practices. Because performance of practices in-series is not well documented, questions persist regarding how to size individual practices with respect to maximizing water quality and hydrologic benefits, while minimizing cost (Brown et al., 2012). Furthermore, to our knowledge no studies have analyzed residential application of

GI in-series. A review of literature found the following studies on the hydrological performance of GI in-series:

- Brown et al. compared a treatment train (0.53 ha of pervious concrete and a 0.05 ha bioretention cell) to using only the bioretention cell. The study demonstrated the hydrologic benefits (peak flow and outflow reduction) gained by having GI practices in-series. The treatment train was effective in reducing the runoff volume by 69%. When compared with a single treatment practice (bioretention) that was monitored at the same site, the two GI practices in-series treated an additional 10% of annual runoff volume, discharged approximately one-half as much outflow volume, and discharged significantly lower peak outflow rates (Brown et al., 2012).

- Jia et al. studied the urban runoff control effectiveness of a GI treatment train in China. The train included three grassed swales, a buffer strip, a bioretention cell, two infiltration pits, and a CW connected in-series. They noted that the bioretention cell provided a peak flow reduction of 50–84% and a runoff volume reduction of 47–80%; whereas the grassed swales provided 17–79% reduction in peak flow rate and 9–74% runoff volume reduction (Jia et al., 2015).

- Four treatments of parking lot surfaces and the presence or absence of swales was studied. These treatments included asphalt without a swale, asphalt with a swale, concrete with a swale, and porous pavement with a swale. Porous pavement with a swale reduced runoff by 32% when compared with asphalt or concrete with a swale, and by 50% when compared with asphalt without a swale (Rushton, 2001).

- Mayer et al. (2012) performed an extensive six-year before and after study (three years before, three after) of the Shepherd Creek watershed (1.8 km^2) near

Cincinnati, Ohio. They monitored hydrological and ecological indicators in the watershed in which they ran a program, which saw the installation of 83 rain gardens and 176 rain barrels onto what amounted to over 30% of the properties. They found that GI measures had a small but statistically significant effect of decreasing stormwater quantity at the sub-watershed scale (Mayer et al., 2012).

- Three commercial sites were compared— one with no stormwater control measures, one with a wet detention basin and one with GI measures (including eight bioretention cells, 0.53 ha of pervious concrete and two CWs) in North Carolina. The runoff to rainfall ratio for the GI site was between that of the no stormwater control measures site and the wet detention basin site. Researchers stated that this was not surprising given that only 34% of the site's area drained to properly functioning stormwater control measures because of problems with the stormwater wetlands (lack of drawdown orifice) and the bioretention cells (undersized, clogged surface, and groundwater interception) (Line et al., 2012).

- Wilson et al. compared runoff from a commercial low-impact and conventional development in Raleigh, North Carolina. The low impact development site was treated by a mix of green (aboveground) and gray (underground) infrastructure including an underground detention chamber and infiltration gallery, underground and aboveground cisterns, and aboveground swales and bioretention; the conventional development was treated with a dry detention basin and swales. Runoff reduction was 98.3% compared to 51.4% for conventional development (Wilson et al., 2015).

3.3   Materials and Methods

3.3.1   System Descriptions
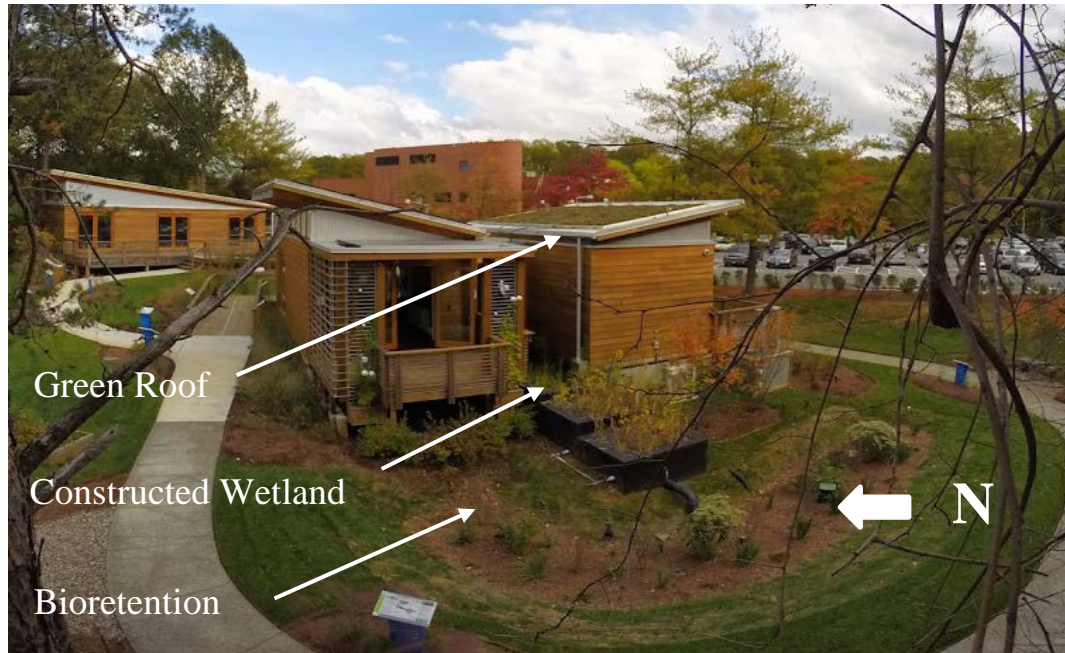
Figure 3-1 *WaterShed's* butterfly roof design allows for stormwater runoff from the 29 m^2 green roof to drain into a three-chamber constructed wetland (8.68 m^2). Finally, surface runoff, and stormwater flowing from the constructed wetland flow into a 32.6 m^2 bioretention.

As depicted in Figure 3-1, the 29 m^2 (312 ft^2) green roof system has a slope of 10 degrees and is 6.35 cm (2.5 in) in depth. Stormwater runoff from the green roof, drains into a three-chamber constructed wetland (8.68 m^2 or 93.4 ft^2) running east to west through the central axis of the house. The first chamber is a free-standing wetland designed to receive direct input of stormwater from the green roof. The final two chambers are horizontal subsurface flow wetlands receiving stormwater from the first chamber. Finally, surface runoff, and stormwater flowing from the CW flow into a 32.6 m^2 (350.9 ft^2) bioretention (7.62 cm or 3 in mulch layer, 70.0 cm or 27.6 in planting media, 15.2 cm or 6

in sand layer, 15.2 cm or 6 in stone layer above the underdrain, and 7.62 cm or 3 in stone layer below the underdrain) with groundwater outlet. For a full description of each system refer to section 2.7 (Site Description: *WaterShed's* Green Infrastructure).

3.3.2 Determining Stormwater Retention

To quantify stormwater retention for each system across 116 storm events (>5 mm) between July 2014 and June 2016, the soil depletion method was applied. Note, precipitation was measured using a rain gauge at the onsite weather station (TB4MM-L Tipping-Bucket Rain Gauge), and storm events were defined as the time precipitation began until the precipitation ceased– independent storm events consisted of events separated by six or more hours. In the event runoff was still occurring 6h after the first event, the two events were combined (Getter et al., 2007).

Green Roof Retention

The soil depletion method uses volumetric water content sensors (CS655 Water Content Reflectometer) within the green roof, or pressure transducers (CS451 Pressure Transducer) measuring water depth in the CW and bioretention, to determine changes in substrate storage between fifteen-minute sensor readings ($\pm\Delta S = S_{t15}-S_{t0}$). Where, $+\Delta S$ signifies retention, and $-\Delta S$ signifies water loss due to substrate drainage or ET. During a storm event, total retention was calculated as the sum of any positive change in storage ($\sum +\Delta S$) (Tjaden, 2014).

More specifically, nine water content reflectometers (Figure 3-2), measuring substrate volumetric water content (VWC) were installed approximately 3.81 cm (1.5 in) below the green roof surface with probes parallel to the roof and perpendicular to the slope

44

(see Figure A-1 for approximate location). VWC sensors operate by calculating the dielectric permittivity of the media from signal attenuation measurements combined with oscillation period measurements. Finally, it applies the Topp equation to estimate VWC from dielectric permittivity (Scientific, 2014). The nine uniformly installed sensors were averaged to determine the average water content (m^3/m^3) across the green roof. After the soil depletion method was applied, total retention ($\sum +\Delta S$) per storm event was determined in millimeters. These steps are summarized in Equation 3-1.
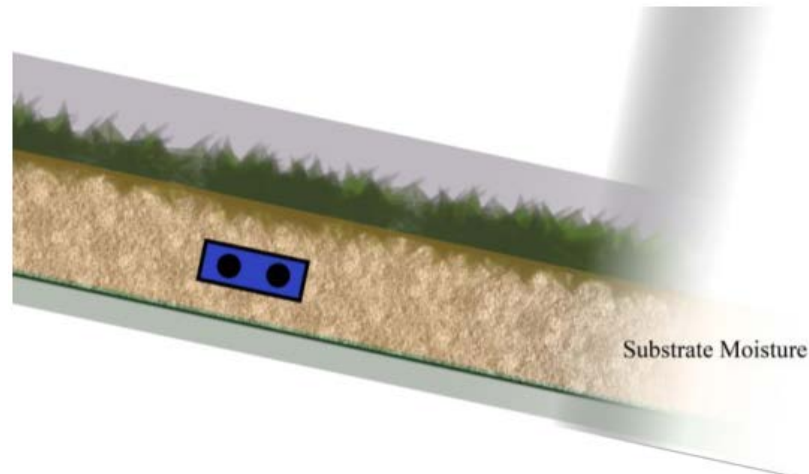
Figure 3-2 Soil Water Content Reflectometer sensors were installed approximately 3.81 cm (1.5 in) below the green roof surface with probes parallel to the roof and perpendicular to the slope (Image credit: Scott Tjaden).

$$\text{Green Roof Retention} = \sum +\Delta \text{ storage } (m^3/m^3) \times \text{Area } (m^2) \times \text{depth } (m) \div \text{Area } (m^2) \times 1000$$

Equation 3-1

Constructed Wetland Retention

Pressure transducers— described as a piezoresistive sensor and a temperature sensor housed in a metal case that can be submerged in water— relate pressure to water depth (pressure can be converted to feet of fresh water using the following equation: 1 psi = 2.31 ft of water) (Scientific, 2010). As illustrated in Figure 3-3, the first and last wetland chamber, referred to as *Wetland East* and *Wetland West*, each contained a pressure transducer (since *Wetland West* and *Wetland Center* were the same sized, they were assumed to retain similar amounts). The soil depletion method was then applied to determine retention depth in meters. Next, retention volumes (m^3) for each chamber were calculated considering water depth, each chamber's area, and the porosity of gravel. Finally, total retention volume (m^3) was calculated, and results were reported in millimeters. These steps are summarized in Equation 3-2.
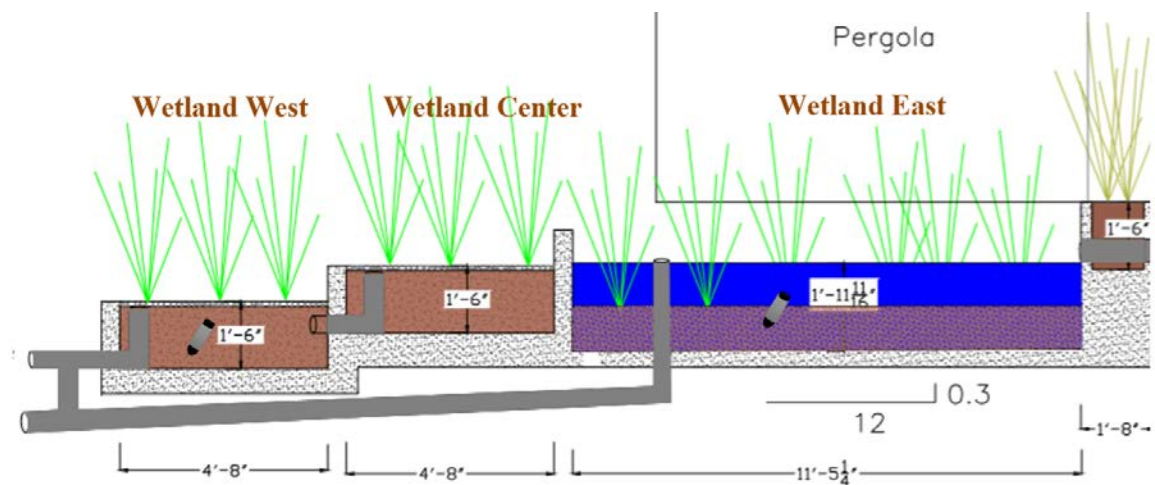
Figure 3-3 Approximate location of pressure transducers in the constructed wetland. Since *Wetland West* and *Wetland Center* were the same sized, they were assumed to retain similar amounts (Image credit: Scott Tjaden).

$$\text{CW Retention} = \sum +\Delta \text{ storage } (m^3) \div \text{Area } (m^2) \times 1000$$

Equation 3-2

Where,

$\sum +\Delta$ storage $(m^3) =$ Wetland West and Center Retention $(m^3) +$ Wetland East Retention (m^3)

Note,

Wetland West and Center Retention $(m^3) = \sum +\Delta$ storage $(m) \times$ Area $(m^2) \times$ 2 chambers $\times$ porosity of gravel

since Wetland East was a free-standing wetland and filled halfway with gravel, the following equation was applied,

Wetland East Retention $(m^3) = (\sum +\Delta$ storage $(m) \times$ Area $(m^2) \div 2) +$ $(\sum +\Delta$ storage $(m) \times$ Area $(m^2) \times$ porosity of gravel $\div 2)$

Bioretention Retention

Regarding bioretention, the average of two submerged pressure transducers was taken (see Figure A-1 for approximate location), then the soil depletion method was applied to determine retention. First, retention volume (m^3) was calculated by multiplying water depth by the area and the porosity of sand. After determining retention volume, results were reported in millimeters. These steps are summarized in Equation 3-3.

$$\text{Bioretention Retention} = \sum +\Delta \text{ storage } (m) \times \text{Area } (m^2) \times \text{porosity of sand} \div \text{Area } (m^2) \times 1000$$

Equation 3-3

3.3.3 Seasonal Effect

Retention data was separated into seasons which were defined as warm (May-October) and cold (November-April) to determine if there was seasonal variation in hydrological performance. Of the 116 storms (>5 mm) identified, 62 were during the warm season and 54 were during the cold season. T-tests (assuming unequal variances) were applied to determine if seasonal variation was statistically significant (correlations were significant at the 0.05 level).

3.3.4 Antecedent Substrate Water Content Effect

The effect of antecedent, or pre-event substrate water content (mm) on hydrological performance was studied. Antecedent water content was defined as the average water content 1 hour prior to a storm event. Volumetric water content sensors in the green roof and pressure transducers in the CW and bioretention used to determine retention were also used to determine antecedent substrate water content. Using regression statistics, retention per storm event was analyzed in respect to antecedent substrate water content.

3.3.5 Storm Characteristics (Size, Intensity, Frequency) Effect

The effect of storm characteristics (size, intensity, frequency) on hydrological performance was studied. Event size (mm), was classified as the total amount of stormwater received by each system during a storm event. Event intensity (mm/min) was defined as the total amount of stormwater received (event size) over the length of the storm event. Event frequency, or time between events (days), was the time between the end one of one storm event and the beginning of the next. Using regression statistics, retention per storm event was analyzed in respect to storm characteristics.

As illustrated in Figure 3-4, event size, or the amount of stormwater received by the green roof was attributed to precipitation. For the CW, the amount of stormwater received was calculated from the volume of stormwater runoff received by the green roof and the volume of precipitation the system received. Finally, stormwater inputted to the bioretention system was calculated from the volume of stormwater received by the CW, the volume of stormwater received from surface runoff, and the volume of precipitation inputted into the system itself. Supplementary information on the methodology used to calculate event size for each system can be found in Appendix B: Determining Event Size.

3.3.6   Vegetation Effect (Green Roof only)

Using regression statistics, monthly retention was analyzed in respect to average leaf area index (LAI) and percent cover. LAI was measured in addition to percent cover because it allowed us to measure the canopy foliage density of the green roof rather than simply area covered (Raji et al., 2015). Supplementary information on the methodology used to calculate LAI and percent cover can be found in Appendix C: Vegetation Development (Green Roof Only).
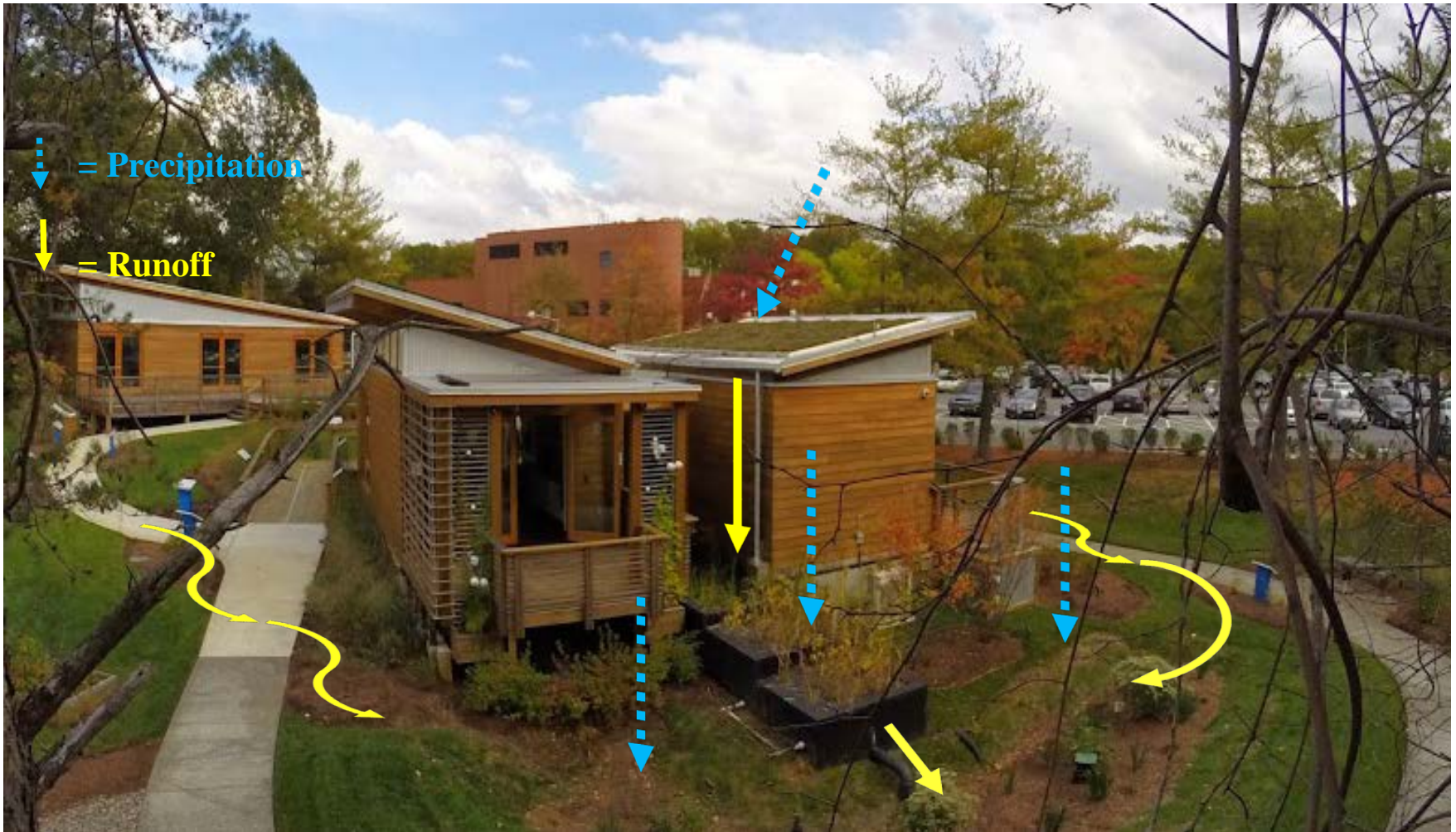
Figure 3-4 Stormwater received by each system: Green Roof = Precipitation Only; Constructed Wetland = Precipitation + Green Roof Runoff; Bioretention = Precipitation + Constructed Wetland Runoff + Surface Runoff.

3.4 Results and Discussion

3.4.1 In-series Hydrological Analysis

As illustrated in Table 3-1, collectively, the green roof, constructed wetland and bioretention stored 6,930.7 mm of stormwater over the two-year study period. Given a total input of 25,974.2 mm, the three systems collectively reduced site runoff by 26.7%. When evaluating each system independently, the CW performed the best considering its size at 8.68 m^2 (retaining 37.6% or 337.3 mm/m^2 of water). In comparison, bioretention only retained approximately 18% (or 1.22 times) more stormwater than the wetland despite receiving almost twice the amount of stormwater and being larger in size at 32.6 m^2 (retaining 22.4% or 109.6 mm/m^2 of water), indicating storage capacity limitations. The green roof was least effective (retention was 19.3% or 14.8 mm/m^2); however, this was expected considering its thin depth and sloped roof.

Table 3-1 In-series hydrological analysis shows collectively, the three systems reduced site runoff by 26.7% over the two-year study period.

	Retention (mm)	Stormwater Depth (mm)	Percent Retention (%)	Effectiveness (mm/m^2)
Green Roof	428.6	2,223.5	19.3	14.8
Constructed Wetland	2,929.1	7,786.3	37.6	337.3
Bioretention	3,573.0	15,964.3	22.4	109.6
Total	6,930.7	25,974.2	26.7	

Although there are no direct comparable studies of GI in-series on a residential building, we did expect to see a significant hydrological benefit based on previous research. For example, Brown et al. (2012) compared a treatment train (0.53 ha of pervious concrete

and a 0.05 ha bioretention cell) to using only the bioretention cell, and demonstrated the hydrologic benefits (peak flow and outflow reduction) gained by having two infiltration GI practices in-series. The treatment train was effective in reducing the runoff volume by 69%. When compared with a single treatment practice (bioretention) that was monitored at the same site, the two GI practices in-series treated an additional 10% of annual runoff volume, discharged approximately one-half as much outflow volume, and discharged significantly lower peak outflow rates (Brown et al., 2012).

Furthermore, Rushton (2001) monitored four treatments of parking lot surfaces and the presence or absence of swales. These treatments included asphalt without a swale, asphalt with a swale, concrete with a swale, and porous pavement with a swale. Results showed that porous pavement with a swale reduced runoff by 32% when compared with asphalt or concrete with a swale, and by 50% when compared with asphalt without a swale (Rushton, 2001). Jia et al. (2015) studied the urban runoff control effectiveness of a GI treatment train in China. The train included three grassed swales, a buffer strip, a bioretention cell, two infiltration pits, and a CW connected in-series. They noted that the bioretention cell provided a peak flow reduction of 50–84% and a runoff volume reduction of 47–80%; whereas the grassed swales provided 17–79% reduction in peak flow rate and 9–74% runoff volume reduction (Jia et al., 2015).

Overall, these findings suggest there is a benefit to designing GI in-series. Though the green roof stored the smallest amount of stormwater, integrating the CW and bioretention in the design of the home allowed for the retention of stormwater that would otherwise have contributed to runoff. Furthermore, it is likely that even though green roof retention was low, it may still be providing an added benefit of delayed runoff into the wetland, and

subsequently the bioretention— vegetated green roof systems have been shown to not only reduce stormwater runoff volumes, but also extend its duration over a period of time beyond the actual storm event (VanWoert et al., 2005). Furthermore, there are several design factors that could affect the hydrological performance of each system, these factors will be discussed in subsequent sections of this chapter.

3.4.2   Green Roof Hydrological Performance

Compared to previous meta-analyses of extensive green roof hydrology— Nawaz et al. (2015) noted 15.5-68% retention and Gregoire and Clausen (2011) reported 34–69%, with an average retention rate of 56%— retention over the study period was low at 19.3%. It is likely that the sloped configuration, modular tray design, and thin substrate depth severely limited retention capacity. In general, comparable studies on extensive modular sloped roofs are lacking, however, results from several studies can be compared.

For example, a study by Gregoire and Clausen (2011) on the effect of a modular extensive green roof system in the Northeastern U.S. on stormwater runoff and water quality showed the green roof retained 51.4% of precipitation during the study period based on area extrapolation (Gregoire and Clausen, 2011). Although the system was modular and extensive like the green roof in our study, it is likely that hydrological performance of this system was higher due to the cumulative effects of slope and depth on our design. The green roof in Gregoire and Clausen's study was not sloped and was slightly deeper at 10.2 cm (≈ 4 in)– our system is 6.35 cm (2.5 in) and sloped at 10 degrees.

This is important as it is well known that decreasing the slope and increasing the depth of green roof growing layers is more likely to reduce runoff (Berardi et al., 2014;

VanWoert et al., 2005; Zhang et al., 2015). For example, depth studies on 12 and 20 cm non-vegetated modules showed the 20 cm module outperformed the 12 cm module. The deeper module was able to reduce runoff by 83% compared to 63% for the shallower module (Nardini et al., 2011). Getter et al. (2007) studied sloped green roof platforms (2-25%) exposed to storm events. Mean retention was least at the 25% slope (76.4% retention) and greatest at the 2% slope (85.6% retention). Although some of these platforms were similar in depth and slope to the green roof in study, they were not modular and for additional water holding capacity, they were designed with a 0.75 cm thick moisture retention fabric (Xero Flor XF159) capable of retaining up to 5.92 kg/m^2 of water when placed over the drainage layer (Getter et al., 2007).

Finally, VanWoert et al. performed a study examining the cumulative effects of slope and depth and concluded that the combination of reduced slope and deeper media clearly reduced the total quantity of runoff. After testing the influence of roof slope (2 and 6.5%) and media depth (2.5, 4.0, and 6.0 cm) on retention, researchers found that for all combined storm events, platforms at 2% slope with a 4-cm media depth had the greatest mean retention (87%) although the difference between the other treatments was minimal (VanWoert et al., 2005).

Based on these finding, there are several potential design lessons learned regarding installing green roofs on sloped residential buildings. First, it is likely that the current design of the green roof – 10° sloped, 6.35 cm (2.5 in) and modular – would only be suitable in this region if designed for additional storage capacity. It would be interesting to study how an improved design, such as the same system designed with a thick moisture retention fabric or deeper substrate would perform. Furthermore, it would be interesting to study the

hydrological performance of the green roof on a flat residential roof.

Table 3-2 Correlation analysis of the effect of antecedent substrate water content, storm characteristics and vegetation characteristics on green roof seasonal retention. Note, (+) indicates a positive correlation and (-) indicates a negative correlation. Furthermore, [a] signifies correlation is significant at the 0.05 level, while NS indicates no significance.

	Antecedent water content (mm)	Event Size (mm)	Event Intensity (mm/min)	Event Frequency (days)	LAI (m^{-2})	Percent Cover (%)
Warm Season	$R^2 = 0.0868$ (-) [a]	$R^2 = 0.4388$ (+) [a]	NS	$R^2 = 0.0947$ (+) [a]	NS	NS
Cold Season	NS	$R^2 = 0.1802$ (+) [a]	NS	NS	NS	NS

Next, the effect of season on green roof retention was evaluated. Then the effect of antecedent substrate water content, storm characteristics and vegetation development on seasonal retention was observed— previous studies indicate green roof retention depends on the season. In the summer green roofs are characterized by higher ET, enabling retention capacity to regenerate quickly (Czemiel Berndtsson, 2010). Our findings show there was no significant difference in retention between the warm 23.1% ± 11.3 (range: 4.2-60.4%) and cold seasons 23.4% ± 17.3 (range: 0-88.6%) when retention percentages were averaged across all 116 storm events (62 were identified during the warm season and 54 were during the cold season). However, retention was more variable in the cold season, with several storm events exhibiting no retention during this time. This was likely attributed to the several occasions it was observed that the green roof's substrate was frozen, which would severely limit retention.

When we evaluated which variables affected seasonal hydrological performance

(Table 3-2), event size was the single biggest predictor of retention. This coincided with previous findings, such as a study where the effect of event size, substrate water content and vegetation on stormwater retention of an un-irrigated extensive green roof system in Central Texas was studied. Event size explained 55.4% of the retention rate in trays with substrate only and 70.6% of the variation observed in vegetated trays (Volder and Dvorak, 2014). Interestingly event size was more strongly correlated in the warm season ($R^2 =$ 0.4388) than the cold season ($R^2 = 0.1802$).
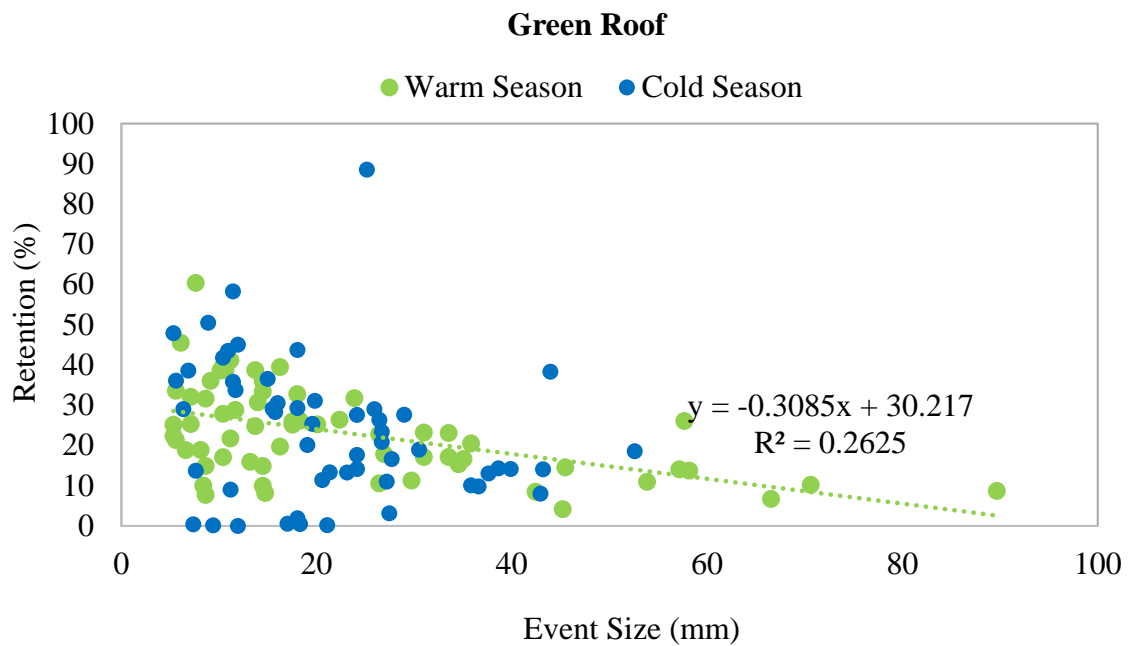
Green Roof

Figure 3-5 Larger storm events produced less retention as a percent of precipitation in the warm season (p<0.05), indicating, the green roof is approaching retention capacity as storms increase in size. From the figure it can be extrapolated that 0% retention will likely occur at storm events 98 mm and greater with the green roof's current design.

Furthermore, event size not only affects the amount of stormwater retained, but the percentage of green roof retention. As seen in Figure 3-5, a smaller percentage of total rainfall was retained with increasing event size during the warm season. In other words, a

larger rainfall events produced a greater proportion of runoff when compared to smaller events (Nawaz et al., 2015). Volder and Dvorak (2014) observed a similar trend, finding a negative correlation between event size and percent retention (Volder and Dvorak, 2014). This trend indicates that the green roof is likely approaching retention capacity as storms increase in size during the warm season. From Figure 3-5, we can extrapolate that 0% retention will likely occur with storm events 98 mm and greater with the green roof's current design. This phenomenon would also explain why retention percentages were lower in the warm season– it was characterized by greater rainfall amounts, especially those greater than >30 mm.
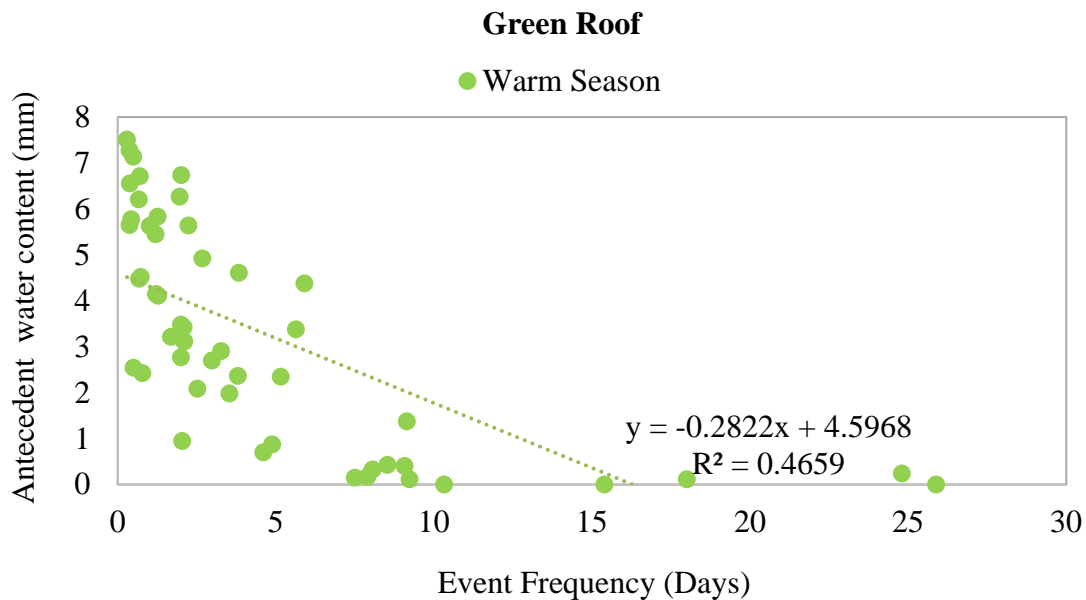
Green Roof

Figure 3-6 Low antecedent water content and days between storm events were correlated, indicating rainfall frequency is imperative to substrate drying out, and the green roof's ability to retain subsequent water.

Another indication that substrate storage capacity was being approached in the warm season is the fact that antecedent substrate water content and event frequency were

significantly correlated to retention. More specifically, greater time between events (R^2 = 0.0947) and low antecedent (pre-event) water content (R^2 = 0.0868) improved retention in the warm season. Furthermore, antecedent water content and event frequency were significantly correlated (R^2 = 0.4569) to each other as seen in Figure 3-6. This coincided with previous findings showing green roof storage capacity usage to be a function of time since last precipitation event, the size of that event, and the rate of water loss from the system through drainage and ET. More specifically, rainfall frequency is imperative to substrate drying out, and a green roof's ability to retain subsequent water (Volder and Dvorak, 2014). It is important to note however that some researchers have suggested that substrate drying time can have a negative impact on stormwater retention. More specifically, one study suggested that at certain VWCs (below 8%) substrates are likely to become hydrophobic, reducing initial capacity to retain water (Griffin, 2014).

Overall, limitations in substrate retention capacity during the warm season point to the importance of designing green roofs so that they effectively regenerate storage capacity in between frequent, large storm events. Studies state that the rate of green roof water loss is through drainage and evapotranspiration (Volder and Dvorak, 2014). Although our analysis did not show that ET was directly correlated with retention, average daily water content and total daily evapotranspiration were correlated (R^2 = 0.5621) (Figure 3-7). This relationship indicates that vegetation is likely playing an intimate role in regenerating storage capacity between storms for improved retention.

There were also several variables that were not significantly correlated to retention when then the effect of antecedent substrate water content, storm characteristics and vegetation development on seasonal retention was evaluated. For example, there was no

correlation between storm intensity and retention for both seasons. However, this trend

may simply be attributed to mostly low to moderately intense storms falling during these

seasons (< 0.33 mm/min). Lee et al. (2013) for example found a high water retention

capacity to rainfall of less than 20 mm/h (≈ 0.33 mm/min). They also observed that as

rainfall intensity increased beyond 0.33 mm/min, runoff ensued. They attributed this

phenomenon to rainfall intensity exceeding infiltration capacity of soils (Lee et al., 2013).
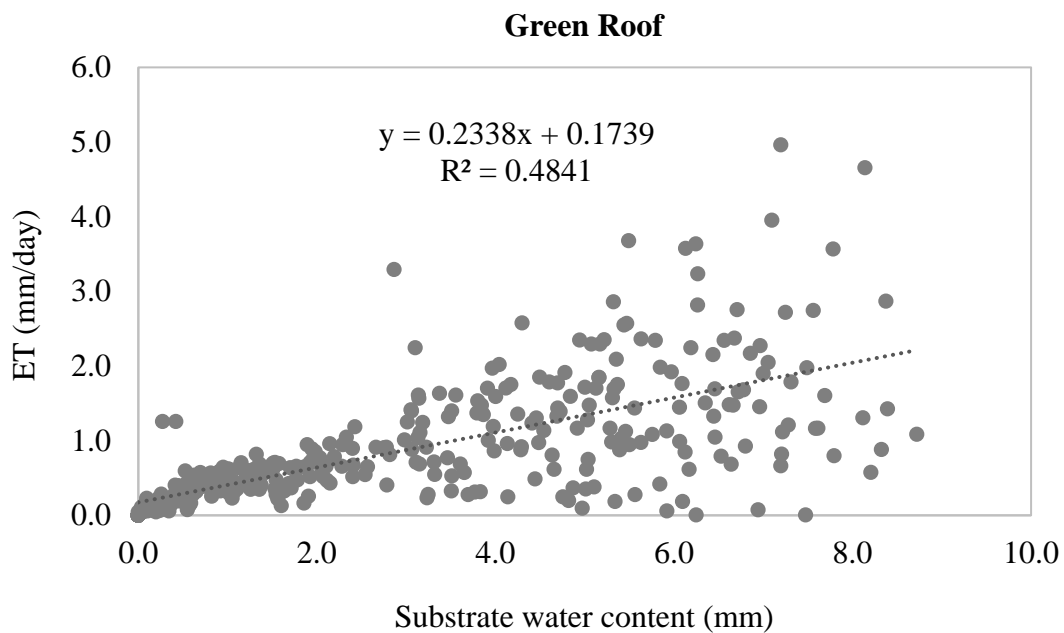
Figure 3-7 Average daily water content and total daily evapotranspiration were correlated, indicating vegetation is likely playing an intimate role in regenerating green roof retention capacity between storms.

Furthermore, no significant relationship was observed between vegetation

characteristics and retention in either season. However, this could simply be attributed to

the green roof exhibiting poor plant growth during the entire two-year study. According to

the manufacturer, minimum installation soil coverage of planted modules is 95%

(LiveRoof, 2009), yet average percent cover was 53.9% ± 12.3 over the course of the study

and average LAI was 1.35 m^{-2} $\pm$ 0.37 (no significant difference in vegetation development between seasons was observed). Previous studies have shown that on average, the presence of vegetation enhances retention efficiency. Volder and Dvorak (2014) for example found that on average, the presence of *Talinum calycinum* enhanced retention efficiency by an additional 7.5% compared to unvegetated modules, and that substrate water content only affected retention capacity when modules were unvegetated (Volder and Dvorak, 2014).

We hypothesized that poor vegetation development is likely due to the green roof's sloped design, which would reduce substrate moisture content over prolonged periods of time without rainfall. In fact, low soil moisture was observed throughout the study– average daily volumetric water content was 2.88 mm (0.045 m^3/m^3) during the warm season, which is low when compared to other findings. Starry et al. (2014) for example studied photosynthesis and water use by *Sedum album* and *Sedum kamtschaticum* and suggested threshold water contents. More specifically, since the lowest average substrate water contents observed for *S. album* and *S. kamtschaticum* were 0.065 m^3/m^3 and 0.04 m^3/m^3, respectively (at this point leaf turgor was visibly reduced for both species, but they quickly recovered upon rewatering), they recommended thresholds at 0.18 and 0.13 m^3/m^3 for *S. album* and *S. kamtschaticum* respectively, which are well above the average water content observed in our study. This has strong implications for green roof design as *Sedum* are widely implemented in green roof installations in the American Northeast and Midwest, and are considered successful in terms of plant coverage and survival, especially due to their drought tolerance (Starry et al., 2014).

Overall, results indicate the need for more hydrological studies of green roofs on residential buildings. With the system's current design, it may 1) not be well-suited for a

slope roof, 2) require irrigation to sustain vegetation, or 3) be best suited for a climate with frequent, small to moderate rainfall amounts that would sustain vegetation, but allow for rapid substrate regeneration capacity. Furthermore, if we had to improve upon the system's design, a water retention layer, a different substrate composition, or a deeper substrate depth would likely reduce runoff and provide additional water to sustain vegetation and ET over prolonged periods of time without rainfall.

Interestingly, there may be a benefit to sloped roofs when considering event size, event frequency and substrate water content. A study evaluating the feasibility of implementing green roof retrofits on pitched residential roofs found that for small storm events, sloped modules had no runoff, while the control module would have substantial runoff. This correlates to the control's much greater volumetric water content over the course of the study, causing runoff to ensue more easily during storm events. In other words, the sloped modules were less saturated and drained more fully between storm events, indicated by their lower water content (Borchers et al., 2015). These findings would further justify implementing sloped green roofs in regions characterized by frequent, low to moderate rainfall that would sustain vegetation, but allow for rapid substrate regeneration capacity.

Ultimately, future hydrological studies should focus on green roof design (slope, depth, and installation type) and management to help designers better select practices with the site in mind. This is especially important considering, many municipalities have started to incentivize or even mandate green roofs on buildings without having a full understanding of how they perform over time. Furthermore, proper system selection and management with the site in mind is imperative considering the future risks of climate change where

rainfall characteristics (size, intensity and frequency) in many regions is expected to change.

3.4.3   Constructed Wetland Hydrological Performance

The constructed wetland retained 37.6% of stormwater over the study period. In terms of comparable studies, CW hydrological studies are lacking, and to our knowledge there are no hydrological studies of CWs integrated with residential buildings– existing studies tend to evaluate large-scale stormwater wetlands. For example, Lenhart and Hunt (2011) found that a 0.14 ha CW in River Bend, North Carolina, reduced peak flows and runoff volumes by 80% and 54%, respectively, and suggested that stormwater wetlands should be considered a viable GI option, especially where there are sandy soils (Lenhart and Hunt, 2011). In another study where the long-term hydraulic and treatment performance of a 19-year old CW treating stormwater from a 320-ha urban catchment was evaluated, there were significant peak flow reductions achieved by the wetland for all storm events (65–89%), and the flow volume reductions for the thirteen events ranged between 12-67%– average flow volume reduction was 22% (Al-Rubaei et al., 2016).

Next, the effect of season on hydrological performance was evaluated. Then the effect of antecedent substrate water content and storm characteristics on seasonal retention was observed. Interestingly, the wetland performed better during the colder months. During the warm season, average percent retention across storm events was 26.3% ± 19.4 (range: 0-79.1%) and during the cold season average percent retention was 37.4% ± 25.9 (range: 0-198.85%). However, it is likely that this was due to outliers skewering the data (retention percentages > 100%), especially since event size was estimated from rainfall into the three chambers and green roof runoff.

Table 3-3 Correlation analysis of the effect of antecedent substrate water content and storm characteristics on constructed wetland seasonal retention. Note, (+) indicates a positive correlation and (-) indicates a negative correlation. Furthermore, [a] signifies correlation is significant at the 0.05 level, while NS indicates no significance.

	Antecedent water content (mm)	Event Size (mm)	Event Intensity (mm/min)	Event Frequency (days)
Warm Season	NS	$R^2 = 0.8305$ (+) [a]	NS	NS
Cold Season	NS	$R^2 = 0.4204$ (+) [a]	NS	NS

Event size was the only variable that significantly affected hydrological performance (warm season $R^2 = 0.8305$, cold season $R^2 = 0.4204$) (Table 3-3), and greater retention was observed as storms increased in size. This was intriguing as other studies have found the hydrological performance of CWs to be related to rainfall intensity and frequency. More specifically, Al-Rubaei et al. (2016) noted that the hydraulic performance of a 19-year old CW in reducing runoff volumes varied from positive to negative reduction for some events, especially with storm events preceded by short dry periods and/or high rainfall intensities (Al-Rubaei et al., 2016). Another interesting finding was larger retention percentages of total rainfall were observed with increasing event size during the warm season ($R^2 = 0.3005$) (Figure 3-8). This was intriguing as the opposite was observed with the green roof– as the events increased in size, it started to reach storage capacity and retention percentages decreased. Altogether, the fact that retention was not correlated to antecedent substrate water content or storm intensity and frequency indicates the wetland was designed with a high storage capacity and/or ET rates are high enough to regenerate retention capacity quickly.

Constructed Wetland
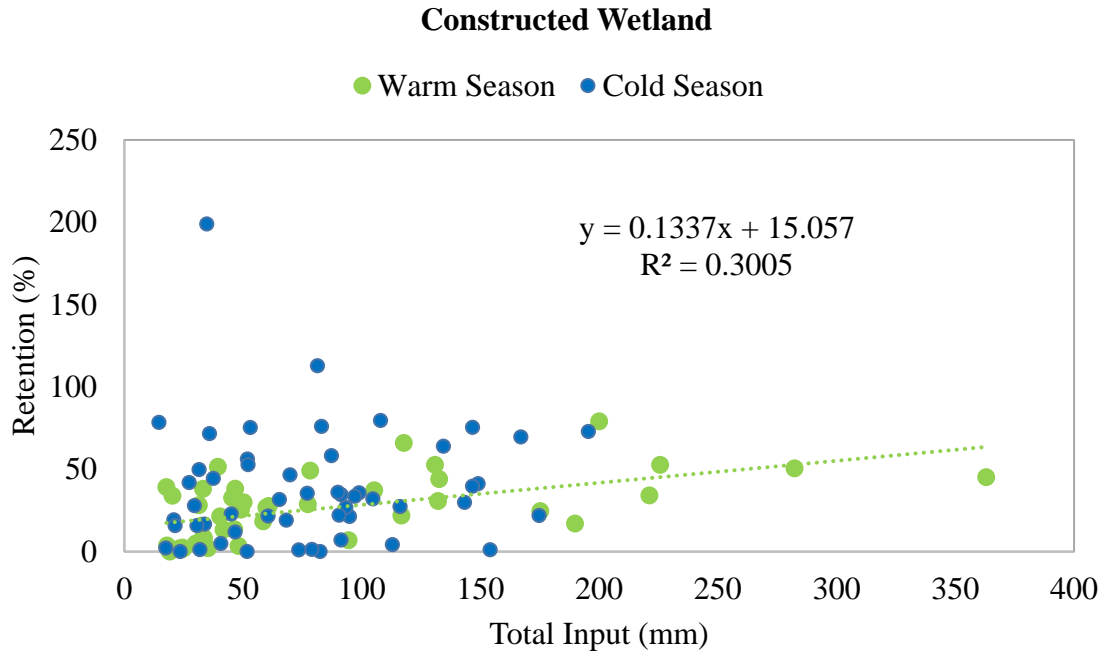
Figure 3-8 Larger storm events produced more wetland retention as a percent of precipitation in the warm season (p<0.05), indicating, the wetland has a high retention capacity.

3.4.4 Bioretention Hydrological Performance

Percent retention over the study period for the bioretention was 22.4%. In terms of studies that have evaluated the hydrological performance of bioretention, Ahiablame et al. (2012) summarized several findings and reported that bioretention reduce runoff by 48-97%. Furthermore, Liu et al. (2014) reviewed several studies and found bioretention reduced peak flow by 44-99%, and reduced runoff volumes by 50-100% .

Seasonal differences in retention percentages were not significant, however it was more variable during the cold season. During the warm season average percent retention across the storm events was 18.3% ± 16.7 (range: 3.3-55.9%), while it was 22.4% ± 22.5 (range: 0-116.1%) during the cold season (note, retention percentages > 100% are likely

attributed to variability in event size estimations). This contrasted with findings that observed seasonal variation in bioretention hydrological performance. For example, Hunt et al. (2006) studied three bioretention systems in North Carolina. Results indicated that efficiencies of runoff volume reduction changed significantly seasonally, partially due to lower ET rates in the winter compared to other seasons (Hunt et al., 2006). Furthermore, Paus et al. (2015) examined the seasonal hydrological effectiveness of bioretention cells in cold climates and found that saturated hydraulic conductivity values during winter/early spring were only 25 to 43% of those during summer.

Table 3-4 Correlation analysis of the effect of antecedent substrate water content and storm characteristics on bioretention seasonal retention. Note, (+) indicates a positive correlation and (-) indicates a negative correlation. Furthermore, [a] signifies correlation is significant at the 0.05 level, while NS indicates no significance.

	Antecedent water content (mm)	Event Size (mm)	Event Intensity (mm/min)	Event Frequency (days)
Warm Season	$R^2 = 0.2194$ (-) [a]	$R^2 = 0.7451$ (+) [a]	NS	NS
Cold Season	NS	$R^2 = 0.2632$ (+) [a]	NS	NS

Event size (warm season $R^2 = 0.7451$, cold season $R^2 = 0.2632$) and antecedent water content (warm season $R^2 = 0.2194$) were the only variables significantly correlated to hydrological performance (Table 3-4). Event size was expected to be a significant factor based on previous findings. For example, Davis (2008) found that during small events bioretention areas can readily capture the entire inflow volume within the media (Davis, 2008). Moreover, Hatt et al. (2009) showed bioretention to be effective in on average,

retaining 33% of the inflow volume (range: 15–83%). Of the five predictor variables, retention of water was found to be most influenced by peak inflow rate and inflow volumes (Hatt et al., 2009). Yang et al. (2013) studied a biphasic rain garden that consisted of a saturated zone to enhance nitrogen removal followed by an unsaturated zone. The peak flow and volume reduction between influent and the unsaturated zone effluent were 67% and 28%, respectively. When studying the effect of rainfall size on the average cumulative volumes and the flow rates of influent and effluent (unsaturated zone effluent), no measurable effluent was observed during light rainfall events (<6 mm) due to the storage capacity of the saturated zone, while during the representative medium (6–12 mm) and heavy (>12 mm) rainfall events, runoff volume reduction percentages decreased (59% for medium rainfall events and 54% for the heavy rainfall events) (Yang et al., 2013).

Antecedent water content during the warm season was also expected to be a significant factor of retention as several studies have also observed its correlation to retention. For example, in a study evaluating the pollutant removal and hydrologic performance of five, 10-year old street-side bioretention systems, the change in measured moisture content during tests was found to be highly variable. In accordance with expectation, the drier the pre-basin, the higher the volume of water was stored within the basin during testing, and consequently lower volumes of water were discharged (Lucke and Nichols, 2015).

Overall, the correlation observed between antecedent water content and retention during the warm season indicates that the biorientation system was likely reaching storage capacity during large storm events. This would explain why although the system stored a vast amount of stormwater (3,573.0 mm), it only stored 18% (or 1.22 times) more-water

than the wetland despite receiving almost twice the amount of stormwater (15,964.3 mm versus 7,786.3 mm, respectively) (Table 3-1). To increase the retention capacity of bioretention, it can be designed with an internal water storage (IWS) zone. Winston et al. found that inclusion of an IWS zone allowed three bioretention cells to reduce runoff by 59%, 42%, and 36% over the monitoring period, despite tight underlying soils. The two cells with lesser runoff reductions were noted to have lower drawdown rates and smaller IWS zone thicknesses (Winston et al., 2016).

Furthermore, at least during the first year, low vegetation cover could have played a role in hydrological performance. Studies have shown that vegetation is important for maintaining bioretention hydraulic capacity, because root growth and senescence counter compaction and clogging (Hatt et al., 2009). Vegetation development would also likely improve ET– evapotranspiration has been cited to play an important role in bioretention retention (Ahiablame et al., 2012). These findings indicate that as vegetation becomes more established over the years, hydrological performance may likely improve.

3.5   Summary and Conclusions

Overall, findings suggest there is a benefit to designing GI in-series. Collectively, the green roof, constructed wetland and bioretention collectively reduced site runoff by 26.7% over the two-year study period. When evaluating each system independently, green roof, CW and bioretention retention percentages were 19.3%, 37.6%, and 22.4%, respectively. The wetland was the most effective system in terms of retention capacity (337.3 mm/m^2) followed by the bioretention (109.6 mm/m^2) and green roof (14.8 mm/m^2). The CW was also the only system whose performance was not impaired by antecedent

water content and storm characteristics (vegetation development was only evaluated for the green roof), further indicating it had the greatest storage capacity.

Though the green roof stored a small amount of stormwater, integrating the wetland and bioretention in the design of the home allowed for the retention of stormwater that would otherwise have contributed to runoff. Furthermore, it is likely that even though green roof retention was low, it may still be providing an added benefit of extending the duration of runoff over a period of time beyond the actual storm event, thus slowing the rate of stormwater into the constructed wetland and bioretention. To improve hydrological performance in this region, several design suggestions were presented such as incorporating a water retention layer or modifying substrate depth or composition for the green roof, furthermore, incorporating an internal water storage for the bioretention.

Chapter 4 Green Roof Thermal Performance

4.1   Objective

The building sector accounts for 40% of total global energy consumption and 33% of GHG emissions (Berardi et al., 2014; Besir and Cuce, 2018), with thermal comfort–space conditioning that includes space heating, cooling and ventilation– accounting for 36% of primary energy use in U.S. buildings alone (Ürge-Vorsatz et al., 2012). In recent years many policy makers and governments have taken decisive measures to systematically reduce carbon emissions and energy use in buildings (Besir and Cuce, 2018). These include advanced eco-technologies, energy efficient systems and renewable energy sources. In this context, green roofs are often identified as a valuable strategy for making buildings more sustainable (Berardi et al., 2014). Cool roof strategies (high albedo and emissivity) are also progressively drawing the attention of the scientific community and the market due to their effective role in reducing building energy requirements and also mitigating UHI effects (Ganguly et al., 2015).

Green roofs essentially prevent the penetration of solar heat to covered building components, and have been found to cool down roof surfaces and reduce building heat flux relative to conventional roofs. Furthermore, green roofs not only impact the energy performance of buildings, but the surrounding environment, and have been found to mitigate the UHI effect (Berardi et al., 2014; Besir and Cuce, 2018). It is believed that green roofs primarily keep roofs cool under the sun by providing additional thermal insulation as well as evapotranspirative cooling (Zinzi and Agnoli, 2012). Furthermore, foliage behaves as a shading device which reflects incident solar radiation (La Roche and Berardi, 2014; Raji et al., 2015).

However, there are several knowledge gaps in green roof thermal performance research. For example, despite widespread application, green roof systems are not standardized (Tan et al., 2017) and there is much uncertainty regarding their thermal performance in real conditions, especially in regional climates characterized by winters, or in comparison to alternatives technologies like cool roofs (Berardi et al., 2014; Bevilacqua et al., 2017; Saadatian et al., 2013). Furthermore, despite the development of computer models that can assist towards analyzing green roof behavior (several authors have used simulation codes for temperatures and heat fluxes analyses to assess the reduction of energy demand for space cooling and heating), there is still a lot of uncertainty regarding the choice of the parameters and values to use in thermal models of simulation codes which may lead to inaccurate estimations of building thermal loads. Other researchers have noted that there is still a relative gap in measured data representing long-term period thermal performance, and in real conditions the development of vegetation varies throughout the year with a strong influence on the thermal performance (Bevilacqua et al., 2017; Theodosiou et al., 2014).

The minority of studies that have been performed in real conditions often lack an understanding of the mechanisms that influence thermal performance. A literature review found several studies attributed improved building thermal performance to green roofs shading, reflecting incident solar radiation, reducing wind speeds, and providing thermal insulation, and evaporative cooling; however, studies to date have not evaluated if these processes directly relate to thermal performance (Besir and Cuce, 2018; Moody and Sailor, 2013; Wang et al., 2014). Furthermore, researchers have evaluated these processes independently, and there is little known on how they interact in a system, or how they vary

with design, climate/season, or site factors. Some researchers for example state the dominant cause of the cooling benefits provided by green roofs is ET, while a large portion of studies have assessed green roof thermal performance based on its heat transfer or resistance property (U-value/R-Value). However, more recent studies report that these processes may be inversely interrelated. More specifically, some studies indicate soil moisture induces heat transfer (impairs thermal resistance) however it is well-known that substrate water content is integral to evapotranspirative cooling (Saadatian et al., 2013).

Thus the purpose of this objective was to 1) characterize the seasonal thermal performance of *WaterShed's* green roof (to the building and surrounding environment) relative to its cool roof, 2) determine the effect of green roof properties (ET, albedo and thermal conductance) on thermal performance, and 3) evaluate the effect of substrate water content, vegetation development (leaf area index and percent cover), and microclimate (net radiation and air temperature, etc.) on ET, albedo and thermal conductance values.

This research is unique because studies simultaneously researching the thermal performance of a green and cool roofs across seasons is lacking. Furthermore, this study evaluates the processes that affect green roof thermal performance which have not been well characterized, especially on a residential home. Findings are relevant to the scientific community in helping us better understand how green roofs operate, which has implications to how we design and maintain them locally to reduce building energy demand. This is increasingly important as global nonrenewable energy sources diminish and has implications to reducing the contribution of buildings to climate change.

4.2   Introduction

Green roofs have been introduced as one of the most efficient mediums of energy savings in the building sector, with their energy-related performance being one of the most common benefit for which they are promoted and adopted (Berardi et al., 2014; Besir and Cuce, 2018; Saadatian et al., 2013). Green roofs benefit buildings through direct and indirect means. Direct effects are those related to the building components, such as reducing the energy balance and energy requirements for building cooling demand through the reduction of roof surface temperatures. In other words, direct effects bring immediate benefits to the building where they are applied. Indirect effects impact building surroundings and become realistic only with widespread deployment within a selected urban area such as the reduction of outdoor temperatures or the UHI effect (an elevation of temperature in urban areas relative to the surrounding rural or natural areas due to the high concentration of heat absorbing dark surfaces such rooftops and pavements). Interestingly, this reduction of the UHI effect has a positive feedback effect on building energy efficiency (Besir and Cuce, 2018; Liu and Baskaran, 2003; Saadatian et al., 2013; Xu et al., 2012).

Although these thermal benefits have been widely attributed to green roofs, there is still a relative gap in measured data representing long-term period thermal performance (Theodosiou et al., 2014). Many of the thermal performance studies found in a literature review are based on computer models and simulations. Thus, we limited the scope of studies described in this chapter to ones with **experimental data**. The following sections of the introduction provide an overview of 1) the thermal benefits of green roofs (with season and relative to cool roofs) and 2) the processes and factors that impact thermal performance.

4.2.1   Green Roofs and Building Energy Demand

Green Roof Building Performance Studies in Warm Seasons/Climates

It is well established that green roofs can reduce building energy consumption and improve the comfort levels inside buildings during the spring and summer seasons by reducing and delaying peak temperatures as well as reducing temperature fluctuations (Liu and Baskaran, 2003; Sonne, 2006). The following are a few of the many experimental studies that have found green roofs to reduce roof surfaces temperatures and building heat flux relative to conventional roofs in warm seasons/climates:

Lui and Baskaran (2003) studied a generic extensive green roof and a modified light gray bituminous roof in Ottawa, Canada on a typical summer day. They found that the reference roof absorbed more solar radiation and reached close to 70 °C during the hottest time of the day, while the membrane on the green roof remained around 25 °C. Furthermore, results showed that across the 660 days of the study, the reference roof exceeded 30 °C on 342 days (52% of time), 40 °C on 291 days (44% of the days), 50 °C on 219 days (33%), 60 °C on 89 days (13%), and 70 °C on 2 days (0.3% of time), while the green roof's surface temperature never reached 40 ℃ during the study. Finally, the reference roof exposed membrane experienced high daily temperature fluctuation, with a median of about 45 °C. However, the green roof reduced the temperature fluctuation in the roof membrane throughout the year, keeping a median fluctuation of about 6 °C (Liu and Baskaran, 2003).

A study performed at the University of Central Florida found that during the summer of 2005, the average maximum temperature of a conventional light-colored roof

was 54 ℃ contrasted to a 33 ℃ average maximum for the green roof (6 in. to 8 in. and planted with native vegetation), with peak surface temperatures for the conventional roof occurring around 1 p.m., while peak green roof surface temperatures occurred around 10 p.m. The weighted average heat flux rate over the period for the green roof was 0.39 Btu/h ·ft^2 (1.23 W/m^2) or 18.3% less than the conventional roof's average heat flux rate of 0.48 Btu/h · ft^2 (1.51 W/m^2) (Sonne, 2006).

According to Morau et al. (2012), an extensive green roof installed in Reunion Island (characterized by tropical humid climate) showed a significant decrease in temperature of the roof surface. While the maximum temperature of the reference bituminous roof surface reached about 73.5 ±1.4 °C, the roof covered with the three succulent plant species (*Plectranthus neochilus*, *Kalanchoe thrysiflora* and *Sedum reflexum*) only reached an average maximum temperature of 34.8 ±0.6 °C (Morau et al., 2012).

Researchers found that on a typical sunny summer day in Estonia the surface of the bituminous roof heated up in the morning and cooled down in the evening (amplitude 35.1 ℃). Substrate layer daily temperature fluctuation of the lightweight aggregates-based green roof was significantly decreased (amplitude 13.8 ℃)– temperature fluctuations have a negative impact on the roof membrane and may cause damage if they occur too often. Note, amplitude represents the difference between the maximum and minimum values (Teemusk and Mander, 2009).

In another study Teemusk and Mander (2010) analyzed the temperature regime of an existing green roof and a sod roof, compared with a modified bituminous membrane roof and a steel sheet roof. They found that the difference between the temperature

amplitude under the planted roofs and the surfaces of the conventional roofs was on average 20 ℃ in the summer (Teemusk and Mander, 2010).

Field measurements during the summer of rooms covered by a lawn garden and roof slab in Japan showed the surface temperature of the roof slab decreased from 60 to 30 ℃ during the daytime, with an estimated heat flux reduction of 50% into the room (Onmura et al., 2001).

A study in Toronto on a typical summer day found that a bituminous reference roof absorbed solar energy and its temperature rose to 66 °C at around 2 p.m. When compared to two extensive green roofs (Green Roof G has deeper and lighter colored growing medium (100 mm) than Green Roof S (75 mm)), the green roofs significantly lowered and delayed peak roof membrane temperature. The roof membrane temperature peaked at 36 °C at 19:30 p.m. for Green Roof G and 38 °C at 6:30 p.m. for Green Roof S (Liu and Minor, 2005).

Data collected on nine green roof plots at the National University of Singapore from July to September 2015 found average exposed concrete surface temperature to reach its peak of 47.2 °C at 16:00 h, whereas average surface temperature of concrete under the planter boxes were between 29.5°C to 31.2 °C. Surface temperature fluctuations were also reduced significantly due to addition of a green roof. The average surface temperature range for exposed concrete roof was 21.2 °C while the combined temperature range under the planter boxes was only 4.1 °C (Tan et al., 2017).

A research conducted in south Italy revealed that an extensive green roof was able to reduce the temperature at the interface with the structural roof, on average, by 12 °C with respect to a black bituminous roof in summer (Bevilacqua et al., 2016).

Niachou et al. (2001) reported there were no significant temperature variations between the external surface of insulated buildings with or without implementation of green roofs in Greece. However, the temperature of green roof upon the non-insulated buildings ranged from 28 to 40 °C, while the corresponding roof temperature of non-insulated buildings without green roof ranged from 42 to 48 °C. They concluded that the exterior surface temperature reductions due to the existence of a green roof on non-insulated buildings were of the order of 10 °C, and that the impact of green roofs of non-insulated building is favorable (Niachou et al., 2001).

Finally, Getter et al. (2011) reported findings of research on a Midwestern U.S. extensive green roof, characterized by hot summers and cold winters. They found that summer cumulative monthly heat flux values showed a net heat gain into the building for the gravel roof while the green roof showed a cooling effect on the building. Peak temperature differences between the gravel and green roofs were greater in the summer than other seasons (sometimes by as much as 20 °C) (Getter et al., 2011) .

Green Roof Building Performance Studies in Cold Seasons/Climates

Many studies show green roofs have different efficiencies for four seasons–generally, its maximum efficiency is reported during summers, while performance of green roofs in winter time is a matter of debate. Some scientists claim it as a medium to save energy during the winter and some view it as a cause of more energy consumption (Berardi

et al., 2014; Saadatian et al., 2013). However, we found many studies that claim green roofs are a detriment in the winter are flawed since they do not compare heat loss from a green roof to a conventional roof in cold periods.

From a literature review the following studies were compiled– we only report experimental studies that compare green and conventional roofs during cold seasons/climates. Overall, studies indicate that green roofs may actually be beneficial in cold seasons/climates when compared to conventional roofs because they reduce heat loss through the building membrane. Note, we did not report thermal performance data of green roofs with snow cover as several studies have shown that due to the insulating properties of snow, temperature regimes between reference roofs and greens roofs are similar (Bass and Baskaran, 2001; Teemusk and Mander, 2009; Zhao et al., 2015).

The first study reviewed highlights experiments conducted over two weeks (one with and without snow) at an outdoor test facility in Pennsylvania, U.S. during the winter. Researchers showed that the buildings with green roof assemblies experienced lower heat losses through the roof compared to reference roof losses (independent of the snow layer). Heat losses from inside of the building to the outdoor environment during the week with no snow were -7.1 $W/m^2 \pm 9.7$ and -9.2 W/m^2 for the green and reference roof, respectively. Since the heat loss from the roof assemblies in winter directly affects heating loads and building energy consumption, researchers concluded that the green roof buildings performed better than the reference buildings due to reduced heat losses of 23%. Interestingly, this energy saving was reduced to 5% when snow accumulated on the roofs, as the snow layer provides extra insulation to the roof. Note, the materials of the reference

roofs in order from the inside to the outside were 6.35 mm OSB sheets, 89 mm fiber glass batting insulation, 19.05 mm plywood, and water proofing layer (Zhao et al., 2015).

Similarly, research on a Midwestern U.S. extensive green roof, characterized by hot summers and cold winters found heat flux strongly influenced by season. More specifically, although more effective in the summer, they found the green roof to be beneficial in the winter relative to a traditional ballasted gravel roof. Average heat flux leaving the building in the winter was 2623 W/m^2 and 3017 W/m^2 for the green and gravel roof, respectively. In the summer they reported 220 W/m^2 heat leaving the building for the green roof and -327 W/m^2 heat entering the building for the gravel roof– where, negative and positive readings measure heat entering and leaving the building, respectively. This translated to the green roof reducing heat flux through the building envelope by an average of 13% in winter and 167% during the summer compared to the gravel roof (Getter et al., 2011).

Lanham (2007) observed a marked decrease in power use when comparing green roof test panels with a conventional built-up roof test panel in cold climate conditions using a hot box apparatus. An analysis of variance comparing 5-hour sample means confirmed that the set of differences among the power use means for the 100 mm and 150 mm green roof test panels were not statistically different at the 99% confidence level, but that the performance of the conventional versus 150 mm green roof test panel and conventional versus the 100 mm green roof test panel were statistically different from each other at the 99% level of confidence. Therefore, it was concluded that the thermal benefit of green roofs in cold climates is at least statistically significant with a confidence level of 95% (Lanham, 2007).

A next study conducted in south Italy revealed that an extensive green roof maintained, on average, a value that is 4 °C higher in respect to a black bituminous roof in winter (Bevilacqua et al., 2016). While Susca et al. compared the thermal performance of a green roof, cool roof and black roof in New York City, and observed that on the soil bottom, below zero temperatures were reached approximately 50% less frequently than on the black roof (Susca et al., 2011).

Teemusk and Mander (2010) analyzed the temperature regime in Estonia of an existing green roof and a sod roof, compared with a modified bituminous membrane roof and a steel sheet roof. They found that the temperatures in the planted roof's substrate layers were much higher than on the surfaces of the conventional roofs, and the thicker sod roof was warmer (average −0.1 °C) than the thinner green roof (average −1.1 °C), which may freeze more easily. Moreover, the average daily temperature amplitude in the planted roof's substrate layers was only 1 °C, while at the same time the temperature fluctuated on average 7–8 °C on the surfaces of the conventional roofs– amplitudes represented the difference between the maximum and minimum values (Teemusk and Mander, 2010).

Finally, the most comprehensive study to date evaluated the thermal performance of a generic green roof (150 mm lightweight soil planted with wild flower meadow) compared to a modified bituminous membrane reference roof in Ottawa for almost a year. Researchers found that overall green roofs are beneficial when one accounts for cumulative energy demand across seasons. To get a better understanding as to why this is, one must look at the thermal pattern of each roof on a typical winter day. They found that on a typical winter day without snow coverage, the membrane temperature on the reference roof fluctuated from -15 to 10 °C depending on the air temperature, while at the same time the

membrane temperature on the green roof remained relatively stable between 1 and 5 °C. The reference roof lost heat at a rate of 10 W/m^2 during early morning and late evening. However, the rate of heat loss decreased during the afternoon as the roof membrane absorbed the solar radiation— during the warmest part of the day, heat even entered the building and resulted in positive heat flow for about 2h around noon. On the other hand, the green roof lost heat at a steady rate of about 7 W/m^2 throughout the day (Bass and Baskaran, 2001).
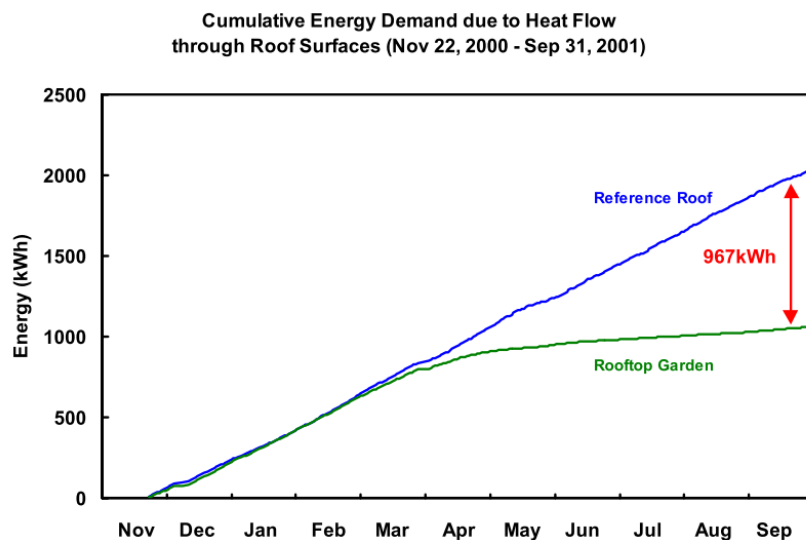
Figure 4-1 Cumulative energy requirement due to heat flow through the roof surfaces (Bass and Baskaran, 2001).

When researchers performed an overall comparison of the cumulative energy demand due to the two roof sections, results showed that the energy demand due to both roof sections was essentially the *same* during the fall and winter seasons (November 2000 to March 2001). Interestingly, the energy demand started to diverge in April 2001, and the difference grew larger through the summer to the point where the difference in space conditioning energy demand was 967 kWh over the 11-month observation period (Figure

). In terms of energy efficiency, the green roof system marginally outperformed (~10%) the reference roof during the colder months but it significantly outperformed (>75%) the reference roof in the warmer months. Researchers concluded that more energy savings was expected if the plant canopy was better developed and provided additional shading and evaporative cooling. They also noted that the actual dollar savings depend on the type and efficiency of the heating and cooling equipment, which is building specific (Bass and Baskaran, 2001).

4.2.2 Green Roofs and Urban Heat Island

The urban heat island phenomenon is one of the main reasons behind the increase in urban air temperature. This primarily occurs due to the removal of natural vegetation and its replacement with buildings and paved surfaces. Building roofs are huge absorbers of heat being directly exposed to solar radiation, thereby increasing the roof temperature up to a great extent and the temperature of the surrounding environment (Ganguly et al., 2015).

Urban Heat Island Studies in Warm Seasons/Climates

Several studies carried out at different latitudes confirm the existence of an UHI. Romeo and Zinzi (2013) report that daytime and daily UHIs around the world typically range between 2 and 6 °C, while UHI intensities up to 12 °C have also been measured (Romeo and Zinzi, 2013). Likewise, a recent review paper reported significant differences in ambient temperature values (from 2 to 4 °C) between urban and rural regions (Besir and Cuce, 2018).

In terms of a region similar in climate to the one in this study, Susca et al. (2011) monitored the UHI in four areas of New York City, and observed an average 2 °C temperature difference between the most and the least vegetated areas, which can be explained by the substitution of greenery areas with man-made building materials (Susca et al., 2011). Similarly, the average difference in New Jersey urban–nonurban minimum temperatures was 3.0 °C for the Newark area and 1.5 °C for Camden (Rosenzweig et al., 2005). Because roof surfaces of building accounts for the 20–25% of total urban surfaces, it is believed that they can be successfully used to reduce air and surface temperatures of urban areas (Zinzi and Agnoli, 2012).

In terms of green roofs reducing ambient air temperatures, results are promising. Field measurements conducted in Singapore to investigate the thermal impacts of a rooftop garden showed a maximum reduction of 4.2 °C at 300 mm height, around 1800 h between ambient air temperatures measured with and without plants (Nyuk Hien Wong et al., 2003). Another study investigated the UHI mitigation of an intensive green roof in Manchester, UK relative to an adjacent concrete roof. Monthly median air temperature was found to be 1.06 °C lower at 300 mm over the green roof. Furthermore, researchers showed that the highest level of contribution of green roofs to cooling was observed during the night, and was 1.58 °C (Speak et al., 2013). Qin et al. showed that a green roof test bed in Singapore can significantly reduce the roof surface temperature by an average of 7.3 ℃, and lower the ambient air temperature by an average of 0.5 ℃ when compared with a bare roof during daytime hours (from 10:00 am to 4:00 pm) (Qin et al., 2012).

With these temperature decreases documented widespread application of green roofs could reduce the UHI effect, which would further lower energy consumption in the

urban area (Liu and Baskaran, 2003). For example, Santamouris (2014) recently reviewed several mitigation technologies to fight UHIs and concluded that the large-scale application of green roofs through existing simulation studies could reduce ambient temperatures between 0.3 to 3 K (or °C) (Santamouris, 2014). Furthermore, Rosenzweig et al. reported that a 50% extensive green roof scenario could reduce New York City's average surface temperature by 0.1 – 1.4°F (<0.1 – 0.8°C) (Rosenzweig et al., 2006).

Urban Heat Island Studies in Cold Seasons/Climates

The urban heat island phenomenon is rarely studied in the winter. It can even be argued that UHIs are currently not as big of a problem for many international cities because they reduce winter heating costs (Speak et al., 2013). However, research indicates warming can still be observed in colder periods/regions. For example, researchers found through fixed point monitoring stations over the city of Manchester that although there is a higher probability of UHI occurrence in the city during the summer, the winter UHI frequency was highest at 1.0 °C during the day and night, and maximum UHI temperature was found to be as high as 10 °C in the winter (summer high of 8 °C was observed) (Cheung, 2011). Furthermore, in New York City researchers observed during winter that the temperature in their more urban site of Columbia was on average 1.5 °C higher than in Fieldston during the daytime. They noted that at their Fieldston site the air temperatures are just slightly affected by the biological activity of trees (Susca et al., 2011).

In terms of green roofs and the UHI effect during the winter, a long-term experimental analysis in the Mediterranean (characterized by cool, wet winters) comparing the thermal performance of a green roof with a conventional bare flat roof was performed. Researchers found that during the winter the external soil surface temperature was cooler

than the ambient air during nighttime by 3–4 °C, whereas in the case of the bare roof it was higher than the ambient air temperature all the day (Theodosiou et al., 2014)**.**

4.2.3   Biophysical Processes and Factors Influencing Thermal Performance

Green roofs essentially absorb less radiant energy than other types of roofs and prevent the penetration of solar heat to covered building components (Berardi et al., 2014; Hashemi et al., 2015). The main drivers thought to occur in green roofs are 1) vegetation reflects incident solar radiation and behaves as a shading device, 2) soil acts as an inertial mass with a high thermal capacity and low thermal transmittance, and 3) soil and foliage induce evapotranspirative cooling (La Roche and Berardi, 2014; Raji et al., 2015).

Though these processes have been widely attributed to thermal performance, most studies have evaluated them independently, and have not directly studied their impact on temperature and heat fluxes to the building and surrounding environment. Furthermore, generalizable results are difficult to make because unlike conventional and cool roofs which are static elements, the ability of green roofs to provide thermal benefits depends on several parameters related to the system's design, as well as local season/climate, and site factors. From a literature review, the following factors were compiled:

Green roof characteristics: systems are not standardized, thus there is a wide variation in green roofs characteristics as determined by the choice of materials used, number of layers, as well as the absolute and relative thickness of different components (Tan et al., 2017) such as:

- Studies have concluded that the quantity and complexity of biomass play a key role in molding the passive cooling functions of green roofs (Jim, 2012). Plant selection

(type and composition) will define the properties of the green roof vegetation layer, like its coverage ratio, leaf area index, foliage height, and water use which is related to stomatal resistance (a pore found in plant functions as a gas exchange) and other biological processes (Raji et al., 2015; Saadatian et al., 2013). These properties affect thermal performance in many ways. For example, it is believed that plant coverage affects thermal insulation properties of green roof through amount of growing substrate exposed to solar radiation (Tan et al., 2017).

- Substrate depth and composition (defines properties like growing medium density and porosity) (Saadatian et al., 2013; Tan et al., 2017) impact substrate water holding content/capacity and vegetation development.

- Other layers such as the presence of a water retention layer or drainage elements (Tan et al., 2017) can also affect substrate water content and green roof vegetation.

Season/climate conditions: green roof thermal performance is affected by factors such as solar radiation, ambient temperature, humidity, wind speed and precipitation, which vary with season, and climate in which the system is being implemented (Bevilacqua et al., 2016; Santamouris, 2014). For example, solar radiation intensity affects vegetation health and ET, thus determining the heat storage and surface temperature of the roof and ultimately the amount of the heat transmitted to the building (Santamouris, 2014).

Other site factors: roof insulation value and type of irrigations can also determine the impact of green roofs on temperature and heat flux (Hashemi et al., 2015).

It is imperative to highlight that a key effect of green roofs design, climate/season and other site factors is their impact on substrate moisture properties. It has been suggested

that the hydrological characteristics of green roofs is a critical property of them that influences overall rooftop surface energy balance and the transmission of heat through the roof (Tan et al., 2017). For example, a wet roof is thought to provide additional ET, which prevents heat flux into the building and acts as a passive cooler by removing heat from the building. However, additional air pockets are also thought to increase the insulating properties of the growing medium (Saadatian et al., 2013). The effect of substrate water content on thermal performance will be extensively discussed in the remainder of the introduction.

Note: Subsequent sections of the introduction will describe the reflective, evapotranspirative and thermal conductance properties of green roofs, as well as the relevant design, climate/season and other site factors that affect them. We focused on these properties due to the availability of sensors on our system of study.

4.2.4 Evapotranspiration Cooling

Green roofs are able provide thermal cooling through evapotranspiration, which is the combined process of soil evaporation and plant transpiration (Tan et al., 2017). The physical process in which water transfers from soil into the atmosphere is called evaporation. Transpiration is a *physiological* process in plants through which moisture retained in the root zone is absorbed by the plants, escapes through the stomata on leaves or the pores of the skin, where it is vaporized (Poë et al., 2015; Raji et al., 2015). These processes are significant factors to cooling because when solar radiation is absorbed by a green roof, energy/latent heat is absorbed and dissipated to turn water into vapor. The latent energy associated with transpiration is typically a large part of the energy balance, and a major pathway for removing heat created by solar and longwave absorption. The effect

entails active cooling of the air immediately above the roof surface while reducing the overall heat transmission to the building (He and Jim, 2010; Ouldboukhitine et al., 2014; Poë et al., 2015; Tjaden, 2014).

Factors Influencing Evapotranspiration

Evapotranspiration can be obtained by direct measurement (Ouldboukhitine et al., 2014). Forces inducing ET losses are a function of the microclimate (i.e. solar radiation, air temperature, wind, relative humidity) and plant physiology. However, the rate at which these forces induce ET depends upon the substrate–water characteristics (i.e. field capacity, permanent wilting point, permeability), any additional moisture storage capacity within the vegetation layer, and the plant's physiological response at the prevailing moisture content (Poë et al., 2015).

In terms of microclimate effects, assuming abundant soil moisture the highest daily ET rates are generally observed in warm summer conditions (Poë et al., 2015). Furthermore, individual climatological factors like increasing the air convection rate near the canopy can effectively enhance ET from the foliage and soil layer, hence improving the latent heat dissipation (Raji et al., 2015). ET is also directly related to temperature– higher temperatures will lead to higher absolute cumulative losses as a greater proportion of the moisture that is held in the small pores of a substrate can be removed under increased levels of heat energy (Poë et al., 2015). There are also factors related to green roof design that specifically affect plant physiology and substrate–water characteristics such as the selection of vegetation and substrate composition and depth.

Regarding vegetation, the type, composition and stage of development influence the inherent physiological traits of a green roof, as different plant types evapotranspire at varying rates. This is related to plant properties such as stomatal resistance (rate that moisture gets through stomata) that controls water loses. More specifically, many extensive green roofs like the system in this study are planted with *Sedum* species that are characterized by crassulacean acid metabolism (CAM) photosynthesis. Under water stress conditions, CAM plants only open their stomata to metabolize at night when temperatures are cooler. ET loss is therefore lower than from C3 or C4 plants that evapotranspire soil–water during warm daylight conditions (He et al., 2017; Poë et al., 2015; Tabares-Velasco and Srebric, 2011; Tan et al., 2017).

Furthermore, the structure and texture of the growing medium governs its substrate–water properties (field capacity, permanent wilting point, retention and release characteristics). Related to these properties is green roof substrate water content, which is often regarded as the most critical factor for ET, with rates expected to decay exponentially with respect to time as available moisture reduces (Poë et al., 2015; Stovin et al., 2013; Tan et al., 2017). Moreover, it is believed that if there is sufficient soil moisture available, then plant type, stage of plant development and weather would affect ET most significantly (Tan et al., 2017).

Substrate depth studies are conflicting. Some findings reveal that ET is higher for intensive green roofs due to the thickness of soil providing more moisture and dense vegetation (Besir and Cuce, 2018; Hilten, 2005). On the other hand, Sun et al. indicated through a simulation model that a thicker medium layer tends to hold less water in the top

as compared to a thinner one. Given that vegetation like *Sedum* only uptakes water from the top layer, ET can be hindered (Sun et al., 2014).

Regarding green roof studies that have simultaneously evaluated these factors in a system, Poe et al. (2015) found cumulative ET was highest from substrates of green roof microcosms with the greatest storage capacity, and significant differences in ET existed between vegetated and non-vegetated configurations. Furthermore, seasonal mean ET was initially affected by climate. Losses were 2.0 mm/day in spring and 3.4 mm/day in summer. However, moisture availability constrained ET, which fell to 1.4 mm/day then 1.0 mm/day (with an antecedent dry weather period of 7 and 14 days) in spring; compared to 1.0 mm/day and 0.5 mm/day in summer (Poë et al., 2015).

Conversely, Jim and Peng studied substrate moisture effect on water balance and thermal regime of a tropical extensive green roof and found that substrate moisture has a limited effect on ET and associated cooling. More specifically, they stated that the dry substrate on sunny days demonstrate an anomalous behavior of high ET which contradicts with previous studies which suggest that ET is proportional to substrate moisture. Instead, evapotranspiration was found to be largely dependent on solar radiation, relative humidity and wind speed. Jim and Peng gave several hypotheses as to why there was a lack of influence of initial substrate moisture on ET, one of them being that the shallow substrate allows solar energy to heat up the entire layer to drive up its temperature and hence ET water depletion (Jim and Peng, 2012).

Evapotranspiration Thermal Performance Studies

Although, evapotranspiration is often cited as the dominant cause of the thermal benefits provided by green roofs (Besir and Cuce, 2018; Cox, 2010; Feng et al., 2010; Hashemi et al., 2015), to our knowledge, no studies have directly backed up this claim by evaluating through correlation analysis if ET has an effect on roof membrane or ambient temperatures. Furthermore, limited studies have experimentally evaluated the factors that affect green roof ET. The following studies support the notion that ET plays a crucial role in thermal performance and have outlined factors that influence ET rates:

In one of the early studies Onmura et al. (2001) investigated the evaporative cooling effect of roof lawn gardens as a way of improving passive cooling. Field measurements during the summer showed that the surface temperature of the roof slab decreased from about 60 to about 30 °C during the daytime, which was estimated to be followed by a 50% reduction in heat flux. The evaporative cooling effect from roof lawn gardens was thought to play an important role in reducing heat flux– as the amount of evaporated water was more in cases with water supply and solar radiation, and lawn surface temperatures were found to decrease under these conditions. Lawn bottom temperatures was greater than surface temperatures in all cases, and were found to decrease in the cases without solar radiation (after wind speed was decreased) and also benefited from water supply (Onmura et al., 2001).

Furthermore, by comparing surface temperatures of bare soil and green roofs tested in plots during August and November in Kobe, Japan, Takebayashi and Moriyama (2007) were able to indirectly validate the significance of ET. More specifically, they reported the surface temperature on the green roof was several degrees lower than that on bare soil in

August. However, in November, the surface temperature on the green surface and bare soil were approximately the same. It was considered that due to ET, the surface temperature on the vegetated roof in summer is lower (Takebayashi and Moriyama, 2007).

Lazzarin et al. (2005) described the findings of a green roof installed in Italy. A data logging system with various sensors (temperature, humidity, rainfall, radiation, etc.) surveyed both the parameters related to the green roof and to the rooms underneath. They found that in dry conditions the temperature at the surface reached up to 55 °C and so the outgoing adduction flux (24 units) was higher than the corresponding one in wet conditions (13 units), where the surface temperature exceeded 40 °C only once. Furthermore, the wet soil gave rise to an evapotranspiration of 25 units whereas in dry conditions that contribution was limited to 12 units. The most important result regards the inside adduction– in dry conditions 1.8 units entered the underneath room, while wet conditions gave rise to passive cooling and 0.4 units left the conditioned room (Lazzarin et al., 2005).

Tan et al. (2017) found temperatures to be significantly reduced in the presence of green roof plots. Interestingly, there were differences between plots depending on their design and soil moisture properties. KA and KB plots were setup using a typical planter box, with KA and KB using K-Soil (lightweight artificial soil) and normal garden soil, respectively. KC differed from KA because it was setup with a water retention layer. Results showed that KC had the lowest surface temperature due to the presence of the water retention layer (which sustained ET during times of low soil moisture content). Interestingly, the water retention layer also led to a slight increase in concrete surface temperature. Researchers hypothesized that this occurred because heat is likely stored in

the water retention layer. Contrastingly, average surface temperature of KB was highest, while it exhibited the lowest temperature concrete surface temperature (Tan et al., 2017).

Jim and Peng studied substrate moisture effect on water balance and thermal regime of a tropical extensive green roof with several interesting findings. They reported the high thermal capacity of substrate moisture and high ET driven by sunshine could suppress subsurface temperatures. Furthermore, on cloudy and rainy days, high substrate moisture played the opposite and dual role of keeping the subsurface and subaerial temperatures at a high level (Jim and Peng, 2012).

4.2.5   Albedo

In addition to latent heat loss, green roofs cool through improved reflectance of incident solar radiation (Castleton et al., 2010). When sunlight hits an opaque surface on the earth like an exposed roof membrane, a fraction of the sunlight is reflected while the rest is absorbed by the surface during the day and its temperature rises (Liu and Baskaran, 2003; Xu et al., 2012).   The ratio of total reflected to incident solar energy is defined as albedo (also described as solar reflectance or the reflection coefficient) (Castleton et al., 2010), and the extent to which temperatures increase depends on the color of the surface. Light color roof membranes (high-albedo) are cooler because they reflect solar radiation but dark color membranes are hotter because they absorb much of the solar radiation (Liu and Baskaran, 2003). High-albedo urban surfaces not only reduce surface temperatures, but have also been found to decrease summertime air temperatures in urban areas (Xu et al., 2012).

Albedo of green roofs is likely in the range of 0.12 to 0.23. The highest albedo found (0.23) was in a study measuring the reflectance of an extensive green roof (20 cm soil layer planted with *Sedum*) installed in the Northeastern Italy (Lazzarin et al., 2005). The lowest albedo reported was in a study of a conventional light-colored roof and a green roof (0.15 m to 0.2 m of plant media and a variety of primarily native grasses and small plants) installed on a two-story building at the University of Central Florida. They found conventional and green roof reflectance values to be 0.58 and 0.12, respectively (Sonne, 2006). A third study reported the surface reflectance of an experimental green roof in Kobe, Japan to be 0.15 (Takebayashi and Moriyama, 2007). While the albedo for a sedum green roof in Bronx, NY (10-cm medium planted with mix of 6 sedum) was found to be 19.6% or ~ 0.20 (Gaffin et al., 2009; Susca et al., 2011).

Although green roof albedos have been reported, studies correlating solar reflectance to temperature and heat flux are lacking. Furthermore, to our knowledge no studies have experimentally evaluated the factors that affect green roof albedo. In terms of studies that have hypothesized these factors, Scharf and Zluwa (2017) published the albedo of three conventional roofs and three different extensive roofs (thickness 12 cm) and one intensive green roof (thickness 30 cm). The albedo of bituminous foil was 7%, the light gray sheet-metal was 24%, gravel was 38% and green roofs ranged between 13 to 21%. They attributed this range to green roof factors such as thickness, color and humidity of the substrate, plants vitality and height (Scharf and Zluwa, 2017). A literature review by Santamouris (2014) stated canopy color, moisture and the structure of the green roof layers vary the transmittance, reflectance and absorptance of solar radiation (Santamouris, 2014). Finally it is thought that as foliage absorbs radiant energy to fuel biological photosynthetic

processes, this effect contributes to increasing the effective albedo of green roof (He and Jim, 2010).

4.2.6   Thermal Insulation (R- and U-values)

It is believed that the addition of a green roof can improve the insulation properties of a building, which reduces annual energy consumption (Castleton et al., 2010). In the building industry it is very common to apply a thermal resistance value, called an R-value, to walls and roof materials to describe their insulating property, where a high thermal resistance material causes low building heat flux, and a low thermal resistance material causes high building heat flux. R-values are often included in building energy calculations as they greatly simplify the calculation of heat transfer through composite materials (Cox, 2010).

Green roof R-value can be determined in the laboratory by fixing a temperature differential across a given thickness of soil and measuring heat flux after the system has reached a steady state (Moody and Sailor, 2013). When steady state conditions are maintained, the effective R-value of the green roof is calculated as $R = \Delta T/Q$, where the temperature difference (ΔT) is calculated as $\Delta T = T_{hot} - T_{cold}$ and Q is the heat flux through the green roof (Ouldboukhitine et al., 2014).

In the green roof scientific community, thermal insulation is also often described in relation to thermal conductance (U-value or heat transfer coefficient), which is the inverse of the R-value (U-value = 1/R-value). Since it is the inverse, the heat transfer coefficient– denotes the total amount of heat which passes through a unit area of a given medium (Lanham, 2007). In terms of buildings, the overall heat transfer coefficient of the roof

defines the heat transferred to the building through building materials and determines its energy load, where a low U-value indicates low heat transfer, and a high U-value indicates high heat transfer (Santamouris, 2014).

Researchers believe one of the benefits of assessing green roofs in relation to U- or R-values, is that they can be easily included in building envelope calculations to determine heating and cooling loads. These loads can then be used to determine building energy performance, and can also be used to compare energy savings with and without the green roof (Cox, 2010). However, some researchers think that treating such a complex system as a simple insulative layer with an enhanced R-value (or U-Value) is problematic, as these values do not capture the transient thermal storage and evaporative cooling that take place on a green roof (Moody and Sailor, 2013). To explore this concept, first we will describe the existing body of literature exploring green roof thermal resistance (R-value) or thermal conductance (U-value). Since this body of literature heavily is simulated, we focused on **experimental** studies.

Factors influencing R- and U-values

U-values have been found to be less when a roof is covered with a green roof than when it is bare. In one study, the heat transfer coefficient for a bare conventional built-up flat roof in Singapore was found to be approximately 0.58 W/m^2 K, as compared to 0.45 W/m^2 K when designed with a green roof (400 mm of growing medium), after daytime fluctuations in temperature were considered (Nyuk Hien Wong et al., 2003). Compared with the bare roof, much less heat gain was observed on the planted roof. Interestingly, referring to these findings Lanham stated this depth value is huge compared to depths of

150 mm currently used in Eastern Ontario and should not be taken as a typical value (Lanham, 2007).

Regarding factors influencing thermal insulation values, several studies have asserted that the thickness of growing media notably affects the thermal insulation feature of green roofs. Deeper green roofs produce lower heat gain and loss, and they often have a better thermal performance (Berardi et al., 2014). In an experimental analysis, Kotsiris et al. explored U-values in real scale and under dynamic conditions. For the study's purposes, five semi-intensive green roof systems were constructed on the roof of an outdoor test cell. It was found that the green roof with 8 cm thick rock wool substrate with 2 cm sod on top had a very low U-value. For the same level of substrate moisture content, the other two green roof systems made of 8 cm deep course aggregate substrates with 2 cm sod on top provided higher U-values. Moreover, deeper amounts of the same substrates (20 cm) reduced the U-value (Kotsiris et al., 2012) .

Furthermore, the effect of vegetation on thermal resistance (R-value) and conductance (U-value) has also been evaluated. For example, a study by Cox focused on the thermal resistance of green roofs with different type of plants. Trays were tested at four different ambient temperatures, ranging from room temperature to 120 ºF. In ascending order, the resulting R-values for sedum (*Sedum hispanicum*) ranged from 1.37 to 3.28 ft^2 h ºF/Btu, for ryegrass (*Lolium perenne*) R-values ranged from 2.15 to 3.62 ft^2 h ºF/Btu, and for vinca (*Vinca minor*) R-values ranged from 3.15 to 5.19 ft^2 h ºF/Btu. Furthermore, the results showed an increase in R-value with increasing temperature. Cox stated that one possible reason why *Sedum* resulted in the lowest R-values is the low water consumption property of the plant— it uses less water which means that it must transpire less water. This

would cause a reduction in evaporative cooling when compared to the other plants, resulting in a lower R-value. Additionally, the author noted that a possible reason for the low values from *Sedum* is its health. It should be noted that when *Sedum* was tested it was not in good health. (Cox, 2010). Referring to the results by Cox, Berardi et al. (2014) stated *Sedum*, one of the most popular types of plants for green roofs, provides high shading against solar radiation, has a short root structure and is compatible with limited water sources. However, it is unable to avoid convective heat transfer under its leaves and consequently, it has a low thermal resistance value (Berardi et al., 2014).

Contrastingly, Morau et al. (2012) observed that *Sedum* performed the best when they compared the U-value, K-value and R-value to two other plant species (*Plectranthus* and *Kalanchoe*) in Reunion Island. The U-value was significantly lower at 2.15 ± 0.22 W/m^2 K, and *Sedum* also exhibited a greater value of thermal resistance (0.47 ± 0.05 m^2 K/W). When the effect of plant type on heat flux was studied, *Sedum* showed a better energy performance compared to the other two plant species (Morau et al., 2012).

Although several studies have validated the importance of vegetation to thermal resistance or conductance, some studies state thermal insulation properties of a green roof is mostly connected to the insulation properties of the growing medium than foliage (Raji et al., 2015). This conclusion was based on the work of Wong et al., who measured similar amounts of heat flux for a roof covered with bare soil and with plants at night. They concluded that plants have a limited effect on stopping heat lost at night when they are compared with the soil layer which has a better insulation property. They further concluded that the thermal protection of vegetation mainly depends on its sun-shading effect rather than the insulation property (N.H. Wong et al., 2003).

In the study by Cox (2010) previously mentioned, in addition to studying the effect of plant type on thermal resistance, another objective was to determine if an increase in ambient temperature would cause an increase in green roof R-value while the relative humidity was maintained constant. Test trays containing green roof materials were tested in a low speed wind tunnel equipped to determine the R-value of the trays. Three different plant species were tested in this study, ryegrass (*Lolium perenne*), sedum (*Sedum hispanicum*), and vinca (*Vinca minor*). As predicted, Cox found an increase in R-value with increasing temperature, and the relationship between temperature and R-value for all three plant species was found to be statistically significant (Cox, 2010).

The influence of water content on R- and U-values

The effect of water content on green roof R- and U-values is a strong area of focus in reviewed studies. It is believed that growing medium moisture alters the efficiency of green roofs through changing the insulation properties, and cooling the roof via evaporative cooling. Some scientists believe that wet growing mediums function as better insulators. Nevertheless, other scientists argue that wet growing mediums are poorer insulators compared to dry growing mediums since air is a better insulator than water (Saadatian et al., 2013). This is an interesting paradigm because when we described evapotranspiration's role in thermal performance (section 4.2.4), many studies show substrate moisture improves ET and results in more cooling. Therefore, if substrate moisture indeed reduces the insulation property of green roofs, this relationship indicates there are likely trade-offs between energy savings and water retention. The following experimental studies summarize research related to water content and green roof R- and U-values.

Kotsiris et al. (2012) explored green roof U-values in real scale and under dynamic conditions in Greece. It was found that the relation between the estimated thermal transmittance and the substrate moisture content was linear, with higher substrate moisture resulting in higher U-values. As a result, researchers recommended that under adequate irrigation, rock wool seems to be an ideal material for green roofs because it provides an adequate plant growth media with high thermal insulating features and quickly discharges rainwater from strong storms (Kotsiris et al., 2012).

Interestingly, because of this relationship with substrate moisture, Lanham states that the way researchers are evaluating thermal insulation is inherently wrong if one considers substrate water content. The author states that R-values are not absolute, because these published values are calculated under standard test conditions which are often not identical to the conditions in which the materials function in the environment. Therefore, the only true method of assessing the thermal performance of a material is to test it under the conditions of which the material's performance is needed. Lanham goes on to state that the thermal performance of green roof systems should be determined while varying moisture conditions. This would determine if any and how the behavior of these systems varies with changes in moisture content (Lanham, 2007).

Moreover, Moody and Sailor state that the steady state R-value is useful as a reference but does not capture the dynamic aspects of the energy balance on a green roof. Thermal performance of green roof soil is further complicated by the fact that, unlike a typical building material, green roof soil retains significant moisture which helps to mitigate storm events and maintain the health of plants. Thus, the thermal properties of the

soil and thermal performance of a green roof is tightly coupled with the time-varying moisture content within the substrate layer (Moody and Sailor, 2013).

4.2.7 Substrate Water Content, Evapotranspiration and Green Roof Thermal Insulating Properties

As previously mentioned, various opinions exist regarding the thermal performance of green roofs in respect to their insulating and evapotranspirative cooling properties. Several studies support the notion that wet green roofs are poor insulators, while other studies state wet green roofs provide more evapotranspirative cooling.

We found that many of the scientific studies that supports the notion that green roof function as insulators are based on simulations. For example, in one of the earliest studies evaluated, Palomo Del Barrio (1998) explored the thermal behavior of green roofs through a mathematical analysis. The main conclusion of this study was that green roofs act as insulation devices rather than cooling ones (Palomo Del Barrio, 1998). On the other hand, many experimental studies seem to support the notion that thermal insulation is not as big of a driver of thermal performance, or that it is more of a factor in the winter. For example, a field experiment conducted on two full-scale rooms of a building in Shanghai– one room was covered by a green roof while the other one was covered by a common roof found that net solar radiation is the major heat gain for green and conventional roofs and dominates the total energy flows. For the green roof, the heat dissipation sequence was: evapotranspiration > net long wave radiation > heat convection > heat conduction > heat storage. For the common roof, heat dissipation sequence was: heat convection > net long wave radiation > heat conduction > heat storage. Researchers stated that the proportion of

heat conduction became smaller for the green roof but larger for the common roof, which means that less heat is absorbed by green roof and more heat enters into the room for common roof. Furthermore, when there was not rich water in soil, the proportion of ET decreased greatly while heat convection rose, showing that soil water ratio has a large effect on energy balance of green roofs and keeping an appropriate level of water ratio is beneficial for the cooling effect of green roofs. Overall, they concluded that the energy balance of a green roof is a dynamic process which changes with meteorological factors, soil water content and indoor conditions. ET and net long wave radiation dominate the whole process of heat dissipation, and soil water content also plays an important role (He et al., 2016).

Other researchers hypothesize that green roof insulating and evapotranspirative properties complement each other. Cox stated that the main cause of decreased roof temperatures is ET by green roof vegetation. This reduction in temperature reduces the heat flux conducted through the green roof and into buildings, and in this way green roofs can act as active insulation. Essentially, as ET increases, the R-value for the green roof increases because the heat flux into the roof is reduced (Cox, 2010). Similarly, when researchers evaluated ET and thermal resistance properties of green roofs, results showed that ET for trays with vegetation was always greater than evaporation of trays with growing media only, and the differences were more pronounced for periwinkle than for ryegrass. Furthermore, results showed that the thermal resistance of the tray without plants was about 0.8 m^2 K/W. However, in the presence of vegetation, the thermal resistance was about 0.92 m^2 K/W in the case of ryegrass and about 1.27 m^2 K/W in the case of periwinkle. Researchers concluded that transpiration accounts for about 13% of the thermal resistance

for ryegrass and about 37% of the thermal resistance for periwinkle as the type of vegetation (Ouldboukhitine et al., 2014)– however, it was unclear how they came to this conclusion.

Another hypothesis is that there may be a temporal/seasonal difference in green roof behavior as an insulating or evapotranspirative device, however this has not been experimentally validated to our knowledge. In a simulation study, researchers highlighted green roof performance strongly depends on the water content of the system, where a well wet green roof has good cooling performance. They also went on to state that water has a negative role in the winter in terms of heating performances, and the dryer the roof, the lower the heating demand (Zinzi and Agnoli, 2012). Similarly, Raji et al. (2015) concluded from summarizing findings of several studies that during the hot seasons or in equatorial climates (where summer-winter temperature differences are not considerable), a wet green roof can increase heat dissipation through evapotranspiratory cooling and reduces the need for indoor cooling. However during the winter, thermal resistance of a green roof improves with less water content in the growing medium due to water having a higher thermal conductivity than air (Raji et al., 2015).

If these findings are experimentally validated, it would make a strong case for water management needs to be calibrated according to local climate conditions and main energy use (Zinzi and Agnoli, 2012). For example, in regions characterized by summers and winters, an effective way to manage green roofs is to use wet substrates in summer and dry substrates during the winter— dry soil can be utilized to increase heat storage and thermal insulation during the winter, while wet substrate can enhance convection and conduction effects in summer periods (Besir and Cuce, 2018). However, relying on substrate water

content to provide cooling in warm seasons/climates can be problematic. Ganguly et al. suggest that although a well wet green roof has good cooling performance, relying on the rainfall does not ensure effective energy performances during dry, hot seasons (Ganguly et al., 2015).

Furthermore, if it is found that a green roof serves more as an insulating device as opposed to an evapotranspirative device, it could impact green roof design. For example, Kotsiris et al. (2012) explored green roof U-values in real scale and under dynamic conditions in Greece. It was found that the relation between the estimated thermal transmittance and the substrate moisture content was linear, with higher substrate moisture resulting in higher U-values. Based on these findings they recommended that under adequate irrigation, rock wool seems to be an ideal material for green roofs because it provides an adequate plant growth media with high thermal insulating features and quickly discharges rainwater from strong storms (Kotsiris et al., 2012). Furthermore, Lin and Lin examined four different plant substrates and concluded that the one with highest porosity (burned sludge) provided the best thermal insulation for the green roof due to the formation of air pockets and water holding capacity (Lin and Lin, 2011).

Finally, results have implications on the applicability of thermal resistance/ conductance values during times of ET. More specifically, researchers have suggested that when green roof substrate layers become saturated, conductivity increases. Traditionally, an increase in thermal conductance due to substrate moisture would be viewed as a negative property of green roofs. However, Pearlmutter and Rosenfeld (2008) suggest that this increase in conductivity augments heat transfer toward the evaporating surface and potentially provides a large cooled mass to absorb heat from the building's roof

(Pearlmutter and Rosenfeld, 2008). Since this is contrary to how many researchers view R- and U-values, it may suggest that the way researchers are evaluating green roofs is inherently wrong.

More specifically, Moody and Sailor state that the steady state R-value is useful as a reference but does not capture the dynamic aspects of the energy balance on a green roof. Thermal performance of green roof soil is further complicated by the fact that, unlike a typical building material, green roof soil retains significant moisture which helps to mitigate storm events and maintain the health of plants. Thus, the thermal properties of the soil and thermal performance of a green roof is tightly coupled with the time-varying moisture content within the substrate layer (Moody and Sailor, 2013). Furthermore, Lanham (2007) states that R-values are not absolute because they are calculated under standard test conditions which are often not identical to the conditions in which the materials function in the environment. It is suggested that only true method of assessing the thermal performance of a material is to test it under the conditions of which the material's performance is needed. Lanham goes on to state that the thermal performance of green roof systems should be determined while varying moisture conditions. This would determine if any and how the behavior of these systems varies with changes in moisture content (Lanham, 2007).

Ultimately these studies highlight a very important issue— green roof thermal performance strongly depends on the water content of the system. However, the unclear relationship between substrate water content, ET and green roof thermal insulating properties warrant the need for more research.

4.2.8   Cool Roofs

Cool roof (or white roof) strategies are progressively drawing the attention of the scientific community and the market due to their effective role in reducing cooling energy demand and mitigating UHI effects. A cool roof technology generally consists of a roof system with a coating characterized by high solar reflectance and high thermal emissivity (Ganguly et al., 2015). These thermal properties limit the rise in roof surface temperatures under the sun and reduce the heat transfer to the built environment by reflecting incident solar radiation away from the building and radiating heat away at night compared to conventional building materials (Ganguly et al., 2015; Zinzi and Agnoli, 2012). It is important to note however that the relative benefits of cool roofs depend on the construction of the building, external weather conditions and use of the building (Kolokotroni et al., 2013).

Cool Roof Studies in Warm Seasons/Climates

In a case study of a building located in Poiters, France, researchers reported that the mean external roof temperature was 30.2 °C during pre-application of cool paint (solar reflectance of 0.88 and a thermal emittance of 0.90) and 19.8 °C during the post-application condition (Bozonnet et al., 2011). Similarly, a study conducted near Sicily found the maximum roof surface temperature difference between the air and roof surface was 48 °C and decreased to 26 °C after application of a cool paint. Monitored data used to calibrate the building model further demonstrated the efficacy of the cool paint– an average reduction of 2.3 °C of the operative temperature during the cooling season and a 54% reduction in cooling energy demand was found. Cool roof application was an eco-friendly white double layer paint on primer finished with a washable gloss emulsion coating. The

calculated solar reflectance of the sphere was 85.9% and the broad band thermal emittance was measured at 0.88 (Romeo and Zinzi, 2013).

Monitoring period	Date	Measured outdoor air temperature and solar radiation (Average from 9 a.m. to 5 p.m.)	West building roof (estimated reflectance)	East building roof (estimated reflectance)
Phase I Pre-coating	January–March	29.1 °C, 653 W/m^2	Concrete roof (0.3)	Concrete roof (0.3)
Phase II Post-coating	March–July	32.4 °C, 643 W/m^2	White roof (0.7)	Black roof (0.1)
Phase III Post-coating	August–December	27.2 °C, 529 W/m^2	White roof (0.7)	White roof (0.7)

Figure 4-2 Monitoring periods and roof-surface reflectance (Xu et al., 2012).

Pre- and post-coating comparison for two commercial buildings monitored in the Metropolitan Hyderabad region of India (Figure 4-2) exhibited the following results (Xu et al., 2012):

- For the concrete roof building (reflectance of 0.3) converted to a cool roof (reflectance of 0.7), the maximum roof-surface temperature decreased from 54.7 °C in pre-coating (Phase I: January to March) to 41.2 °C (a reduction of 13.5 °C) in post-coating (Phase II: March-July) even though the average outdoor air temperature increased from 29.1 °C in Phase I to 32.4 °C in Phase II.

- For the east building, the maximum roof-surface temperature increased from 54.7 °C in Phase I to 71.3 °C in Phase II (an increase of 16.6 °C), after a black coating was applied to the original concrete roof.

- Finally, in Phase III (August-December), with both roofs having the similar white coating under the same weather condition, the maximum roof temperatures of both roofs were similar.

106

- Furthermore, the measured annual energy savings from roof-whitening of the previously black roofs ranged from 20-22 kWh/m^2 of roof area, while the application of white coatings to uncoated concrete roofs resulted in annual savings of 13-14 kWh/m^2 of roof area. The annual direct CO_2 reductions associated with the reduced cooling energy use were estimated to be 11-12 kg CO_2/m^2 of flat roof area.

Zinzi and Fasano (2009) studied the properties and performance of advanced reflective paints to reduce cooling loads near Rome. One of their conclusions was that the white coating lowers by many degrees surface temperatures compared to conventional Italian construction materials (concrete blocks, clay tiles, asphalt, brown paint and stone marble). Furthermore, the white paint was found to have a surface temperature seldom higher than the air (above 35 °C only for 3% of the time), an important factor that mitigates the UHI effect (Zinzi and Fasano, 2009).

A study that took place in an open office building in London consisted of a pre-application and post-application study period of cool paint (May–June and August-September, respectively and the cool roof paint was applied in July). Every parameter showed a better performance from a cooling point of view after application of the cool paint. After comparing two particular days pre and post-application (June 1, 2009 and August 16, 2009– each having approximately similar external average temperature and average global radiation during the daytime, results showed that the roof surface temperature was higher on June 1st as compared to August 16th by a maximum of 7.7 °C and an average of 6 °C during working hours. Furthermore, internal ceiling surface temperature was higher by a maximum of 3.1 °C on June 1st (Kolokotroni et al., 2013).

Cool Roof Thermal Studies in Cold Seasons/Climates

While cool roofs can reduce building cooling load during warm months, some researchers believe they may regrettably increase heating loads in cool months; thus reducing their overall effectiveness (Testa and Krarti, 2017). Other researchers state the penalty is minor (Synnefa et al., 2007). For example, when an innovative cool fluorocarbon coating on an industrial building in the Netherlands (temperate climate) was assessed pre- and post-application to an aluminum roof, researchers observed a decrease of 73% for cooling while there was a minor heating penalty of 5% (Mastrapostoli et al., 2014).

Other researchers state cool roofs do not have a heating penalty. For example, Susca et al. (2011) found that on average, considering both the diurnal and nocturnal fluxes of heat through roofs, the cool roof in their study did not have any penalty during the winter. This was because the heat fluxes from indoors to outdoors were less than those through the black roof. More specifically, the cool roof had heat penalties during the warmest hours of the day, when its surface temperatures were lower than those on the black membrane. However during the night, the cool roof (because of its emissivity) slowly releases stored heat, keeping the surface temperature higher than the black membrane (Susca et al., 2011).

Cool versus Green Roofs Thermal Performance

An interesting evaluation of the effectiveness of green roofs comes by comparing their performance with that of cool roofs. Different studies have shown different results (Berardi et al., 2014). In terms of experimental studies, the following conclusions were found:

Susca et al. (2011) indicate that cool and green roofs perform similarly when they compared the thermal performance of a green roof, cool roof and black roof in New York City. During the summer they observed the summer daily thermal oscillation on the black surface to be approximately 60 °C, while it was approximately 30 °C on the cool roof and green roof surface (thermal oscillation on the soil bottom was less than 20 °C). Moreover, they found that during the winter, temperatures recorded on the soil bottom of the green roof were almost constant with peak of oscillation of approximately 10 °C, while the thermal oscillations on the black membrane were approximately 30 °C with peaks of more than 40 °C; and on the cool roof, they were approximately 10-20 °C with peaks of 30 °C. After considering energy savings, construction impacts, replacement phase impacts and surface albedo, they concluded that the cool and green roofs result in less impact than the black roof (Susca et al., 2011).

Contrastingly, Simmons et al. (2008) reported green roofs outperform cool roofs when they compared the thermal performance of six types of extensive green roofs against a cool and a conventional roof in a former pasture in Austin, Texas (climate is subhumid, subtropical with a bimodal rainfall pattern peaking in spring and fall). By comparing green roof performance to other surfaces, they aimed to help explore the general conclusion that the greatest environmental benefits from green roofs might be achieved in subtropical climates characterized by high temperatures and intense rain events despite little research to supporting this notion. The structure of the green roofs was almost identical across all types (a membrane root barrier, a drainage layer and 100 mm of substrate). Furthermore, the cool roof was a white membrane (acrylic surfaced 2-ply APP modified bituminous membrane). Measurements showed that when ambient temperature reached 33 °C, the

surface temperature of the black and cool roofs reached 68 °C and 42 °C, and the membrane temperatures of the green roofs ranged between 31 and 38 °C (Simmons et al., 2008).

Other studies have reported the opposite trend. An analysis by Takebayashi and Moriyama (2007) found the cool roof to outperform the green roof. The cool roof (white paint with solar reflectance of 0.74) and lawn-grass green roof, along with a several other surfaces (cement concrete surface, a surface painted with a highly reflective gray paint, and a surface of bare soil) were placed and tested in plots in Kobe, Japan, during August and November. Results in August showed the surface temperature of the cement concrete slab and the highly reflective gray paint were almost the same and higher by about 10 °C than the highly reflective white paint. They also found the surface temperature on the green surface to be several degrees lower than that on bare soil, however it was several degrees higher than that on the highly reflective white paint (Takebayashi and Moriyama, 2007).

Factors to consider when evaluating Cool and Green Roofs

Ultimately the effectiveness of green and cool roofs depends on several factors like season/climate, green and cool roof properties, and other related factors. For example, season/climate and substrate water content are likely strong factors in performance efficiencies of green roofs relative to cool roofs. When researcher performed a numerical comparative analysis between cool and green roofs in the Mediterranean, researchers concluded that cool roofs are the most effective solutions for the center and southern areas of the Mediterranean basin. The study highlighted a very important issue– green roof performance strongly depends on the water content, with a well wet green roof having good cooling performance (Zinzi and Agnoli, 2012). Moreover, Li et al. modeled the effectiveness of cool and green roofs as UHI mitigation strategies. They found that green

roofs with relatively abundant soil moisture have an effect in reducing surface and near-surface UHIs comparable to cool roofs with an albedo value of 0.7 (Li et al., 2014).

In terms of cool roof properties, Gaffin et al. (2005) performed a simulation where they evaluated what albedo is needed on a bright or white roof to reproduce the cooling observed on a green roof. This was estimated by raising the albedo on the calibrated non-green model until it simulated the reduced temperatures observed on the green roofs. Findings suggested that green roofs cool as effectively as the brightest possible white roofs, with an equivalent albedo of 0.7–0.85 (Gaffin et al., 2005).

Furthermore, Santamouris (2014) performed a review of green and cool roof UHI effectiveness studies (some experimental, but most we simulations) and concluded that when the albedo of cool roofs is equal or higher than 0.7, cool roofs present a much higher heat island mitigation potential than green roofs during the peak period. Santamouris noted however that in all studies evaluated, the comparison has been performed against green roofs of extensive type and low leaf area index. The peak latent heat associated with ET in those roofs ranged between 100 and 250 W/m^2 which may not compensate for the reflective benefit of cool roofs that is higher than 400 W/m^2. Thus, it was suggested that green roofs may present a similar or higher mitigation potential during the peak period, when latent heat losses exceed 400 W/m^2. This is possible for very well irrigated green roofs presenting a LAI higher than 4 or 5 and for quite dry climates (Santamouris, 2014).

Some of these hypotheses have been experimentally validated. Coutts et al. (2013) for example compared four experimental rooftops– including a green roof (extensive green roof planted with *Sedum*) and a cool roof (uninsulated rooftop coated with white elastomeric paint)– over the summer of 2011-2012 in Melbourne, Australia. Results

suggested that cool roofs, combined with insulation, provide the greatest overall benefit in terms of urban heat mitigation and energy transfer into buildings. Researchers attributed this to the high albedo of the cool roof, which substantially reduced net radiation, leaving less energy available at the surface for sensible heating during the day. Furthermore, they noted that ET from the green roof was low, leading to high sensible heat fluxes during the day under warm and sunny conditions, when soil moisture was limited. This phenomenon was further confirmed as irrigation improved the performance of the green roof by increasing ET (Coutts et al., 2013).

Overall, Coutts et al. concluded that green roofs could provide as much benefits as cool roofs if they are regularly irrigated and planted with a dense mix of actively transpiring vegetation. Interestingly, they report that the common green roof species of choice, *Sedum*, provided no significant benefit over a soil substrate roof alone. They attributed this to the resistance of *Sedum* to ET since it does not transpire actively during the daytime. In fact, they stated that latent heat flux rarely reached the 400 W/m^2 suggested by Santamouris to make green roofs comparable to cool roofs (with albedos >0.7), except for the day after irrigation where the latent heat of evapotranspiration was measured as high as 600 W/m^2. They concluded that although *Sedum* can provide benefits (shallow rooting depth and drought tolerance, and sustained stormwater management) they are not suited to achieving a cooling performance objective (Coutts et al., 2013).

4.3 Materials and Methods

4.3.1 System Descriptions and Overview of Sensors

Figure 4-3 *WaterShed's* extensive green roof sits upon a cool roof (TPO membrane).

The sloped extensive green roof system is a LiveRoof Lite extensive modular system (6.35 cm or 2.5 in deep, 10° sloped, 29 m^2 or 312 ft^2, north-facing)– for a full description of the system refer to section 2.7 (Site Description: *WaterShed's* Green Infrastructure). The green roof is waterproofed by a cool roof (white thermoplastic polyolefin membrane material), which has a border ranging from 38.1-50.8 cm (15–20 in) between the vegetation and edge of the roof (Figure 4-3). The emissivity and reflectance values of the cool roof are unknown, however prior research has reported the initial solar reflectance of a TPO membrane in New York City to be 0.79 (Gaffin et al., 2012).

Sensors were installed across the green and cool roofs to help validate their thermal performance over a two-year period (July 2014-June 2016). These included temperature sensors (under and at the surface of the green roof, at the surface of the cool roof membrane,

and at the onsite weather station), a net radiometer on the green roof, as well as heat flux and substrate moisture sensors within the green roof. Detailed information on how each sensor was used, as well as basic information regarding their location is outlined in subsequent sections. Supplementary information regarding the brand, quantity and specific location of each sensor can be found in Appendix A: List of Sensors and Location.

4.3.2 Characterizing Green and Cool Roof Seasonal Thermal Performance
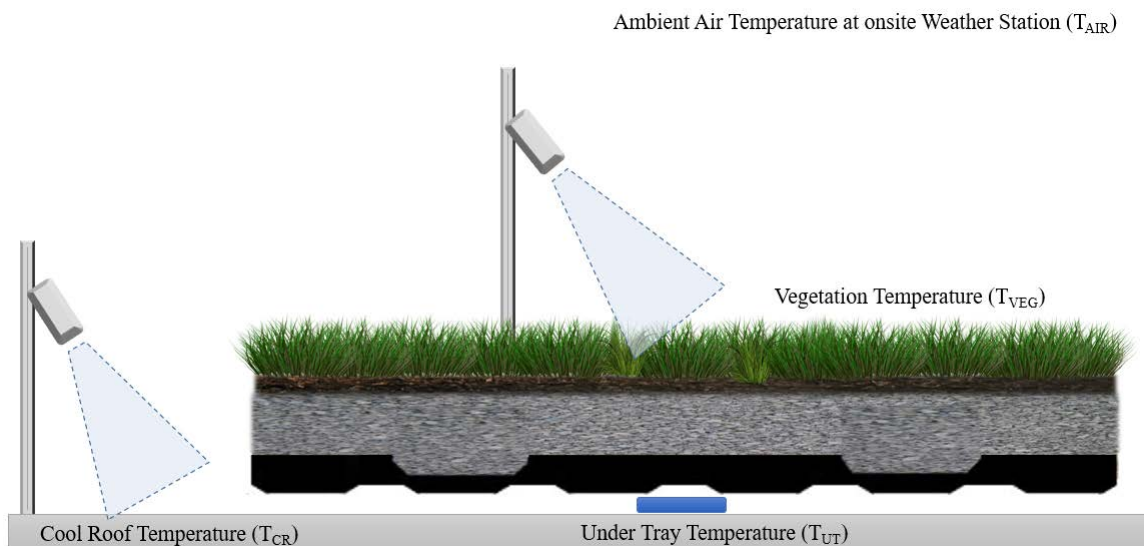
Figure 4-4 Temperature sensors used to evaluate thermal performance.

As seen in Figure 4-4, temperature sensors at the surface of the green roof (T_{VEG}), on the roof membrane under the green roof (T_{UT}), at the surface of the exposed cool roof membrane (T_{CR}), and at the weather station (T_{AIR}) were used to 1) evaluate how roof membrane temperatures under the green roof compared to the exposed cool roof and 2) to evaluate if the green roof provided an UHI benefit by comparing vegetation surface and ambient air temperatures. Vegetation and cool roof temperature sensors were infrared radiometers (SI-111 Infrared Radiometer) elevated approximately 33.02 cm (13 in) off the

surface. Under tray temperature sensors consisted of thermocouples (109 Thermocouple Probe). The SI-111 consists of a thermopile, while the 109 measures temperature via a thermistor. Additionally, ambient temperature was measured with a temperature probe (CS215-L Temperature and Relative Humidity Probe) at the onsite weather station.

Temperatures were averaged daily for the warm (May-October) and cold seasons (November-April) for each sensor location. Then, we examined average temperature differences between the various sensor locations, where, $-\Delta T$ corresponded to a cooling effect and $+\Delta$ corresponded to a warming effect. Statistical analysis using T-Tests (Paired Two Sample for Means) was applied to determine if average temperatures were significantly different— correlations were significant at the 0.05 level.

4.3.3 Determining the effect of Evapotranspiration, Solar Reflectance and Thermal Conductance on Thermal Performance

Determining Evapotranspiration

Evapotranspiration was derived from the soil depletion method, which utilizes volumetric water content sensors (CS655 Water Content Reflectometer) within the substrate of the green roof (Figure 4-5) to determine changes in substrate moisture between 15-minute sensor measurements ($\pm \Delta S = S_{t15} - S_{t0}$). Volumetric water content sensors operate by calculating the dielectric permittivity of the media from signal attenuation measurements combined with oscillation period measurements. Finally, it applies the Topp equation to estimate VWC (m^3/m^3) from dielectric permittivity (Scientific, 2014).
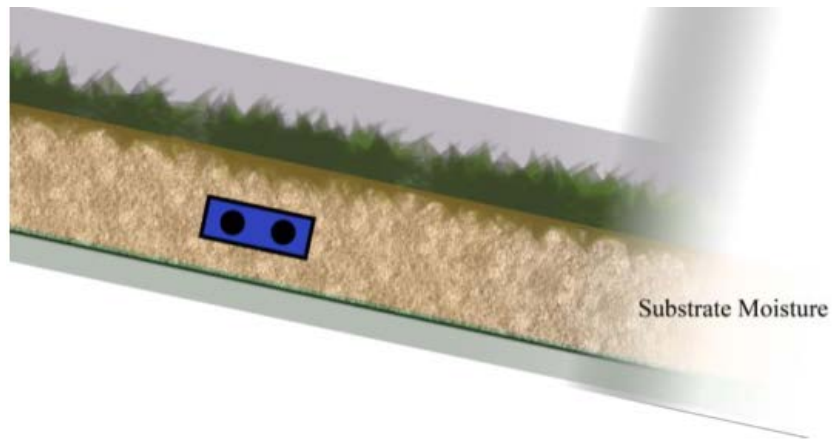
Figure 4-5 Soil Water Content Reflectometer sensors were installed approximately 3.81 cm (1.5 in) below the green roof surface with probes parallel to the roof and perpendicular to the slope (Image credit: Scott Tjaden).

With the soil depletion method, the assumption is that any gain in water $(+\Delta S)$ is retention, and any water loss $(-\Delta S)$ is due to ET or substrate drainage. Thus, any water loss in between rain events can be attributed to ET while substrate drainage was assumed to largely occur during storms. Because ET is a very small portion of the overall water balance of a green roof during storms, it was estimated to be equal to the average rate of ET between one rain event and the next. Once these values were calculated, total ET per day (mm/day) was determined. It should be noted that since ET was attributed to the change in water status, the soil depletion method could only be confidently applied during warmer months (May-October). During colder months, plant cover and ET diminishes, and any water loss over prolonged periods of time could be due to substrate drainage.

Determining Solar Reflectance (Albedo)

A net radiometer (NR01-L 4-Component Net Radiation Sensor**)** measuring shortwave and longwave radiation fluxing in and out of the green roof was used to calculate

albedo. Albedo was defined as the ratio of reflected radiation from a surface to the amount of solar radiation that hits it (α = Shortwave reflected/ Incoming Shortwave). Figure 4-6 helps depict what component of the net radiometer (facing Up/Down) corresponds to the net radiation in and out of the system for both short and longwave. Up corresponds to incident solar and down measures radiation reflected. Albedo per day was calculated by dividing total shortwave radiation reflected per day by total incident solar radiation per day.
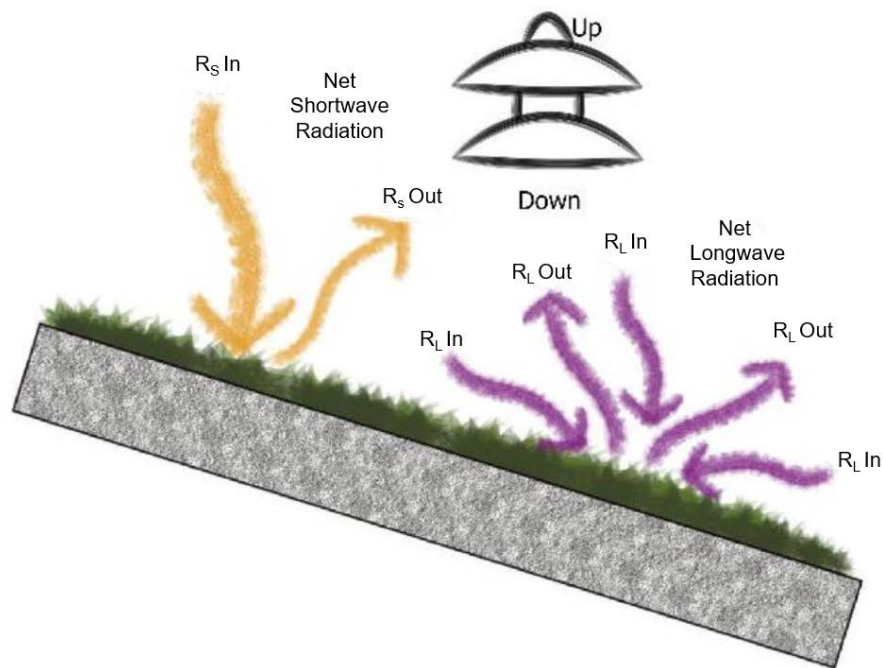
Figure 4-6 Albedo was calculated using a net radiometer sensor. This figure shows that the sensor facing up measured shortwave and longwave radiation coming into the roof, while the sensor facing down measured outgoing shortwave and longwave radiation (Image credit: Scott Tjaden).

Assessing Thermal Conductance (U-value)

As depicted in Figure 4-7, heat flux sensors (HFP01-L Soil Heat Flux Plates) within the substrate, as well as surface and below tray temperature sensors were used to

calculate heat transfer coefficients ($U_{GR} = Q/\Delta T$) at 15-minute intervals. Where, U = heat

transfer coefficient (W/ m^2 K), Q = heat flux through green roof (W/ m^2), and ΔT = change

in temperature between vegetation and under tray areas (K). Heat flux sensors operate by

outputting a voltage signal proportional to substrate heat flux. Under tray sensors (109

Thermocouple Probe) measure temperature via a thermistor, while vegetation sensors (SI-

111 Infrared Radiometer) measure temperature via a thermopile. Note that because U-value

calculations do not account for net radiation, heat transfer coefficients were only analyzed

at night. Once U-values were calculated, they were averaged daily.
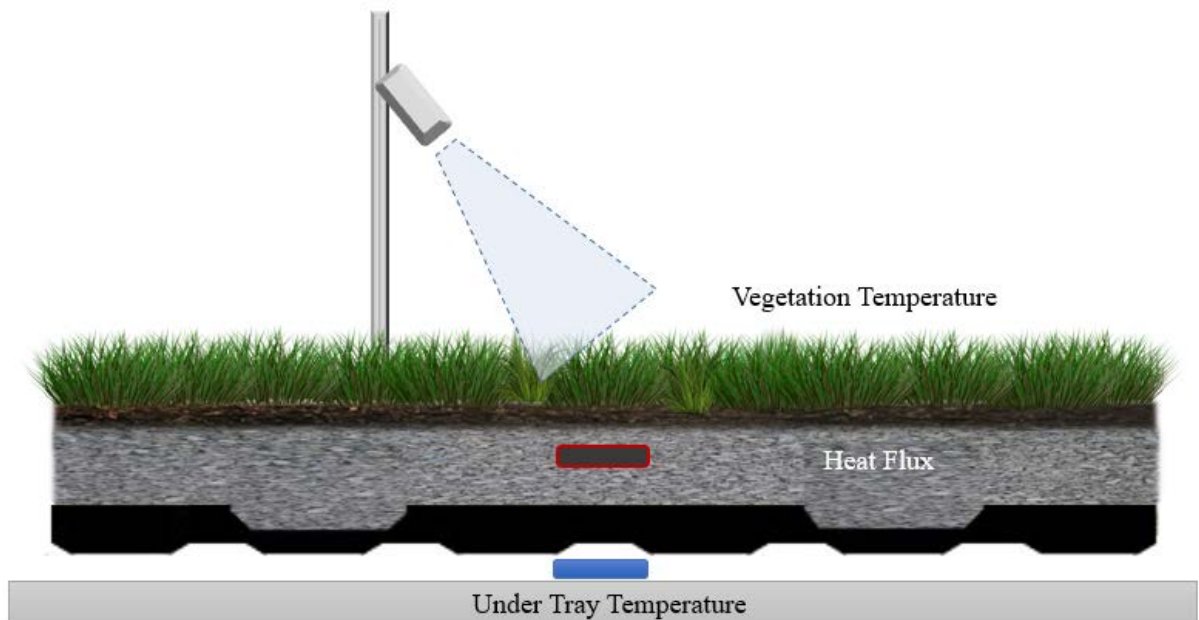
Figure 4-7 U-value was calculated from soil heat flux, and the temperature difference between the vegetation and under tray areas. Heat flux sensors were installed approximately 3.81 cm (1.5 in) below surface.

Finally, regression analysis was used to evaluate the effect of ET, solar reflectance

and thermal conductance on average daily temperature differences ($\pm\Delta T$) between the

vegetation of the green roof, the roof membrane under the green roof, and the ambient air (T_{VEG} – T_{AIR} and T_{UT} – T_{AIR}). Where, $-\Delta T$ corresponded to a cooling effect and $+\Delta$ corresponded to a warming effect.

4.3.4 Evaluating the effect of Substrate Water Content, Vegetation Development, and Microclimate Characteristics on Thermal Performance

Regression analysis was also used to evaluate the effect of substrate water content, vegetation development, and microclimate characteristics on ET, solar reflectance and thermal conductance. Average daily water content was determined using the same CS655 Water Content Reflectometer sensors previously described. Microclimate factors evaluated were net radiation and air temperature— since net radiation was the sum of the incoming shortwave and longwave minus the sum of the reflected shortwave and emitted longwave, it was considered the energy input to the green roof. Net radiation was averaged per day and measured using the NR01-L 4-Component Net Radiation sensor previously described. Additionally, air temperature was averaged per day and measured with the temperature probe (CS215-L Temperature and Relative Humidity Probe) at the weather station.

Finally, biomass changes of the green roof's vegetation over time was evaluated using monthly measurements of leaf area index and percentage of vegetation cover. LAI was measured in addition to percent cover because it allowed us to measure the canopy foliage density of the green roof rather than simply area covered (Raji et al., 2015). Supplementary information on vegetation methodologies can be found in Appendix C: Vegetation Development (Green Roof Only).

4.4 Results and Discussion

4.4.1 Warm Season Thermal Performance

T_{AIR} = 20.1 ± 4.94 °C (Range: 5.33 - 29.0 °C)

T_{VEG} = 19.6 ± 6.30 °C (Range: 1.19 - 32.7 °C)

T_{CR} = 19.1 ± 6.39 °C (Range: -1.39 - 30.2 °C)

T_{UT} = 22.8 ± 6.30 °C (Range: 5.63 - 35.2 °C)
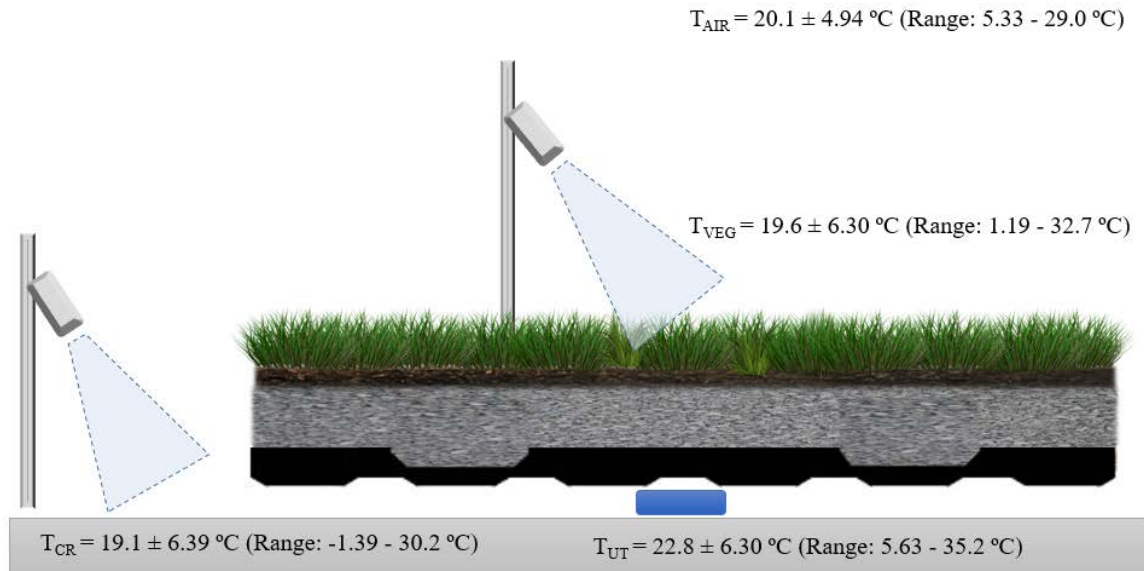
Figure 4-8 Average temperature for each sensor location during the warm season.

As depicted in Figure 4-8, average temperatures during the warm season for T_{AIR}, T_{VEG}, T_{UT}, and T_{CR} were 20.1 ± 4.94 °C, 19.6 ± 6.30 °C, 22.8 ± 6.30 °C and 19.1 ± 6.39 °C respectively. Several key results were observed when average temperature difference for each sensor location was evaluated (Table 4-1). First, it was observed that relative to T_{AIR} and T_{VEG}, T_{UT} was higher than both on average by 2.63 °C and 3.17 °C, respectively. This was not unusual as greater under green roof temperatures relative to ambient and vegetation temperatures have been documented. Morau et al. (2012) for example studied an extensive green roof installed in Reunion Island (tropical humid climate) and found that although the green roof performed significantly better than the reference roof, the maximum ambient air temperature (28.7±0.4°C) was much lower than the temperature under the green roof which

was 34.8 ±0.6 °C (Morau et al., 2012). It should also be noted that ambient temperature likely benefitted from the location of our study in Rockville, MD where the UHI is likely lower than a more urban setting like Washington, DC. Moreover, although Tan et al. found average vegetation surface temperature and average surface temperature of concrete under planter boxes to be significantly reduced in the presence of green roof plots, they noted that under temperatures were greater than vegetation temperatures for all treatments (Tan et al., 2017).

Table 4-1 Average temperature differences for each sensor location in the warm season. Negative values signify cooler temperatures and positive values signify warmer temperatures. Note, [a] signifies temperature difference is significant at the 0.05 level.

	$T_{UT} - T_{AIR}$	$T_{UT} - T_{VEG}$	$T_{UT} - T_{CR}$	$T_{VEG} - T_{AIR}$	$T_{VEG} - T_{CR}$
Warm Season	2.63 °C [a]	3.17 °C [a]	3.70 °C [a]	-0.54 °C [a]	0.53 °C [a]

Next, it was observed that the green roof is likely providing a thermal benefit to the building. Although we were unable to compare average under tray temperature (22.8 ± 6.30°C) to a conventional roof, published studies (Table 4-2) document conventional roof temperatures ranging between 42 and 73.5 °C. Furthermore, it is also likely that the green roof is also delaying peak temperatures as well as reducing temperature fluctuations as noted in several studies described in the Introduction (section 4.2.1: Green Roofs and Building Energy Demand), where reduced temperature fluctuations have the additional benefit of protecting the roof membrane from damage (Liu and Baskaran, 2003; Sonne, 2006; Tan et al., 2017; Teemusk and Mander, 2009).

Table 4-2 Summary of studies from the Introduction (section 4.2.1: Green Roofs and Building Energy Demand) that reported surface temperature data of conventional and green roofs.

Reference	Methodology	Reference Roof Temperature	Green Roof Temperature
(Liu and Baskaran, 2003)	Researchers compared temperatures on a typical summer day of a generic extensive green roof and a modified light-gray bituminous roof in Ottawa, Canada.	70 °C	25 °C
(Sonne, 2006)	Average maximum temperature of a conventional light-colored roof and green roof in Central Florida.	54 °C	33 °C
(Morau et al., 2012)	Maximum temperature of an extensive green roof comprised of succulent plant species compared to a reference bituminous roof surface installed in Reunion Island.	73.5 ±1.4 °C	34.8 ±0.6 °C
(Onmura et al., 2001).	Surface temperature of rooms covered by a lawn garden and roof slab in Japan during the summer.	60 °C	30 °C
(Liu and Minor, 2005).	A bituminous reference roof was compared to two green roofs in Toronto on a typical summer day. Green Roof G has a deeper and lighter colored growing medium (100 mm) than Green Roof S (75 mm).	66 °C	38°C for Green Roof S and 36 °C for Green Roof G
(Tan et al., 2017).	Average surface temperatures under nine green roof planter boxes at the National University of Singapore relative to an exposed concrete surface.	47.2 °C	29.5-31.2 °C
(Niachou et al., 2001)	Exterior surface temperatures of green roofs on non-insulated buildings in Greece.	42 to 48 °C	28 to 40 °C

Next, a slight UHI benefit was observed– T_{VEG} (19.6 ± 6.30 ºC) was on average 0.54 ºC cooler than T_{AIR} (20.1 ± 4.94 ºC). Green roof UHI studies are lacking, however preliminary results are promising. For example, field measurements conducted in Singapore to investigate the thermal impacts of a rooftop garden, showed a maximum reduction of 4.2 °C at 300 mm height, around 1800 h between ambient air temperatures measured with and without plants (Nyuk Hien Wong et al., 2003). Another study investigated the UHI mitigation of an intensive green roof in Manchester, UK relative to an adjacent concrete roof. Monthly median air temperature was found to be 1.06 °C lower at 300 mm over the green roof (Speak et al., 2013). Moreover, Qin et al. (2012) showed that a green roof test bed in Singapore can significantly lower the ambient air temperature by an average of 0.5ºC when compared with a bare roof during daytime hours (from 10:00 am to 4:00 pm) (Qin et al., 2012). Overall these studies show the beneficial role of green roofs in mitigating UHIs. It should be noted that a greater UHI benefit would likely have occurred in our study if it had taken place in a more urban setting as opposed to the study's location in Rockville, MD which is partially forested.

Finally, interesting results were observed when green and cool roof performance was compared. More specifically, relative to the cool roof (T_{CR} = 19.1 ± 6.39 ºC), T_{UT} and T_{VEG} were warmer on average by 3.70 ºC and 0.53 ºC, respectively. As described in the Introduction (section 4.2.8: Cool Roofs), there is debate regarding the effectiveness of green roofs relative to cool roofs, with different studies reporting different results (Berardi et al., 2014). Our results are in line with the hypothesis that cool roofs outperform green roofs. For example, Takebayashi and Moriyama (2007) evaluated the comparative performance of a cool roof (white paint with solar reflectance of 0.74), green roof (lawn-

grass), and other roof surfaces in test plots in Kobe, Japan. Results in August showed the surface temperature on the green surface to be several degrees higher than that on the highly reflective white paint (Takebayashi and Moriyama, 2007).

However, it should be noted that the comparison of cool and green roofs is still an active area of research, with other studies reporting green roofs outperform cool roofs. For example, Simmons et al. (2008) compared the thermal performance of six types of extensive green roofs against a reflective and conventional roof in a former pasture in Austin, Texas. Measurements showed that when ambient temperature reached 33 °C, the surface temperature of the black and cool roofs reached 68 °C and 42 °C, while membrane temperatures of the green roofs ranged between 31 and 38 °C (Simmons et al., 2008).

Furthermore, (although lacking in experimental data) active research shows there may be several factors to consider when comparing green and cool roof efficiency such as season/climate, green and cool roof properties, and other related factors. For example, Coutts et al. (2013) compared four experimental rooftops– including a green roof (extensive green roof planted with *Sedum*) and a cool roof (uninsulated rooftop coated with white elastomeric paint)– over the summer of 2011-2012 in Melbourne, Australia. Results suggested that cool roofs, combined with insulation, provide the greatest overall benefit in terms of urban heat mitigation and energy transfer into buildings. Researchers attributed this to the high albedo of the cool roof, which substantially reduced net radiation, leaving less energy available at the surface for sensible heating during the day. Furthermore, they noted that ET from the green roof was low, leading to high sensible heat fluxes during the day under warm and sunny conditions, when soil moisture was limited. This phenomenon was further confirmed as irrigation improved the performance of the green roof by

increasing ET. Overall, they concluded that green roofs could provide as much benefits as cool roofs if they are regularly irrigated and planted with a dense mix of actively transpiring vegetation (Coutts et al., 2013). As described in the next section, we found ET and substrate water content to be integral to thermal performance.

4.4.2 Drivers of Warm Season Thermal Performance

Table 4-3 Describes the effect of evapotranspiration, solar reflectance, and thermal conductance on average temperature differences between T_{UT}, T_{VEG} and T_{AIR}. Note, (+) indicates a positive correlation and (-) indicates a negative correlation. Furthermore, [a] signifies correlation is significant at the 0.05 level, [b] denotes significantly different than cold season at the 0.05 level, [c] indicates not evaluated in the cold season, while NS indicates no significance.

	Average Daily Warm Season Value	$T_{UT} - T_{AIR}$	$T_{VEG} - T_{AIR}$
ET	0.81 mm [c]	$R^2 = 0.1548$ (-) [a]	$R^2 = 0.0137$ (-) [a]
Albedo	0.13 [b]	$R^2 = 0.0155$ (-) [a]	$R^2 = 0.0880$ (-) [a]
U-value	3.16 W/m^2 K	NS	$R^2 = 0.0295$ (+) [a]

Warm season averages were 0.81 mm/day for ET, 0.13 for albedo, and 3.16 W/m^2 K for U-value (Table 4-3). Correlation analyses confirmed that higher ET rates and albedo resulted in cooler under tray and vegetation temperatures, with T_{UT} being more correlated with ET ($R^2 = 0.1548$), while T_{VEG} was more correlated with albedo ($R^2 = 0.0880$). Additionally, cooler vegetation temperatures were observed when U-values were low. When we evaluated these parameters independently, several key trends were noted.

First, we observed that on days where no ET occurred, T_{UT} was as much as 8.99 °C warmer than the ambient air— when ET was greatest (4.65 mm/day), temperature

differences between T_{UT} and the ambient air reduced to 1.99 °C. It should also be noted that although the correlation between T_{VEG} and ET was not as strong, on days where no ET occurred, T_{VEG} tended to be warmer than the ambient air (maximum of 3.52 °C).

ET was expected to be a significant driver of cooling based on previous green roof research. For example, Lazzarin et al. (2005) described the findings of a green roof installed in Italy. A data logging system with various sensors (temperature, humidity, rainfall, radiation, etc.) surveyed both the parameters related to the green roof and to the rooms underneath. Researchers found that in dry conditions, the temperature at the surface reached up to 55 °C and so the outgoing adduction flux (24 units) was higher than the corresponding one in wet conditions (13 units), where the surface temperature exceeded 40 °C only once. They also noted that the wet soil gave rise to an evapotranspiration of 25 units, whereas in dry conditions that contribution was limited to 12 units. Ultimately, they concluded that ET positively impacted building thermal performance– in dry conditions 1.8 units entered the underneath room, while wet conditions gave rise to passive cooling and 0.4 units left the conditioned room (Lazzarin et al., 2005).

When the factors that were driving evapotranspirative cooling were examined (Table 4-4), ET was found to be strongly correlated to substrate water content ($R^2 = 0.4841$) and to a lesser extent net radiation ($R^2 = 0.0429$), but was not significantly related to vegetation characteristics (LAI or percent cover) or ambient air temperature. In respect to published works, green roof soil moisture is often regarded as the most critical factor for ET, with rates expected to decay exponentially with respect to time as available moisture reduces (Poë et al., 2015; Stovin et al., 2013; Tan et al., 2017). We observed a similar trend as ET was greatest (4.65 mm/day) when soil moisture was highest (8.14 mm).

Table 4-4 The effect of substrate water content, vegetation development and microclimate factors on evapotranspiration, albedo and U-value. Note, (+) indicates a positive correlation and (-) indicates a negative correlation. Furthermore, [a] signifies correlation is significant at the 0.05 level, [b] denotes significantly different than cold season at the 0.05 level, while NS indicates no significance.

	Average Daily Warm Season Value	ET	Albedo	U Value
VWC	2.88 mm [b]	$R^2 = 0.4841$ (+) [a]	$R^2 = 0.0334$ (+) [a]	$R^2 = 0.0638$ (+) [a]
LAI	1.50 m^{-2}	NS	NS	NS
% Cover	55.6%	NS	NS	$R^2 = 0.6736$ (+) [a]
Net Radiation	112.5 W/m^2 [b]	$R^2 = 0.0429$ (+) [a]	$R^2 = 0.1191$ (-) [a]	NS
Air Temperature	20.1 ℃ [b]	NS	$R^2 = 0.0314$ (-) [a]	NS

It is likely that substrate moisture was the strongest driver of ET due to the media being limited in water– average daily water content was 2.88 mm (0.045 m^3/m^3) during the warm season, which is low when compared to other findings. More specifically, Starry et al. (2014) studied photosynthesis and water use by *Sedum album* and *Sedum kamtschaticum*. In addition to observing that ET was reduced for both species with decreasing substrate moisture, they suggested threshold water contents. More specifically, since the lowest average substrate water contents observed for *S. album* and *S. kamtschaticum* were 0.065 m^3/m^3 and 0.04 m^3/m^3, respectively (at this point leaf turgor was visibly reduced for both species, but they quickly recovered upon rewatering), they recommended thresholds for both species at 0.18 and 0.13 m^3/m^3 for *S. album* and *S. kamtschaticum* respectively, which are well above the average water content observed in our study. Thus, it is likely under that these dry conditions, *Sedum* species are being

induced into crassulacean acid metabolism (CAM) photosynthesis. More specifically, many extensive green roofs like the system in this study are planted with *Sedum* species that are characterized by CAM photosynthesis. Under water stress conditions, CAM plants only open their stomata to metabolize at night when temperatures are cooler. ET loss is therefore lower than from plants that evapotranspire soil–water during warm daylight conditions (He et al., 2017; Poë et al., 2015; Tabares-Velasco and Srebric, 2011; Tan et al., 2017).

Overall, these findings suggest that if the green roof was well-watered above the thresholds suggested by Starry et al. (2014), ET rates would have likely been higher and resulted in more cooling of T_{UT} and T_{VEG}. Furthermore, results have implications for the green roof industry as *Sedum* are widely implemented in green roof installations in the American Northeast and Midwest, and are considered successful in terms of plant coverage and survival, especially due to their drought tolerance and CAM metabolism (Starry et al., 2014). It is likely that the extensive sloped nature of the studied roof results in an extremely dry climate that even drought tolerant species may not be well adapted to. Furthermore, this phenomenon is likely why vegetation characteristics were consistently low throughout the two-year study period (across both seasons LAI was 1.35 m^{-2} ± 0.37 and percentage cover was 53.9% ± 12.3— according to the manufacturer, minimum installation soil coverage of planted modules is 95%), which would in turn explain why vegetation characteristics were not correlated to ET.

Since green roof hydrological characteristics are determined by several factors such as the characteristics of growing substrate and drainage elements (Tan et al., 2017), improving the water status of the green roof by irrigating, modifying its depth or substrate

composition, or implementing a water retention layer may be beneficial to plant health, ET and ultimately cooling. Moreover, it is likely that once sufficient soil moisture is achieved, then other factors like plant type, stage of plant development and weather would affect ET most significantly (Tan et al., 2017). There are even studies that indicate once vegetation is well developed, its shading properties may largely dominate cooling. For example, studying the thermal performance of *Pennisetum clandestinum*, *Aptenia cordifolia*, *Sesuvium verrucosum* and *Halimione portulacoides*, researchers concluded that shading proved to be much more efficient than the evaporative cooling mechanism of the moist soil (Schweitzer and Erell, 2014).

Next, we evaluated the effect of albedo on thermal performance (to our knowledge, this is the first study directly evaluating this relationship). Average daily albedo in the warm season was 0.13, which is on the low end of the range we compiled (0.12 to 0.23) from a literature review in the Introduction (section 4.2.5: Albedo) (Gaffin et al., 2009; Lazzarin et al., 2005; Scharf et al., 2012; Scharf and Zluwa, 2017; Sonne, 2006; Susca et al., 2011; Takebayashi and Moriyama, 2007). Nonetheless, albedo was significantly correlated to reducing T_{VEG} and T_{UT} temperatures ($R^2 = 0.0155$ and $R^2 = 0.0880$, respectively).

Studies report that green roof factors such as thickness, color and humidity of the substrate, plants vitality and height (Scharf et al., 2012; Scharf and Zluwa, 2017), as well as canopy color, moisture and the structure of the green roof layers vary the transmittance, reflectance and absorptance of solar radiation (Santamouris, 2014). In terms of factors we evaluated, daily albedo values were most correlated with solar radiation ($R^2 = 0.1191$). More specifically, as net radiation increased, albedo decreased in value as the green roof

reflected a smaller fraction of incident radiation. Similarly, as temperature increased, solar reflectance decreased (R^2 = 0.0314). Finally, substrate water content was also a small yet significant factor to solar reflectance (R^2 = 0.0334), with albedo values increasing with more substrate moisture.

From these observations it is likely that green roof albedo was impaired by radiation and high temperatures because these are conditions that would cause the substrate to dry out most readily. Although we were unable to directly confirm this, dry substrates are likely inducing physiological stress and having a negative impact on vegetation development, which would in turn reduce solar reflectance. In other words, by improving substrate moisture, vegetation physiology and health would likely improve, which would increase the albedo effect. He and Jim (2010) made a similar hypothesis– they stated that as foliage absorbs radiant energy to fuel biological photosynthetic processes, this effect contributes to increasing the effective albedo of green roofs (He and Jim, 2010). Furthermore, this phenomenon would explain why LAI and vegetation cover (which were consistently low throughout the two-year study period) were not directly related to albedo.

U-value findings were most perplexing. Portions of our results aligned with prior research, while other aspects were conflicting. First, average U-value over the warm season was 3.16 W/m^2 K, which is higher than the value (2.15 $\pm$ 0.22 W/m^2 K) reported by Morau et al., who studied a *Sedum* green roof (220 mm or 8.66 in) installed in Reunion Island (Morau et al., 2012). Differences in U-value between the two roofs can be attributed to several factors (extensively described in section 4.2.6), the most relevant being substrate thickness. More specifically, the thickness of growing media notably affects the thermal insulation feature of green roofs– deeper substrate amounts have been found to reduce the

U-value (Kotsiris et al., 2012). Relative to the system evaluated by Morau et al. (2012), *WaterShed's* green roof was shallow, and was characterized by poor vegetation health.

Next, we observed a low but significant correlation between daily U-values and T_{VEG} ($R^2 = 0.0295$)— there was no correlation to T_{UT}. More specifically, cooler vegetation temperatures were generally observed when U-values (thermal conduction) were low. For example, on a day where thermal conductance was abnormally high at 47.4 W/m^2 K, T_{VEG} was 2.23 °C warmer than the ambient air.

One aspect of thermal conductance findings that was perplexing was the fact that vegetation cover was highly correlated with higher U-values ($R^2 = 0.6736$). This contrasted with expectations, as we hypothesized lower U-values with greater vegetation development.
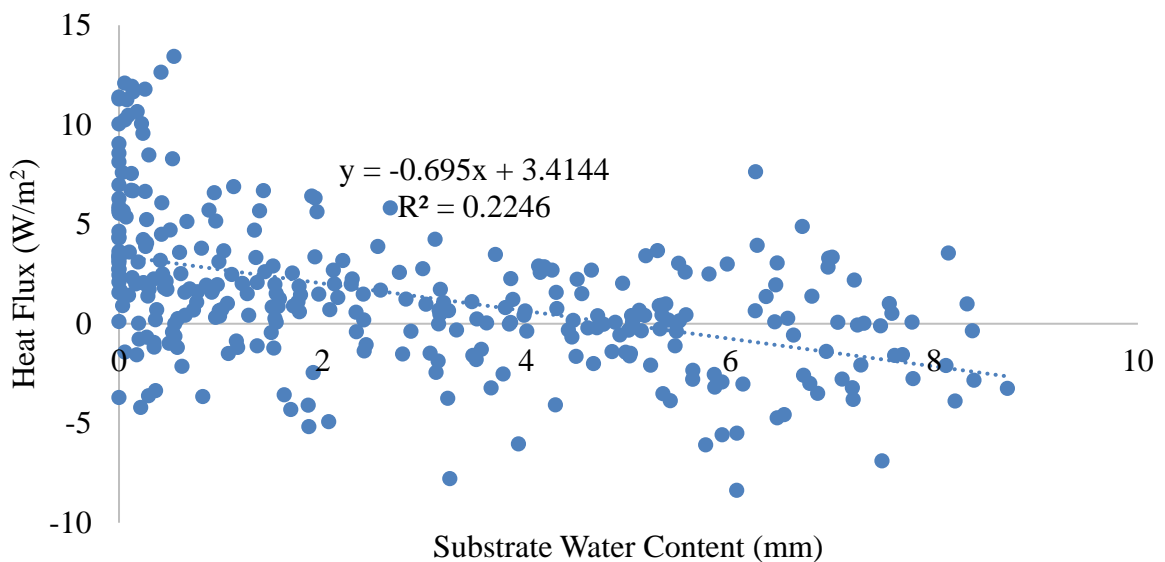
Figure 4-9 Heat flux out of the green roof (negative values) is correlated to higher substrate water content. Correlation is significant at the 0.05 level.

In line with the hypotheses of several researchers, low U-values were generally observed when substrate moisture was low ($R^2 = 0.0638$). However, this was confounding when we evaluated the relationship between heat flux and substrate water content (Figure 4-9)— we evaluated this relationship only after realizing ET, albedo and U-value were all significantly correlated to substrate water content. It was observed that on days where high substrate moisture occurred, more heat generally fluxed out of the roof ($R^2 = 0.2246$), and higher fluxes out the roof were significantly correlated to cooler T_{UT} ($R^2 = 0.2078$) and T_{VEG} ($R^2 = 0.1948$) temperatures as seen in Figure 4-10. Thus overall, it appears substrate moisture is beneficial to warm season thermal performance.
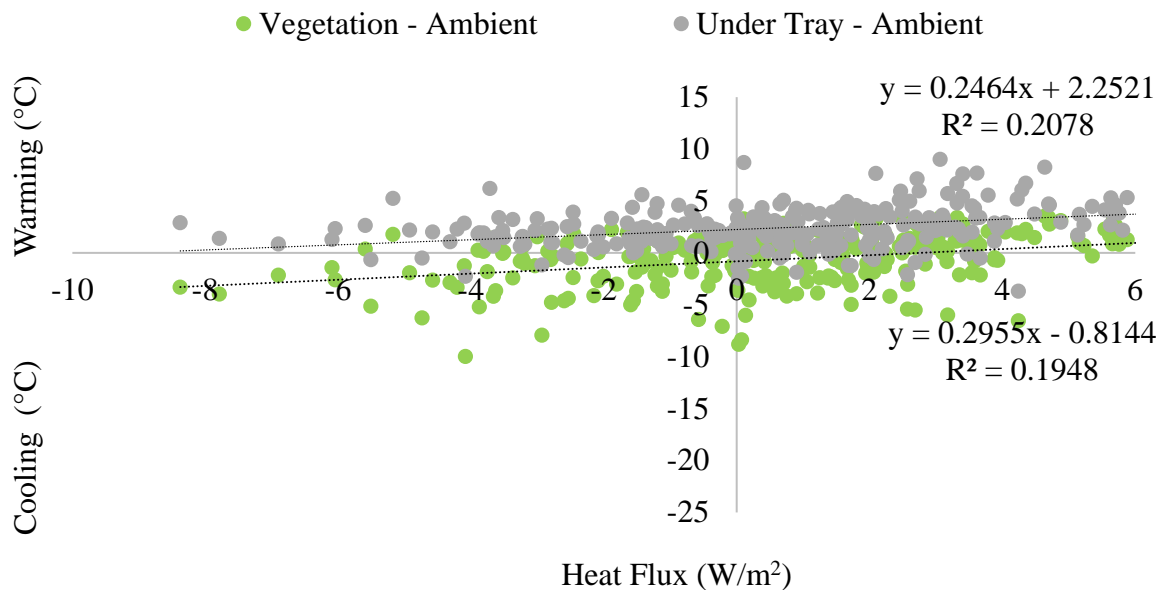
Figure 4-10 Heat flux out of the green roof (negative values) is correlated to cooler under tray and vegetation tempeatures. Correlations are significant at the 0.05 level.

Overall, these findings point to the complex nature of green roofs, which is increasingly a point of discussion in literature. More specifically, these results align well with the hypothesis that ET is likely the greatest driver of thermal performance.

Furthermore, it is also likely that there is a temporal benefit to substrate moisture– where in warm seasons/climates, moisture is beneficial when ET is high, however in transitional months, or where climatic conditions are less favorable, water can be detrimental to thermal performance due to its conductive property.

Finally, results indicate that the use of U-values or R-values which are frequently used in the building community to quickly estimate energy loads can be problematic— especially since daily U-values were not correlated to T_{UT}. Some researchers hypothesize that treating a complex system like a green roof as a simple insulative layer with an enhanced R-value (or U-Value) is problematic and fundamentally wrong as it does not capture the transient thermal storage and evaporative cooling that take place on a green roof (Moody and Sailor, 2013).

More specifically, Moody and Sailor state that the steady state R-value is useful as a reference but does not capture the dynamic aspects of the energy balance on a green roof. Thermal performance of green roof soil is further complicated by the fact that, unlike a typical building material, green roof soil retains significant moisture which helps to mitigate storm events and maintain the health of plants (Moody and Sailor, 2013). Furthermore, Lanham (2007) states that R-values are not absolute because they are calculated under standard test conditions which are often not identical to the conditions in which the materials function in the environment. It is suggested that only true method of assessing the thermal performance of a material is to test it under the conditions of which the material's performance is needed. Lanham goes on to state that the thermal performance of green roof systems should be determined while varying moisture

conditions. This would determine if any and how the behavior of these systems varies with changes in moisture content (Lanham, 2007).

4.4.3 Cold Season Thermal Performance
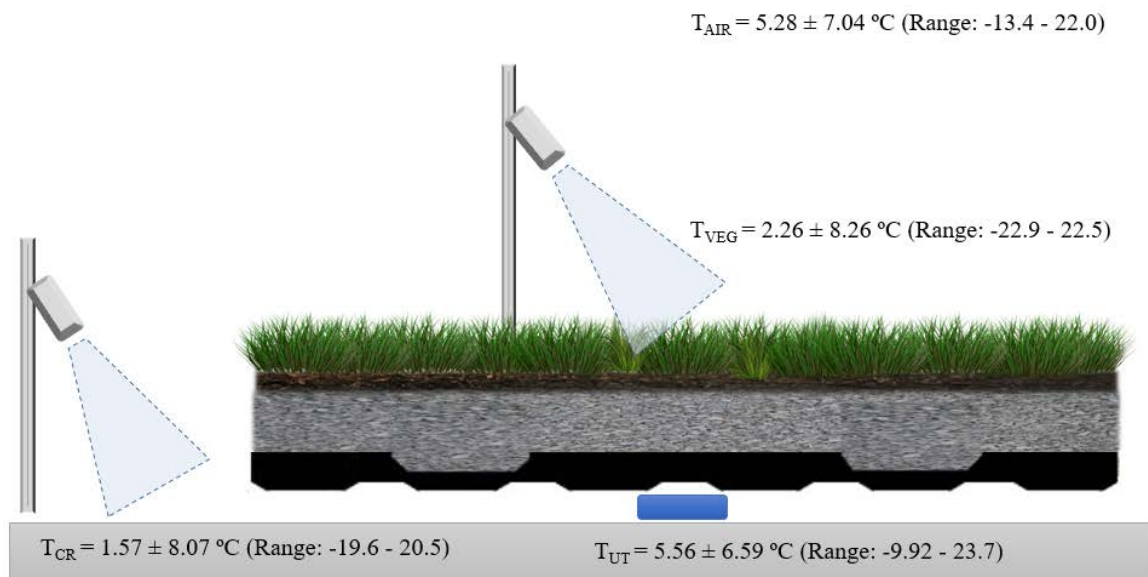
Figure 4-11 Average temperature for each sensor location during the cold season.

Average temperatures during the cold season for T_{AIR}, T_{VEG}, T_{UT}, and T_{CR} were 5.28 ± 7.04 °C, 2.26 ± 8.26 °C, 5.56 ± 6.59 °C, and 1.57 ± 8.07 °C, respectively (Figure 4-11). Several key results were observed when average temperature difference for each sensor location was evaluated (Table 4-5). First, it was observed that T_{UT} was warmer than T_{VEG} on average by 3.30 °C, while it was not significantly different than T_{AIR}. Next, it was observed that the green roof is likely providing a thermal benefit to the building.

Although we were unable to compare under tray temperature to a conventional roof, published studies indicate that green roofs generally perform similarly or outperform conventional roofs in cold seasons/climates (Table 4-6). For example, experiments

conducted over a week in Pennsylvania, USA compared heat losses between green roof assemblies to reference roof losses. Heat losses from the building to the outdoor environment during the week were -7.1 $W/m^2 \pm 9.7$ and -9.2 W/m^2 for the green roof and reference roof, respectively (Zhao et al., 2015).

Table 4-5 Average temperature differences for each sensor location in the cold season. Negative values signify cooler temperatures and positive values signify warmer temperatures. Note, [a] signifies temperature difference is significant at the 0.05 level, while NS signifies no significance.

	$T_{UT} - T_{AIR}$	$T_{UT} - T_{VEG}$	$T_{UT} - T_{CR}$	$T_{VEG} - T_{AIR}$	$T_{VEG} - T_{CR}$
Cold Season	NS	3.30 ℃ [a]	3.99 ℃ [a]	-3.03 ℃ [a]	0.69 ℃ [a]

In another study, the thermal performance of a generic green roof (150 mm lightweight soil planted with wild flower meadow) was compared to a modified bituminous membrane roof in Ottawa, Canada for almost a year. Researchers found that not only did the green roof slightly outperform the conventional roof in the winter, but overall the green roof was beneficial when they accounted for cumulative energy demand across seasons. More specifically, Bass and Baskaran (2001) found that after accounting for the steady heat loss from the green roof, and the fluctuating heat loss and gain for the conventional roof, the green roof marginally outperformed (~10%) the reference roof during the colder months. Furthermore, when they accounted for cumulative energy demand across seasons, the difference in space conditioning energy demand was 967 kWh over the 11-month period (Figure 4-1). This was due to the green roof significantly outperforming (>75%) the reference roof in the warmer months (Bass and Baskaran, 2001).

Table 4-6 Summary of studies from the Introduction (section 4.2.1: Green Roofs and Building Energy Demand) that compared conventional and green roofs in cold seasons/climates.

Reference	Methodology	Key Findings
(Zhao et al., 2015)	Experiments conducted over two weeks (one with and without snow) at an outdoor test facility in Pennsylvania, USA compared heat losses between green roof assemblies to reference roof losses.	Heat losses from the building to the outdoor environment during the week with no snow were -7.1 W/m^2 ± 9.7 and -9.2 W/m^2 for the green roof and reference roof, respectively— note, because snow is a good insulator, heat loss was similar that week.
(Getter et al., 2011)	Research on a Midwestern USA extensive green roof relative to a traditional ballasted gravel roof.	Monthly cumulative heat losses averaged over the winter were 2623 W/m^2 and 3017 W/m^2 for the green roof and gravel roof, respectively.
(Lanham, 2007)	Compared green roof test panels with a conventional built-up roof test panel in cold climate conditions using a hot box apparatus.	It was concluded that the thermal benefit of green roofs in cold climates is at least statistically significant with a confidence level of 95%.
(Bevilacqua et al., 2016)	Conducted in south Italy, researchers compared an extensive green roof to a black bituminous roof in the winter.	The green roof was on average 4 °C higher than the black bituminous roof in the winter.
(Teemusk and Mander, 2010)	Analyzed the temperature regime of an existing green roof and a sod roof, compared with a modified bituminous membrane roof and a steel sheet roof in Estonia.	The temperatures in the planted roof's substrate layers were much higher than on the surfaces of the conventional roofs.
(Bass and Baskaran, 2001)	The thermal performance of a generic green roof (150 mm lightweight soil planted with wild flower meadow) was compared to a modified bituminous membrane reference roof in Ottawa for almost a year.	The energy demand due to both roof sections was essentially the same during the fall and winter seasons. In terms of energy efficiency, the green roof system marginally outperformed (~10%) the reference roof during the colder months but it significantly outperformed (>75%) the reference roof in the warmer months.

Next, we aimed to determine if the green roof was providing an UHI benefit during the cold season, especially since the UHI phenomenon is rarely studied during the winter. It can even be argued that UHIs are currently not as big of a problem for many international cities because they reduce winter heating costs (Speak et al., 2013). However, research indicates warming can still be observed in colder seasons/climates.

For example, researchers found through fixed point monitoring stations over the city of Manchester that although there is a higher probability of UHI occurrence in the city during the summer, the winter UHI frequency was highest at 1.0 ℃ during the day and night, and maximum UHI temperature was found to be as high as 10 °C in the winter (summer high of 8 °C was observed) (Cheung, 2011). Furthermore, in New York City researchers observed during winter that the temperature in their more urban site of Columbia was on average 1.5 ℃ higher than in Fieldston during the daytime. They noted that at their Fieldston site the air temperatures are just slightly affected by the biological activity of trees (Susca et al., 2011).

Overall, an UHI benefit of 3.03 ℃ was observed, where T_{VEG} was 2.26 ± 8.26 ℃ and T_{AIR} was 5.28 ± 7.04 ℃. This finding aligned with the results of another study, where a long-term experimental analysis in the Mediterranean (characterized by cool, wet winters) comparing the thermal performance of a green roof with a conventional bare flat roof was performed. Researchers found that during the winter the external soil surface temperature was cooler than the ambient air during nighttime by 3–4 °C, whereas in the case of the bare roof it was higher than the ambient air temperature all the day (Theodosiou et al., 2014).

Finally, interesting results were observed when green and cool roof performance was compared— relative to the cool roof, the green roof was more beneficial to building energy demand (the opposite was observed during the warm season). More specifically, T_{CR} (1.57 ± 8.07 ℃) was on average 3.99 ℃ cooler than and T_{UT} (5.56 ± 6.59 ℃). Results indicate that in sunny climates, cool roofs present an important advantage, while in moderate and cold climates green roofs seem to present higher benefit (Santamouris, 2014). Ultimately an experiment evaluating the effect of cool and green roofs on building energy demand across the seasons would provide more insight on this theory.

Furthermore, it should be noted that it is very likely that cool roofs are still overall beneficial in cold seasons/climates relative to conventional roofs. This is because 1) they may perform similarly to conventional roofs in cold seasons/regions, and 2) generally perform better than conventional roofs when one considers their overall impact on building energy demand across the year.

More specifically, researchers traditionally hypothesized that cool roofs increase heating loads in cool months (Testa and Krarti, 2017). However, other researchers state cool roofs do not have a heating penalty at all. For example, Susca et al. (2011) found that on average, considering both the diurnal and nocturnal fluxes of heat through roofs, the cool roof in their study did not have any penalty during the winter. This was because the heat fluxes from indoors to outdoors were less than those through the black roof— the cool roof had heat penalties during the warmest hours of the day, when its surface temperatures were lower than those on the black membrane. However during the night, the cool roof (because of its emissivity) slowly releases stored heat, keeping the surface temperature higher than the black membrane (Susca et al., 2011).

Other researchers indicate the penalty is minor and negligible when one considers cool roof performance across the year. For example, when an innovative cool fluorocarbon coating on an industrial building in the Netherlands (temperate climate) was assessed pre- and post-application to an aluminum roof, researchers observed a decrease of 73% for cooling while there was a minor heating penalty of 5% (Mastrapostoli et al., 2014). Ultimately more experiments comparing conventional and cool roofs across the seasons would provide more insight on this theory.

4.4.4 Drivers of Cold Season Thermal Performance

Table 4-7 Describes the effect of solar reflectance and thermal conductance on average temperature differences between T_{UT}, T_{VEG} and T_{AIR}. Note, (+) indicates a positive correlation and (-) indicates a negative correlation. Furthermore, [a] signifies correlation is significant at the 0.05 level, [b] denotes significantly different than warm season at the 0.05 level, while NS indicates no significance.

	Average Daily Cold Season Value	**$T_{UT} - T_{AIR}$**	**$T_{VEG} - T_{AIR}$**
Albedo	0.21 [b]	$R^2 = 0.0880$ (+) [a]	NS
U-value	3.33	$R^2 = 0.0152$ (-) [a]	$R^2 = 0.0215$ (+) [a]

During the cold season, the effect of albedo and U-value on thermal performance was evaluated (Table 4-7)— it should be noted that although there is likely some biological activity during cold months, ET was assumed to be zero due to limitations of the soil depletion method. Overall, average albedo increased from 0.13 in the warm season to 0.21 in the cold season, while U-value was not significantly different between seasons (3.16 W/m^2 K and 3.33 W/m^2 K, respectively).

The relationships between green roof temperatures (T_{UT} and T_{VEG}), solar reflectance

and thermal conductance were somewhat perplexing, with some findings corresponding with published research, and others being contrary to what other studies have found. First, a low but significant correlation between T_{UT} and albedo was observed. More specifically, under tray temperatures were generally found to increase with solar reflectance ($R^2 = 0.0880$). This is contrary to what was expected because one would think that absorbed solar radiation would heat up the green roof substrate and induce warming; this was observed in the warm season (T_{UT} and T_{VEG} both generally increased as solar reflectance decreased).

Table 4-8 The effect of substrate water content, vegetation development and microclimate factors on albedo and U-value. Note, (+) indicates a positive correlation and (-) indicates a negative correlation. Furthermore, [a] signifies correlation is significant at the 0.05 level, [b] denotes significantly different than warm season at the 0.05 level, while NS indicates no significance.

	Average Daily Cold Season Value	Albedo	U Value
VWC	4.50 mm [b]	$R^2 = 0.0342$ (-) [a]	$R^2 = 0.012$ (+) [a]
LAI	1.20 m^{-2}	NS	NS
% Cover	50.0%	NS	NS
Net Radiation	40.2 W/m^2 [b]	$R^2 = 0.0661$ (-) [a]	NS
Air Temperature	5.29 °C [b]	$R^2 = 0.2001$ (-) [a]	$R^2 = 0.012$ (+) [a]

Furthermore, when the effect of substrate water content, vegetation development and microclimate factors on solar reflectance was evaluated (Table 4-8), albedo values were found to generally decrease with greater temperatures ($R^2 = 0.2001$), greater amounts of net radiation ($R^2 = 0.0661$), and increased substrate water content ($R^2 = 0.0342$). Based on this observation, findings indicate that greater solar radiation, temperature and substrate moisture are likely detrimental to T_{UT} because they cause albedo to decrease. This finding

was also contrary to what was expected– one would think that higher solar radiation and warmer temperatures would heat up the green roof substrate and induce warming.

One would also think vegetation development would be a strong driver of albedo, particularly across season, however vegetation development was not significantly different between the warm and cold seasons, and LAI and percent cover were not correlated to solar reflectance. As discussed in section 4.4.2, vegetation development was likely the same across seasons due to plant physiological stress and consistently low substrate moisture.

Next, the effect of thermal conductance on thermal performance was explored— T_{UT} generally decreased with U-value or heat transfer ($R^2 = 0.0152$), while T_{VEG} generally increased with U-value ($R^2 = 0.0215$). This was logical because during cold periods, heat is likely to be transferred from the warmer under tray space to the colder vegetation area.

When the effect of substrate water content, vegetation development and microclimate factors on thermal conductance was evaluated (Table 4-8), U-values were generally found to increase with both substrate water content ($R^2 = 0.012$) and temperature ($R^2 = 0.012$). Based on this finding, results further suggest higher temperatures and substrate water content are likely detrimental to T_{UT} during the cold season.

Interestingly, when compared to published studies, results both coincided and conflicted with conclusions. For example, the temperature finding is contrary to what Cox (2010) observed– experimental results showed an increase in R-value with increasing temperature. Since R-value and U-value are inversely related, we can assume that higher temperatures would be correlated to lower U-values (we observed the opposite trend) (Cox, 2010). On the other hand, some researchers have hypothesized that wet growing mediums

are poorer insulators compared to dry growing mediums since air is a better insulator than water (Saadatian et al., 2013). This coincided with our observation that U-values (heat transfer) increased with greater substrate moisture.
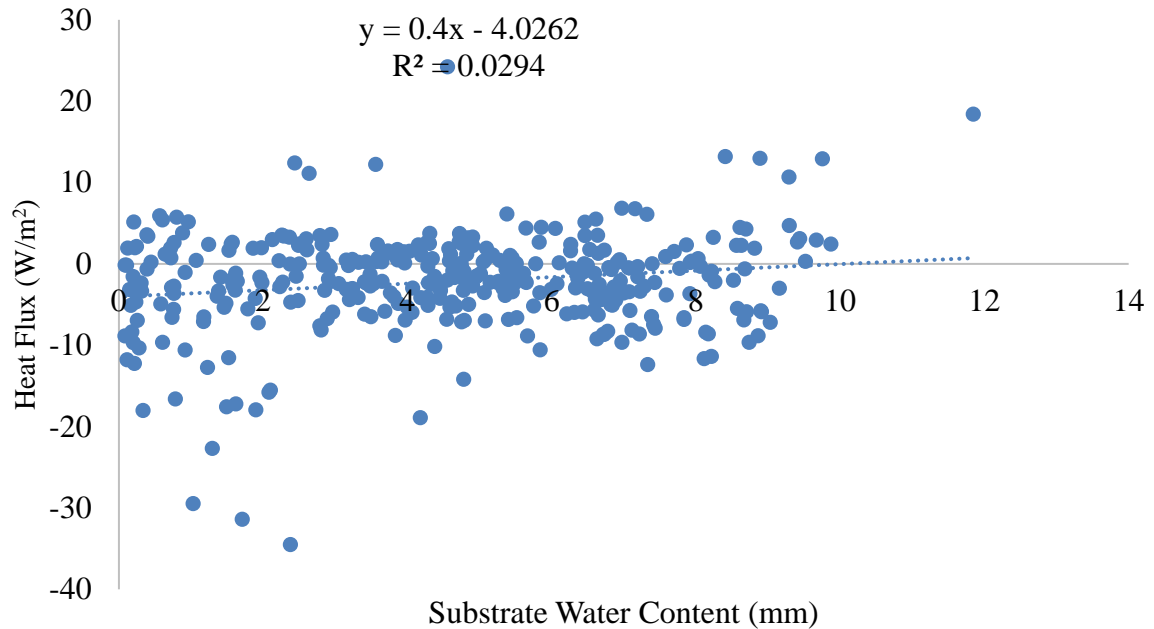
Figure 4-12 Heat flux into the green roof (positive values) is correlated to higher subsstrate water content. Correlation is significant at the 0.05 level.

Finally, we explored the relationship between heat flux and substrate water content. In the warm season, we found substrate moisture to have a positive impact on thermal performance, as more cooling was observed when heat fluxed out of the roof (more heat loss was observed during wetter periods). Interestingly, the opposite trend was observed during the cold season. More specifically, a low but significant correlation showed greater heat flux into the green roof during wetter periods (Figure 4-12, $R^2 = 0.0294$). However, it was also observed that heat flux into the green roof was detrimental to under tray temperatures— greater heat gain was correlated to cooler T_{UT} temperatures ($R^2 = 0.1055$)

and warmer T_{VEG} temperatures ($R^2 = 0.0505$) (Figure 4-13). This is contrary to what was expected because one would expect heat gain into the roof to warm under tray temperatures. Nonetheless, this finding largely correlates with the previous finding that substrate water content is likely detrimental to T_{UT} during the cold season because it caused solar reflectance to decrease. One possible explanation for this phenomenon is that heat gain due to wetter substrate is primarily warming the vegetation layer of the green roof, however temperatures are still low enough where heat is still being lost from the under tray region to the green roof's surface.
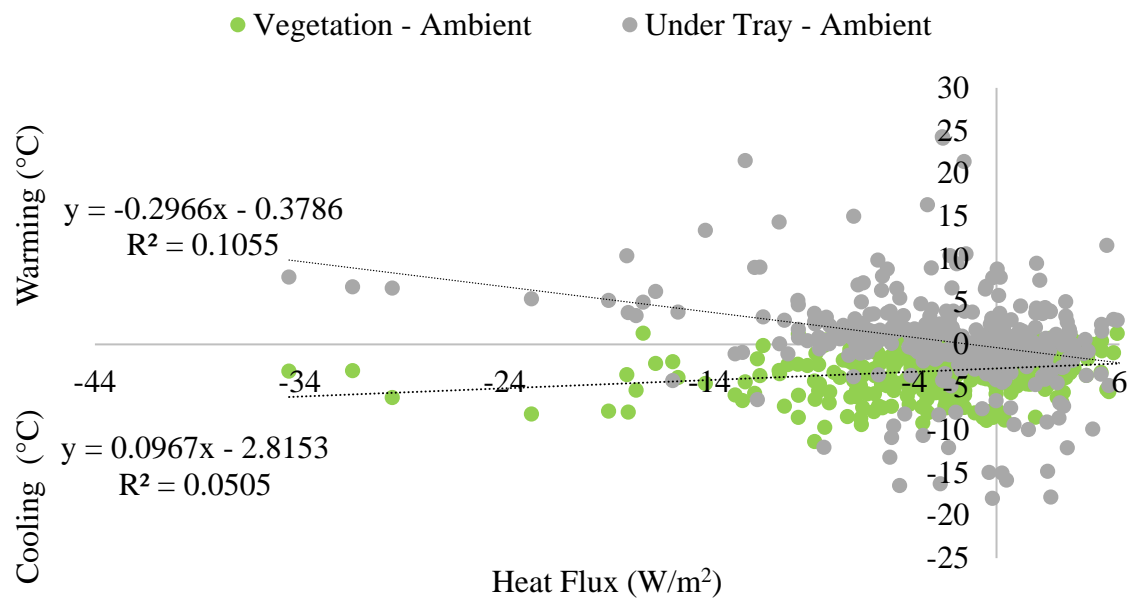
Figure 4-13 Heat flux into the green roof (positive values) is correlated to cooler under tray temperatures and warmer vegetation temperatures. Correlations are significant at the 0.05 level.

Overall, although cold season results were less conclusive, results indicate that substrate moisture in the cold season may likley be detrimental to building energy demand. This has several implications for green roof management. Zinzi and Agnoli (2012) for

example suggest calibrating water management needs according to climate conditions and main energy use in cold periods to limit substrate moisture and lower heating demand (Zinzi and Agnoli, 2012). Furthermore, perplexing results indicate a strong need for more thermal performance studies in cold seasons/climates.

4.5 Summary and Conclusions

Summary of Key Findings

- During the warm season the cool roof outperformed the green roof, being cooler than the green roof by 3.70 ºC. However, the green roof was more beneficial than the cool roof in the cold season as it was 3.99 ºC warmer. Nonetheless, both roofs are likely benefiting building energy demand relative to conventional roofs when compared to published research— an experiment evaluating the effect of conventional, cool and green roofs on building energy demand across seasons would provide more insight on this hypothesis.

- A slight 0.54 ºC UHI benefit was observed during the warm season, which increased to 3.03 ºC during the winter (some may argue this is detrimental to building heating demand). UHI benefits would likely have been greater if the study took place in a more urban setting.

- ET was the most significant driver of under tray thermal cooling in the warm season ($R^2 = 0.1548$), while green roof vegetation temperatures were more correlated with albedo ($R^2 = 0.0880$).

- Hydrological parameters are likely playing a strong role in thermal performance. In the warm season, substrate water content was highly correlated to ET ($R^2 = 0.4841$)

and to a lesser extent solar reflectance ($R^2 = 0.0334$) and thermal conduction ($R^2 = 0.0638$).

- The effect of albedo and thermal conductance on cold season thermal performance was unclear, making it difficult to draw strong conclusions. Furthermore, U-value findings across both seasons were confounding, resulting in us questioning its applicability to green roofs.

Implications for Green and Cool Roof Selection

The first objective aimed to characterize green roof seasonal thermal performance (to the building and surrounding environment) across seasons. We found that in the both seasons, the green roof is likely beneficial to building energy demand relative to conventional roofs based on published findings. Furthermore, a slight 0.54 ℃ UHI benefit was observed during the warm season, which increased to 3.03 ℃ during the winter (some may argue this is detrimental to building heating demand). Overall, it was suggested that UHI benefits would likely have been greater if the study took place in a more urban setting.

Next, we explored how the green roof performed relative to the cool roof TPO membrane. In the warm season, it was suggested that the green roof was not as effective in reducing roof membrane temperature as the cool roof (T_{UT} -T_{CR} = 3.70 ℃). It should be noted however that green roof cooling may have been low relative to the cool roof because of poor ET. In fact, Coutts et al. (2013) hypothesized that green roofs can provide as much benefits as cool roofs if they are regularly irrigated and planted with a dense mix of actively transpiring vegetation. Interestingly, they also report that the common green roof species of choice, *Sedum* (a dryland species), provide no significant benefit over soil substrate roofs

alone. They attribute this to the resistance of *Sedum* to ET since it does not transpire actively during the daytime (Coutts et al., 2013). Thus, it is likely that extensive green roofs characterized by *Sedum* may not perform as effectively in warm seasons/regions as cool roofs, but other types of green roofs may.

Interestingly, in the cold season it was suggested that the green roof was more beneficial to the building as roof membrane temperatures under the green roof were on average significantly warmer than the cool roof (T_{UT} -T_{CR} = 3.99 °C). Thus, based on findings across seasons, results indicate green roofs may be the best thermal solution for more temperate or cooler regions, while cool roofs may be preferable in hot climates. Santamouris for example hypothesized that in sunny climates, cool roofs present an important advantage while in moderate and cold climates green roofs seem to present higher benefit (Santamouris, 2014).

Ultimately a long-term study evaluating conventional, green and cool roof thermal performance across seasons is greatly needed, especially as some studies indicate that cool roofs are still overall beneficial in cold seasons/climates relative to conventional roofs. This is because they generally perform better than conventional roofs when one considers their overall impact on building energy demand across the year. For example, when an innovative cool fluorocarbon coating on an industrial building in the Netherlands (temperate climate) was assessed pre-and post-application to an aluminum roof, researchers observed a decrease of 73% for cooling while there was a minor heating penalty of 5% (Mastrapostoli et al., 2014).

Next, we aimed to determine the effect of ET, solar reflectance and thermal conductance on green roof thermal performance. Moreover, the effect of substrate water content, vegetation development (LAI and percent cover), and microclimate characteristics (net radiation and air temperature) on ET, albedo, and U-values was explored. This was important as many researchers have largely attributed ET, albedo and U-value to thermal performance, however studies evaluating their direct effect on roof surface and ambient temperatures in a single system are lacking. Overall, this part of our analysis was somewhat confounding, with many aspects contradicting published findings.

First, it was observed that ET and albedo improved under tray and vegetation temperatures during the warm season, with ET being more strongly correlated to T_{UT} and albedo being more strongly correlated to T_{VEG}. This was expected as latent heat loss and improved reflectivity of incident solar are often regarded as two main parameters of green roofs that cool buildings (Saadatian et al., 2013). Furthermore, ET was most correlated to substrate water content, then net radiation, which largely aligned with previous findings. Substrate moisture also had a positive effect on albedo, while it decreased with greater net radiation and ambient air temperatures.

An in-depth analysis of substrate moisture indicated that ET was severely restricted due to low moisture throughout the warm season– average daily volumetric water content was 2.88 mm (0.045 m^3/m^3), which is low when compared to threshold recommendations for *Sedum spp.*— Starry et al. (2014) recommended threshold values of 0.18 and 0.13 m^3/m^3 for *S. album* and *S. kamtschaticum*, respectively. This indicated that vegetation was

likely under physiological stress and was being induced into CAM photosynthesis to conserve water loss.

This observation has strong implications for green roof management as many extensive systems like the one in this study are planted with *Sedum* species. *Sedum* are widely implemented in green roof installations in the American Northeast and Midwest, and are considered successful in terms of plant coverage and survival, especially due to their drought tolerance and CAM metabolism (Starry et al., 2014). Because we observed poor vegetation health throughout the study period (across both seasons LAI was 1.35 m^{-2} ± 0.37 and percentage cover was 53.9% ± 12.3), results indicate that the sloped extensive nature of the green roof creates and environment that even the most drought tolerant green roof species are not well adapted to.

Based on these observations, we concluded that improving the water status of the green roof in warm seasons/regions by irrigating, modifying its depth and substrate composition, or implementing a water retention layer may be beneficial to plant health, ET and ultimately cooling. Moreover, it is likely that once sufficient soil moisture is achieved, then other factors like plant type, stage of plant development and weather would affect ET most significantly (Tan et al., 2017).

It should be noted however, that substrate moisture may likely be detrimental to building energy demand in cold seasons/regions. More specifically, a low but significant correlation showed greater heat flux into the green roof during wetter periods, however, it was also observed that heat flux into the green roof was detrimental to under tray temperatures. This has several implications for green roof management. Zinzi and Agnoli for example suggest calibrating water management needs according to climate conditions

and main energy use in cold periods to limit substrate moisture and lower heating demand (Zinzi and Agnoli, 2012). More specifically, it has been suggested that the effective way to manage a green roof is to use wet substrate in summer and dry soil in winter (Besir and Cuce, 2018). We would also add that even in the warm seasons/climates, substrate moisture should be limited on days where ET is not conducive (i.e. cloudy or rainy days).

Finally, of all the parameters evaluated, U-value findings were the most confounding, especially in the warm season. This was somewhat expected as the use of U-values for green roofs is highly contested, with researchers debating its relevance and the factors that influence it. First, it was observed that U-values were only correlated to T_{VEG} in the warm season, which would make it difficult to justify the use of these values in building energy demand calculations.

Other portions of our results that were perplexing was the observation that low U-values were observed when substrate moisture was low in the warm season, however, substrate moisture was overall observed to be beneficial to heat fluxing out of the roof and cooler T_{VEG} and T_{UT} temperatures. Thus, it was hypothesized that there may be a temporal benefit to substrate water content in warm seasons/climates, where moisture is beneficial when ET is high, however in transitional months of the warm season or where climatic conditions are less favorable to ET, stored water may be detrimental to cooling.

Overall, findings suggest that green roof thermal performance is not as simplistic as many researchers suggest, which would likely make it more difficult to simulate energy savings from simple calculations like U- or R-values, especially as values drastically fluctuated with substrate water content, and were not correlated to T_{UT} temperatures in the warm season. Some researchers have started to suggest this– Moody and Sailor (2013) for

example state that treating a complex system like a green roof as a simple insulative layer with an enhanced R-value (or U-Value) is problematic and fundamentally wrong as it does not capture the transient thermal storage and evaporative cooling that take place on a green roof (Moody and Sailor, 2013).

More specifically, Moody and Sailor state that the steady state R-value is useful as a reference but does not capture the dynamic aspects of the energy balance on a green roof. Thermal performance of green roof soil is further complicated by the fact that, unlike a typical building material, green roof soil retains significant moisture which helps to mitigate storm events and maintain the health of plants (Moody and Sailor, 2013). Furthermore, Lanham (2007) states that R-values are not absolute because they are calculated under standard test conditions which are often not identical to the conditions in which the materials function in the environment. It is suggested that only true method of assessing the thermal performance of a material is to test it under the conditions of which the material's performance is needed. Lanham goes on to state that the thermal performance of green roof systems should be determined while varying moisture conditions. This would determine if any and how the behavior of these systems varies with changes in moisture content (Lanham, 2007).

Reccommended Future Studies

Ultimately, the results of the study indicate a greater need for green roof thermal performance research. More specifically, it would be optimal to design a study where researchers evaluate conventional, green and cool roof surface temperature and heat fluxes, and their effect on building energy demand over a year.

Furthermore, since green roof systems are not standardized and there exist wide variability in design, it is important to study the impact of design factors on thermal performance such as the choice of materials used, number of layers, as well as the absolute and relative thickness of different components (Tan et al., 2017). For example, energy savings is likely to differ for shallow, extensive roofs, with low plant density relative to intensive systems, which are characterized by deeper substrates and a more diverse plant palette.

Other variables researchers should consider include the effect of different climate conditions, the insulation level of the roof element, as well as the irrigation and overall hydrological status of the roof. Exploring green roof hydrological status is imperative as it is a key property of green roofs, and has substantial implications for green roof retention and thermal performance— more extensive evaluation is needed to better understand how substrate moisture should be managed to maximize both benefits.

Chapter 5 Green Roof Evapotranspiration

5.1   Objective

As was explored in Chapter 3 (Green Infrastructure Hydrological Performance) and Chapter 4 (Green Roof Thermal Performance), green roofs play an important role in mitigating runoff and providing thermal benefits to buildings and the surrounding environment. One of the important drivers of these benefits is thought to be evapotranspiration (ET), which is a combined process of soil evaporation and plant transpiration (Tan et al., 2017). The physical process in which water transfers from soil into the atmosphere is called evaporation. Transpiration is a *physiological* process in plants through which water uptaken by the root system escapes through the stomata on leaves or the pores of the skin, where it is vaporized (Poë et al., 2015; Raji et al., 2015).

Evapotranspiration can be obtained by direct measurement (Ouldboukhitine et al., 2014). Forces inducing ET losses are a function of the microclimate (i.e. solar radiation, air temperature, wind, relative humidity) and plant physiology. However, the rate at which these forces induce ET depends upon substrate–water characteristics (i.e. field capacity, permanent wilting point, permeability), any additional moisture storage capacity within the vegetation layer, and the plant's physiological response at the prevailing moisture content (Poë et al., 2015). Moreover, there are several factors related to green roof design (selection of substrate and vegetation) that affect ET, which will be discussed in the Introduction (section 5.3.2: Factors affecting Evapotranspiration).

Although ET is important to the energy and water balance of green roofs, it has not been well studied, especially in real conditions and there is little experimental data

examining ET rates and attributing factors. Another area of active research is the use of ET model— there are several approaches with models that achieve ET in a time step by taking into account a number of physical parameters (radiation, pressure, wind, etc.) and characteristics of the plants (Ouldboukhitine et al., 2014). These models are important since direct measurements of ET are rarely available, and it is difficult to quantify in real-time because of changing environmental fluxes (Starry, 2013; Sumner and Jacobs, 2005).

In terms of evaluated models, the FAO-56 version of the Penman–Monteith model has been shown to provide a better prediction amongst other methods for green roofs (Berretta et al., 2014). However, many methods of estimating ET assume that moisture is in abundant supply (Poë et al., 2015), and several ET equations, including the FAO-56 version, have been found to overestimate ET for *Sedum* species common on green roof systems, even after correcting for water limited conditions (Starry, 2013; Tjaden, 2014). Thus, it has been suggested that agricultural models are not appropriate for estimating green roof ET when water is limited and one should limit the use of models to the well-watered condition, a condition that may not be applicable on a green roof (Voyde, 2011).

The purpose of this objective was to 1) characterize the evapotranspirative nature of *WaterShed's* sloped extensive green roof, 2) evaluate the effect of substrate water content, vegetation characteristics (LAI and percent cover) and microclimate characteristics (net radiation, air temperature, relative humidity, wind speed) on ET rates, and 3) compare measured ET to rates predicted with the FAO-56 Penman–Monteith model.

The determination of the evapotranspiration is important because rates of ET have been directly linked to stormwater retention efficiency (Starry, 2013) – we were also able to show its significance to thermal performance (Chapter 4). Furthermore, modelled ET is

often used in continuous hydrologic simulations to establish the efficiency and effectiveness of green roofs as a stormwater management tool (Voyde, 2011), thus investigating and calibrating ET equations used in predictive models is vital to the precision and accuracy of model outputs (Starry, 2013).

This study is also of significance because green roof ET has not been comprehensively evaluated in real conditions, and this is the first ET study to our knowledge of a residential system. The studied green roof is unique as it is sloped, modular and extensive, which is indicative of a design that is well-suited for many residential homes. Thus, we believe this analysis of observing ET helps show how a green roof operates under normal weather conditions considering the different stress types which can be experienced over longer periods of observation. Moreover, this research is of significance because preliminary studies indicate that the FAO-56 model should be limited in application to the well-watered condition. Since many modelling studies were found to be short-term or laboratory based, this study is unique in evaluating the application of the FAO-56 model on a full-scale green roof under real conditions.

5.2   Introduction

5.2.1   Evapotranspiration and Green Roof Benefits

It is thought that evaporation and transpiration processes are one of the biggest drivers of stormwater retention– during dry periods between storm events ET reduces substrate water content and regenerates green roof retention capacity (Poë et al., 2015). At the same time, ET plays a significant role in green roof cooling. When solar radiation is absorbed by a green roof, energy/latent heat is absorbed and dissipated to turn water into vapor. The latent energy associated with transpiration is typically a large part of the energy

balance, and a major pathway for removing heat created by solar and longwave absorption. The effect entails active cooling of the air immediately above the roof surface while reducing the overall heat transmission to the building (He and Jim, 2010; Ouldboukhitine et al., 2014; Poë et al., 2015; Tjaden, 2014).

5.2.2   Green Roof Evapotranspiration and Factors

Evapotranspiration can be obtained by direct measurement (Ouldboukhitine et al., 2014). Forces inducing ET losses are a function of the microclimate (i.e. solar radiation, air temperature, wind, relative humidity) and plant physiology. However, the rate at which these forces induce ET depends upon substrate–water characteristics (i.e. field capacity, permanent wilting point, permeability), any additional moisture storage capacity within the vegetation layer, and the plant's physiological response at the prevailing moisture content (Poë et al., 2015).

In terms of microclimate effects, highest daily ET rates are generally observed in warm summer conditions assuming abundant soil moisture (Poë et al., 2015). Furthermore, individual climatological factors like increasing the air convection rate near the canopy can effectively enhance ET from the foliage and soil layer (Raji et al., 2015). ET is also directly related to temperature– higher temperatures will lead to higher absolute cumulative losses as a greater proportion of the moisture that is held in the small pores of a substrate can be removed under increased levels of heat energy (Poë et al., 2015). There are also factors related to green roof design that specifically affect plant physiology and substrate–water characteristics such as the selection of vegetation and substrate composition and depth.

Regarding vegetation, the type, composition and stage of development influence the inherent physiological traits of a green roof, as different plant types evapotranspire at varying rates. This is related to plant properties such as stomatal resistance (rate that moisture gets through stomata) that controls water loses. More specifically, many extensive green roofs like the system in this study are planted with *Sedum* species that are characterized by crassulacean acid metabolism (CAM) photosynthesis. Under water stress conditions, CAM plants only open their stomata to metabolize at night when temperatures are cooler. ET loss is therefore lower than from C3 or C4 plants that evapotranspire soil–water during warm daylight conditions (He et al., 2017; Poë et al., 2015; Tabares-Velasco and Srebric, 2011; Tan et al., 2017).

Furthermore, the structure and texture of the growing medium governs its substrate–water properties (field capacity, permanent wilting point, retention and release characteristics). Related to these properties is green roof substrate water content, which is often regarded as the most critical factor for ET, with rates expected to decay exponentially with respect to time as available moisture reduces (Poë et al., 2015; Stovin et al., 2013; Tan et al., 2017). Moreover, it is believed that if there is sufficient soil moisture available, then plant type, stage of plant development and weather would affect ET most significantly (Tan et al., 2017).

Substrate depth studies are conflicting. Some findings reveal that ET is higher for intensive green roofs due to the thickness of soil providing more moisture and dense vegetation (Besir and Cuce, 2018; Hilten, 2005). On the other hand, Sun et al. (2014) indicated through a simulation model that a thicker medium layer tends to hold less water

in the top as compared to a thinner one. Given that vegetation like *Sedum* only uptakes water from the top layer, ET can be hindered (Sun et al., 2014).

Regarding green roof studies that have evaluated these factors in a system, Poe et al. (2015) found cumulative ET was highest from substrates of green roof microcosms with the greatest storage capacity, and significant differences in ET existed between vegetated and non-vegetated configurations. Furthermore, seasonal mean ET was initially affected by climate. Losses were 2.0 mm/day in spring and 3.4 mm/day in summer. However, moisture availability constrained ET, which fell to 1.4 mm/day then 1.0 mm/day (with an antecedent dry weather period of 7 and 14 days) in spring; compared to 1.0 mm/day and 0.5 mm/day in summer (Poë et al., 2015).

Conversely, Jim and Peng (2012) studied substrate moisture effect on water balance and thermal regime of a tropical extensive green roof and found that substrate moisture has a limited effect on ET and associated cooling. More specifically, they stated that the dry substrate on sunny days demonstrate an anomalous behavior of high ET which contradicts with previous studies which suggest that ET is proportional to substrate moisture. Instead, evapotranspiration was found to be largely dependent on solar radiation, relative humidity and wind speed. Jim and Peng gave several hypotheses as to why there was a lack of influence of initial substrate moisture on ET, one of them being that the shallow substrate allows solar energy to heat up the entire layer to drive up its temperature and hence ET water depletion (Jim and Peng, 2012).

5.2.3 FAO-56 Penman Monteith Model and Green Roof Application

Quantifying green roof evapotranspiration using an empirical approach provides valuable information to supplement current data; however, the process is time and labor intensive— using models to predict ET is more practical (Voyde, 2011). Although there are several models that achieve ET in a time step by taking into account a number of physical parameters (radiation, pressure, wind, etc.) and characteristics of the plants (Ouldboukhitine et al., 2014), there is no single universally-adopted approach for calculating potential ET; with several methods widely adopted, including Priestley-Taylor, Hargreaves, Thornthwaite and Penman–Monteith. There is a significant body of literature evaluating the suitability of each method, however, the FAO-56 version of the Penman–Monteith model has been adopted due to its physical basis (Poë et al., 2015), and because a few studies have shown the FAO-56 model to provide a better prediction amongst other methods for green roofs (Berretta et al., 2014).

For example, Hilten (2005) compared the FAO-56 Penman-Monteith and Hargreaves' methods for predicting ET for reference crop evapotranspiration from February to June 2005. The simpler method of Hargreaves' often resulted in over-prediction of ET during periods of cloudiness, and under-prediction during times of high wind compared to ET predicted using the FAO-56 method, which takes these effects into account directly (Hilten, 2005). Furthermore, Voyde (2011) tested several agricultural models and found the FAO-56 version of the Penman-Monteith to be one of two models that performed best at predicting ET for green roof trays using *D. australe* and *S. mexicanum* (Voyde, 2011).

The FAO-56 equation is derived from the Penman-Monteith equation (Equation

5-1) which combines two approaches– a mass balance approach and an energy balance approach– to calculate ET. The mass balance approach assumes water will diffuse away from the leaf surface in direct proportion to the vapor pressure deficit of the surrounding air and the velocity of the wind at any given time. The energy balance approach infers ET from the difference between energy going into and out of the leaf, assuming no storage component (Starry, 2013).

$$\textbf{Equation 5-1} \qquad ET = \frac{\Delta(Rn-G) - \rho_a c_p \frac{(e_s - e_a)}{r_a}}{\Delta + \gamma \left(1 + \frac{r_s}{r_a}\right)}$$

Described by Allen et al. (1998), the FAO-56 Penman–Monteith model (Equation 5-2) is the updated equation recommended by FAO (Food and Agricultural Organization of the UN) and the World Meteorological Organization to estimate reference potential ET from a grass surface (Allen et al., 1998; Berretta et al., 2014). The FAO-56 equation basically simplifies the standard Penman-Monteith equation used to predict ET by assuming the stomatal conductance and albedo of a reference grass crop. It is assumed that the definition for the reference crop is a hypothetical reference crop with crop height of 0.12 m, a fixed surface resistance of 70 s m^{-1}, and an albedo value (i.e., portion of light reflected by the leaf surface) of 0.23 (Starry, 2013; Zotarelli and Dukes, 2010). The reference surface most closely resembles an extensive surface of well-watered, actively growing green grass of uniform height that completely shades the surface (Hilten, 2005). Using the assumptions mentioned, the Penman-Monteith method reduces to the following equation:

Equation 5-2

$$ET_o = \frac{0.408\Delta(R_n\text{-}G)+\gamma\frac{c_n}{T+273}(e_s\text{-}e_a)u_2}{\Delta+\gamma\,(1+c_du_2)}$$

Where, ET_o = reference evapotranspiration from a well-watered crop (mm/day)

Δ = slope of saturation vapor pressure curve (kPa/°C)

R_n = net radiation at crop surface (MJ/m^2 day)

G = heat flux density to the soil (MJ/m^2 day)

γ = psychrometric constant (kPa/°C)

T = mean daily temperature 2 m above the ground (°C)

u_2 = mean daily wind speed 2 m above the soil surface (m/s)

e_s = mean saturation vapor pressure (kPa)

e_a = mean actual vapor pressure (kPa)

C_n = numerator constant that depends on reference crop

C_d = denominator constant that depends on reference crop

However, a major limitation of agricultural methods of estimating ET is that they assume that moisture is in abundant supply (Poë et al., 2015). As a result, several ET equations, including the FAO-56 version, have been found to overestimate ET for *Sedum* species common on green roof systems, even after correcting for water limited conditions (Starry, 2013; Tjaden, 2014).

To correct for overestimations the FAO-56 model has been further modified by a crop coefficient (K_C) to account for physiological attributes of different plant species and a coefficient (K_S) to account for drought stress (Starry, 2013). A crop coefficient approach

calculates ET for a specific crop (ET_C) while accounting for all the physical and physiological differences between the specific and reference crops (Equation 5-3) (Hilten, 2005). Moreover, Voyde describes K_C as the relative ability of a specific crop (and stage of growth) and soil surface to meet evaporative demand under well-watered conditions (Voyde, 2011). It is important to note however that K_C values are not well-defined for green roof species (Starry, 2013).

$$\textbf{Equation 5-3} \qquad ET_C = K_C ET_O$$

Where, ET_C is the expected crop evapotranspiration in the absence of environmental or water stresses,

K_C is the crop coefficient,

ET_O is reference ET calculated from the FAO-56 method

Furthermore, a key focus of research on adapting ET equations for green roofs has been to adjust the calculations for less than well-watered conditions. An adjustment can be made to the FAO-56 to account for the available water, by introducing a water stress coefficient multiplier, K_S (Chapter 8; Allen et al. 1998) which can be calculated using Equation 5-4 (Starry, 2013).

$$\textbf{Equation 5-4} \qquad K_S = \frac{TAW \text{-} D_r}{TAW \text{-} RAW}$$

Where, TAW is total available water,

D_r is root zone depletion, i.e., water deficit relative to field capacity,

RAW is water that is readily available to the plant

Once K_C and K_S coefficients are determined, Allen et al. suggests Equation 5-5 to determine actual (adjusted) crop evapotranspiration as a result of environmental or water stresses ($ET_{C\ adj}$) (Allen et al., 1998).

Equation 5-5 $\qquad ET_{C\ adj} = K_S K_C ET_O$

Where, $ET_{C\ adj}$ is the actual (adjusted) crop evapotranspiration because of environmental or water stresses,

K_C is the crop coefficient,

K_S is the water stress coefficient,

ET_O is reference ET calculated from the FAO-56 method

In terms of studies that have applied these coefficients when predicting green roof ET, Starry applied the FAO-56 model to green roof platforms while correcting for less than well-watered conditions using the K_S factor and found the model to overpredict ET. Since less was known about how to adjust this equation using crop coefficients to account for physiological adaptations by CAM plant species to drought stress, K_C factors for *Sedum* species (which were previously undefined) were then calculated using Equation 5-6, and used to further adjust the model (Equation 5-5). Note, Starry chose to estimate K_C values after estimating K_S, not before as recommended in the FAO-56 manual. This was done to eliminate variation due to known relationships between K_S and substrate water content before attempting to explain unknown variation (Starry, 2013).

Equation 5-6 $\qquad K_C = \dfrac{ET_A}{K_S ET_O}$

Where, K_C is the crop coefficient,

ET_A is actual measured evapotranspiration,

K_S is the water stress coefficient,

ET_O is reference ET calculated from the FAO-56 method

Despite both corrections being applied, the model was still observed to poorly predicted ET, and there were cases where the model even underpredicted ET (Starry, 2013). Thus, findings bring into question the applicability of the model to green roofs, especially considering the fact that it does not account for available water and physiological characteristics of CAM plants. Other researchers have already suggested that agricultural models are not appropriate for estimating green roof ET when water is limited and one should limit the use of models to the well-watered condition, a condition that may not be applicable on a green roof (Voyde, 2011). It should be noted however, that many of modelling studies were found were short-term or laboratory based. This study is unique in evaluating the application of the FAO-56 model over a 2-year study period on a full-scale green roof under real conditions.

5.3 Materials and Methods

5.3.1 Determining Actual Evapotranspiration

Evapotranspiration across a two-year observation period (July 2014-June 2016) was derived from the soil depletion method, which utilizes volumetric water content sensors (CS655 Water Content Reflectometer) within the substrate of the green roof (Figure 5-1) to determine changes in soil moisture between 15-minute sensor measurements ($\pm \Delta S = S_{t15}\text{-}S_{t0}$). Note, volumetric water content sensors operate by calculating the dielectric permittivity of the media from signal attenuation measurements

combined with oscillation period measurements. Finally, it applies the Topp equation to estimate VWC (m^3/m^3) from dielectric permittivity (Scientific, 2014).

With the soil depletion method, the assumption is that any gain in water ($+\Delta S$) is retention, and any water loss ($-\Delta S$) is due to ET or substrate drainage. Thus, any water loss in between rain events can be attributed to ET while substrate drainage was assumed to largely occur during storms. Because ET is a very small portion of the overall water balance of a green roof during storms, it was estimated to be equal to the average rate of ET between one rain event and the next. Once these values were calculated, total ET per day (mm/day) was determined. It should be noted that since ET was attributed to the change in water status, the soil depletion method could only be confidently applied during warmer months (May-October). During colder months, plant cover and ET diminishes, and any water loss over prolonged periods of time could be due to substrate drainage.

Figure 5-1 Soil Water Content Reflectometer sensors were installed approximately 1.5 in (3.81 cm) below the green roof surface with probes parallel to the roof and perpendicular to the slope (Image credit: Scott Tjaden).

5.3.2 Factors affecting Evapotranspiration

Correlation analyses were performed to evaluate the effect of substrate water content, vegetation characteristics (LAI and percent cover) and microclimate characteristics (net radiation, air temperature, relative humidity, wind speed) on evapotranspiration rates. Average daily substrate water content was determined using the same CS655 Water Content Reflectometers described in the previous section, while vegetation characteristics were measured monthly and compared to monthly ET rates. Note, LAI was measured in addition to percent cover because it allowed us to measure the canopy foliage density of the green roof rather than simply area covered (Raji et al., 2015)— supplementary information on the methodology used to calculate LAI and percent cover can be found in Appendix C.

Finally, average daily values of air temperature and relative humidity (CS215-L Temperature and Relative Humidity Probe)¸ as well as wind speed (05103-L Wind Monitor) were measured with sensors at the onsite weather station, while net radiation (NR01-L 4-Component Net Radiation) was measured at the green roof. Supplementary information regarding the brand, quantity and location of each sensor in respect to others can be found in Appendix A. It should be noted that since net radiation was the sum of the incoming shortwave and longwave minus the sum of the reflected shortwave and emitted longwave, it was considered the energy input to the green roof.

5.3.3 Predicting Evapotranspiration

To predict evapotranspiration from a plant and surface, the FAO-56 Penman-Monteith method computes ET for a reference surface using standard meteorological data along with radiation and heat flux data. The reference surface is a hypothetical reference

crop with an assumed crop height of 0.12 m, a fixed surface resistance of 70 s m^{-1} and an albedo of 0.23. The reference surface most closely resembles an extensive surface of well-watered, actively growing green grass of uniform height that completely shades the surface.

Equation 5-7
$$ET_o = \frac{0.408\Delta(R_n\text{-}G)+\gamma\frac{900}{T+273}(e_s\text{-}e_a)u_2}{\Delta+\gamma\,(1+0.34u_2)}$$

Using the assumptions mentioned, the Penman-Monteith method reduces to Equation 5-7 (Hilten, 2005), where the C_n numerator constant that depends on the reference crop is 900 and the denominator constant (C_d) that depends on the reference crop is 0.34. Note, that when applying the equation the use of onsite, versus regional, climatic data considerably improves agreement between model estimates and actual measurements (Marasco et al., 2015).

The format of the equation allows calculations of ET on short intervals and in many studies ET is calculated using this method on hourly intervals that are summed to daily totals (Hilten, 2005). According to Zotarelli and Dukes, if the model is applied using hourly data, the constant value "900" should be divided by 24 for the hours in a day and the R_n and G terms should be expressed as MJ m^{-2} h^{-1} (Zotarelli and Dukes, 2010). Since our data was in 15-minute intervals, the model was adjusted accordingly and summed over the day (mm/day).

Sensor data measuring net radiation (Rn), substrate heat flux (G), wind speed (u_2), and ambient green roof temperature (T) were inputted into the equation. Furthermore, Δ which is the slope of saturation vapor pressure curve (kPa/°C) was calculated with Equation 5-8,

Equation 5-8
$$\Delta = \frac{4098\left[0.6108\exp\left(\frac{17.27T}{T+237.3}\right)\right]}{T+(237.3)^2}$$

γ which is the psychrometric constant (kPa/°C) was calculated with Equation 5-9,

Equation 5-9
$$\gamma = 0.000665P$$

Where, $P = 101.3\left[\frac{293-0.00065z}{293}\right]^{5.26}$

and z = elevation above sea level, m.

e_s which is the mean saturation vapor pressure (kPa) was calculated with Equation 5-10,

Equation 5-10
$$e_s = 0.6108\exp\left[\frac{17.27T}{T+237.3}\right]$$

and finally, e_a which is the mean actual vapor pressure (kPa) was calculated using Equation 5-11 (relative humidity was measured at the onsite weather station).

Equation 5-11
$$e_a = RH \times e_s$$

For detailed information on how to calculate ET step-by-step using the FAO-56 model, we recommend consulting Zotarelli and Dukes (2010).

5.4 Results and Discussion

5.4.1 Evapotranspiration Analysis

As described in Table 5-1, average ET rates were 25.47 ± 7.05 mm/month and 0.81 ±0.24 mm/day, with the lowest rates observed in August. It is difficult to compare ET rates

to other studies, however, Starry reported an ET range for *S. album* of 2.15 to 0.28 mm/day, and a range of 2.91 to 0.12 mm/day for *S. kamtschaticum* (after dividing by the surface area of the containers) (Starry, 2013). Furthermore, Voyde summarized and reported ET from several studies. The range of daily ET for green roofs in the well-watered condition was 0.1–6.6 mm/day. When water became scarce, ET from both planted and unplanted trials was <1 mm/day, in all temperature ranges (Voyde, 2011). Finally, Poe et al. reported the ranges of cumulative ET for microcosms following a 28-day dry weather period; ranges were 0.6–1.0 mm/day in spring and 0.7–1.25 mm/day in summer. These ranges reflect the influence of configuration on ET which will be discussed shorty (Poë et al., 2015).

Table 5-1 Summary of green roof evapotranspiration.

	Total Monthly ET (mm)	Average Daily ET (mm)
May	29.07	0.74 ± 0.75
June	37.29	1.24 ± 1.00
July	25.18	0.89 ± 1.50
August	18.35	0.59 ± 0.49
September	18.89	0.63 ± 0.69
October	29.47	0.95 ± 0.50
Average	25.47 ± 7.05	0.81 ± 0.24

Next, we aimed to explore the factors driving ET of the sloped, extensive green roof. Correlation analyses (Table 5-2) revealed ET was most significantly correlated to substrate water content ($R^2 = 0.4841$). ET was also correlated to net radiation ($R^2 = 0.0429$), while ambient temperature, relative humidity, wind speed and vegetation characteristics (LAI and percent cover) were not related.

The influence of substrate moisture was clear when a linear regression analysis was plotted (Figure 5-2)— highest rate of ET (4.96 mm/day) was observed when substrate water content was 7.19 mm. This relationship is further seen in a monthly time series that was plotted; average daily ET closely followed trends in substrate moisture (Figure 5-3). From this figure it can also be seen that lowest substrate moisture was observed in August (1.54 mm/day), which would explain why ET was lowest this month (0.59 ± 0.49 mm/day).

Overall, the observed trend was expected as generally green roof substrate water content is often regarded as the most critical factor for ET to occur, with rates expected to decay exponentially with respect to time as available moisture reduces (Poë et al., 2015; Stovin et al., 2013; Tan et al., 2017). Moreover, it is believed that if there is sufficient soil moisture available, then plant type, stage of plant development and weather would affect ET most significantly (Tan et al., 2017).

Table 5-2 Correlation coefficients between ET, substrate water content, vegetation characteristics and microclimate factors. Where, [a] signifies correlation is significant at the 0.05 level, while NS indicates no significance.

	Average Daily Value	**Correlation**
Substrate Water Content	2.88 mm	$R^2 = 0.4841$ [a]
Net Radiation	112.5 W/m^2	$R^2 = 0.0429$ [a]
Ambient Temperature	20.1 °C	NS
Relative Humidity	73.5%	NS
Wind Speed	0.523 m/s	NS
LAI	1.50 m^{-2}	NS
Vegetation Cover	55.6%	NS
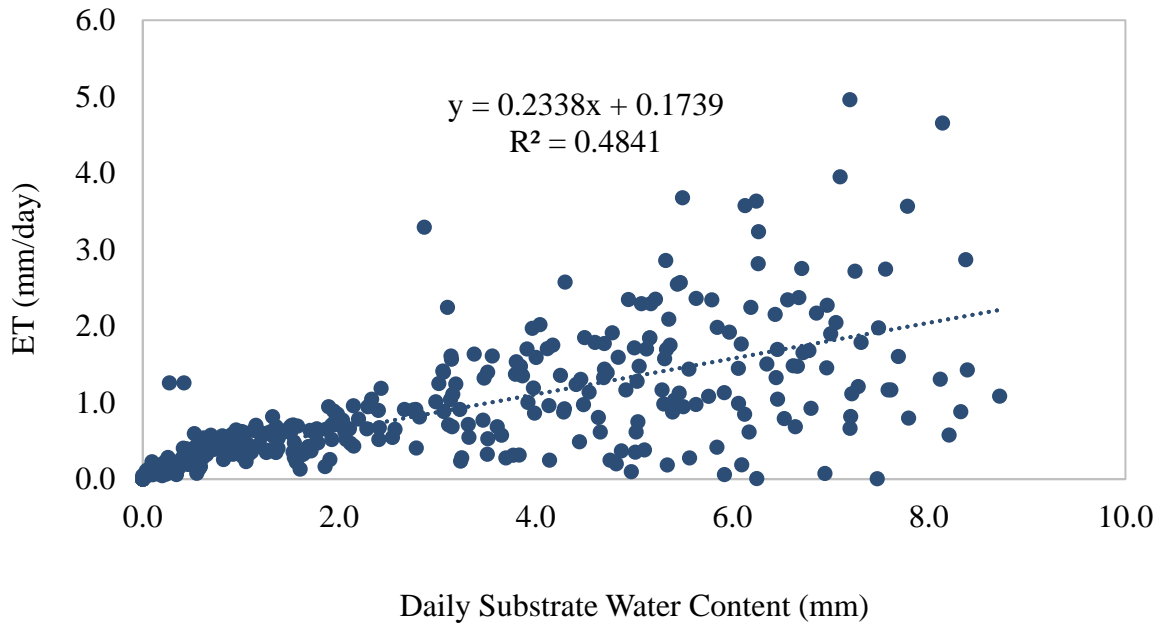
Figure 5-2 ET was most correlated to substrate water content.
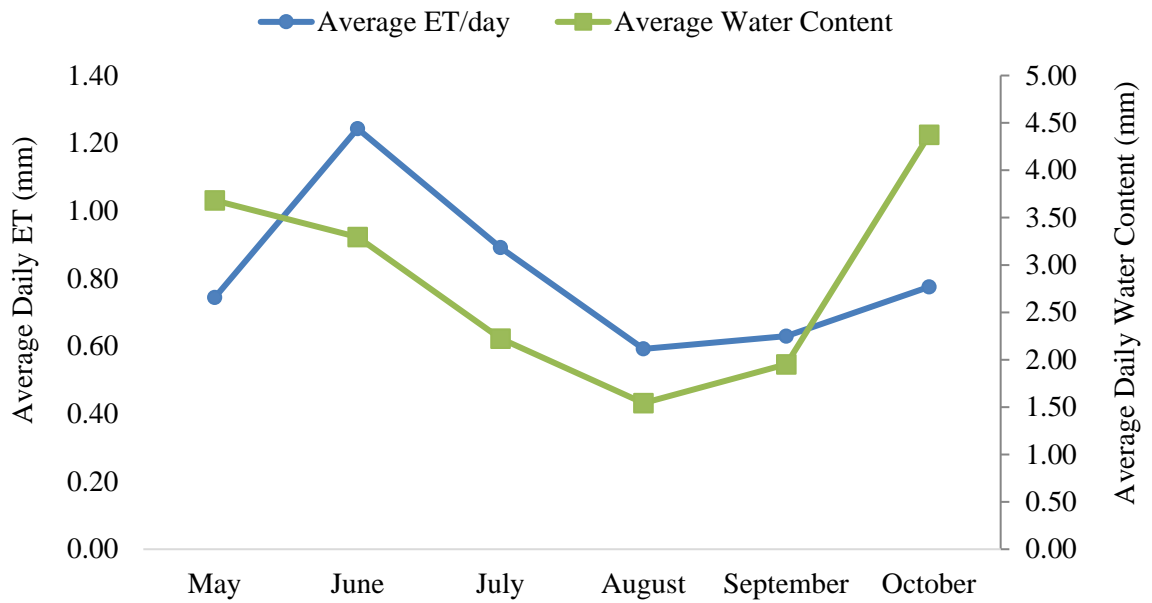
Figure 5-3 Average ET per day and daily substrate water content.

More specifically, Voyde (2011) concluded after reviewing several green roof ET studies that water availability had the greatest overall influence on ET rates. Additional influential factors identified were radiation, relative humidity, temperature, roof slope, roof aspect, and plant architecture (Voyde, 2011). Furthermore, Poe et al. (2015) reported the ranges of cumulative ET for microcosms following a 28-day dry weather period to be 0.6–1.0 mm/day in spring and 0.7–1.25 mm/day in summer. These ranges reflect the influence of configuration on ET. More specifically, cumulative ET was highest from substrates with the greatest storage capacity (significant differences in ET existed between vegetated and non-vegetated configurations) (Poë et al., 2015).

The influence of available moisture could also be seen when they explored ET across seasons— losses were 2.0 mm/day in the spring and 3.4 mm/day during the summer, which fell to 1.4 mm/day then 1.0 mm/day (with an antecedent dry weather period of 7 and 14 days) in spring; compared to 1.0 mm/day and 0.5 mm/day in summer. Overall, they concluded that seasonal climate differences were significant to ET and that the decay of ET over time reflects the effects of reduced moisture availability (Poë et al., 2015). Finally, in another study researchers found daily moisture loss rates were influenced by both temperature and moisture content, with reduced moisture loss/ET when soil moisture was restricted (the presence of vegetation also resulted in higher daily moisture loss) (Berretta et al., 2014).

It is likely that substrate moisture was the strongest driver of ET due to the media being limited in water– average daily water content was 2.88 mm ($0.045 \ m^3/m^3$) during the warm season, which is low when compared to other findings. More specifically, Starry et al. (2014) studied photosynthesis and water use by *Sedum album* and *Sedum*

171

kamtschaticum. In addition to observing that ET was reduced for both species with decreasing substrate moisture, they suggested threshold water contents. More specifically, since the lowest average substrate water contents observed for *S. album* and *S. kamtschaticum* were 0.065 m^3/m^3 and 0.04 m^3/m^3, respectively (at this point leaf turgor was visibly reduced for both species, but they quickly recovered upon rewatering), they recommended thresholds for both species at 0.18 and 0.13 m^3/m^3 for *S. album* and *S. kamtschaticum* respectively, which are well above the average water content observed in our study. Thus, it is likely under that these dry conditions, *Sedum* species are being induced into crassulacean acid metabolism (CAM) photosynthesis. More specifically, many extensive green roofs like the system in this study are planted with *Sedum* species that are characterized by CAM photosynthesis. Under water stress conditions, CAM plants only open their stomata to metabolize at night when temperatures are cooler. ET loss is therefore lower than from plants that evapotranspire soil–water during warm daylight conditions (He et al., 2017; Poë et al., 2015; Tabares-Velasco and Srebric, 2011; Tan et al., 2017).

Overall, these findings suggest that if the green roof was well-watered above the thresholds suggested by Starry et al. (2014), ET rates would likely have been higher. Furthermore, results have implications for the green roof industry as *Sedum* are widely implemented in green roof installations in the American Northeast and Midwest, and are considered successful in terms of plant coverage and survival, especially due to their drought tolerance and CAM metabolism (Starry et al., 2014). It is likely that the extensive sloped nature of the studied roof results in an extremely dry climate that even drought tolerant species may not be well adapted to. Furthermore, this phenomenon is likely why

vegetation characteristics were consistently low throughout the two-year study period (across both seasons LAI was 1.35 m^{-2} ± 0.37 and percentage cover was 53.9% ± 12.3— according to the manufacturer, minimum installation soil coverage of planted modules is 95%), which would in turn explain why vegetation characteristics were not correlated to ET.

Since green roof hydrological characteristics are determined by several factors such as the characteristics of growing substrate and drainage elements of green roof systems (Tan et al., 2017), improving the water status of the green roof by irrigating, modifying its depth or substrate composition, or implementing a water retention layer may be beneficial to plant health and ET. Moreover, it is likely that once sufficient soil moisture is achieved, then other factors like plant type, stage of plant development and weather would affect ET most significantly (Tan et al., 2017).

5.4.2 FAO-56 Penman Monteith Model

With such a dry substrate, it was not surprising that the FAO-56 model did not predict ET well when compared to measured values (Figure 5-4), and most of the time it was observed to overpredict ET. This was further confirmed as when the ratio of actual to predicted ET was plotted against substrate water content (Figure 5-5), a significant correlation was observed (R^2 = 0.5546). Essentially as substrate moisture increased, the model was more likely to predict ET correctly– where the closer the ratio is to 1, the more accurate the FAO-56 prediction. Interestingly, the model is also more likely to overpredict ET with greater substarte moisture.
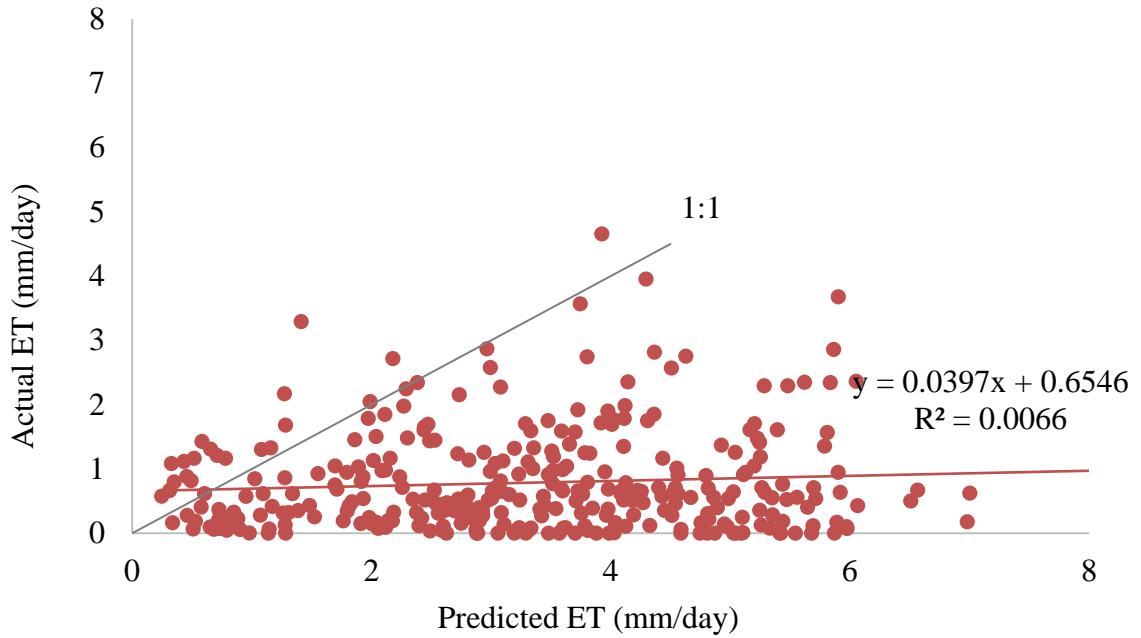
Figure 5-4 The FAO-56 Penman Monteith model overpredicts ET.
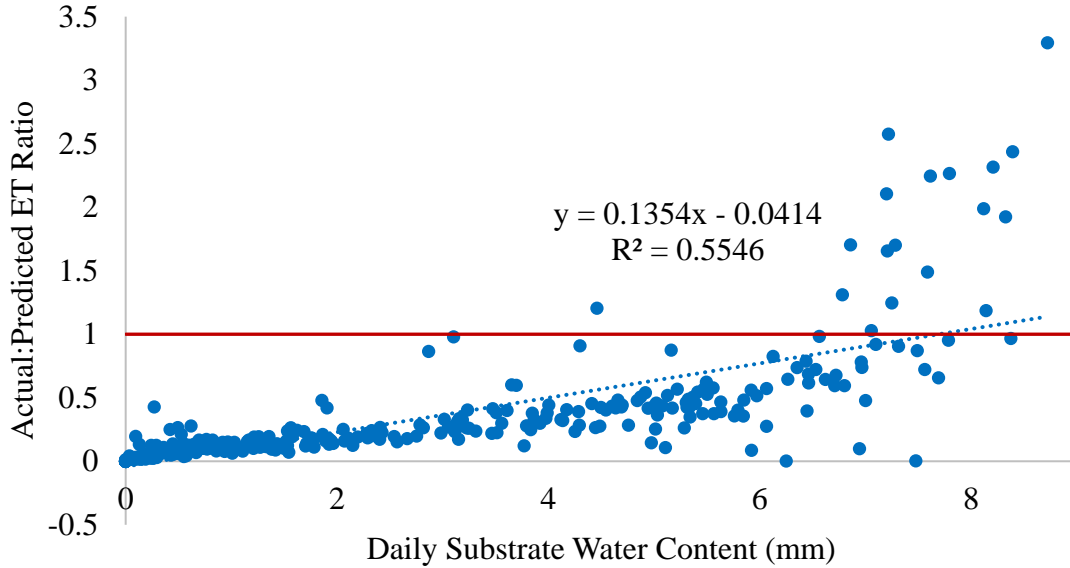
Figure 5-5 The ratio of actual to predicted ET was correlated to substrate water content, where the closer the ratio is to 1, the more accurate the FAO-56 prediction. Although the model generally improves in accuracy with substrate moisture, it is also more likely to overpredict ET at higher substarte moisture content.

Overall, these results were expected considering the FAO-56 model has been found to overestimate ET for *Sedum* species common on green roof systems, even after correcting for water limited conditions (Starry, 2013; Tjaden, 2014). For example, this study was partially a long-term continuation of research by Tjaden (2014), who studied the application of the FAO-56 model to the same green roof system in this study from June-September of 2014. It was found that predicted ET fluctuated with over- and underestimating ET rates. Tjaden hypothesized this was related to the lack of available soil moisture for the thin, sloped green roof (Tjaden, 2014).

More specifically, Tjaden stated that measured ET drastically increased during times following precipitation, and decreased at a diminishing rate between rain events due to reduced moisture availability. Tjaden went on to conclude that because substrate moisture is not a parameter in the FAO-56 model, it is imperative that caution be used when applying the model to green roofs because they can be water-stressed. He suggested applying additional variables to the equation to better predict ET, such as the K_C and K_S values (Tjaden, 2014).

Interestingly, Starry (2013) found the model to inaccurately predict ET even after applying K_C and K_S values to correct the model. More specifically, Starry examined the accuracy of the FAO-56 equation for experimental green roof platforms planted with *Sedum album*, *Sedum kamtschaticum*, and *Sedum sexangulare*. First, it was found that the model consistently overpredicted rates of ET even though it was corrected (K_S) for having less than well-watered conditions. This disparity was greatest during the summer months, when predicted daily ET rates were nearly double measured rates (Starry, 2013).

Since less was known about how to adjust the equation using crop coefficients to account for physiological adaptations by CAM plant species to drought stress, Starry then calculated species specific K_C values— Starry chose to estimate K_C values after estimating K_S, not before as recommended in the FAO-56 manual. This was done to eliminate variation due to known relationships between K_S and substrate water content before attempting to explain unknown variation. It was found that even after K_C adjustments, the FAO-56 still over-predicted measured ET, although the data was much closer to a 1:1 line after the second adjustment (Starry, 2013).

Overall, results have major implications to applying the FAO-56 model to green roofs as they typically not irrigated, and actual ET rates fall with time following a rainfall event as available moisture becomes increasingly restricted (Berretta et al., 2014). Moreover, Poe et al. (2015) state that since many methods of estimating ET assume that moisture is in abundant supply, it is important to differentiate potential evapotranspiration (PET) from ET, as they will only be equal for the relatively short period of time when the green roof is at, or very near to maximum moisture storage capacity. Thereafter, ET will be constrained by the soil moisture deficit (Poë et al., 2015).

Poe et al. go on to state that any models that function on the premise that ET equals PET will typically overpredict ET losses, and that the decay of ET as a proportion of PET (ET/PET) is a key modelling parameter that must account for moisture availability– moisture availability is variably influenced by climatic conditions and plant and soil characteristics (Poë et al., 2015). On the other hand, Voyde (2011) states that a K_C value of 1.0 may not be a realistic assumption for green roofs because it suggests that green roof

species are able to transpire at the same rate as a well-watered actively growing grass or alfalfa crop (Voyde, 2011).

Altogether, these findings indicate that it is likely that even if we corrected our modeled results, the FAO-56 model may still not predict ET with precision and accuracy. Future green roof studies should test the model's accuracy to extensive green roofs in well-watered conditions, and at various water contents to determine threshold water contents where predictions are likely to be closer to actual values. This would enable researchers to have a better understanding of when the model is applicable, and should lead to the development of more accurate modelling approaches for long-term simulations. Such predictions are necessary to support decision-making in stormwater management; both in terms of projecting green roof performance in response to changing climatic scenarios and for estimating plant stress conditions (Berretta et al., 2014).

5.5   Summary and Conclusions

The purpose of this objective was to 1) characterize the evapotranspirative nature of *WaterShed's* sloped extensive green roof, 2) evaluate the effect of substrate water content, vegetation characteristics (LAI and percent cover) and microclimate characteristics (net radiation, air temperature, relative humidity, wind speed) on ET rates, and 3) compare green roof ET to rates predicted with the FAO-56 Penman–Monteith model.

We believe this analysis of observing ET helped show how a green roof operates under normal weather conditions considering the different stress types which can be experienced over longer periods of observation. Moreover, this research is of significance

because preliminary studies indicated that the FAO-56 model should be limited in application to the well-watered condition. Since many modelling studies were found to be short-term or laboratory based, this study is unique in evaluating the application of the FAO-56 model on a full-scale green roof under real conditions.

Overall, it was observed that average ET rates were 25.47 ± 7.05 mm/month and 0.81 ±0.24 mm/day, with the lowest rates observed in August (August had the lowest substrate water content). ET was most tied to substrate moisture and to a lesser extent net radiation. It was hypothesized that soil moisture was the strongest driver of ET due to the substrate of the sloped extensive green roof being limited in water– average daily volumetric water content was 2.88 mm (0.045 m^3/m^3) during the warm season, which is low when compared to thresholds recommended by Starry et al. for *Sedum* spp. (0.18 and 0.13 m^3/m^3 for *S. album* and *S. kamtschaticum*, respectively) (Starry et al., 2014).

Based on this observation, it is likely that under these dry conditions *Sedum* species are stressed and being induced into CAM photosynthesis. It was hypothesized that if the green roof was well-watered above suggested thresholds (0.18 and 0.13 m^3/m^3 for *S. album* and *S. kamtschaticum*, respectively), ET rates would likely improve. Moreover, it is likely that once sufficient soil moisture is achieved, then other factors like plant type, stage of plant development and weather would affect ET most significantly (Tan et al., 2017).

We also noted the implications of water content thresholds for the green roof industry as *Sedum* are widely implemented in green roof installations in the American Northeast and Midwest, and are considered successful in terms of plant coverage and survival, especially due to their drought tolerance and CAM metabolism (Starry et al., 2014). It is likely that the extensive sloped nature of the studied roof results in an extremely

dry climate that even drought tolerant species are not well adapted to. Thus, improving the water status of the green roof by irrigating, modifying its depth and substrate or implementing a water retention layer depending on the site/region may be beneficial to plant health and ET (Tan et al., 2017).

Finally, we concluded that the FAO-56 Penman-Monteith does not accurately predict ET in its original form when moisture availability is low. This is because the original Penman-Monteith equation was intended for a well-watered system with tall fescue like grass. Although it is possible that applying a K_S water stress coefficient in conjunction with a K_C crop coefficient would have resulted in more accurate predictions, Starry (2013) did so with no success. As a result, we recommended future green roof studies test the model's accuracy to extensive green roofs in well-watered conditions, and at various water contents to determine threshold water contents where predictions are likely to be closer to actual values. This would enable researchers to have a better understanding of when the model is applicable, and should lead to the development of more accurate modelling approaches for long-term simulations. Such predictions are necessary to support decision-making in stormwater management; both in terms of projecting green roof performance in response to changing climatic scenarios and for estimating plant stress conditions (Berretta et al., 2014)

Chapter 6 Green Infrastructure Sustainability and Resilience

6.1   Objective

In 2016, over half (54.5%) of the world's population lived in urban settlements, and it is estimated that by 2030, urban areas will house 60% of people globally (United Nations, 2016). To meet the rapid rise of populations, a new city is needed to accommodate one million new urban inhabitants around the world every week (Raji et al., 2015). However, the rapid rise and development of large urban centers in the developing world will be among the greatest challenges to ensuring human well-being and a viable global environment (Borgström et al., 2006).

First, there are tremendous consequences to constructing buildings to meet rising populations– construction practices are one of the major contributors of environmental problems, particularly due to the utilization of non-renewable materials. United States Green Building Council estimates for example, that commercial and residential construction buildings release 30% of greenhouse gases and consume 65% of electricity in the US (Bianchini and Hewage, 2012a). Furthermore, urban development has resulted in the loss of important natural ecosystems and services (Borgström et al., 2006). For example, without urban vegetation, many cities are suffering from the effects of UHIs– thermal energy requirements now account for 36% of primary energy use in buildings in the U.S. (Borgström et al., 2006; Ürge-Vorsatz et al., 2012). Due to this and other well-known environmental issues (i.e. climate change, water quality degradation, deforestation, waste generation, etc.), the concept of sustainability has been introduced to the urban communities.

Green infrastructure– such as green roofs, bioretention areas, porous pavements, rain barrels/cisterns, and green roofs– is increasingly being recognized as a sustainable approach to urban environmental problems. GI is defined as natural and constructed green spaces that utilize vegetation, soil, and other components to replicate natural processes that provide benefits for human populations in the urban setting such as stormwater management, mitigation of the UHI effect, decreased energy use, improved air and water quality, carbon sequestration, benefits to human physical and mental health, access to recreational opportunities, and improved habitat for biota (Law et al., 2017).

However, although GI has been touted as a sustainable technology, it is currently designed to manage downstream impacts of urbanization without consideration of broader, "up-stream" environmental, economic, and social impacts associated with its implementation and operation. This gap in knowledge incites unanswered questions such as: Do GI benefits outweigh these "up-stream" environmental impacts? What and where are the non-monetary costs and benefits throughout the life of a practice? Are some GI practices "greener" than others (Flynn and Traver, 2013)? This final question is pertinent as there are many types of GI, and there has been limited comparison of sustainability between types (Law et al., 2017). Finally, GI sustainability relative to gray infrastructure or natural ecosystems in which they are designed to mimic have not been fully explored.

The most prominent environmental accounting methods currently used to explore GI sustainability are cost-benefit analysis (CBA) and life-cycle assessment (LCA), however each model has its limitation. One of the most controversial criticisms of CBA is that it evaluates environmental impacts and ecosystem services to humans using economic analysis when many environmental impacts such as human life and some irreversible

effects on ecology are not convertible into monetary values (Reza, 2013). Furthermore, LCA has been criticized as a utilitarian user-side approach to sustainability, only focusing on environmental impacts due to resource consumption and emissions while ignoring the work of ecosystems to provide 'freely available' services and products (e.g. rainfall, soil organic matter, etc.) (Reza, 2013). Thus, it has been proposed that sustainability cannot be assessed simply by counting mass and energy flows, but by accounting for the direct and *indirect* energy supporting flows. *Emergy* is proposed as a more holistic ecological accounting method for determining if the direct and indirect energy requirements of GI are less than produced benefits over each system's life-span.

In addition to sustainability, resilience has become an important goal of many communities as global populations have become increasingly urbanized and as climate change progresses— with many communities viewing GI as a means of improving urban resilience due the multifaceted benefits they provide. Resilience, as applied to integrated systems of people and the natural environment, has three interrelated characteristics, one of them being the amount of change a system can undergo and still retain the same controls on function and structure. In the resilience discourse, management of diversity per se is considered to be a key attribute for building resilience in complex adaptive systems (Colding and Barthel, 2013). This is because diversity functions as insurance– it spreads risks, creates buffers, and opens up for multiple strategies from which humans can learn in situations when uncertainty is high. Diversity also plays an important role in the reorganization and renewal processes of disturbed systems (Colding and Barthel, 2013), and makes systems less vulnerable to natural and human-induced changes such as resource availability fluctuations.

In ecology, the Shannon diversity index, has been used often to assess ecosystem diversity (Ulgiati et al., 2011)— since GI benefits are diverse and not easily 'additive', it has been proposed that the environmental accounting technique of *emergy* evaluation could be extended using information theory (the basis of the Shannon diversity index) to enumerate the energetic diversity of GI and provide a new metric of resilience. Previously, this system-level *emergy diversity index* (derived from the Shannon diversity index) was used to quantify the diversity of species in ecological systems, and diversity of energy and resources in economic systems (Brown et al., 2006; Ulgiati et al., 2011). The new emergy based indicator differs from the typical way of estimating *H*— which is based on simply counting individuals, biomass or other stocks— because it uses the flows of energy and materials in *emergy* terms. Where, resilient systems are thought to be supported by a variety of emergy flows that make it more likely to develop complex structures, while systems that only rely on a small set of sources out of a large number of potentially available ones are thought to possess a built-in fragility that may determine their collapse in times of shrinking or changing resource basis (Ulgiati et al., 2011).

Altogether, the purpose of this final objective was to explore the sustainability and resilience of *WaterShed's* green roof, constructed wetland and bioretention relative to a wastewater system and natural forest using emergy synthesis. *Emergy* enabled us to evaluate if the direct and indirect energy requirements of GI are less than produced benefits over each system's life-span. Furthermore, by integrating information theory with emergy evaluation, we were able to quantify how much the green roof, CW and bioretention increase the flow of information at the ecological, environmental, social and economic levels compared to a typical wastewater treatment plant and natural forest.

This research is unique because we were able to quantify GI benefits for the sustainability and resilience analyses using a combination of live sensor and published data. Furthermore, this research is of significance as communities are using GI as a means of mitigating and adapting to urbanization and climate change, however the sustainability and resilience of different GI has not been well characterized. Furthermore, GI sustainability and resilience relative to gray infrastructure or natural ecosystems in which they are designed to mimic have not been fully explored. Finally, sustainability analyses are crucial to improving GI design, operation and maintenance, which can vary greatly across regions.

6.2   Introduction

6.2.1   From Gray to Green Infrastructure

The rapid rise and development of large urban centers in the developing world will be among the greatest challenges to ensuring human well-being and a viable global environment. This is because urban development frequently decreases the amount and quality of green space, which leads to fragmentation and isolation of the remaining parcels of natural ecosystems. We are increasingly understanding that human well-being and a viable global environment depend on these natural ecosystems and the services they provide (Borgström et al., 2006).

Many of these critical ecosystem services are related to energy-water balance. For example, without urban vegetation many cities are suffering from the effects of UHIs–thermal energy requirements now account for 36% of primary energy use in buildings in the US (Borgström et al., 2006; Ürge-Vorsatz et al., 2012). Furthermore, an increase in area of impervious surfaces has caused stormwater runoff problems. Runoff has put heavy pressure on water resources in many semiarid regions, while in other regions, it has

degraded water quality and increased flood risks (Czemiel Berndtsson, 2010; Rowe, 2011; Yang and Cui, 2012). There are also major energy requirements and GHG emissions associated with managing stormwater– a typical medium sized wastewater treatment plant in the U.S. consumes 1200 kWh of energy to treat one million gallon of wastewater (Flynn and Traver, 2013). Other ecosystem services green spaces provide include reduced air pollution, noise pollution, and enhanced health. Furthermore, urban vegetation has important recreational and cultural values for urban citizens (Borgström et al., 2006).

To meet these challenges, many urban communities have traditionally relied heavily on engineered solutions such as air conditioning systems and stormwater infrastructure. However, conventional 'hard' engineering solutions to restoring urban energy-water balance are vulnerable and failure prone, especially considering climate change projections of more intense storms and heat waves. This is because conventional infrastructure relies on a few nonrenewable energies and resources to provide cities with one or two benefits, often with unintended consequences (Figure 6-1).

Figure 6-1 Traditional infrastructure relies on a few nonrenewable energies and resources to provide cities with one or two benefits, often with unintended consequences.

For example, increasing reliance on fossil fuels to meet building thermal demands makes cities vulnerable to energy shortages, while there is the unintended consequence of further contributing to climate change as fossil fuel use results in greenhouse gases being emitted to the atmosphere. Furthermore, in many communities there are combined sewer systems to manage raw sewage and stormwater for transport to fossil fuel dependent wastewater treatment plants. There are unintended consequences associated with this as runoff of heavy storms frequently overwhelm gray infrastructure, resulting in combined sewers overflowing into water bodies with adverse effects (Czemiel Berndtsson, 2010; Rowe, 2011).

Due to these challenges the concept of sustainability has been introduced to the urban communities, with green infrastructure– such as green roofs, bioretention areas, porous pavements, rain barrels/cisterns, and green roofs– increasingly being recognized as a sustainable approach to urban environmental problems. GI is defined as natural and constructed green spaces that utilize vegetation, soil, and other components to replicate natural processes that provide benefits for human populations in the urban setting. In addition to stormwater management GI can provide multiple benefits including mitigation of the UHI effect, decreased energy use, improved air and water quality, carbon sequestration, benefits to human physical and mental health, access to recreational opportunities, and improved habitat for biota. Many of these additional benefits play a role in urban settings mitigating and adapting to the effects of changing climate, and can have positive impacts on local economies (Law et al., 2017). As a result, GI are increasingly seen as a more sustainable alternative to traditional engineering practices because in providing these multitude of benefits, they make use of the natural abilities and functions

of ecosystems (e.g., soil, plants, bacteria)– Figure 6-2.

Figure 6-2 Green infrastructure is increasingly seen as a more sustainable alternative to traditional engineering practices because in providing a multitude of benefits, they make use of the natural abilities and functions of ecosystems.

6.2.2   Sustainability Assessments

In recent years, sustainability appraisals of the built environment have gained increasing focus and have resulted in the integration of sustainable development policies and legislations in day-to-day decision-making. Regarding the goal of sustainable development, built environment construction and operation processes would shift from using nonrenewable to renewable resources and fuels, and from waste productive options to reuse and recycling alternatives (Reza, 2013).

Performing more holistic and system-based sustainability appraisals can provide improved understanding to make informed decisions on the basis of choosing lower impact materials and design alternatives, and result in the creation of a built environment that is in balance with the local climate, traditions, culture, and surrounding environment (Reza,

2013). According to Reza (2013), in the field of construction and infrastructure, sustainability tools can be classified into three main categories:

- Sustainability rating systems such as: LEED (U.S.) and BREEAM (U.K.)

- Environmental Systems Analysis tools such as: material flow analysis, embodied energy analysis, cost-benefit analysis, ecological footprint, and emergy synthesis

- Life Cycle Assessment based tools such as: BEES (U.S.) and ATHENA (Canada)

In terms of GI, cost-benefit analysis and life cycle assessment were found to be commonly applied sustainability tools. CBA is a socio-economic based method which estimates the total impacts (including environmental impacts) of a project, investment, or decision on society by measuring social costs and benefits. In CBA, costs and benefits are expressed on a basis of monetary values and are adjusted based on the time value of money. The main propose of CBA is to predict if the benefits of a policy outweigh its costs, and by how much relative to other alternatives (Reza, 2013). A summary of major CBA findings of GI can be found in Table 6-1 and Table 6-2.

LCA is an environmental management tool that considers all material and energy flows from "cradle to grave" including, extraction and provisions of raw materials, manufacturing, transportation, operation and maintenance activities, reuse or recycling, and finally disposal, decommissioning, or replacement. LCA can be used to evaluate impacts of a product, process, service, or other complex systems throughout all stages of its life cycle. Studying complex systems, such as green infrastructure practices, through a life cycle lens allows for the estimation of cumulative impacts and net impacts of these systems (Flynn and Traver, 2013). A summary of major LCA findings of GI can be found in Table 6-3.

188

Table 6-1 Cost-benefit analysis studies of green infrastructure.

Cost-Benefit Analyses of Green Infrastructure
Summarizing U.S. EPA data, Montalto et al. indicates that while the installation costs of green infrastructure technologies (porous pavement, porous concrete, infiltration/detention basins) are generally more expensive than conventional stormwater infrastructure, they can be more cost-effective on a volumetric basis (Montalto et al., 2007).
Researchers concluded that tax incentives and the overall combination of green systems can make installation and the maintenance costs economically sustainable during the life span of a greening system (Perini and Rosasco, 2016)
In general, installing green roofs is a low risk investment– the probability of profits out of this technology is much higher than the potential financial losses. It is evident that the inclusion of social costs and benefits of green roofs improves their value (Bianchini and Hewage, 2012b).
The net present value (NPV) of the studied green roof ranged from 10-14% more expensive than its conventional counterpart. A reduction of 20% in green roof construction cost would make the social NPV of the practice less than traditional roof NPV (Carter and Keeler, 2008).
Net present value (NPV) analysis comparing a conventional roof system to an extensive green roof system demonstrates that at the end of the green roof lifetime the NPV for the green roof is between 20.3 and 25.2% less than the NPV for the conventional roof over 40 years. Researchers concluded that the additional upfront investment is recovered at the time when a conventional roof would be replaced (Clark et al., 2008).
Compared to a black roof, a 3-inch to 6-inch green roof covering 10,000 feet has a net present value of $2.70 per square foot per year, payback of 6.2 years and an internal rate of return of 5.2% nationally. The longevity of green roofs has the greatest effect on savings, whereas installation and maintenance have the greatest effect on cost (United States General Services Administration, 2011).
Taking a 1795 m^2 roof area in Washington DC, researchers determined that the installation cost of green roofs is 27% higher than that of conventional roofs. However, considering the benefits over the life time (40 years), the net present value of the green roof is about 25% lower than that of a conventional roof (NIU et al., 2010).
Results from a 50-year life-cycle cost analysis showed that relative to black roofs, white roofs provide a 50-year net savings of $25/m^2 ($2.40/ft^2) and green roofs have a negative net savings of $71/m^2 ($6.60/ft^2). Despite lasting at least twice as long as white or black roofs, they concluded that green roofs cannot compensate for their installation cost premium (Sproul et al., 2014).

Table 6-2 Cost-benefit analysis studies comparing of green infrastructure types.

Cost-Benefit Analyses Comparing Green Infrastructure Types
A model was presented that was used to simulate the cost-effectiveness of reducing CSOs through incremental installation of low impact development (LID) technologies across urban watersheds, when they are introduced alone, or in combination with conventional CSO abatement technologies.
Results indicate that individual LID systems have differing levels of cost-effectiveness in terms of CSO reduction, but that under a variety of performance and cost scenarios a public subsidy to encourage LID installation represents a cost-effective alternative for public agencies to consider in their efforts to reduce CSOs. Future LID installation investment path would promote (in order) porous pavement, the treatment wetland/curbside channel scheme, and then green roofs (Montalto et al., 2007).
Life cycle cost assessment found porous pavement is the most cost-effective for peak flow reduction, followed by bioretention and then green roofs. Furthermore, life cycle cost was estimated for different designs, and the optimal design, defined as the design with the lowest cost and at least 20% peak runoff reduction, was identified. The optimal design of green roofs tends to be larger in area but thinner, while the optimal designs of bioretention and porous pavement tend to be smaller in area. They also noted however, that to handle larger storms, it is more effective to increase the green roof depth, and to increase the area of the bioretention and porous pavement (Chui et al., 2016).
The cost efficiency of implementing a wide range of low impact development (LID) techniques in a proposed land development in the City of London, Ontario, Canada was investigated using continuous hydrologic simulation and a recently developed LID costing tool. The results indicate that infiltration trenches and infiltration trenches in combination with green roofs are the most cost efficient solutions for runoff reduction (Joksimovic and Alam, 2014).

Table 6-3 Life cyle assesment studies of green infrastructure.

Life Cycle Assessments of Green Infrastructure
Researchers observed annual energy savings and avoided GHG emissions of 7.3 GJ and 0.4 metric tons, respectively, for a GI strategy implemented in a neighborhood in New York City. Annual savings were small compared to the energy and GHG intensity of the GI materials, resulting in slow environmental payback times (78 to 110 years for energy; 100 to 150 years for GHG emissions) (Spatari et al., 2011).

Results of a bioretention case study show that the construction phase is the main contributing life cycle phase for all adverse environmental impacts, as well as total life cycle cost and labor impacts (Flynn and Traver, 2013).
A comparative life cycle assessment of an intensive green roof, an extensive green roof and a conventional ballasted roof showed that despite the need for additional resources initially, green roofs are the environmentally preferable choice when constructing a building due to the small reduction in energy demand and the increased life of the roofing membrane (Kosareo and Ries, 2007).
An optimization model for selecting the optimal GI systems found that the implementation of green systems was effective in terms of thermal comfort, energy consumption, life cycle cost, and life cycle assessment (Kim et al., 2016).
Life cycle analysis of a new modular greening system found that the curing process has a major impact on GHG emissions. By changing the curing process, it became possible to reduce the overall global warming potential (GWP) of the system by 74%. The GWP is directly related to fossil fuel dependency for energy production and transportation (Manso et al., 2018).
In general, air pollution due to green roof polymer production can be balanced in 13-32 years. However, the manufacturing process of low density polyethylene and polypropylene has many other negative impacts to the environment than air pollution– total pollutants released show that non-recycled LDPE releases 2.8 times more toxic substances to air than recycled LDPE. Thus, current green roof materials need to be replaced by more environmentally friendly and sustainable products (Bianchini and Hewage, 2012a).
LCA of four roof systems showed that the extensive green roof with recycled rubber had a significantly lower environmental impact compared to a non-insulated conventional roof (7% reduction) and compared to another green roof with a pozzolana drainage layer (6.7% reduction), while it had a similar environmental impact to the insulated conventional roof (2% increase) (Rincón et al., 2014).
A LCA conducted on a 120-year-old house found that although the green roof would require more retrofit embodied energy than the cool roof (it requires soil transportation, soil pan fabrication, roof joist retrofit kit, and ceiling replacement, while the cool roof requires only the manufactured paint), the green roof would still outperform the cool roof over a 10-year period on total energy consumption. Furthermore, both options would provide energy savings over the no-retrofit option (Dale et al., 2013).
LCA was used to quantify environmental impacts of climate change adaptation strategies. The GI adaptation plan had significantly lower impacts than the traditional alternative in all analyzed impact categories (Brudler et al., 2016).
Two complete lightweight green roofs were analyzed with the aim of determining the potential environmental impact of the different layers of the systems. Results showed that the water retention, drainage and substrate layers had the greatest negative environmental impact. More specifically, 1) rockwool, virgin polystyrene and expanded clay should be avoided; 2) simple roof systems may be recommendable whenever feasible; 3) recycled and local materials are better than virgin and those requiring long distance transport; and 4) the use of compost on the roofs may be recommendable (Bozorg Chenani et al., 2015).

However, there are several limitations to the studies reviewed. First, there is a tremendous amount of variability in results of sustainability analyses, which often reflects assumptions made for the calculations involved (Castleton et al., 2010) such as the boundary of the analysis and benefits analyzed. Ideally an effective sustainability appraisal tool should address the complete life cycle of a system including design, construction, operation, maintenance as well as demolition and disposal (Reza, 2013). Researchers also note that few studies have considered all three types of benefits (i.e., economic, environmental, and social) (Zhan and Chui, 2016). Many green roof CBA studies for example ignore important benefits, which biases final observations. This is because some benefits, like improvement of air quality and reduction of the UHI effect, are extremely complex to quantify. Other benefits of green roofs such as aesthetics, ecological preservation and noise reduction are individual-centric and they do not translate to direct savings for building owners (Vijayaraghavan, 2016). Contrasting results also reflect variability in different geographic locations (Vijayaraghavan, 2016). Other limitations of research include the type of analyses; although GI has been touted as a sustainable technology, its sustainability relative to gray infrastructure or natural ecosystems in which they are designed to mimic have not been fully explored. There are also many types of GI, and there has been limited comparison of sustainability between types (Law et al., 2017).

There are also several limitations to assessing sustainability with cost-benefit analysis and life cycle assessment. Although CBA is one of the well-established decision-support tools used for economic evaluation of projects on higher strategic levels, one of the most controversial criticisms of CBA is that it evaluates environmental impacts and ecosystem services to humans using economic analysis when many environmental impacts

192

such as human life and some irreversible effects on ecology are not convertible into monetary values (Reza, 2013). Furthermore, LCA has been criticized as a utilitarian user-side approach to sustainability, only focusing on environmental impacts due to resource consumption and emissions while ignoring the work of ecosystems to provide 'freely available' services and products (e.g. rainfall, soil organic matter, etc.) (Reza, 2013).

6.2.3   Assessing Sustainability with Emergy

Due to the limitations of CBA and LCA, it has been proposed that sustainability cannot be assessed simply by counting mass and energy flows, but by accounting for the direct and *indirect* energy supporting flows. *Emergy* is proposed as a more holistic ecological accounting method for determining if the direct and indirect energy requirements of GI are less than produced benefits over each system's life-span. More specifically, *Emergy* synthesis is the process of determining the sorts of energies and resources used up directly or indirectly in the biosphere in order to produce a specific product or service (i.e., joules of electricity used or produced by a system). Emergy accounting is unique because it is possible to tangibly evaluate the contribution of environmental, economic, and social impacts in a single energy-based unit known as solar energy joules (sej, or solar emjoules), and to determine an overall unbiased value for sustainability objectives (Reza et al., 2014).

A key concept in the emergy evaluation process is *solar transformity* or *unit emergy value* (UEV). Solar transformity values convert flows (e.g., grams, joules, dollars) to solar energy joules– in other words, it represents the amount of emergy required to produce one unit of an output or benefit (Equation 6-1) (Reza et al., 2014). The transformity of solar radiation equals one by definition (1.0 sej/J), while the transformities of all other flows and

193

storages (including those related to human societies) are calculated based on their convergence patterns through the biosphere hierarchy (Ulgiati et al., 2011). Ultimately, this principle differentiates emergy synthesis from other sustainability appraisal tools as emergy implies that 'with resource use comes responsibility'— high-emergy resources are valuable because of the amount of physical and thermodynamic work that went into producing them and should not be squandered (Raugei et al., 2014).

$$\textbf{Equation 6-1} \qquad UEV = \frac{\text{Solar energy joules (seJ)}}{\text{Available energy flow (Joule, grams, dollars)}}$$

$$\textbf{Equation 6-2} \qquad Emergy = UEV \times \text{Available energy flow}$$

The following example shows how one would convert a value to emergy terms. If 12E+04 sejs of coal and 4E+04 sejs of labor are required to generate 1 J of electricity, the UEV of electricity is 16E+04 sej/J (Reza et al., 2014). Where, solar energy joules account for the amount of "free" environmental work done by nature to generate flows. To determine total emergy if 2 J of electricity is used to produce a green roof, one would apply Equation 6-2 and total emergy would be 32E+04 sej. Once inputs and benefits are converted to emergy values, sustainability can be assessed with several ratios that evaluate total emergy of inputs (e.g. manufacturing, installation and maintenance) and benefits produced over a system's lifetime. In this study we focused on the Emergy Yield Ratio and Environmental Loading Ratio.

The Environmental Loading Ratio is the emergy of purchased (Y) and non-renewable resources (N) divided by the emergy of renewable inputs (R) (ELR = (F + N)/R). Natural systems commonly have ELR = 0 when operating on 100% renewable inputs.

Thus, the ratio indicates the pressure of a system on the surrounding environment– the ELR will decrease when the EYR is high, indicating less stress on the environment (Buranakarn, 1998; Coffman, 2007; Winfrey, 2012).

The Emergy Yield Ratio (EYR) is the ratio of emergy yielded (Y) to the purchased inputs (F) of the system and is obtained by dividing the emergy output by the emergy of all inputs coming from the human economy (EYR = Y/F). In other words, it expresses the emergy value of a material as a function of the purchased emergy from the economy required to make it. With high amounts of local, renewable emergy inputs to the system and low purchased inputs, the EYR will increase, indicating high yield of utilizing local resources and using less purchased emergy. More specifically, an EYR greater than 1.0 indicates that the system in question is making a positive contribution to the economy, on the other hand an EYR of less than 1.0 indicates that the system is absorbing resources of higher emergy value than the products it creates (Buranakarn, 1998; Droguett, 2011; Winfrey, 2012).

6.2.4   Emergy Studies of Green Infrastructure

To date, emergy has been used to evaluated GI sustainability in a few studies– a summary of major findings of GI are summarized below:

- Researchers conducted a comparative emergy analysis of two green engineered roofs (planted and cool/reflective) and a traditional modified bitumen roof. They found that the energy embodied in highly processed materials such as engineered soils can greatly impact a product's total sustainability despite its operational sustainability (Schramski et al., 2009).

- An emergy analysis of a modeled south-facing green façade revealed that the total emergy consumed could be balanced by the electricity saved from reduced air conditioning if the cooling load was reduced by at least 14%. Furthermore, the solar emergy required to manufacture, install, maintain, and decommission the green façade was 9.8 E12 sej/m^2/year, with nearly 55% embodied in human services, 14% in non-renewable materials, and 31% in renewable materials (Price, 2010).

- Researchers examined the benefits and detriments of current GI designs (rain gardens, green roofs, porous pavements, and tree plantings) using emergy analysis. Porous pavements performed the worst when evaluated using standard emergy-based environmental sustainability indices and the best when using economic indices. Indices calculated for green roofs and tree plantings indicated that these types of GI might inherently be more environmentally sustainable. Furthermore, emergy inputs of stone and soil were dominant inputs for all systems, as was the emergy cost of disposal of excavated materials. Porous asphalt was a high emergy input for the porous pavement projects examined. Labor and equipment inputs were high for most projects, but were overshadowed by stone and soil inputs. Researchers concluded that these dominant emergy inputs show areas where efficiency of designs could be improved by practices such as recycling excavated sediments or utilizing construction materials that are less emergy intensive. In addition, researchers concluded that the results of this study showed that not all GI projects are created equally (Law et al., 2017).

- Rain gardens, bioswales, new tree planting, extensive green roofs, CWs and permeable pavement were analyzed considering the valuation of three ecosystem

services; education incomes, biodiversity protection and stormwater treatment. The results indicate that GI practices are more sustainable than gray infrastructure, that the construction stage represents high environmental impacts for all practices. It was also observed that the operation stage of rain gardens, bioswales and green roofs are less resource intensive than tree planting and standard constructed subsurface wetlands. Overall it was concluded that porous pavement is the least sustainable strategy, achieving emergy indexes closer to gray infrastructure (Droguett, 2011).

- An emergy evaluation of a living wall and grass wall was performed to assess potential 'environmental costs' relative to their benefits– which were estimated as energy saving for cooling. Results demonstrated that, in certain conditions (i.e. Mediterranean climate context, south-oriented facade and massive envelope), the installation of living and grass wall systems is a sustainable operation for building retrofitting (Pulselli et al., 2014).

- The total energy required to manufacture, install and maintain an extensive, sedum-planted green roof over an assumed life of 20 years in the Mid-Atlantic region of the U.S. was analyzed using emergy analysis. Data on benefits was modeled based on published literature. The low-density, engineered growing media constituted 59% of the total energy requirements, while the petroleum-based root barrier and filter fabric contributed less than 4% combined. Electricity savings provided the largest benefit, but the sum of the three benefits equaled only 12% of total energy inputs, indicating that this type of green roof design used more energy than it saved or produced. Despite this, the green roof did reduce the local ELR of the building

by increasing the amount of locally renewable emergy captured by the vegetation. Researchers concluded that this extensive green roof design increased the overall ecological footprint of the building, and indicated that the energy footprint of the roof could be reduced by removing some of the engineered growing media (Rustagi et al., 2009).

- Emergy analysis was used to quantify and compare the sustainability of three different green roof systems. The roof systems were also compared to agricultural systems, constructed landscapes, and a city in order to determine how each system performed as a sustainable development technology relative to other landscapes. The shallow substrate green roof was the most sustainable of the three, followed by the deep substrate green roof, and lastly the agricultural roof garden. The levels of sustainability were associated with low percentage usage of renewable resources (extensive 6%, intensive 3%, agriculture 2%). All three systems were more sustainable than conventional landscapes, urban gardens and a city while being less sustainable than various agricultural practices (Coffman, 2007).

6.2.5   Extending Emergy to Enumerate Resilience

As global populations have become increasingly urbanized and as climate change progresses, urban resilience may greatly depend on the implementation of GI. Resilience, as applied to integrated systems of people and the natural environment, has three interrelated characteristics: (1) the amount of change the system can undergo and still retain the same controls on function and structure; (2) the degree to which the system is capable of self-organization; and (3) the ability to build and increase the capacity for learning and adaptation. In the resilience discourse, management of diversity per se is considered to be

198

a key attribute for building resilience in complex adaptive systems (Colding and Barthel, 2013).

Diversity spreads risks, creates buffers, and opens up for multiple strategies from which humans can learn in situations when uncertainty is high. In addition to functioning as insurance, diversity also plays an important role in the reorganization and renewal processes of disturbed systems, or events that require change in social–ecological systems by creating a frame for creativity and adaptive capacity to deal with change in constructive ways. Diversity is thus seen as key for dealing with disturbance and change in productive ways, with self-organization and the capacity for learning and adaptation constituting important resilience characteristics (Colding and Barthel, 2013).

The critical role of diversity and redundancy has been examined in many systems (e.g. genetic, ecological, and governance systems). In biological systems diversity facilitates functional redundancy, i.e. if a species declines or is lost, other species providing the same function in the system can continue providing this function. Hence, management of many species within a single functional group promotes resilience by reducing the risk of a specific ecosystem function being entirely lost in a biological community or ecosystem. Moreover, diversity in ecosystems promotes 'response diversity'. This capacity is mainly related to the diversity of 'functional groups' of species in a system, like organisms that pollinate, graze, predate, fix nitrogen, and decompose. Response diversity means that different organisms within a functional group respond differently to diverse types and frequencies of disturbance. For example, if honeybees are affected by a pathogen, other pollinator species not affected by the pathogen may take over the function of

pollination. In this way diversity creates redundancy in ecological systems (Colding and Barthel, 2013).

In ecology, the Shannon diversity index (*H*), has been used often to assess ecosystem diversity. Derived from information theory, *H* evaluates species richness (*S*), the abundance of species in the community, and species evenness (*E*), how similar the abundance of different species are in an area (Ulgiati et al., 2011). *H* is calculated using Equation 6-3, where p_i is the proportion of the number individuals in a species to the total number of individuals in *i*th species sampled (N_i) (Equation 6-4). A large *H* value indicates a diverse community.

$$\textbf{Equation 6-3} \qquad H= -\sum P_i \log[P_i]$$

$$\textbf{Equation 6-4} \qquad P_i = N_i / \sum N_i$$

Since GI benefits are diverse and not easily 'additive', it has been proposed that the environmental accounting technique of *emergy* evaluation could be extended using information theory— the basis of the Shannon Index— to enumerate the energetic diversity of GI and provide a new metric of resilience. Previously, this system-level *emergy diversity index* (derived from the Shannon diversity index) was used to quantify the diversity of species in ecological systems, and diversity of energy and resources in economic systems (Brown et al., 2006; Ulgiati et al., 2011).

The new emergy based indicator (described in the Methods— section 6.4.2) differs from the typical way of estimating *H*— which is based on simply counting individuals, biomass or other stocks— because it uses the flows of energy and materials in *emergy*

terms. Resilient systems are supported by a variety of emergy flows that make it more likely to develop complex structures, while systems that only rely on a small set of sources out of a large number of potentially available ones possess a built-in fragility that may determine their collapse in times of shrinking or changing resource basis (Ulgiati et al., 2011). By integrating information theory with emergy evaluation, were able to quantify how much the green roof, constructed wetland and bioretention increase the flow of information at the ecological, environmental, social and economic levels compared to a typical wastewater treatment plant and natural forest.

6.3   Materials and Methods

6.3.1   System Description
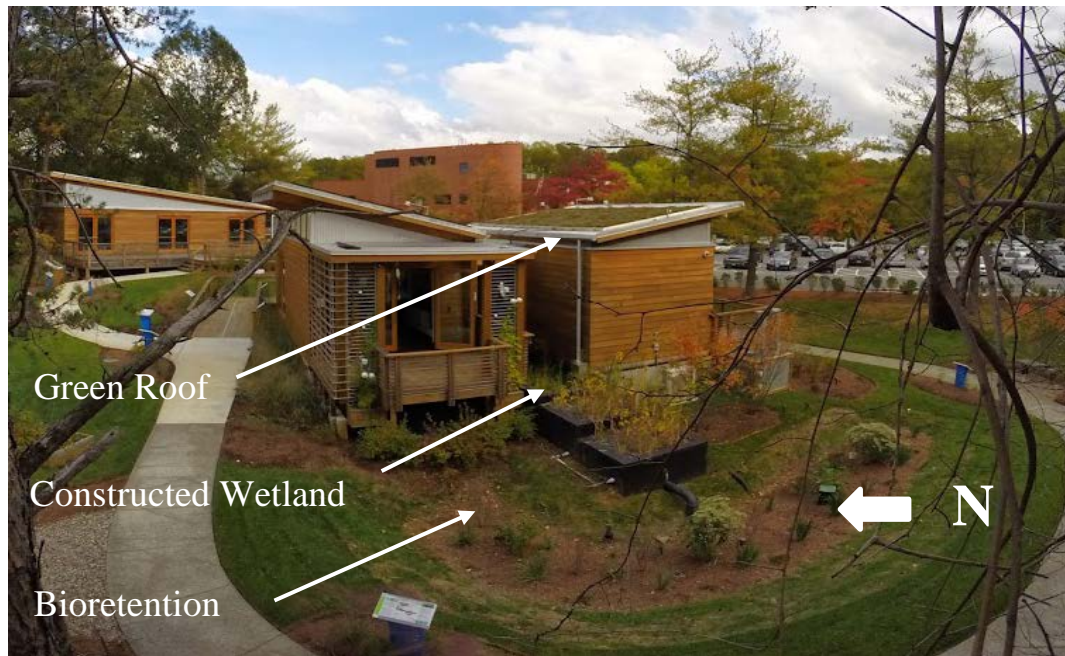
Figure 6-3 *WaterShed's* butterfly roof design allows for stormwater runoff from the 29 m^2 green roof to drain into a three-chamber constructed wetland (8.68 m^2). Finally, surface runoff, and stormwater flowing from the constructed wetland flow into a 32.6 m^2 bioretention.

As depicted in Figure 6-3, the 29 m^2 (312 ft^2) green roof system has a slope of 10 degrees and is 6.35 cm (2.5 in) in depth. Stormwater runoff from the green roof, drains into a three-chamber constructed wetland (8.68 m^2 or 93.4 ft^2) running east to west through the central axis of the house. The first chamber is a free-standing wetland designed to receive direct input of stormwater from the green roof. The final two chambers are horizontal subsurface flow wetlands receiving stormwater from the first chamber. Finally, surface runoff, and stormwater flowing from the CW flow into a 32.6 m^2 (350.9 ft^2) bioretention (7.62 cm or 3 in mulch layer, 70.0 cm or 27.6 in planting media, 15.2 cm or 6 in sand layer, 15.2 cm or 6 in stone layer above the underdrain, and 7.62 cm or 3 in stone layer below the underdrain) with groundwater outlet. For a full description of each system refer to section 2.7 (Site Description: *WaterShed's* Green Infrastructure).

6.3.2 Emergy Analysis

WaterShed's Green Infrastructure

An emergy analysis of the green roof, CW, and bioretention was performed. The boundary for each analysis was the manufacturing, installation, and operation of the system over a 30-year lifetime (Figure 6-5). Although maintenance and end of life processes are important, we did not evaluate them for a consistent comparison to the wastewater system and natural forest. Inputs for each system were calculated by consulting engineering documents, published data, and product specifications. Furthermore, benefits were derived from 2-year sensor data (data collection period July 2014-June 2016) and published data. For details on how all inputs and benefits were calculated for the green roof, CW, and bioretention, see Appendix D, Appendix E, and Appendix F, respectively.

Wastewater system

The domestic wastewater system (WWTP) used in our analysis was adapted from Winfrey (2012), who used emergy methodology to evaluate the effectiveness of various waste treatment technologies. The 9,000 m^2 WWTP was a conventional treatment system designed for a small town (population of approximately 5,000), with primary clarification, aeration and sedimentation, and disinfection unit processes, similar to conventional treatment in the U.S. (Figure 6-4). The case study was designed and modeled using construction and performance criteria from the literature (Winfrey, 2012). We adapted the data to reflect the 30-year lifetime we assumed for GI.
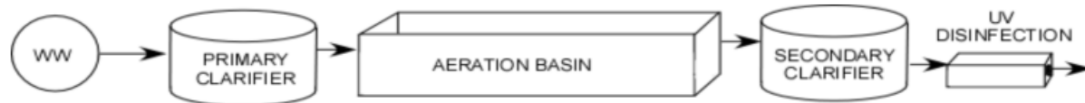
Figure 6-4 shows a schematic of the model WWTP (Winfrey, 2012).

Natural forest

The U.S. National Forest System (NFS) used in our analysis, which encompass 192.7 million acres (78 million hectares) of land, was adapted from Campbell and Brown (2012), who performed an environmental accounting of natural capital and ecosystem services for the system. The spatial boundaries of flows supporting the system were defined by the extent of NFS lands and the economic assets (roads, buildings, and machinery) and the natural capital (mineral resources, tree biomass, and miscellaneous natural resources) contained within them. Data for evaluations were taken primarily from NFS publications (Campbell and Brown, 2012).
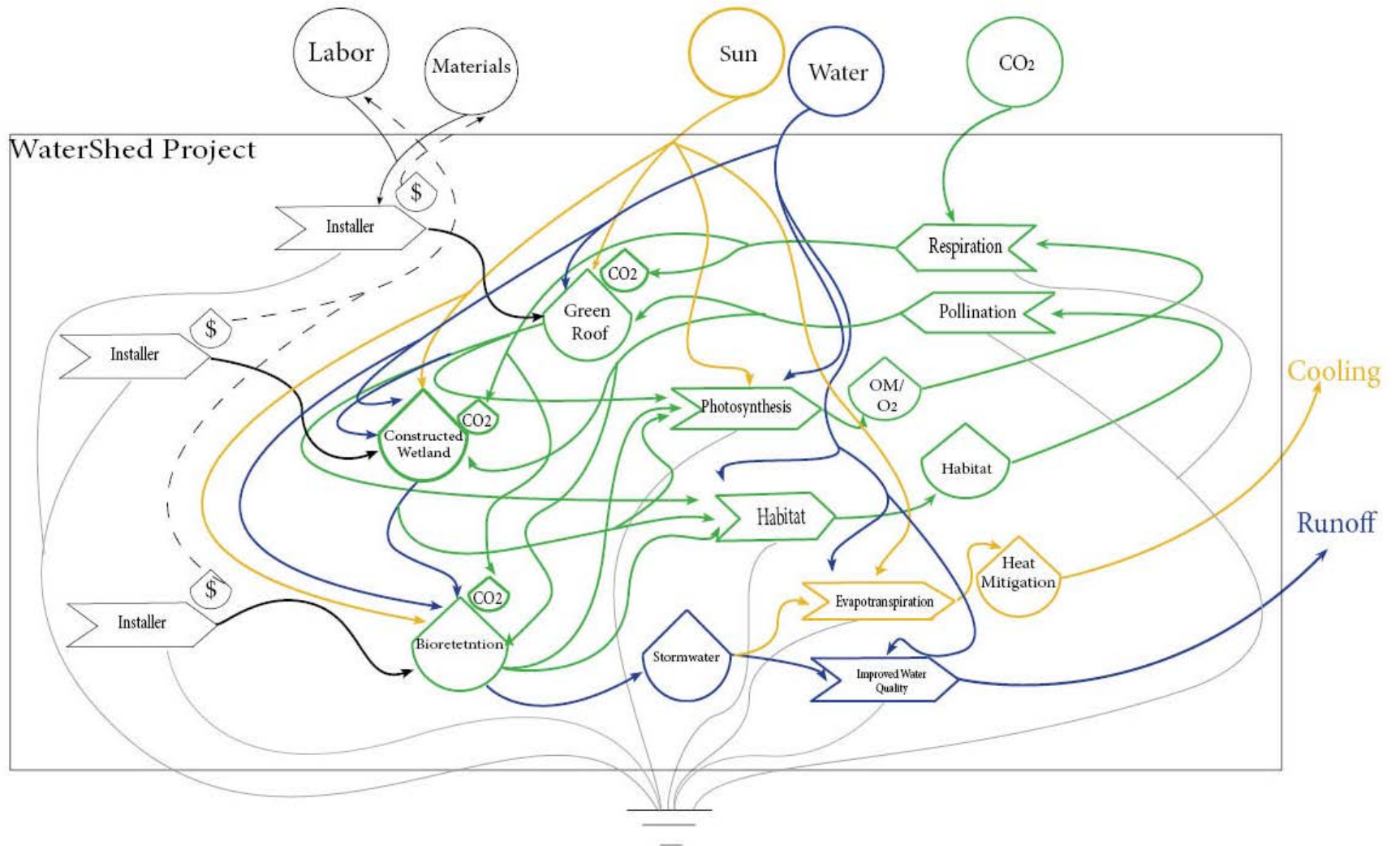
Figure 6-5 Systems diagram of *WaterShed's* green infrastructure.

6.3.3   Sustainability Analysis

The following measures and indices were calculated to assess sustainability: total renewable inputs (R), total purchased inputs (F), total benefits (Y), Emergy Yield Ratio (EYR = Y/F), Environmental Loading Ratio (ELR = F/R) and payback time (F × year/Y).

6.3.4   Resilience Analysis

A system-level *emergy diversity index* (Equation 6-5) derived from the Shannon diversity index (*H*) was used to enumerate the diversity of *WaterShed's* GI systems. The new emergy based indicator differs from the typical way of estimating *H*— which is based on simply counting individuals, biomass or other stocks— because it uses the flows of energy and materials in emergy terms. Resilient systems are supported by a variety of emergy flows, whereas systems that rely on a small set of sources possess a built-in fragility, that may determine their collapse in times of shrinking or changing resource basis (Ulgiati et al., 2011).

$$\textbf{Equation 6-5} \qquad \text{Emergy diversity (ED)} = - \sum \text{EIV}_i \, \log[\text{EIV}_i]$$

$$\textbf{Equation 6-6} \qquad \text{EIV}_i = \frac{\text{NP}_i \times \tau_i}{\sum \text{NP}_i \times \tau_i}$$

Where EIV_i is the emergy importance value,

NP_i is the net production (e.g. J/year),

τ_i is the computed transformity of component *i* (e.g. sej/J)

This quality-adjusted diversity index differs as the probability of each individual or species (p_i = number individuals in a species/total number of individuals in *i*th species) is

replaced by an emergy importance value (EIV_i = emergy of component/emergy of all components, Equation 6-6). By replacing the probability p_i with the EIV_i the Shannon information index translates into an ecosystem-scale Shannon diversity index as follows, where biodiversity is maximized when the probability of observing each component is equal (Ulgiati et al., 2011):

6.4   Results and Discussion

6.4.1   Sustainability Analysis

Table 6-4 *Emergy* based sustainability analysis of *Watershed's* green infrastructure compared to a wastewater treatment plant (WWTP) and natural forest system (NFS). Green to red color gradient represents how well the system scored in that category, where green = high score and red = low score.

System	Renewable Inputs (sej/m^2/yr)	Purchased Inputs (sej/m^2/yr)	Benefits (sej/m^2/yr)	ELR	EYR	Payback Time (yr)
Green Roof	2.26E+10	1.57E+13	7.12E+12	694	0.453	66.2
Constructed Wetland	7.31E+11	1.88E+14	1.09E+13	257	0.058	517
Bioretention	1.19E+12	6.63E+13	3.65E+12	55.9	0.055	544
WWTP	1.06E+14	2.28E+14	3.54E+13	799	0.099	305
NFS	4.13E+10	2.27E+10	4.80E+11	0.55	21.1	1.42

Overall, the sustainability analysis revealed the National Forest System to be the most sustainable system evaluated. Although it is low in emergy (i.e. E+11<) relative to the other systems evaluated, it operates primarily on renewable inputs (ELR = 0.55), and benefits are high relative inputs purchased from the economy (EYR = 21.1, payback time = 1.42 years).

Being that GI are designed to mimic the benefits of natural ecosystems, and are to thought to minimize the impacts of gray infrastructure, a comparison to the NFS and WWTP was an important and unique aspect of this study. This part of our analysis revealed that overall GI are generally low in renewable inputs relative to purchased inputs (ELR >1). Furthermore, benefits generally do not outweigh costs (EYR< 1). Similar results were also observed for the WWTP.

More specifically, the green roof had an ELR value of 694, an emergy yield ratio of 0.453, and a high payback time (66.2 years). It should be noted however that the green roof was a much more sustainable option compared the CW, bioretention or WWTP. The constructed wetland exhibited an ELR value of 257, EYR value of 0.058, and payback period of 517 years, while values were 55.9, 0.055 and 544 years for bioretention, and 799, 0.099 and 305 years for the wastewater facility. It should be noted however that due to the plethora of green roof studies, we were able to model significantly more benefits relative to the other systems. Furthermore, water quality improvement is a key benefit of bioretention that could not be modeled due to the lack of available data that would allow us to calculate its benefit in emergy terms (i.e., $g/m^2/year$).

In respect to other GI *emergy* analyses, Droguett (2011)— who performed an emergy analysis of raingardens, bioswales, new tree planting, extensive green roofs, constructed wetlands and permeable pavement considering three ecosystem services; education incomes, biodiversity protection and stormwater treatment— found GI practices to be more sustainable than gray infrastructure, but noted that the construction stage represents high environmental impacts for the systems evaluated. Furthermore, it was noted that GI strategies such as rain gardens, bioswales, and extensive green roofs were

207

more sustainable in emergy terms than tree planting and constructed subsurface wetlands; most notably during the operation stage rain gardens, bioswales and green roofs were less resource intensive than tree planting and standard CWs. Overall, porous pavement was the least sustainable strategy achieving emergy indices closer to gray infrastructure (Droguett, 2011).

Interestingly, Law et al. compared several GI systems (rain gardens, green roofs, porous pavements, and tree plantings) using emergy analysis and results indicated that green roofs and tree plantings were inherently more environmentally sustainable. Aside from pointing out high emergy inputs for improved design (stone and soil were dominant inputs for all systems, as was the emergy cost of disposal of excavated materials), researchers concluded that the results of their study show that not all GI projects are created equally (Law et al., 2017).

Finally, high payback time for GI was somewhat expected based on prior research. Spatari et al. (2011) for example performed a life cycle assessment of a GI strategy (street trees and permeable pavement) implemented in New York City and found annual energy savings and avoided GHG emissions of 7.3 GJ and 0.4 metric tons, respectively. According to estimates, annual savings were small compared to the energy and GHG intensity of the GI materials, resulting in slow environmental payback times (78 to 110 years for energy; 100 to 150 years for GHG emissions). Spatari et al. (2011) noted this slow environmental payback was due to high energy inputs and GHG emissions in the construction phase; and they overall concluded that while GI strategies lead to energy and GHG emissions reduction benefits, they can be small and slow to accrue compared to the materials needed

to implement them— they also noted however that this finding was a function of design decisions employing the use of specific construction materials (Spatari et al., 2011).

Green Roof Sustainability

To better understand observed trends, it is imperative to look at the emergy breakdown of each system. The green roof analysis (Table D-1) revealed that expanded shale (59.8%) was the most emergy intense purchased input, followed by *Sedum* cuttings (16.6%) and labor (9.5%). Emergy of benefits were mostly attributed to energy savings in cooling (54.3%), carbon dioxide emissions avoided due to energy savings (16.4%), and biophilia (15.5%)— which was modeled as the biophilic relationship between views of nature and daylighting in the workplace and their impacts on sick leave of office workers.

Compared to other green roof *emergy* studies, this evaluation was performed using a combination of actual and modeled data. Even so, similar trends can be observed— other researchers for example have found green roof substrates to dominate the emergy of extensive green roofs. Schramski et al. (2009) for example used emergy to explore the total energy required to manufacture, install and maintain an extensive, *Sedum*-planted green roof over an assumed life of 20 years in the Mid-Atlantic region of the U.S (data on benefits was modeled based on published literature). Researchers found the green roof's emergy investment was comparatively high with the drainage media and the engineered soil comprising 79% of the total emergy cost (32.05E+12 sej/m^2/year). Overall they concluded that the emergy cost increase of a green roof is significant and is dominated by only a few components (Schramski et al., 2009).

Furthermore, using emergy theory Rustagi et al., (2009) found low-density, engineered growing media to constitute 59% of the total energy requirements of an extensive green roof, while the petroleum-based root barrier and filter fabric contributed less than 4% combined. Interestingly when benefits were evaluated (energy savings, primary production and stormwater reduction), electricity savings provided the largest benefit. However, Rustagi et al. (2009) noted that the sum of the three benefits modeled equaled only 12% of total energy inputs, indicating that this type of green roof design used more energy than it saved or produced. Despite this, they noted the green roof did reduce the local environmental loading ratio of the building by increasing the amount of locally renewable emergy captured by the vegetation (ELR of a building with or without a green roof was 1,710 vs. 23,800). Researchers concluded that this extensive green roof design increased the overall ecological footprint of the building, and indicated that the energy footprint of the roof could be reduced by removing some of the engineered growing media (Rustagi et al., 2009).

An emergy analysis of a shallow substrate green roof revealed the expanded clay, which constituted part of the growing material, was the largest input (1.52E+16 sej) due to its high quantity (4.99E+06 g) and transformity (3.04E+09 sej/g). This accounted for 35% of all purchased inputs, while compost, which was mixed with the expanded clay, was the second major input for the extensive roof at 25% (1.07E+16 sej). The third was human labor at 17% (7.31E+15 sej). Coffman also noted that machinery, sand, and plants each accounted for 6% of the purchased resources; the protective membranes accounted for 5%; lastly, irrigation accounted for less than 1% because it was used only for one season during plant establishment (Coffman, 2007).

Finally, Droguett (2011) performed an emergy analysis comparing an extensive green roof to other GI and found the highest emergy content in the green roof was represented by the waterproof barrier, the drainage layer for plant uptake and storm buffering, and the geosynthetic layer which prevents fine soil media from clogging the porous media (Droguett, 2011).

As we take a closer look at green roof sustainability, it is not surprising that purchased inputs were high considering researchers have noted that green roof design is still based on conventional materials such as expanded clay, polypropylene or polyester geotextiles membranes, poly-ethylene or polystyrene panels, natural puzolana, and bitumen or PVC membranes (Pérez et al., 2012).

More specifically, green roof substrates composed of expanded aggregates are thought to represent the greatest portions of the embodied energy and environmental impact potential over a system's lifetime because they are produced by either super-heating materials such as slate, shale, or clay; or by mining naturally expanded materials like pumice. Furthermore, researchers have noted that there other impacts associated with green roof production such as increased carbon footprint and the release of GHGs from hydrocarbon fuels during heat-expansion, material processing, and transportation (Matlock and Rowe, 2016).

This has major implications for the green roof industry because in North America the main component of green roof substrates is often lightweight stable aggregates such as heat expanded slate, shale, or clay (Eksi and Rowe, 2016). The production of lightweight aggregates are particularly important considering weight limitations of green roof systems, which have led several manufacturers to develop their own growing mediums. Generally,

growing medium have a high content of porous minerals and a low content of organic matter to maintain the balance between weight and performance (Bianchini and Hewage, 2012a). Green roof experts have also justified the need to introduce other conventional materials like plastics into the market because it can reduce the overall weight and improve the performance of waterproofing layers without compromising the benefits of green roofs (Bianchini and Hewage, 2012a). Despite the benefits of these materials to reducing weight loads, findings across multiple studies suggest the need to substitute green roof materials with lower environmental impact ones such as recycled materials (Rincón et al., 2014).

Constructed Wetland Sustainability

A breakdown of inputs and benefits to the constructed wetland (Table E-1) revealed that the top three purchased inputs were nursery pots (16.6%), concrete (15.9%), and gravel (5.9%), while benefits were dominated by sediment removal (72.1%), biophilia (10.1%), and primary production (6.7%).

In respect to other GI *emergy* analyses, there is not much performed on CWs to put these results in context. Droguett (2011) however performed an emergy analysis of raingardens, bioswales, new tree planting, extensive green roofs, constructed subsurface wetlands and permeable pavement considering three ecosystem services; education incomes, biodiversity protection and stormwater treatment. GI strategies such as raingardens, bioswale, and extensive green roofs were found to be more sustainable in emergy terms than tree planting and CWs; most notably during the operation stage raingarden, bioswale and green roofs were found to be less resource intensive than tree planting and standard CWs (Droguett, 2011).

212

Droguett further noted that wetlands have a higher construction costs than raingardens, living swales and tree plantings. The increased emergy cost during the construction stage of CWs is produced by the different requirements such as excavation, backfilling, compaction, filling, finish grading and soil replacement. These requirements also require more skilled labor, equipment and machinery; therefore, increasing energy input. Overall, it was recommended that to create more sustainable GI during the operation and maintenance stage, inputs should be decreased— more specifically, for the construction stage, renewable energy and on-site compost strategies were suggested (Droguett, 2011).

Bioretention Sustainability

Finally, a breakdown of inputs and benefits to bioretention (Table F-1) revealed that the top three purchased inputs were the 21" planting media (assumed to be mostly sand) (34.3%), 9"stone layer (29.7%), and 6" sand bed (20.6%). For this analysis, media specifications were not provided, thus emergy of bioretention media was approximated based on the assumption that the state of Maryland recommends bioretention planting soil should contain a minimum 35 to 60% sand, by volume (MDE, 2009). Based on this specification, we assumed the substrate was comprised of native soils amended with sand for simplicity. Thus, since the 21" planting media (assumed to be mostly sand) and the 6" sand bed were high in emergy terms (34.3 and 20.6% respectively), alternatives should be considered to improve sustainability.

Benefits were dominated by primary production (32.4%), biophilia (30.2%), and wastewater energy savings (17.7%). It should be noted however, that water quality improvement was a key benefit of bioretention that could not be modeled due to the lack

213

of available data that would allow us to calculate its benefit in emergy terms (i.e., $g/m^2/year$).

In respect to other studies, a few *emergy* evaluations of bioretention can be compared to this analysis. For example, Droguett (2011) found GI strategies such as raingardens, bioswale, and extensive green roofs to be more sustainable in emergy terms than tree planting and CWs; it was noted that rain gardens and bioswales had the lowest construction costs. This is because rain gardens and bioswales require small depth excavation and less equipment for soil movement (Droguett, 2011).

Furthermore, researchers examined the benefits and detriments of current GI designs (rain gardens, green roofs, porous pavements, and tree plantings) using emergy analysis. Emergy inputs of stone and soil were dominant for all systems, as was the emergy cost of disposal of excavated materials. Furthermore, labor and equipment inputs were high for most projects, but were overshadowed by stone and soil inputs. Based on these findings researchers concluded that these dominant emergy inputs show areas where efficiency of designs could be improved by practices such as recycling excavated sediments or utilizing construction materials that are less emergy intensive (Law et al., 2017).

Trends can also be put into perspective when compared to the results of a life cycle assessment of a bio-infiltration rain garden performed by Flynn and Traver (2013). Results of this study showed the construction phase to be the main contributing life cycle phase for all adverse environmental impacts. Construction phase environmental impacts for bioretention was attributed to the use of silica sand as a soil amendment and the use of bark mulch to provide ground cover, repress invasive vegetation, and establish target vegetation (mulch was a small emergy input for us 0.4%; Table F-1) (Flynn and Traver, 2013).

214

Interestingly, the bio-infiltration rain garden operation phase was found to provide significant avoided environmental impacts relative to construction phase impacts. These avoided impacts were attributed to urban forest benefits from vegetation, benefits due to stormwater runoff pollutant treatment by the practice, and benefits to combined sewer systems due to reduced stormwater volume through infiltration and ET (Flynn and Traver, 2013).

Overall, based on these findings Flynn and Traver recommended that alternatives be investigated to the use of silica sand as a soil amendment to produce rain garden media. An alternative could be to use the natural soil as rain garden media and to accept a lower infiltration rate. They did note however that this could require a larger rain garden footprint to achieve the same stormwater management performance. Another alternative design is to replace the silica sand with another material such as naturally occurring sand, a sandy soil, or an engineered rain garden media. Another suggestion was to reduce the volume of silica sand by reducing the depth of the rain garden media (Flynn and Traver, 2013).

Although mulch was a small component of our emergy analysis, Flynn and Traver had several suggestions to reduce its environmental impact such as using mulch produced onsite from tree clippings and other organic waste generated by maintenance activities, or to use rubber mulch produced from recycled tires. Furthermore, if bark mulch must be used it was recommended that it is only applied during the initial establishment phase of the rain garden vegetation and not reapplied throughout the operation phase of the practice unless deemed necessary for the health of the vegetation. Finally, they suggested that any design alternatives for silica sand, bark mulch, or any other materials and processes should be evaluated using the same life cycle assessment methodology. Only then can alternative

designs be properly assessed and compared for both cost and environmental impacts; it may be found that some alternatives simply shift adverse impacts to other impact areas (Flynn and Traver, 2013).

6.4.2 Resilience Analysis

Table 6-5 Emergy diversity index (ED) was used as an indicator of resilience. B $_{Inputs}$ (renewable and purchased) and B $_{Benefits}$ of *Watershed's* green infrastructure was compared to a wastewater treatment plant (WWTP) and natural forest (NFS). The difference between benefits and inputs (Generativity = ED $_{Benefits}$ - ED $_{Inputs}$) was taken to evaluate whether the system made a positive contribution towards higher complexity and resiliency. Green to red color gradient represents how well the system scored, where green = high score and red = low score. See Appendix G for Emergy Diversity Index Calculations.

System	ED $_{Inputs}$ (bits/emergy)	ED $_{Benefits}$ (bits/emergy)	Generativity (bits/emergy)
Green Roof	1.94	2.04	0.10
Constructed Wetland	1.75	1.52	-0.23
Bioretention	2.15	2.26	0.10
WWTP	1.26	1.75	0.49
NFS	0.39	2.31	1.92

In the resilience discourse, management of diversity per se is considered to be a key attribute for building resilience in complex adaptive systems. Diversity is seen as key for dealing with disturbance and change in productive ways, with self-organization and the capacity for learning and adaptation constituting important resilience characteristics (Colding and Barthel, 2013).

Previously, the system-level *emergy diversity index* (derived from the Shannon diversity index) was used to quantify the diversity of species in ecological systems, and diversity of energy and resources in economic systems (Brown et al., 2006; Ulgiati et al.,

2011). Where, Ulgiati (2011) stated that systems that only rely on a small set of sources out of the large number potentially available possess a built-in fragility, that may determine their collapse in times of shrinking or changing resource basis. More specifically, Ulgiati stated that high source diversity means that the system relies on a larger set of resource options that make it more likely to develop complex structures (both environmental and human-dominated) and therefore more resilient in the face of fluctuations— the extreme negative case would be a system driven by only one category of input flows, for which the diversity index would be equal to zero. Such a system would be very endangered, because of its reliance on one resource option only (Ulgiati et al., 2011). To our knowledge, the application of the emergy diversity index to explore resiliency of GI inputs and benefits is unique to this study.

Since the premise of the emergy diversity index is the Shannon diversity index, the index was essentially used to enumerate the diversity of *WaterShed's* GI inputs and benefits based on their richness and evenness. In contrast to Ulgiati (2011), high emergy diversity of inputs was seen as a negative case since it indicated that the systems we evaluated are were likely very reliant on purchased inputs from the economy. Moreover, high emergy diversity of benefits was seen as a positive case since it indicated the system is likely producing a variety of different benefits for urban communities. Next, the difference between emergy diversity benefits and inputs (Generativity) was taken to evaluate whether the system made a positive contribution towards higher complexity and resiliency.

Overall, the NFS scored high in benefits (2.31) and low in inputs (0.39). The system also created information when the difference between emergy diversity of benefits and inputs was evaluated (Generativity = 1.92), indicating the NFS made a positive

217

contribution towards higher complexity and resiliency. The WWTP had emergy diversity values of 1.26 for inputs and 1.75 for benefits, making a slightly positive contribution towards higher complexity and resiliency (Generativity = 0.49).

Relative to the NFS and WWTP, GI scored poorly in the resilience analysis. More specifically, although GI was generally high in emergy diversity of benefits (except the constructed wetland where ED $_{Benefits}$ was 1.52), GI was also generally high in emergy diversity of inputs (1.75-2.15). The bioretention system for example, which scored poorly in the sustainability analysis, had emergy diversity values for inputs and benefits of 2.15 and 2.26, with a generativity value of 0.10. Interestingly, the constructed wetland was the only system to have an overall negative contribution towards higher complexity and resiliency— ED $_{Inputs}$ and ED $_{Benefits}$ were 1.75 and 1.52, with a generativity value of -0.23.

Another interesting observation was that emergy diversity of benefits was greater for bioretention (2.26) than the green roof (2.04). This is because although the green roof was rich in benefits (23 benefits were modeled), evenness was lower as it was highly concentrated in emergy for a few benefits— energy savings in cooling (54.3%), carbon dioxide emissions avoided due to energy savings (16.4%), and biophilia (15.5%). Emergy diversity of bioretention benefits on the other hand was more even: primary production (32.4%), biophilia (30.2%), and wastewater energy savings (17.7%).

From a diversity standpoint, these benefits are important because in the resilience discourse, diversity spread risks, create buffers, and by doing so functions as insurance for a system. More specifically, improved diversity of GI benefits in urban communities is likely to play an important role in the reorganization and renewal processes of communities in the face of disturbance (like climate change related weather events), by creating a frame

for creativity and adaptive capacity to deal with change in constructive ways (Colding and Barthel, 2013).

More specifically, in biological systems diversity facilitates functional redundancy, i.e. in ecology, if a species declines or is lost, other species providing the same function in the system can continue providing this function. Hence, management of stormwater reduction benefits with multiple GI for example, is likely to promote resilience by reducing the risk of that benefit from being entirely lost in urban communities during times of disturbance. Other benefits of improved diversity include 'response diversity'. In ecology response diversity means that different organisms within a functional group respond differently to diverse types and frequencies of disturbance. Thus, for GI that means that if one system is affected by a disturbance or event, other systems may not be affected by that disturbance or event, and may continue providing that function. In this way diversity creates redundancy in ecological systems (Colding and Barthel, 2013).

Overall, the concept of diversity as a metric of resilience using the emergy diversity index is a new framework of thinking, however these preliminary findings indicate that the current design of gray and green infrastructure— they are highly reliant on a diverse amount of purchased inputs relative to renewable inputs or benefits— puts these systems at risk to perturbations such as resource scarcity or potentially climate change in comparison to the natural forest system. This is concerning considering global populations have become increasingly urbanized, and as climate change progresses urban resilience may greatly depend on the implementation of gray and green infrastructure. For green and gray infrastructure, this then makes the case for improving the richness and evenness of renewable inputs and benefits with improved design and implementation.

6.5   Summary and Conclusions

Green infrastructure is increasingly being recognized as a sustainable approach to urban environmental problems. They are designed to be natural and constructed green spaces that utilize vegetation, soil, and other components to replicate natural processes that provide a multitude of benefits for human populations in the urban setting. However, before these benefits can be realized and accounted for, environmental debts (e.g., energy subsidies), which are being incurred usually beyond the local boundaries (Schramski et al., 2009) must be accounted for.

This analysis was unique in using actual and modeled data to explore the sustainability and resilience of GI relative to a wastewater system and natural forest. Overall, these analyses revealed the beneficial value of natural ecosystems as the NFS scored the highest in both evaluations. From these initial analyses, it is very clear that with the current design of gray and green infrastructure, benefits provided do not compare to the benefits provided by natural ecosystems. This has implications for prioritizing the management and preservation of existing ecosystems where possible.

It was also observed from comparing GI and the WWTP that the green roof was the most sustainable option, while the WWTP was the most resilient system considering emergy diversity of benefits relative to inputs. There are several potential lessons from these findings. First, this finding indicates the importance of assessing both GI sustainability and resilience— based on current findings there may be a strong case for prioritizing certain systems over others depending on goals. For example, it may be likely that from a sustainability perspective green roofs may be the best option, while WWTPs may be the best option for improving urban resilience. However, it should be noted that

improving system design or benefits would likely alter the outcome of sustainability and resilience analyses. This is because sustainability appraisal tools like emergy synthesis reflect parameters inputted in the model such as design, construction, operation and maintenance, and benefits. Thus, extensive measures for example should be taken to optimize GI design and implementation based on the site and region to optimize performance. It should further be noted that this analysis could be improved by evaluating the whole cradle to grave life cycle of gray and green infrastructure— maintenance and end of life processes are important aspects we did not evaluate.

Since GI benefits were generally low relative to the emergy required to make them, it was concluded that a movement towards minimizing materials and replacing heavily processed products would significantly improve the long-term sustainability (Law et al., 2017) and potentially resilience of GI. We would also suggest that maximizing benefits by improving GI design and implementation is another important area that could greatly improve results.

More specifically, in terms of reducing inputs we outlined several aspects of each system's design that was emergy intense and could be improved to lower dependence on conventional materials (e.g. green roof expanded shale, or the use of concrete in CWs). It should be noted however that GI can vary considerably in their components or design. Some green roofs, for example, consist solely of organic compost, eliminating engineered soils entirely (Schramski et al., 2009). Furthermore, the cost of retrofitting green roofs is an important input that many other sustainability analyses would have to account for. Some researchers even hypothesize that if strengthening works are required to support the green roof, the additional costs would likely outweigh any benefits (Castleton et al., 2010).

Furthermore, GI design could be improved to maximize benefits in several ways. For example, as described in Chapter 3 (Green Infrastructure Hydrological Performance), both the green roof and bioretention systems had lower stormwater reduction efficiencies relative to the CW. For the green roof this was largely attributed to its sloped roof and thin depth. Thus, it is likely that if the system was placed on a home with a flat roof, emergy of benefits would improve. It is also likely that improving design by increasing green roof depth would improve retention, but it is also likely that this action may have a negative effect on the emergy of purchased inputs as well. Therefore, it is imperative that design alternatives be evaluated using the same assessment methodology. Only then can alternative designs be properly assessed and compared; it may be found that some alternatives simply shift adverse impacts to other impact areas (Flynn and Traver, 2013).

It is also important to note that many benefits were modeled conservatively. For example, *WaterShed's* roof membrane is highly insulated (R value of 50 h ft^2 F/Btu or 8.805 K m^2/ W), thus the green roof would likely provide more energy-related benefits on a more conventional home. Furthermore, water quality improvement is a key benefit of bioretention that could not be modeled due to the lack of available data that would allow us to calculate its benefit in emergy terms (i.e., g/m^2/year). Finally, many benefits of GI are downstream of the system itself, and transcend well beyond each system's boundary, or are even difficult to evaluate. Thus, future studies should try and quantify these benefits, such the reduction of stream erosion, the positive benefit of GI on aquatic health like reduced algal blooms, or the benefits of reusing graywater.

Other factors that many widely affect sustainability and resilience analyses include local factors. For example, variability in stormwater related benefits may be attributed to

quantities of annual precipitation, with greater annual savings likely to coincide with years in which higher precipitation is observed (Spatari et al., 2011).

Finally, it is important to note that there are some limitations to using emergy methodology to enumerate the sustainability and resilience of GI. For example, transformity values can be difficult to find or quantify. Furthermore, emergy does not always show other environmental impacts of systems or processes. For example, LCA can be beneficial in quantifying the acidification potential (production of acidifying pollutants like sulfur containing gases), and global warming potential (release of carbon dioxide, nitrous oxide, and methane gas) of systems (Eksi and Rowe, 2016), while economic analyses such as CBA are imperative in today's economy to determine the feasibility of implementing gray or green infrastructure in many communities— there may even be cases where systems score differently using various sustainability appraisal tools. For example, researchers examined the benefits and detriments of current GI designs (rain gardens, green roofs, porous pavements, and tree plantings) using emergy analysis. Porous pavements performed the worst when evaluated using standard emergy-based environmental sustainability indices and the best when using economic indices (Law et al., 2017). Thus, it may be useful to evaluate multiple GI strategies using various sustainability appraisal tools. Such an approach would allow municipalities to track and quantitatively weigh the full set of environmental and economic tradeoffs of conventional versus green infrastructure to ensure that scarce public resources be spent wisely to achieve the broadest increase in economic, social, and environmental benefit (Spatari et al., 2011).
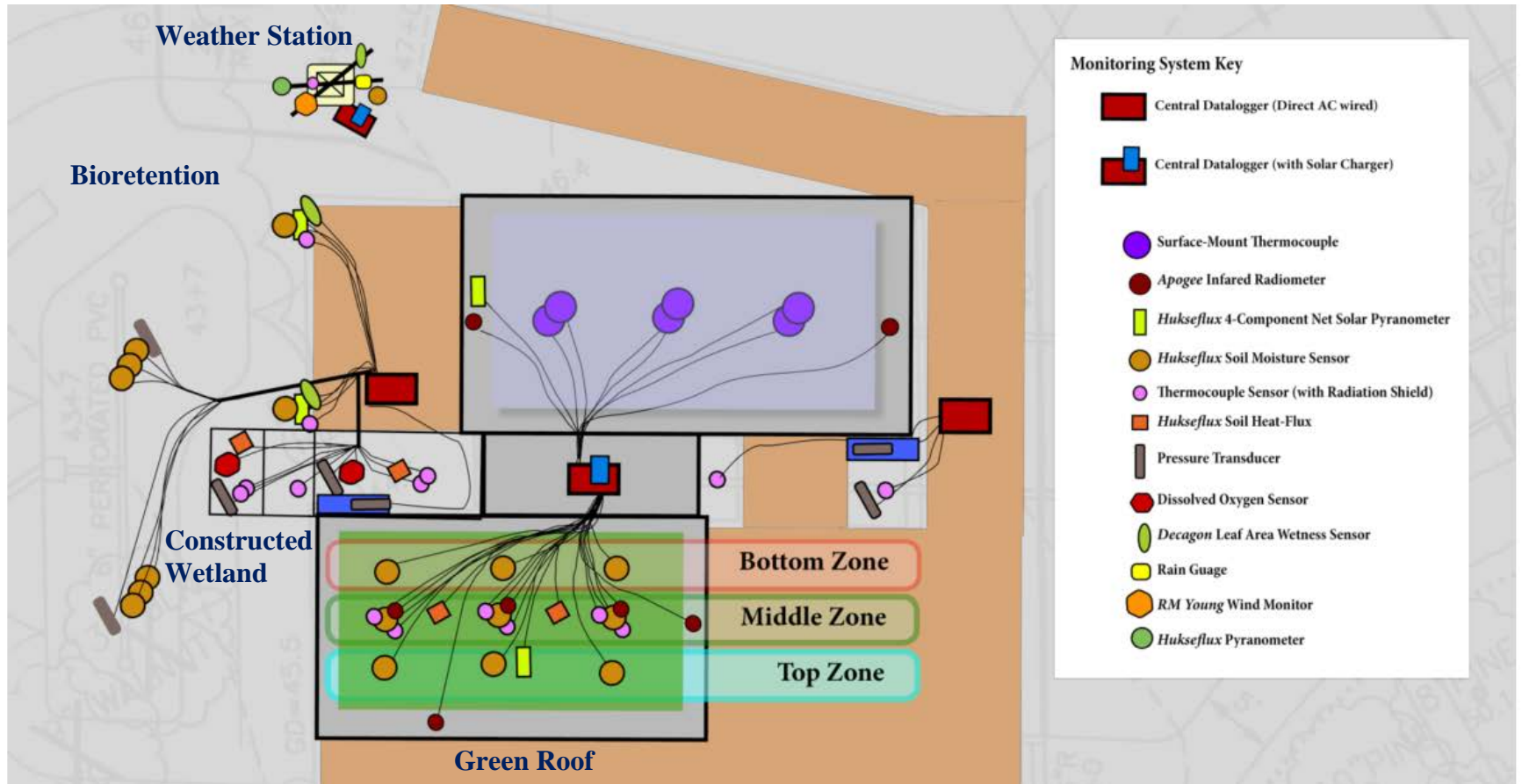
Figure A-1 General sensor layout on the exterior of *WaterShed* (Image credit: Scott Tjaden).

This section provides supplemental information for the monitoring system installed on *WaterShed*. The various sensors listed were selected based on the desired parameters needed for either energy or water analyses. Data was collected every 15 minutes, with varying sub-scan intervals. These sub-scans were averaged or totaled within the 15-minute window to provide the collected data. Finally, data was wirelessly transmitted and downloaded for analyzation.

Weather Station Sensor	Description	Model #	Qty.
Radiation	Pyranometer	LP02-L	1
Rain Gauge	Tipping-Bucket Rain Gauge	TB4MM-L	1
Temperature & Humidity	Temperature and Relative Humidity Probe	CS215-L	1
Water/Soil Temperature	Temperature Probe	109	1
Wind Speed and Direction	Wind Monitor	05103-L	1
Leaf wetness	Leaf Wetness Sensor	LWS-L	2

Table A-1 Weather Station sensors.

Photovoltaic Roof Sensor	Description	Model #	Qty.
Panel Surface Temperature	Surface-Mount Thermistor	110PV-L	3
Exposed Roof Temperature	Infrared Radiometer	SI-111	2
Shaded Roof Temperature	Thermocouple Probe	109	3
Net Radiation	4-Component Net Radiation Sensor	NR01-L	2
Roof Runoff	Pressure Transducer	CS451	1

Table A-2 Photovoltaic Roof Sensors.

Green Roof Sensor	Description	Model #	Qty.
Vegetation Temperature	Infrared Radiometer	SI-111	3
Under-Tray Temperature	Thermocouple Probe	109	3
TPO Surface Temperature	Infrared Radiometer	SI-111	2
Net Solar Radiation	4-Component Net Radiation Sensor	NR01-L	1
Soil Heat-Flux	Soil Heat Flux Plate	HFP01-L	2
Substrate Moisture & Temperature	12cm Water Content Reflectometer Plus	CS655	9
Total Roof Runoff	Pressure Transducer	CS451	1

Table A-3 Green Roof Sensors.

Sensor Purpose	Description	Model #	Qty.
Water Depth	Pressure Transducer	CS451	1
Water/Substrate Temperature	Temperature Probe	109	6
Soil Heat Flux	Soil Heat Flux Plate	HFP01-L	2
Dissolved Oxygen	Dissolved Oxygen Sensor	CS511-L	2

Table A-4 Constructed Wetland Sensors.

Sensor Purpose	Description	Model #	Qty.
Water Depth	Pressure Transducer	CS451	2
Substrate Moisture & Temperature	12cm Water Content Reflectometer Plus	CS655	6

Table A-5 Bioretention Sensors.

Appendix B Determining Event Size
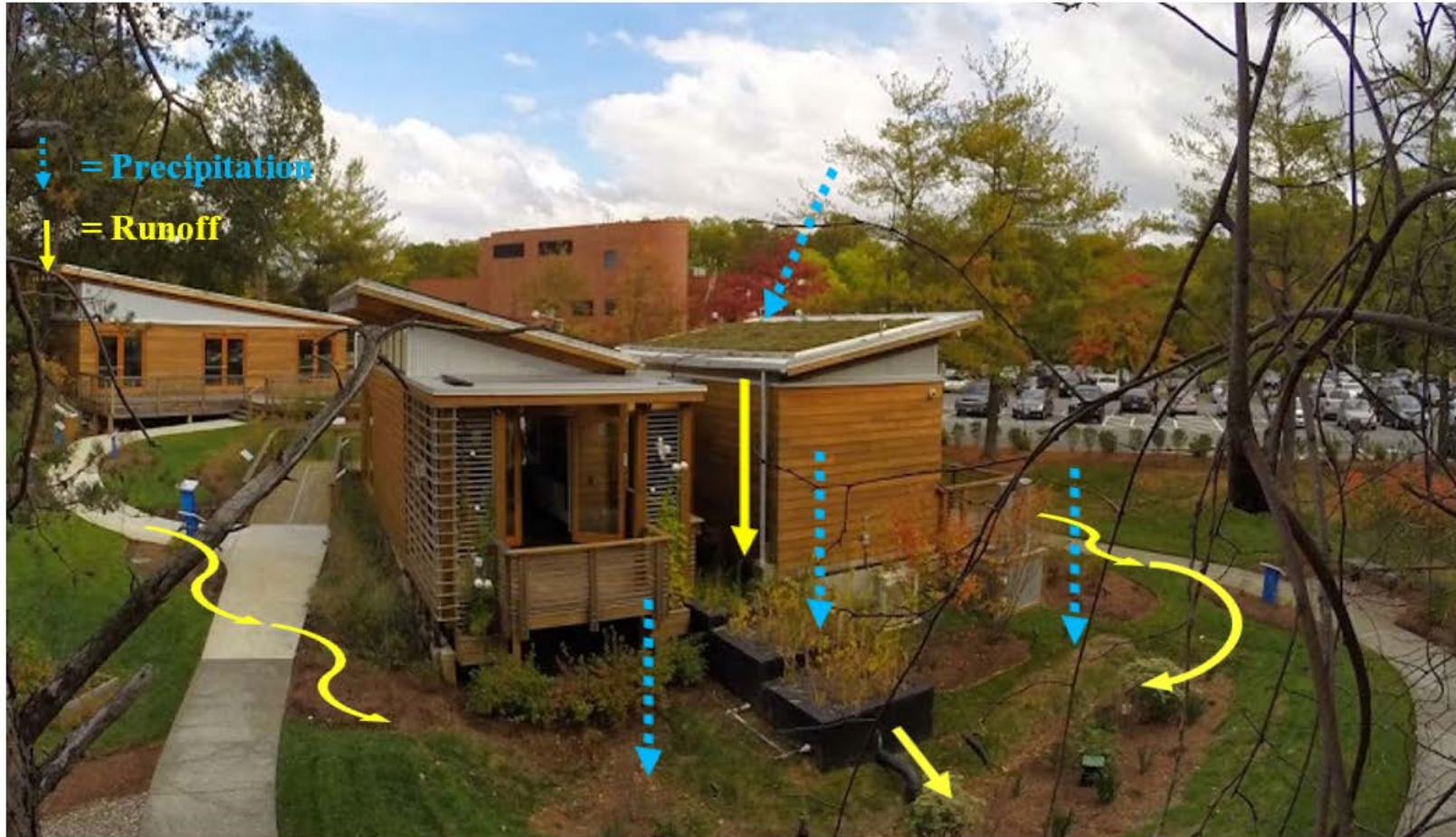
Figure B-1 Stormwater received by each system: Green Roof = Precipitation Only; Constructed Wetland = Precipitation + Green Roof Runoff; Bioretention = Precipitation + Constructed Wetland Runoff + Surface Runoff.

This section provides supplemental information for quantifying event size (mm), or the amount of stormwater received by the green roof, constructed wetland and bioretention system. As illustrated in Figure B-1, the amount of stormwater received by the green roof was attributed to precipitation— green roof retention was calculated using Equation B-1. For the CW, the amount of stormwater received was calculated from the volume of stormwater runoff received by the green roof and the volume of precipitation received (Equation B-2). Finally, stormwater inputted to the bioretention system was calculated from the volume of stormwater received by the CW, the volume of stormwater received from surface runoff, and the volume of precipitation inputted into the system itself (Equation B-3).

Equation B-1   Green Roof Event Size = Precipitation (mm)

CW Event Size = [Precipitation (m^3)+ Green Roof Runoff (m^3)] ÷ Area (m^2) ×1000

Equation B-2

Where,

Green Roof Runoff (m^3) = Precipitation (m^3) − Retention (m^3)

Bioretention Event Size = [Precipitation (m^3)+ CW Runoff (m^3) + Surface Runoff (m^3)] ÷ Area (m^2) ×1000

Equation B-3

Where, CW Runoff (m^3) = Precipitation (m^3) − Retention (m^3)

Equation B-4 is Surface Runoff (m^3) = Precipitation (m) × Surface Runoff Area (m^2) × Surface Type (%) × Runoff Coefficient

228
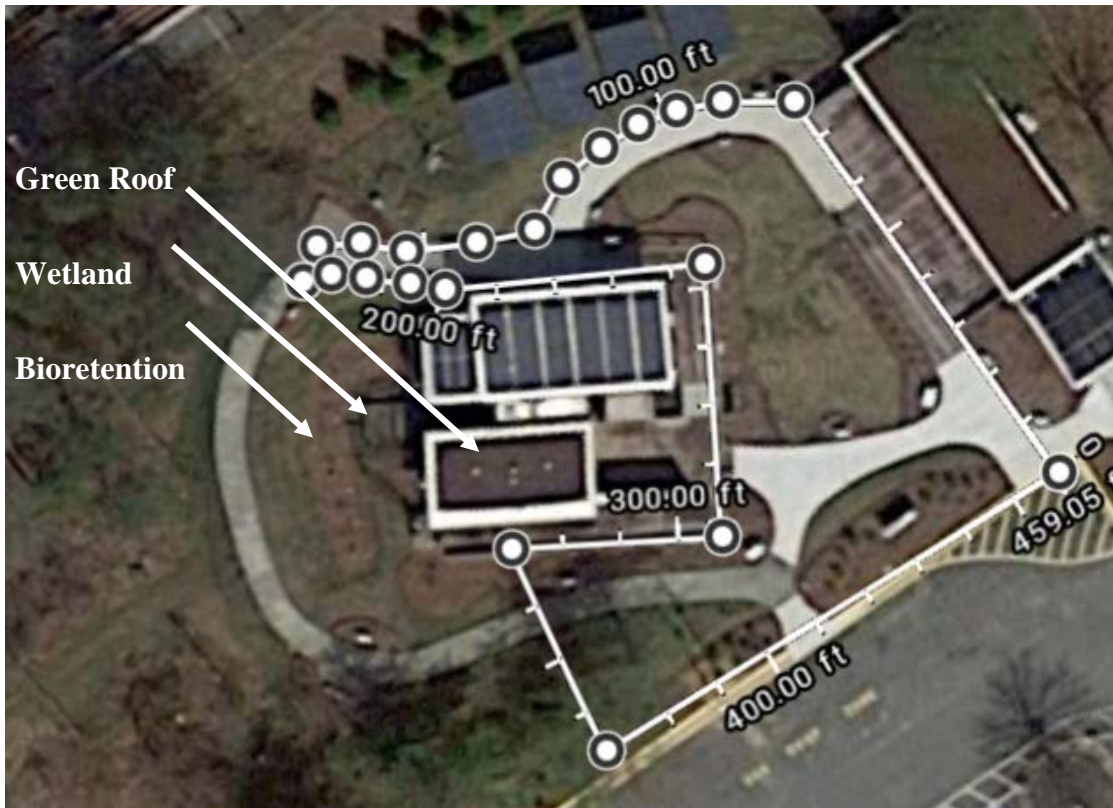
Figure B-2 Surface area contributing to runoff. The ratio of the lawn to impervious concrete and pervious concrete is 68.9%, 21.3% and 9.8%, respectively.

The area of land contributing to surface runoff was determined after a land survey and spatial mapping of land elevation with Google Maps (Figure B-2). Surface runoff was calculated using Equation B-4, which accounts for surface type of the land surveyed– in this case it was a combination of lawn, impervious concrete and pervious concrete (68.9%, 21.3% and 9.8%, respectively). Runoff coeeficents used for calculations were: 0.22 for lawn (assuming clay soil with an average slope of 2-7%), 0.95 for impervious concrete, and 0.48 for pervious concrete. Rationional coefficients for pervious concrete have not been well studied, thus we calculated an average value from a study where rational coefficients for different permeable pavement types was estimated (Figure B-3) (Bean, 2005).

	Surface Infiltration	Cary	Swansboro	Kinston	Wilmington	Standard Impervious
SCS Curve Number			36	88	85	98
A Soil	68					
B Soil	79					
Rational C Equivalent		0.44	0.00	0.76	0.70	0.96
% Grassed	84		>100	71	33	0

Figure B-3 Summary table of curve numbers, rational coefficients, and equivalent percent grassed area from different permeable pavement performance comparisons along with impervious surfaces (Bean, 2005). An average rational coefficient value of 0.48 was calculated and used for this analysis.

Appendix C Vegetation Development (Green Roof Only)

Biomass changes of the green roof's vegetation over time was evaluated using monthly measurements of leaf area index (LAI) and percentage of vegetation cover done during the data collection period. LAI was measured in addition to percent cover because it allowed us to measure the canopy foliage density of the green roof rather than simply area covered (Raji et al., 2015). To assess vegetation changes, the sloped green roof was strategically sectioned off into nine 1 m^2 quadrants within zones (related to elevation) (Figure C-1).
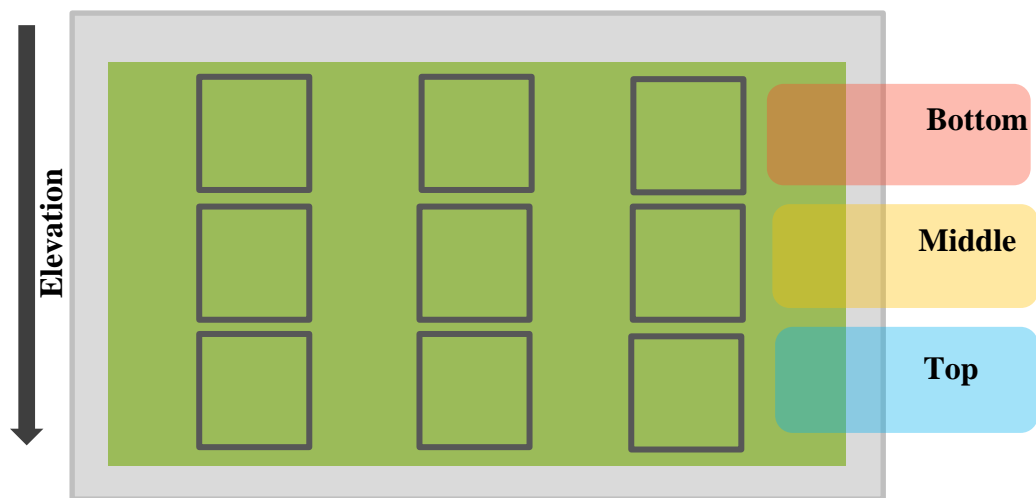
Figure C-1 To assess vegetation changes, the sloped green roof was strategically sectioned off into nine 1 m^2 quadrants within zones (related to elevation).

Determining Leaf Area Index

To calculate, a 1 m × 1 m square grid with 2.54 cm (1-inch) intervals was made (Figure C-2). Within each of the nine quadrants on the roof, 5 points (XY-coordinate) were randomly generated. At this coordinate a count was done for the number of leaves touching the object inserted through the media. This number was averaged, then divided by the

231

measured area of the quadrant ($1\ m^2$) to yield the quadrant LAI (number of leaves per area). Finally, LAI was averaged across the nine quadrants to estimate LAI for the entire roof (Tjaden, 2014).

Figure C-2 Grid pattern used for measuring LAI, 1m x 1m in size.

Determining Percent Cover

To assess vegetation cover, we took photographs of each quadrant within the zones. We analyzed the pictures using a software called *ImageJ*, which enables users to trim and crop an image and select a certain color spectrum to focus on an area of interest. These color spectrums are determined by changing the hue, saturation, and brightness of pixels to select an area of interest. Next, the software computes the pixel quantities for the total area and the area of interest, providing a pixel ratio, which represents percent cover. This method is widely used for various percent cover applications along with other analyses (Tjaden, 2013).

232

The steps below were modified from Tjaden (2013) and outline how to process green roof pictures to calculate a percent cover value using *ImageJ*.

1. *ImageJ* software can be downloaded from the following link: http://imagej.nih.gov/ij/download.html.

2. Once software is downloaded open the desired picture of the area needed to be analyzed: File > Open > 'file.'

3. Crop the designated area you want analyzed by using a polygon tool in the top toolbar. End polygon by clicking on first point.

4. To erase outside pixels, select Edit > Clear Outside to get a new image cropped to the canvas size.

5. Select File > Save as to obtain separate images of cropped area and vegetation area for future reference.

6. At this point with the area still selected take a measurement of the entire area by selecting Analyze > Measure or (Ctrl + M). This will bring up a table with the file name and pixel count (under the column header "Area"). Other variables can be added but for this application the pixel count is all that is needed.

7. Next, adjust the color threshold of the image by selecting Image > Adjust > Color Threshold.

8. Once the threshold window appears, ensure the settings are in the HSB Color mode (at the bottom under Color space), with the rest of the settings as follows: Hue: 0 – 100, Saturation: 46 – 255, Brightness: 1 – 255, Thresholding method: Default,

Threshold color: Red, and Dark background selected. Refer to Figure C-3 for reference.
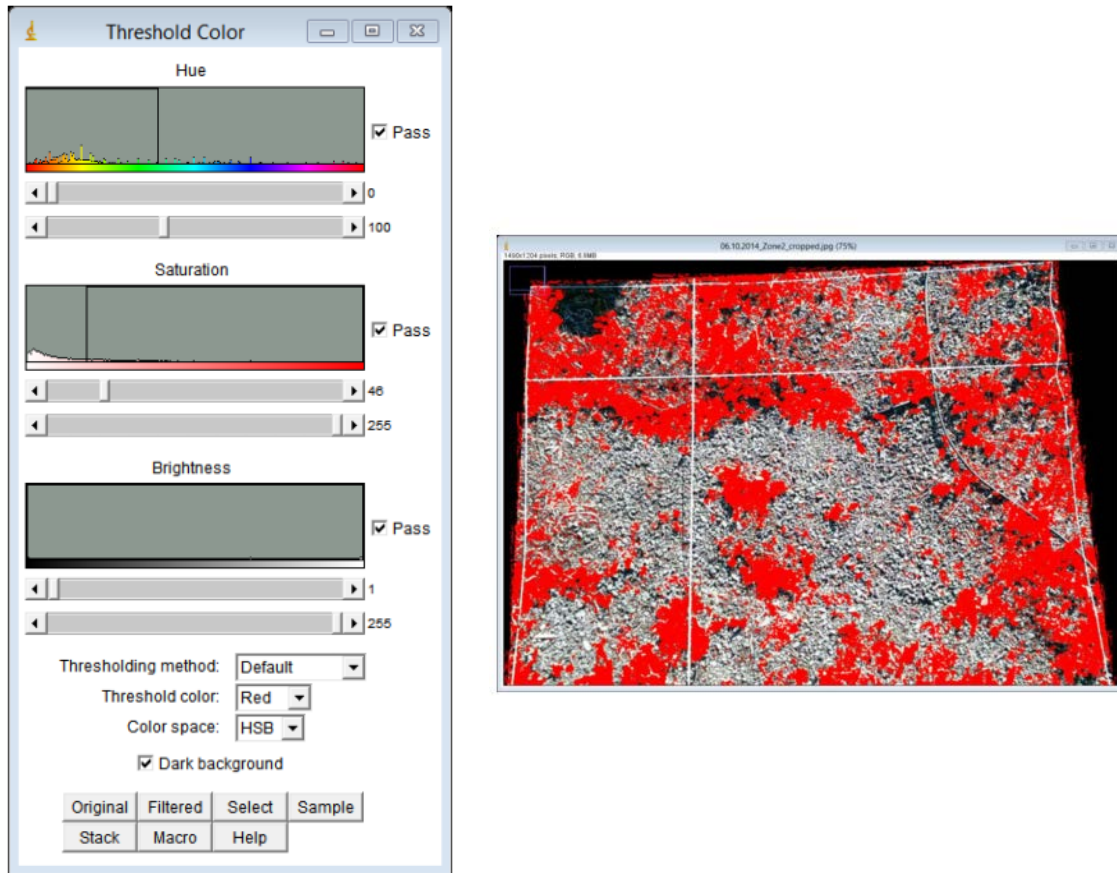
Figure C-3 Screenshot of *ImageJ* software showing how the Threshold color feature was used to select vegetation only within respective green roof quadrants (Tjaden, 2013).

9. Once the settings have been set, click "Select." At this point, you should see only the vegetation selected.

10. To remove the background so that only vegetation is left, select Edit > Clear outside.

11. The vegetation should be the only thing left. At this point take a new measurement by selecting Analyze > Measure or (Ctrl + M), which will populate a new pixel

count of just the vegetation. Select File > Save as to keep this image as well for future reference.

12. Finally, calculate percent cover (% cover = Vegetation Pixels/All Pixels × 100). Figure C-4 is a visual representation of the steps outlined to calculate percent cover.
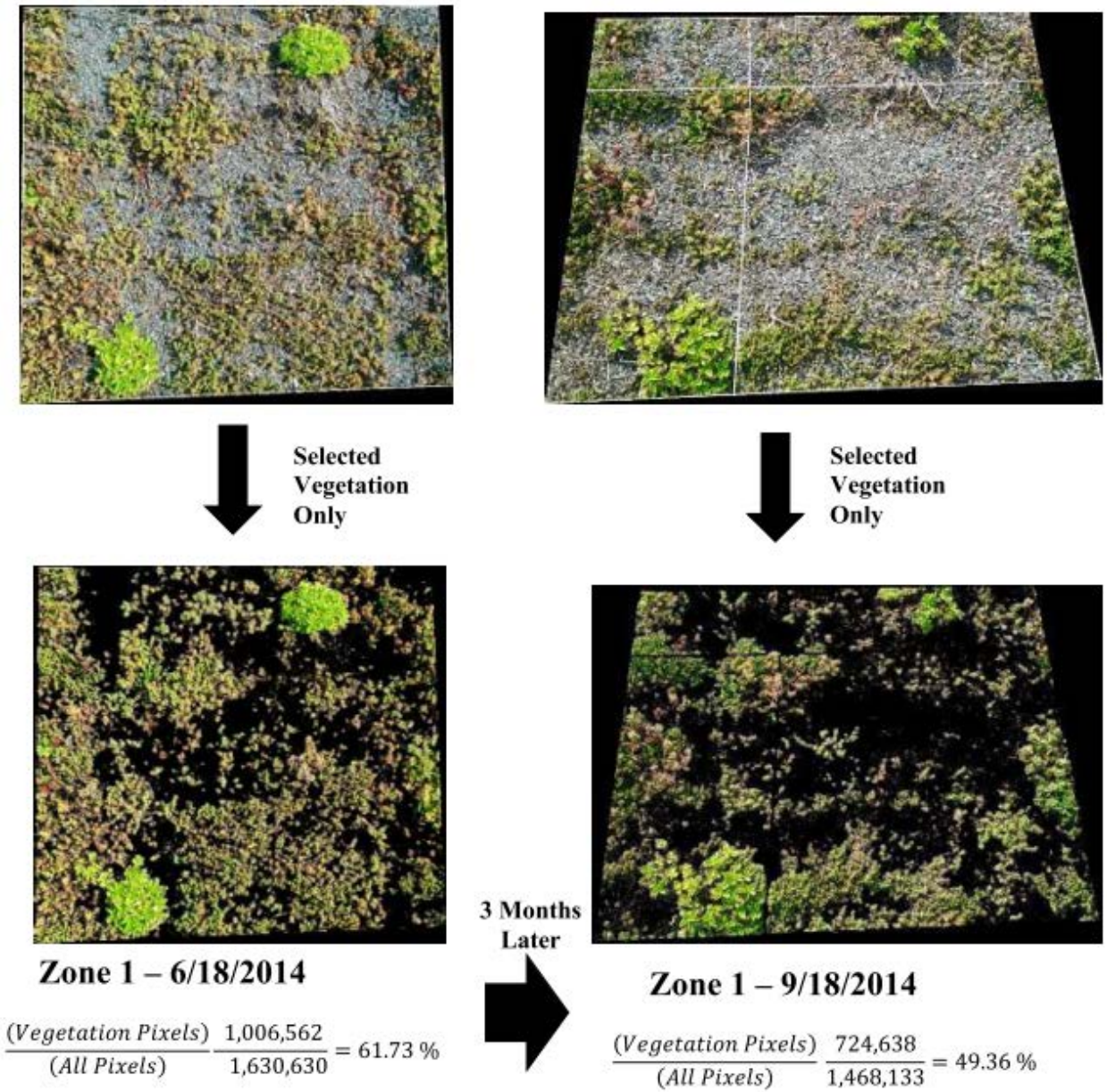
Figure C-4 Visual results of green roof percent cover using *ImageJ* software (Tjaden, 2013).

Appendix D Green Roof Emergy Table and Calculations

Table D-1 Green roof emergy analysis.

Index	Item	Value	Unit	Transformity	Unit	Emergy (sej/year/ m²)	% Total
Renewable							
1	Sun	3.12E+09	J/m²/year	1	sej/J	3.12E+09	13.8%
2	Evapotranspiration	6.37E+05	J/m²/year	3.06E+04	sej/J	1.95E+10	86.2%
						2.26E+10	
Purchased							
3	Polypropylene Module	1.42E+02	g/m²/year	5.27E+09	sej/g	7.51E+11	4.8%
	Engineered Soil						
4	*Expanded Shale*	3.09E+03	g/m²/year	3.04E+09	sej/g	9.40E+12	59.8%
5	*Sand*	1.63E+02	g/m²/year	1.12E+09	sej/g	1.82E+11	1.2%
6	*Compost*	9.20E+06	J/m²/year	1.91E+04	sej/J	1.76E+11	1.1%
7	Sedum Cuttings	1.63E+02	g/m²/year	1.60E+10	sej/g	2.60E+11	16.6%
8	Snow Guard	2.11E+01	g/m²/year	1.25E+10	sej/g	2.63E+11	1.7%
9	Roof Edge	2.84E+01	g/m²/year	1.25E+10	sej/g	3.55E+11	2.3%
10	Labor	1.79E+00	$/m²/year	8.32E+11	sej/$	1.49E+12	9.5%
11	Transportation	7.37E+06	J/m²/year	6.58E+04	sej/J	4.85E+11	3.1%
						1.57E+13	
Benefits							
	Energy Savings						
12	*Heating*	1.59E+06	J/m²/year	2.69E+05	sej/J	4.28E+11	6.0%
13	*Cooling*	1.44E+07	J/m²/year	2.69E+05	sej/J	3.87E+12	54.3%
14	Primary Production	6.37E+05	J/m²/year	3.06E+04	sej/J	1.95E+10	0.3%
15	Urban Heat Island	2.92E+08	J/m²/year	1.26E+01	sej/J	3.67E+09	0.1%
16	Stormwater Reduction	1.43E+06	J/m²/year	3.06E+04	sej/J	4.37E+10	0.6%
17	Habitat Birds	9.35E+02	J/m²/year	5.16E+06	sej/J	4.83E+09	0.1%
18	Habitat Insects	2.31E+03	J/m²/year	6.37E+04	sej/J	1.47E+08	0.0%

	Air Pollution						
19	*Ozone*	4.42E+00	g/m^2/year	6.23E+10	sej/g	2.75E+11	3.9%
20	*Nitrogen dioxide*	2.30E+00	g/m^2/year	6.84E+09	sej/g	1.57E+10	0.2%
21	*Particulate matter*	1.19E+00	g/m^2/year	2.04E+10	sej/g	2.43E+10	0.3%
22	*Sulfur dioxide*	5.95E-01	g/m^2/year	5.26E+10	sej/g	3.13E+10	0.4%
23	Carbon Sequestration	1.25E+01	g/m^2/year	5.80E+08	sej/g	7.25E+09	0.1%
	Energy Savings Emissions Avoided						
24	*Carbon dioxide*	2.02E+03	g/m^2/year	5.80E+08	sej/g	1.17E+12	16.4%
25	*Nitrogen dioxide*	3.09E-02	g/m^2/year	6.84E+09	sej/g	2.11E+08	0.0%
26	*Methane*	3.02E+03	J/m^2/year	4.35E+04	sej/J	1.32E+08	0.0%
	Water Quality						
27	*Ammonia nitrogen*	1.29E-01	g/m^2/year	2.41E+10	sej/g	3.11E+09	0.0%
28	*Lead*	1.10E-02	g/m^2/year	4.80E+11	sej/g	5.28E+09	0.1%
29	*Zinc*	2.50E-02	g/m^2/year	7.20E+10	sej/g	1.80E+09	0.0%
30	Wastewater Energy Savings	3.29E+05	J/m^2/year	2.69E+05	sej/J	8.85E+10	1.2%
	Wastewater Emissions Avoided						
31	*Carbon dioxide*	4.15E+01	g/m^2/year	5.80E+08	sej/g	2.41E+10	0.3%
32	*Nitrogen dioxide*	6.36E-04	g/m^2/year	6.84E+09	sej/g	4.35E+06	0.0%
33	*Methane*	6.23E+01	J/m^2/year	4.35E+04	sej/J	2.71E+06	0.0%
34	Biophilia	1.33E+00	$/m^2/year	8.32E+11	sej/$	1.10E+12	15.5%
						7.12E+12	

Renewable Inputs

1. Sun

   Energy input to the green roof was considered net radiation, which was the sum of incoming shortwave and longwave radiation minus the sum of the reflected shortwave and emitted longwave radiation.

   Net radiation was measured on site with a Huskeflux 4-Component Net Radiation Sensor. Data was automatically collected every second and averaged over 15 minutes; therefore, each data point was multiplied by 900. Finally, data was totaled over the month and averaged over two years.

	Net Radiation (J/month/m^2)
January	1.11E+08
February	1.45E+08
March	2.39E+08
April	3.20E+08
May	3.51E+08
June	3.78E+08
July	4.32E+08
August	3.72E+08
September	3.16E+08
October	2.34E+08
November	1.34E+08
December	8.96E+07
Total	**3.12E+09 J/year/ m**

   Table D-2 Total net radiation per month was averaged across the two-year study period, then summed over the year.

   Sun emergy = Annual Net Radiation × Transformity of Sunlight

   Sun emergy = 3.12E+09 J/m^2 /year × 1 sej/J (Odum, 1996) = 3.12E+09 sej/m^2/year

2. Evapotranspiration

   ET was derived from the soil depletion method, which utilizes volumetric water content sensors (CS655 Water Content Reflectometer) within the substrate of the green roof to determine changes in soil moisture between 15-minute sensor measurements ($\pm \Delta S = S_{t15}$-S_{t0}).

   With the soil depletion method, the assumption is that any gain in water (+ΔS) is retention, and any water loss (–ΔS) is due to ET or substrate drainage. Thus, any water

loss in between rain events can be attributed to ET while substrate drainage was assumed to largely occur during storms. Because ET is a very small portion of the overall water balance of a green roof during storms, it was estimated to be equal to the average rate of ET between one rain event and the next. Once these values were calculated, total ET per month (mm/month) was determined. Then, ET per month was averaged across the two-year study period. It should be noted that since ET was attributed to the change in water status, the soil depletion method could only be confidently applied during warmer months (May-October). During colder months, ET diminishes, and any water loss could be due to substrate drainage.

	ET (mm/month)
May	29.1
June	37.3
July	25.2
August	18.4
September	18.9
October	29.5
Total	**128.8 mm/year**

Table D-3 Total green roof ET per month was averaged across the two-year study period, then summed over the year.

ET emergy = Annual ET × Density of water × Gibbs potential energy of water × Transformity of ET

ET emergy = 128.8 mm/year × 1 m / 1000 mm × 1000 kg/m^3 × 4,949J/kg × 3.06 E+04 sej/J (Odum, 1996) = 1.95E+10 sej/m^2/year

Purchased Inputs

3. Polypropylene Module

   Emergy of module = Mass of layer × Transformity of High Density Polyethylene / Lifetime of roof

   Emergy of module = 14 oz/ft² (LiveRoof specifications) × 1 ft² / 0.0929 m² × 28.35 g/oz × 5.27E+09 sej/g (Buranakarn, 1998) / 30 years= 7.51E+11 sej/m^2/year

   Engineered Soil

4. Expanded Shale

   Emergy of shale = Mass of layer × Transformity of calcined clay [a] / Lifetime of roof

---

[a] Transformity of expanded shale was approximated as being equal to that of expanded clay. The transformity of calcined clay was calculated in Coffman, 2007.

Emergy of shale =19 lb/ft² (LiveRoof specifications) x 1 ft² / 0.0929 m² × 453.6 g/lb x 3.04E+09 sej/g (Coffman, 2007) / 30 years = 9.40E+12 sej/m^2/year

5. Sand

Emergy of sand = Mass of layer × Transformity of sand / Lifetime of roof

Emergy of sand = 1 lb/ft² (LiveRoof specifications) × 1 ft² / 0.0929 m² × 453.6 g/lb × 1.12E+09 sej/g (Odum, 1996) / 30 years = 1.82E+11 sej/m^2/year

6. Compost

Emergy of compost = Mass of layer × Energy content of compost [b] × Transformity of compost/ Lifetime of roof

Emergy of compost = 2.5 lb/ft² (LiveRoof specifications) × 1 ft² / 0.0929 m² × 453.6 g/lb x 5.4 kcal/g (Orrell, 1998) × 4186 J/kcal × 1.91E+04 sej/J (Orrell, 1998) / 30 years = 1.76E+11 sej/m^2/year

7. Emergy of Sedum Cuttings

Emergy of sedum cuttings = Mass of layer × Transformity of tomato production [c] / Lifetime of roof

Emergy of sedum cuttings = 1 lb/ft² (LiveRoof specifications) × 1 ft² / 0.0929 m² × 453.6 g/lb × 1.60E+10 sej/g (Brandt-Williams, 2002) / 30 years = 2.60E+12 sej/m^2/year

Figure D-1 Snow guard with roof edging (Image credit: LiveRoof).

---

[b] Rustagi et al. approximated the energy content of compost and transformity as being equal to that of soil organic matter (Rustagi et al., 2009). They referenced Orrell, 1998, who stated that the energy content of soil organic matter in a "southern mixed hardwood forest ecosystem" is 5.4 kcal/g.
[c] Transformity of *Sedum* was approximated as being equal to that of tomato production.

8. Emergy of Snow Guard

Emergy of snow guard = Mass of layer × Transformity of aluminum / Lifetime of roof

Emergy of snow guard = 631.7 g/m^2 × 1.25E+10 sej/g (Buranakarm and Brown, 2000) / 30 years = 2.63E+11 sej/m^2/year

> Where, a sample of the snow guard was provided by the Solar Decathlon Team and the following specifications were measured: mass = 358.7 g, radius = 0.5 in and height = 24 in.
>
> First, the surface area (SA) of the sample was calculated:
>
> SA of sample (cylinder) = $2\pi rh + 2\pi r^2$ = (2 *pi* x .5 in x 24 in) + (2 *pi* x .5 in ^{2}) =76.9 in^2 = 0.0496 m^2
>
> Then, the SA of the snow guard spanning the length of the roof (312 in.) was calculated:
>
> SA spanning roof = $2\pi rh + 2\pi r^2$ = (2 *pi* x .5 in x 312 in) + (2 *pi* x .5 in ^{2}) = 981.8 in^2 = 0.633 m^2
>
> Next, the total mass of the snow guard was calculated:
>
> Total mass = Mass of sample /SA of sample x SA spanning roof = 358.7 g / 0.0496 m^2 x 0.633 m^2 = 4519.6 g
>
> Finally, the mass of the layer given green roof area was calculated and multiplied by four snow guards:

9. Emergy of Roof Edge

Emergy of roof edge = Mass of layer × Transformity of aluminum / Lifetime of roof

Emergy of roof edge = 851.4 g/m^2 × 1.25E+10 sej/g (Buranakarm and Brown, 2000) / 30 years = 3.55E+11 sej/m^2/year

> Where, sample of the roof edge was provided by the Solar Decathlon Team and the following specifications were measured: mass = 1101.0 g, length = 40.5 in, width$_1$ = 3.5 in and width$_2$ = 4.5 in.
>
> First, the surface area (SA) of the sample was calculated:
>
> SA of sample = $lw + lw$ = (40.5 in x 3.5 in) + (40.5 in x 4.5 in) = 324.0 in^2 = 0.209 m^2
>
> Then, the surface area the roof edge spanning the length (312 in.) and width (144 in.) of the roof was calculated:
>
> SA along length of the roof = $lw + lw$ = (312 in x 3.5 in) + (312 in x 4.5 in) = 2496 in^2= 1.610 m^2
>
> SA along width of the roof = $lw + lw$ = (144 in x 3.5 in) + (144 in x 4.5 in) = 1152 in^2 = 0.743 m^2
>
> Next, the total mass of the roof edge was calculated considering there were four of them:
>
> Total Mass = Mass of sample /SA of sample × SA of roof edge spanning roof
>
> Total Mass = 2 (1101 g / 0.209 m^2 × 1.610 m^2) + 2 (1101 g /0.209 m^2 × 0.743 m^2) = 24563.4 g
>
> Finally, the mass of the layer given green roof area was calculated:
>
> Mass of layer = Total mass/ green roof area = 24563.4 g / 29 m^2 = **851.4 g/ m^2**

10. Labor

Emergy of labor = Cost of LiveRoof installation × Emergy Money-Dollar Ratio / Lifetime of roof

Emergy of labor = 5 \$/ft^2 (Solar Decathlon Team specifications) × 1 ft^2 / 0.0929 m^2 × 8.32E+11 sej/\$ (Tilley, 2006) / 30 years = 1.49E+12 sej/m^2/year

11. Transportation

Emergy of transportation = Distance from nursery × Fuel efficiency [d] × Transformity of petroleum derivatives / Roof area / Lifetime of roof

Emergy of transportation = 282 mi [e] × 1 gallon / 5.8 mi × 125,000 Btu/gallon gasoline x 1,055 J/Btu × 6.58E+04 sej/J (Bastianoni et al., 2009) / 29 m^2 / 30 years = 4.85E+11 sej/m^2/year

Benefits

Energy Savings

Emergy of energy savings = Average heat flux difference between conventional and green roof × Transformity of electricity / Coefficient of performance [f]

12. Energy Saved in Heating

Emergy of heating savings = 0.454 J/s m^2 × 1.051E+07 s/year [g] × 2.69E+05 sej/J (Odum, 1996) / 3 COP = 4.28E+11 sej/m^2/year

> Where,
>
> Heat Flux = (ΔT between green and conventional roof)/ R-value of *Watershed's* roof membrane
>
> Heat Flux = (278.71 K - 274.71) / 8.805 K m^2/ W = **0.454 W/m^2**
>
> The average roof temperature under *WaterShed's* green roof during the cold season was observed to be 5.56 ± 6.59 °C or 278.71 K (Figure 4-11). A study conducted in south Italy found that a green roof was on average 4 °C higher than the black bituminous roof in the winter (Bevilacqua et al., 2016). Thus, the temperature of the conventional roof was estimated to be 1.56 °C or 274.71 K. The R-value of *WaterShed's* roof membrane is 50 h ft^2 F/Btu or 8.805 K m^2/ W.

---

[d] Fuel efficiency of a class 7-8 combination trucks is 5.8 mpg (Davis et al., 2016).

[e] Estimated distance from Riverbend Nursery in Riner, VA to *WaterShed* site in Rockville, Maryland.

[f] A coefficient of performance of 3 was assumed for a heat pump, which is a ratio of heating or cooling provided to electricity consumed.

[g] Assumed that peaking heating demand during the cold season (November-April) was for four months (1.051E+07 s).

13. Energy Saved in Cooling

Emergy of cooling savings = 4.11 J/s m^2 × 1.051E+07 s/year ^{h} × 2.69E+05 sej/J (Odum, 1996) / 3 COP = 3.87E+12 sej/m^2/year

> Where,
>
> Heat Flux = (ΔT between conventional and green roof)/ R-value of *Watershed's* roof membrane
>
> Heat Flux = (332.15 K - 295.95 K) / 8.805 K m^2/ W = **4.11 W/m^2**
>
> The average temperature found in a literature review of conventional roofs (Table 4-2) was calculated to be 59.0 °C or 333.15 K, while the average roof temperature under *WaterShed's* green roof during the warm season was observed to be 22.8 ± 6.30 ºC or 295.95 K (Figure 4-8). The R-value of *WaterShed's* roof membrane is 50 h ft^2 F/Btu or 8.805 K m^2/ W.

14. Production

The emergy yielded by green roof primary production was assumed to equal the emergy of evapotranspiration.

15. Urban Heat Island

UHI emergy = Annual ET × Density of water × Latent heat of vaporization × Transformity of global latent heat

UHI emergy = 128.8 mm/year ^{i} × 1 m / 1000 mm × 1000 kg/m^3 × 2264.76 kJ/kg × 1000 J/kJ × 12.6 sej/J (Odum et al., 2000) = 3.67E+09 sej/m^2/year

16. Stormwater Reduction

To quantify stormwater retention across storm events (>5 mm), the soil depletion method was applied— refer to section 3.3.2 for a detailed description of how retention was determined. Storm events were defined as the time precipitation began until the precipitation ceased. Independent storm events consisted of events separated by six or more hours. In the event runoff was still occurring 6h after the first event, the two events were combined (Getter et al., 2007). Total retention per month was calculated then averaged across the two-year study period.

---

[h] Assumed that peaking cooling demand during the warm season (May-October) was for four months (1.051E+07 s).
[i] See step 2 for evapotranspiration calculation methodology.

	Retention (mm/month)
January	23.4
February	24.6
March	20.4
April	22.1
May	23.5
June	36.8
July	27.4
August	15.2
September	19.9
October	22.2
November	22.7
December	30.2
Total	**288.4 mm/year**

Table D-4 Total green roof retention per month was averaged across the two-year study period, then summed over the year.

Stormwater emergy = Retention × Density of water × Gibbs chemical energy of water × Transformity of rain water/ Roof area

Stormwater emergy = 288.4 mm/year × 1 m/ 1000 mm × 1000 kg/m^3 × 4,949J/kg × 3.06 E+04 sej/J (Odum, 1996) = 4.37E+10 sej/m^2/year

17. Birds

Emergy of birds found on the green roof was modeled based on a study of bird species found to breed on green roofs (Fernandez-Canero and Gonzalez-Redondo, 2010). The list of birds was restricted based on the availability of mass and basal metabolic rate (BMR) data found in McNab, 2009.

	Species	Scientific Name	Mass (g)	BMR (kJ/h)
1	Blue tit	*Parus caeruleus*	9.6	0.6
2	Willow warbler	*Phylloscopus trochilus*	10.7	0.75
3	Black redstart	*Phoenicurus ochruros*	13.8	0.87
4	Spotted flycatcher	*Muscicapa striata*	14.4	0.89
5	Great tit	*Parus major*	16.5	1.26
6	White wagtail	*Motacilla alba*	18	1.08
7	Meadow pipit	*Anthus pratensis*	18.9	1.08
8	Chaffinch	*Fringilla coelebs*	21	1.34
9	Tree sparrow	*Passer montanus*	22.3	1.46

10	House sparrow	*Passer domesticus*	23	1.32
11	Greenfinch	*Carduelis chloris*	28.2	1.71
12	Skylark	*Alauda arvensis*	31.7	2.6
13	Little ringed plover	*Charadrius dubius*	36	1.5
14	Black bird	*Turdus merula*	82.6	3.34
15	Magpie	*Pica*	158.9	4.31
16	City dove	*Columba livia*	368	5.97
17	Common gull	*Larus canus*	431	8.1
18	Carrion crow	*Corvus corone*	518	11.93
19	Oystercatcher	*Haematopus ostralegus*	554	10.48
20	Mallard	*Anas platyrhynchos*	1020	14.64

Table D-5 Due to large varations in bird mass and BMR, the medians were calculated at 25.6 g and 1.515 kJ/h, respectively.

Bird emergy = Bird density × Bird mass × Metabolism × Time there × Bird transformity

Bird emergy = 0.01 ind/m^2 [j] × 25.6 g/ind × 59.18 J/hr g [k] × 0.17 hr/day [l] × 365 day/year × 5.16E+06 sej/J (Riposo and Kangas, 2009) = 4.83E+09 sej/m^2/year

18. Insects

Insect density was modeled from a study of insect species composition and diversity on intensive green roofs (MacIvor and Lundholm, 2011). The top 4 orders used for this calculation represented 94.5% of insects sampled.

	Species Density (ind/m^2)	Mass (g)	Metabolism (J/s g)
Heteroptera (True Bugs)	0.1345	0.00371	1.46E-02
Coleoptera (Beetles)	0.198	0.00009	3.82E-03
Diptera (Flies)	0.142	0.01326	1.97E-02
Hymenoptera (Bees, wasps, ants)	1.20	0.01541	5.07E-03
	1.67	**8.12E-03**	**1.08E-02**

Table D-6 Total insect density, average mass and average metabolism were calculated. Insect mass and metabolism values were adapted from Makarieva et al., 2008.

---

[j] Bird density was modeled from a study of birds in urban parks. Densities of 48.5 ± 16.4 ind/ha and 51.0 ± 15.6 ind/ha for parks in the breeding and wintering seasons, respectively were observed (Zhou and Chu, 2012).

[k] Bird metabolism = 1.515 kJ/h × 1000 J/kJ / 25.6 g = 59.18 (J/ hr g)

[l] It was assumed that birds were present 10 minutes per day.

Insect emergy = Total insect density × Average insect mass × Average insect metabolism × Time there × Insect transformity

Insect emergy = 1.67 ind/m^2 × 8.12E-03 g/ind × 1.08E-02 J/s g × 2.628E+06 s/month × 6 month/year × 6.37E+04 sej/J (Cohen 2004) [m] = 1.47E+08 sej/m^2/year

Air pollution

Emergy of air pollution was modeled from a dry deposition model used to quantify the impact of green roofs on air pollution in Chicago. Researchers found that air pollutants were removed at a rate of 85 kg/ha/year with ozone accounting for 52% of the total followed by NO_2 (27%), PM_{10} (14%), and SO_2 (7%) (Yang et al., 2013).

Air pollutant emergy = Pollutant removed × Transformity of pollutant

19. Ozone

    Ozone emergy = 4.42 g/m^2/year × 6.23E+10 sej/g (Campbell and Tilley, 2014a) = 2.75 E+11 sej/m^2/year

20. Nitrogen Dioxide

    Nitrogen dioxide emergy = 2.3 g/m^2/year × 6.84E+09 sej/g (Campbell and Tilley, 2014a) = 1.57 E+10 sej/m^2/year

21. Particulate Matter

    Particulate matter emergy = 1.19 g/m^2/year × 2.04E+10 sej/g (Campbell and Tilley, 2014a) = 2.43E+10 sej/m^2/year

22. Sulfur Dioxide

    Sulfur dioxide emergy = 0.595 g/m^2/year × 5.26 x10^{10} sej/g (Campbell and Tilley, 2014a) = 3.13E+10 sej/m^2/year

23. Carbon Sequestration

    Emergy of carbon sequestered was modeled from a study of the carbon sequestration potential of extensive green roofs. Researchers found that the green roof system sequestered 375 g/C·m^2 in above- and belowground biomass and substrate organic matter (total carbon averaged at the end of the two growing seasons) (Getter et al., 2009).

---

[m] Transformity for large aquatic insects.

Carbon sequestration emergy = Carbon sequestered × Transformity of carbon / Lifetime of roof

375 g/m^2 × 5.80E+08 sej/g (Campbell and Tilley, 2014a) / 30 years = 7.25E+09 sej/m^2/year

Energy Savings Emissions Avoided

Carbon dioxide, nitrogen dioxide and methane emissions avoided due to energy savings in heating and cooling was modeled (see steps 12-13). Where,

Energy savings = Heat Flux difference between conventional and green roof / Coefficient of performance [n]

Heating savings = 0.454 J/s m^2 [o] × 1.051E+07 s/year [p] / 3 COP = 1.59E+06 J/m^2/year

Cooling savings = 4.11 J/s m^2 [q] × 1.051E+07 s/year [r] / 3 COP = 1.44E+07 J/m^2/year

Total energy savings = 1.59E+06 J/m^2/year + 1.44E+07 J/m^2/year = 1.60E+07 J/m^2/year

Emission avoided emergy = Total energy savings × Emission factor [s] × Transformity of pollutant

24. Carbon Dioxide

Emergy of carbon dioxide avoided = 1.60E+07 J/m^2/year × 1 kWh / 3.6E+06 J × 454.4 g/kWh (EPA, 2014) × 5.80E+08 sej/g (Campbell and Tilley, 2014a) = 1.17E+12 sej/m^2/year

25. Nitrogen Dioxide

Emergy of nitrogen dioxide avoided = 1.60E+07 J/m^2/year × 1 kWh / 3.6E+06 J × 0.007 g/kWh (EPA, 2014) × 6.84E+09 sej/g (Campbell and Tilley, 2014a) = 2.11E+08 sej/m^2/year

---

[n] A coefficient of performance of 3 was assumed for a heat pump, which is a ratio of heating or cooling provided to electricity consumed.
[o] See step 12 for heating savings calculation.
[p] Assumed that peaking heating demand during the cold season (November-April) was for four months (1.051E+07 s).
[q] See step 13 for cooling savings calculation.
[r] Assumed that peaking cooling demand during the warm season (May-October) was for four months (1.051E+07 s).
[s] An emission factor is defined as the annual amount of air pollutant emission by the annual amount of electricity production at local power stations (Peng and Jim, 2015).

26. Methane

Emergy of methane avoided = 1.60E+07 J/m^2/year $\times$ 1 kWh / 3.6E+06 J $\times$ 0.012 g/kWh (EPA, 2014) $\times$ 5.55E+04 J/g ^{t} x 4.35E+04 sej/J (Bastianoni et al., 2009) = 1.32E+08 sej/m^2/year

Water Quality

Water quality benefits were modeled from a study of the effect of a modular extensive green roof on stormwater runoff and water quality (Gregoire and Clausen, 2011). It should be noted that we assumed that the green roof is only a sink, and not a source of pollutants, even though researchers found certain mean concentrations of pollutants in runoff were higher than in precipitation. We excluded these pollutants and narrowed our list to pollutants that the green roof was a sink for: NH$_3$–N, Zn, and Pb.

Pollutant	Input (kg/ha/year)	Output (kg/ha/year)	Removal (kg/ha/year)
NH$_3$–N	1.47	0.18	1.29
Pb	0.11	0	0.11
Zn	0.38	0.13	0.25

Table D-7 Mass input and export of nutrients and metals in runoff from a modular extensive green roof. Source: Gregoire and Clausen (2011).

Emergy of water quality improvement = Pollutant removed $\times$ Transformity of pollutant

27. Ammonia Nitrogen

Emergy of ammonia nitrogen removed = 0.129 g/m^2/year $\times$ 2.41E+10 sej/g (Brandt-Williams, 1999) = 3.11E+09 sej/m^2/year

28. Lead

Emergy of lead removed = 0.011 g/m^2/year $\times$ 4.80E+11 sej/g (Cohen et al., 2007) = 5.28E+09 sej/m^2/year

29. Zinc

Emergy of zinc removed = 0.025 g/m^2/year $\times$ 7.20E+10 sej/g (Cohen et al., 2007) = 1.80E+09 sej/m^2/year

---

^{t} Energy content of methane is 55.5 MJ/kg.

30. Wastewater Treatment Energy Savings

Indirect energy savings was modeled based on the assumption that a typical medium sized wastewater treatment (WWTP) plant in the U.S. consumes 1200 kilowatt hours (kWh) per million gallons (MG) of wastewater (Flynn and Traver, 2013).

Emergy of WWTP energy savings = Retention × 1200 kWh/MG × Transformity of electricity

Emergy of WWTP energy savings = 288.4 mm/year [u] × 1 m / 1000 mm × 1 MG / 3785.4 m³ × 1200 kWh/MG × 3.6E+06 J/kWh × 2.69E+05 sej/J (Odum, 1996) = 8.85E+10 sej/m^2/year

Wastewater Treatment Emissions Avoided

Emergy of WWTP emission avoided = Retention [v] × 1200 kWh/MG × Emission factor [w] × Transformity of pollutant

31. Carbon Dioxide

Emergy of carbon dioxide avoided = 288.4 mm/year × 1 m / 1000 mm × 1 MG / 3785.4 m³ x 1200 kWh/MG × 454.4 g/kWh (EPA, 2014) × 5.80E+08 sej/g (Campbell and Tilley, 2014a) = 2.41E+10 sej/m^2/year

32. Nitrogen dioxide

Emergy of nitrogen dioxide avoided = 288.4 mm/year × 1 m / 1000 mm × 1 MG / 3785.4 m³ × 1200 kWh/MG × 0.007 g/kWh (EPA, 2014) × 6.84E+09 sej/g (Campbell and Tilley, 2014a) = 4.35E+06 sej/m^2/year

33. Methane

Emergy of methane avoided = 288.4 mm/year × 1 m / 1000 mm × 1 MG / 3785.4 m³ 1200 kWh/MG × 0.012 g/kWh (EPA, 2014) × 5.55E+04 J/g [x] × 4.35E+04 sej/J (Bastianoni et al., 2009) = 2.71E+06 sej/m^2/year

34. Biophilia

Biophilia was modeled from a study that attempted to quantify an important yet not scientifically proven assumption concerning the biophilic relationship between views

---

[u] See step 16 for stormwater reduction calculation.
[v] See step 16 for stormwater reduction calculation.
[w] An emission factor is defined as the annual amount of air pollutant emission by the annual amount of electricity production at local power stations (Peng and Jim, 2015).
[x] Energy content of methane is 55.5 MJ/kg.

of nature and daylighting in the workplace and their impacts on sick leave of office workers. Researchers found that someone working in an office with the best view would be expected to use, on average, about 57 hours of sick leave (a little more than 7 days), but someone with no view at all would be expected to use almost 68 hours (11 hours or close to one and one-half days more per year) (Elzeyadi, 2011).

Emergy of biophilia = Sick hours saved × Hourly wage × Number of inhabitants × Emergy Money-Dollar Ratio / *WaterShed* site area

Emergy of biophilia = 11 hr/person/year × 2 persons [y] × 28 \$/hr [z] × 8.32E+11 sej/\$ (Tilley, 2006) / 464.5 m^2 = 1.10E+12 sej/m^2/year

---

[y] *WaterShed* was designed for two persons.
[z] According to the state of Maryland, average personal income in 2016 was \$57,936 or approximately \$28/hr.

Appendix E Constructed Wetland Emergy Table and Calculations

Table E-1 Constructed wetland emergy analysis.

Index	Item	Value	Unit	Transformity	Unit	Emergy (sej/year/ m²)	% Total
Renewable							
1	Sun	3.12E+09	J/m²/year	1	sej/J	3.12E+09	0.4%
2	Evapotranspiration	2.38E+07	J/m²/year	3.06E+04	sej/J	7.28E+11	99.6%
						7.31E+11	
Purchased							
3	Concrete	2.07E+04	g/m²/year	1.44E+09	sej/g	2.99E+13	15.9%
4	PVC Pipes	1.53E+02	g/m²/year	5.87E+09	sej/g	8.99E+11	0.5%
5	Waterproofing spray	2.85E+01	g/m²/year	4.39E+09	sej/g	1.25E+11	0.1%
	Vegetation						
6	*Nursery Pots*	2.15E+04	g/m²/year	5.27E+09	sej/g	1.13E+14	16.6%
7	*Soil*	2.67E+03	g/m²/year	1.68E+09	sej/g	4.48E+12	1.7%
8	*Cattail Plants*	3.29E+01	$/m²/year	8.32E+11	sej/$	2.74E+13	2.3%
9	Gravel	6.64E+03	g/m²/year	1.68E+09	sej/g	1.12E+13	5.9%
10	Land Value	6.21E-01	$/m²/year	8.32E+11	sej/$	5.17E+11	0.3%
11	Labor	3.87E-01	$/m²/year	8.32E+11	sej/$	3.22E+11	0.2%
						1.88E+14	
Benefits							
12	Primary production	2.38E+07	J/m²/year	3.06E+04	sej/J	7.28E+11	6.7%
13	Urban heat island	1.09E+10	J/m²/year	1.26E+01	sej/J	1.37E+11	1.3%
14	Stormwater reduction	8.43E+06	J/m²/year	3.06E+04	sej/J	2.58E+11	2.4%
	Water quality						
15	*Sediment*	4.68E+03	g/m²/year	1.68E+09	sej/g	7.86E+12	72.1%
16	*Phosphorus*	6.67E+00	g/m²/year	2.16E+10	sej/g	1.44E+11	1.3%
17	Wastewater energy savings	1.95E+06	J/m²/year	2.69E+05	sej/J	5.23E+11	4.8%
	Wastewater emissions						

	avoided							
18		*Carbon dioxide*	2.46E+02	g/m²/year	5.80E+08	sej/g	1.42E+11	1.3%
19		*Nitrogen dioxide*	3.78E-03	g/m²/year	6.84E+09	sej/g	2.59E+07	0.0%
20		*Methane*	3.60E+02	J/m²/year	4.35E+04	sej/J	1.57E+07	0.0%
21	Biophilia		1.33E+00	$/m²/year	8.32E+11	sej/$	1.10E+12	10.1%
							1.09E+13	

1. Sun

   It was assumed the energy input to the wetland was the same as the green roof– see Appendix D for details on how net radiation was calculated.

   Sun emergy = Annual Net Radiation × Transformity of Sunlight

   Sun emergy = 3.12E+09 J/m^2/year × 1 sej/J (Odum, 1996) = 3.12E+09 sej/m^2/year

2. Evapotranspiration

   Evapotranspiration was derived from the soil depletion method, which utilizes pressure transducer sensors (CS451 Pressure Transducer) within the substrate of the wetland to determine changes in soil moisture between 15-minute sensor measurements ($\pm \Delta S = S_{t15}\text{-}S_{t0}$).

   With the soil depletion method, the assumption is that any gain in water (+ΔS) is retention, and any water loss (–ΔS) is due to ET or substrate drainage. Thus, any water loss in between rain events can be attributed to ET while substrate drainage was assumed to largely occur during storms. Because ET is a very small portion of the overall water balance of a green roof during storms, it was estimated to be equal to the average rate of ET between one rain event and the next. Once these values were calculated, total ET per month (mm/month) was determined. Then, ET per month was averaged across the two-year study period.

	ET (mm/month)
May	200.0
June	809.0
July	747.0
August	1287.5
September	1015.5
October	746.5
Total	**4805.5 mm/year**

   Table E-2 Total wetland ET per month was averaged across the two-year study period, then summed over the year.

   It should be noted that since ET was attributed to the change in water status, the soil depletion method could only be confidently applied during warmer months (May-October). During colder months, ET diminishes, and any water loss could be due to substrate drainage.

   ET emergy = Annual ET × Density of water × Gibbs potential energy of water × Transformity of ET

   ET emergy = 4805.5 mm/year × 1 m / 1000 mm × 1000 kg/m^3 × 4,949 J/kg × 3.06 E+04 sej/J (Odum, 1996) = 7.28E+11 sej/m^2/year

Purchased Inputs

3. Concrete cell

   Emergy of concrete cells was estimated based on the assumption that a typical 80 lb. bag of concrete has a volume of 0.6 ft^3 (estimated from product specifications). Volume covered was estimated based on engineering documents provided by the Solar Decathlon Team.

   Concrete emergy = Concrete density × Volume covered × Transformity of cement / Wetland area / Lifetime of wetland

   Cement emergy = 80 lb / 0.6 ft^3 × 453.6 g/lb × 35.3 ft^3 / 1 m^3 × 2.53 m^3 (Engineering design specifications) × 1.44E+09 sej/g (Buranakarn, 1998) / 8.68 m^2 / 30 years = 2.99E+13 sej/m^2/year

4. PVC Pipes

   Using dimensional analysis of engineering design documents, emergy of PVC pipes was estimated based on the assumption that 6-inch pipes were used. Pipe density was estimated from product specifications. Area covered was estimated based on engineering documents provided by the Solar Decathlon Team.

   PVC pipe emergy = PVC pipe density × Area covered × Transformity of PVC / Wetland area / Lifetime of wetland

   PVC pipe emergy = 36.63 lb/ 10 ft × 24 ft × 453.6 g/lb × 5.87E+09 sej/g (Buranakarn, 1998) / 8.68 m^2 / 30 years = 8.99E+11 sej/m^2/year

5. Waterproofing Spray

   Emergy of waterproofing was estimated based on the assumption that waterproofing spray was used— density (12 oz, area covered is 10 ft^2) was estimated from product specifications. Area covered was estimated based on engineering documents provided by the Solar Decathlon Team.

   Waterproofing spray emergy = Spray density × Area covered × Transformity of rubber / Wetland area / Lifetime of wetland

   Waterproofing spray emergy = 12 oz/ 10 ft^2 × 217.9 ft^2 x 28.34 g/oz x 4.39E+09 sej/g (Buranakarn, 1998) / 8.68 m^2/ 30 years =1.25E+11 sej/m^2/year

<u>Vegetation</u>

6. Nursery Pots

   Emergy of vegetation was estimated based on the assumption that 3-gallon nursery pots (diameter = 9.5 in, mass = 0.34 lb) were used— density was estimated from product specifications. Number of pots was estimated based on engineering documents provided by the Solar Decathlon Team (wetland area/ area of pot).

   Nursery pot emergy = Pot density × Number of pots × Transformity of High Density Polyethylene / Lifetime of wetland

   Nursery pot emergy = 0.34 lb / 70.9 in^2 × 1550 in^2/m^2 × 453.6 g/lb × 191 pots × 5.27E+09 sej/g (Buranakarn, 1998) / 30 years = 1.13E+14 sej/m^2/year

7. Soil

   Emergy of soil used in nursery pots was estimated based on the assumption that a 2 ft^3 bag weighs approximately 40 lbs. Soil density was estimated from product specifications. Number of pots was estimated based on engineering documents provided by the Solar Decathlon Team (wetland area/ area of pot).

   Soil emergy = Soil density × Number of pots × Volume of pots × Transformity of soil / Wetland area / Lifetime of wetland

   Soil emergy = 40 lb/ 2 ft^3 × 453.6 g/lb × 1ft^3 / 7.48 gal × 3 gal × 191 pots × 1.68E+09 sej/g (Campbell and Ohrt, 2009) [aa] / 8.68 m^2 / 30 years = 4.48E+12 sej/m^2/year

8. Cattail Plants

   Common Cattail (*Typha latifolia*) was listed as one of the species planted in the wetland.

   Emergy of cattail plants = Cost × Number of pots × Emergy Money-Dollar Ratio / Wetland area / Lifetime of wetland

   Emergy of cattail plants = 14.95 \$/gal × 3 gallons/pot × 191 pots × 8.32E+11 sej/\$ (Tilley, 2006) / 8.68 m^2/ 30 years = 2.74E+13 sej/m^2/year

9. Gravel

   Emergy of gravel was estimated based on the assumption that a 50 lb bag of gravel with a coverage volume of 1.5 ft^3 was used (generic product specifications). Volume covered was estimated based on engineering documents provided by the Solar Decathlon Team.

[aa] Campbell and Tilley (2014b) used this value as a transformity for rock, sand, and gravel.

Gravel emergy = Gravel density × Volume covered × Transformity of gravel / Wetland area / Lifetime of wetland

Gravel emergy = 50 lb / 1.5 ft^3 × 453.6 g/lb × 35.3 ft^3 / 1 m^3 × 3.24 m^3 ×1.68E+09 sej/g (Campbell and Ohrt, 2009) [bb] / 8.68 m^2 / 30 years = 1.12E+13 sej/m^2/year

10. Land Value

Emergy of land value was estimated based on the assumption that Maryland value of land per acre is $75,429 (Larson, 2015).

Land value emergy = Land value × Emergy Money-Dollar Ratio / Lifetime of wetland

Land value emergy = 75,429 $/acres × 1 acre / 4046.9 m^2 × 8.32E+11 sej/$ (Tilley, 2006) / 30 years = 5.77E+11 sej/m^2/year

11. Labor

Emergy of labor was estimated based on the assumption that typical construction cost of constructed wetlands in 2004 ranged from approximately $30,000 to $65,000 per acre ("Pennsylvania Stormwater Best Management Practices Manual," 2006). Average cost was calculated to be $47,000 per acre or (11.61 $/m^2).

Labor emergy = Labor cost × Emergy Money-Dollar Ratio / Lifetime of wetland

Labor emergy = 47,000 $/acres × 1 acre / 4046.9 m^2 × 8.32E+11 sej/$ (Tilley, 2006) / 30 years = 3.22E+11 sej/m^2/year

Benefits

12. Primary Production

The emergy yielded by constructed wetland primary production was assumed to equal the emergy of evapotranspiration.

13. Urban Heat Island

UHI emergy = Annual ET × Density of water × Latent heat of vaporization × Transformity of global latent heat

UHI emergy = 4805.5 mm/year [cc] × 1m/1000mm × 1000 kg/m^3 × 2264.76 kJ/kg × 1000J/kJ × 12.6 sej/J (Odum et al., 2000) = 1.37E+11 sej/m^2/year

---

[bb] Campbell and Tilley (2014b) used this value as a transformity for rock, sand, and gravel.
[cc] See step 2 for evapotranspiration calculation methodology.

14. Stormwater Retention

To quantify stormwater retention across storm events (>5 mm), the soil depletion method was applied— refer to section 3.3.2 for a detailed description of how retention was determined. Storm events were defined as the time precipitation began until the precipitation ceased. Independent storm events consisted of events separated by six or more hours. In the event runoff was still occurring 6h after the first event, the two events were combined (Getter et al., 2007). Retention volumes per month were calculated then averaged across the two-year study period.

	Retention (m^3/month)
January	1.50
February	1.15
March	0.75
April	0.3
May	0.61
June	2.70
July	0.57
August	1.21
September	0.87
October	1.63
November	1.04
December	2.44
Total	**14.8 m^3/year**

Table E-3 Total wetland retention per month was averaged across the two-year study period, then summed over the year.

Stormwater emergy = Retention volume x Density of Water × Gibbs chemical energy of water × Transformity of rain water / Wetland area

Stormwater emergy = 14.8 m^3/year × 1000 kg/m^3 × 4,949J/kg × 3.06 E+04 sej/J (Odum, 1996) / 8.68 m^2 = 2.58E+11 sej/m^2/year

Water Quality

Emergy of water quality benefits was modeled from as study that analyzed phosphorus and particle retention in seven constructed wetlands, situated in agricultural catchments. Average net accumulation of sediment (t/ha/year) and phosphorus (kg/ha/year) of the seven wetlands for the two years of study was taken and used for

this anaysis (Johannesson et al., 2015).

Emergy of water quality = Pollutant accumulated × Transformity of pollutant

15. Sediment

Emergy of sediment accumulation = 51.6 t/ha/year x 90,7185 g/t × 1 ha / 10,000 m^2 × 1.68E+09 sej/g (Campbell and Ohrt, 2009) [dd] = 7.86E+12 sej/m^2/year

16. Phosphorus

Emergy of phosphorus accumulation = 66.7 kg/ha/year x 1000 g/kg × 1 ha/ 10,000 m^2 × 2.16E+10 sej/g (Campbell and Ohrt, 2009) [ee] = 1.44E+11 sej/m^2/year

17. Wastewater Treatment Energy Savings

Indirect energy savings was modeled based on the assumption that a typical medium sized wastewater treatment (WWTP) plant in the U.S. consumes 1200 kilowatt hours (kWh) per million gallons (MG) of wastewater (Flynn and Traver, 2013).

Emergy of WWTP energy savings = Retention volume × 1200 kWh/MG × Transformity of electricity / Wetland area

Emergy of WWTP energy savings= 14.8 m^3/year [ff] × 1 MG / 3785.4 m³ × 1200 kWh/MG × 3.6E+06 J/kWh × 2.69E+05 sej/J (Odum, 1996) / 8.68 m^2 = 5.23E+11 sej/m^2/year

Wastewater Treatment Emissions Avoided

Emergy of WWTP emission avoided = Retention [gg] × 1200 kWh/MG × Emission factor [hh] × Transformity of pollutant

18. Carbon Dioxide

Emergy of carbon dioxide avoided = 14.8 m^3/year × 1 MG / 3785.4 m³ × 1200 kWh/MG × 454.4 g/kWh (EPA, 2014) × 5.80E+08 sej/g (Campbell and Tilley, 2014a) / 8.68 m^2 = 1.42E+11 sej/m^2/year

---

[dd] Campbell and Tilley (2014b) used this value as a transformity for sediment.
[ee] Campbell and Tilley (2014b) used this value as a transformity for phosphorus.
[ff] See step 14 for stormwater reduction methodology.
[gg] See step 14 for stormwater reduction methodology.
[hh] An emission factor is defined as the annual amount of air pollutant emission by the annual amount of electricity production at local power stations (Peng and Jim, 2015).

19. Nitrogen Dioxide

Emergy of nitrogen dioxide avoided = 14.8 m^3/year $\times$ 1 MG / 3785.4 m³ $\times$ 1200 kWh/MG $\times$ 0.007 g/kWh (EPA, 2014) $\times$ 6.84E+09 sej/g (Campbell and Tilley, 2014a) / 8.68 m^2 = 2.59E+07 sej/m^2/year

20. Methane

Emergy of methane avoided = 14.8 m^3/year $\times$ 1 MG / 3785.4 m³ $\times$ 1200 kWh/MG $\times$ 0.012 g/kWh (EPA, 2014) $\times$ 5.55E+04 J/g [ii] $\times$ 4.35E+04 sej/J (Bastianoni et al., 2009) / 8.68 m^2 = 1.57E+07 sej/m^2/year

21. Biophilia

Biophilia was modeled from a study that attempted to quantify an important yet not scientifically proven assumption concerning the biophilic relationship between views of nature and daylighting in the workplace and their impacts on sick leave of office workers. Researchers found that someone working in an office with the best view would be expected to use, on average, about 57 hours of sick leave (a little more than 7 days), but someone with no view at all would be expected to use almost 68 hours (11 hours or close to one and one-half days more per year) (Elzeyadi, 2011).

Emergy of biophilia = Sick hours saved $\times$ Hourly wage $\times$ Number of inhabitants $\times$ Emergy Money-Dollar Ratio / *WaterShed* site area

Emergy of biophilia = 11 hr/person/year $\times$ 2 persons [jj] $\times$ 28 \$/hr [kk] $\times$ 8.32E+11 sej/\$ (Tilley, 2006) / 464.5 m^2 = 1.10E+12 sej/m^2/year

---

[ii] Energy content of methane is 55.5 MJ/kg.
[jj] *WaterShed* was designed for two persons.
[kk] According to the state of Maryland, average personal income in 2016 was \$57,936 or approximately \$28/hr.

Appendix F Bioretention Emergy Table and Calculations

Table F-1 Bioretention emergy analysis. It should be noted that water quality improvement is a key benefit of bioretention that could not be modeled due to the lack of available data that would allow us to calculate its benefit in emergy terms (i.e., $g/m^2/year$).

Index	Item	Value	Unit	Transformity	Unit	Emergy (sej/year/ m^2)	% Total
Renewable							
1	Sun	3.12E+09	$J/m^2/year$	1	sej/J	3.12E+09	0.3%
2	Evapotranspiration	3.87E+07	$J/m^2/year$	3.06E+04	sej/J	1.18E+12	99.7%
						1.19E+12	
Purchased							
3	3" Mulch layer	9.04E+02	$g/m^2/year$	2.75E+08	sej/g	2.49E+11	0.4%
4	21" Planting media	1.35E+04	$g/m^2/year$	1.68E+09	sej/g	2.27E+13	34.3%
5	6" Sand bed	8.14E+03	$g/m^2/year$	1.68E+09	sej/g	1.37E+13	20.6%
6	9" Stone layer	1.17E+04	$g/m^2/year$	1.68E+09	sej/g	1.97E+13	29.7%
7	Perforated PVC pipes	3.06E+01	$g/m^2/year$	5.87E+09	sej/g	1.79E+11	0.3%
	Vegetation						
8	*Nursery pots*	1.69E+03	$g/m^2/year$	5.27E+09	sej/g	8.89E+12	13.4%
9	*Soil*	5.58E+01	$g/m^2/year$	1.68E+09	sej/g	9.37E+10	0.1%
10	*Switchgrass*	1.83E-01	$\$/m^2/year$	8.32E+11	sej/$	1.52E+11	0.2%
11	Land value	6.21E-01	$\$/m^2/year$	8.32E+11	sej/$	5.17E+11	0.8%
12	Labor	4.31E+00	$\$/m^2/year$	8.32E+11	sej/$	8.96E+10	0.1%
						6.63E+13	
Benefits							
13	Primary production	3.87E+07	$J/m^2/year$	3.06E+04	sej/J	1.18E+12	32.4%
14	Urban heat island	1.77E+10	$J/m^2/year$	1.26E+01	sej/J	2.23E+11	6.1%
15	Stormwater reduction	1.04E+07	$J/m^2/year$	3.06E+04	sej/J	3.20E+11	8.7%

16	Wastewater energy savings	2.41E+06	J/m^2/year	2.69E+05	sej/J	6.47E+11	17.7%
	Wastewater emissions avoided						
17	*Carbon dioxide*	3.04E+02	g/m^2/year	5.80E+08	sej/g	1.76E+11	4.8%
18	*Nitrogen dioxide*	4.68E-03	g/m^2/year	6.84E+09	sej/g	3.20E+07	0.0%
19	*Methane*	4.45E+02	J/m^2/year	4.35E+04	sej/J	1.94E+07	0.0%
20	Biophilia	1.33E+00	\$/m^2/year	8.32E+11	sej/\$	1.10E+12	30.2%
						3.65E+12	

Renewable Inputs

1. Sun

   It was assumed the energy input to the wetland was the same as the green roof– see Appendix D for details on how net radiation was calculated.

   Sun emergy = Annual Net Radiation × Transformity of Sunlight

   Sun emergy = 3.12E+09 J /m^2/year × 1 sej/J (Odum, 1996) = 3.12E+09 sej/m^2/year

2. Evapotranspiration

   Evapotranspiration was derived from the soil depletion method, which utilizes pressure transducer sensors (CS451 Pressure Transducer) within the substrate of the wetland to determine changes in soil moisture between 15-minute sensor measurements ($\pm \Delta S = S_{t15} - S_{t0}$).

   With the soil depletion method, the assumption is that any gain in water ($+\Delta S$) is retention, and any water loss ($-\Delta S$) is due to ET or substrate drainage. Thus, any water loss in between rain events can be attributed to ET while substrate drainage was assumed to largely occur during storms. Because ET is a very small portion of the overall water balance of a green roof during storms, it was estimated to be equal to the average rate of ET between one rain event and the next. Once these values were calculated, total ET per month (mm/month) was determined. Then, ET per month was averaged across the two-year study period.

	ET (mm/month)
May	1462.5
June	1778.0
July	832.2
August	1942.5
September	1077.0
October	720.0
Total	**7812.2 mm/year**

   Table F-2 Total bioretention ET per month was averaged across the two-year study period, then summed over the year.

   It should be noted that since ET was attributed to the change in water status, the soil depletion method could only be confidently applied during warmer months (May-October). During colder months, plant cover and ET diminishes, and any water loss over prolonged periods of time could be due to substrate drainage.

   ET emergy = Annual ET × Density of water × Gibbs potential energy of water × Transformity of ET

   ET emergy = 7812.2 mm/year × 1 m / 1000 mm × 1000 kg/m^3 × 4,949 J/kg × 3.06 E+04 sej/J (Odum, 1996) = 1.18E+12 sej/m^2/year

Purchased

3. 3" Mulch Layer

Emergy of mulch was estimated based on the assumption that typical mulch products weigh between 400-800 lbs per cubic yard. For this analysis we took the average of these values. Volume covered was estimated based on engineering documents provided by the Solar Decathlon Team.

Mulch layer emergy = Mulch density × Volume covered × Transformity of mulch / Bioretention area / Lifetime of bioretention

Mulch layer emergy = 600 lb/yd^3 × 453.6 g/lb × 1.31 yd^3/m^3 × 2.48 m^3 × 2.75E+08 sej/g (Nelson et al., 2001) / 32.6 m^2 / 30 years = 2.49E+11 sej/m^2/year

4. 21" Planting Media

Media specifications were not provided, thus emergy of the soil bed was approximated based on the assumption that the state of Maryland recommends bioretention planting soil be a sandy loam, loamy sand, loam (USDA), or a loam/sand mix (should contain a minimum 35 to 60% sand, by volume) (MDE, 2009). The average of these percentage values was taken for the analysis. It was also assumed that native soil was used for simplicity. Volume covered was estimated based on engineering documents provided by the Solar Decathlon Team.

Planting media emergy = Sand density [ll] × Volume covered × Transformity of soil / Bioretention area / Lifetime of bioretention

Planting media emergy = 50 lb / 0.5 ft^3 × 453.6 g/lb × 35.3 ft^3 / 1 m^3 × 17.4 m^3 × 47.5% × 1.68E+09 sej/g (Campbell and Ohrt, 2009) [mm] / 32.6 m^2 / 30 years = 2.27E+13 sej/m^2/year

5. 6" Sand Bed

Emergy of the sand bed was approximated based on the assumption that a typical 50 lb bag of sand has as coverage volume of 0.5 ft^3. Sand density was estimated from product specifications. Volume covered was estimated based on engineering documents provided by the Solar Decathlon Team.

Sand bed emergy = Sand density × Volume covered × Transformity of sand / Bioretention area / Lifetime of bioretention

Sand bed emergy = 50 lb / 0.5 ft^3 × 453.6 g/lb × 35.3 ft^3 / 1 m^3 × 4.96 m^3 × 1.68E+09 sej/g (Campbell and Ohrt, 2009) [nn] / 32.6 m^2 / 30 years = 1.37E+13 sej/m^2/year

---

[ll] Emergy of the sand bed was approximated based on the assumption that a typical 50 lb bag of sand has as coverage volume of 0.5 ft^3. Sand density was estimated from product specifications.
[mm] Campbell and Tilley (2014b) used this value as a transformity for rock, sand, and gravel.
[nn] Campbell and Tilley (2014b) used this value as a transformity for rock, sand, and gravel.

6. 9" Stone Layer

Emergy of the stone layer was estimated based on the assumption that a typical 48 lb bag of stone has as coverage volume of 0.5 ft^3. Stone density was estimated from product specifications. Volume covered was estimated based on engineering documents provided by the Solar Decathlon Team stating there was a 6" stone layer above the underdrain and a 3" stone layer below the underdrain.

Stone layer emergy = Stone density × Volume covered × Transformity of stone / Bioretention area / Lifetime of bioretention

Stone layer emergy = 48 lb / 0.5 ft^3 × 453.6 g/lb × 35.3 ft^3 / 1 m^3 × 7.45 m^3 × 1.68E+09 sej/g (Campbell and Ohrt, 2009) [oo] / 32.6 m^2 / 30 years = 1.97E+13 sej/m^2/year

7. Perforated PVC Pipes

Emergy of the 18 linear feet of 6" perforated PVC pipes used was calculated. Pipe density (36.63 lb/ 10 ft) was estimated from product specifications. Area covered was estimated based on engineering documents provided by the Solar Decathlon Team.

Perforated PVC pipe emergy = PVC pipe density × Area covered × Transformity of PVC / Wetland area / Lifetime of wetland

Perforated PVC pipe emergy = 36.63 lb/ 10 ft × 18 ft × 453.6 g/lb × 5.87E+09 sej/g (Buranakarn, 1998) / 32.6 m^2 / 30 years = 1.79E+11 sej/m^2/year

Vegetation

8. Nursery Pots

Emergy of vegetation was estimated based on the assumption that 3-gallon nursery pots were used— density was estimated from product specifications (diameter = 9.5 in, mass = 0.34 lb). It was assumed that 15 pots were bought based on photographs of bioretention in the early phases of establishment.

Nursery pot emergy = Pot density × Number of pots × Transformity of High Density Polyethylene / Lifetime of bioretention

Nursery pot emergy = 0.34 lb / 70.9 in^2 × 1550 in^2/m^2 × 453.6 g/lb × 15 pots × 5.27E+09 sej/g (Buranakarn, 1998) / 30 years = 8.89E+12 sej/m^2/year

9. Soil

Emergy of soil used in nursery pots was estimated based on the assumption that a 2 ft^3 bag weighs approximately 40 lbs. Soil density was estimated from product specifications. It was assumed that 15 pots were bought based on photographs of

---

[oo] Campbell and Tilley (2014b) used this value as a transformity for rock, sand, and gravel.

bioretention in the early phases of establishment.

Soil emergy = Soil density × Number of pots × Volume of pots × Transformity of soil / Bioretention area / Lifetime of bioretention

Soil emergy = 40 lb/ 2 ft^3 × 453.6 g/lb × 1ft^3 / 7.48 gal × 3 gal × 15 pots × 1.68E+09 sej/g (Campbell and Ohrt, 2009) [pp] / 32.6 m^2 / 30 years = 9.37E+10 sej/m^2/year

10. Switchgrass

A plant list was not provided, however commonly used species for bioretention areas are provided in [Table A.4] of *Maryland's Stormwater Design Manual* (MDE, 2009). Switchgrass (*Panicum virgatum*) was listed as a commonly used shrub species for bioretention areas. It was assumed that 15 pots were bought based on photographs of bioretention in the early phases of establishment.

Emergy of switchgrass plants = Cost × Number of pots × Emergy Money-Dollar Ratio / Bioretention area / Lifetime of bioretention

Emergy of switchgrass plants = 11.95 \$/pot × 15 pots × 8.32E+11 sej/\$ (Tilley, 2006) / 32.6 m^2 / 30 years = 1.52E+11 sej/m^2/year

11. Land value

Emergy of land value was estimated based on the assumption that Maryland value of land per acre is \$75,429 (Larson, 2015).

Land value emergy = Land value × Emergy Money-Dollar Ratio / Lifetime of bioretention

Land value emergy = 75,429 \$/acres × 1 acre / 4046.9 m^2 × 8.32E+11 sej/\$ (Tilley, 2006) / 30 years = 5.17E+11 sej/m^2/year

12. Labor

Emergy of labor was approximated based on the assumption that the cost to hire a professional to design and install bioretention, it will cost roughly \$10-\$14 per square feet (Winooski Natural Resources Conservation District, 2007). The average of these values was taken and used for the analysis.

Labor emergy = Labor cost × Emergy Money-Dollar Ratio / Lifetime of wetland

Labor emergy = 12 \$/ft^2 × 10.76 ft^2/m^2 × 8.32E+11 sej/\$ (Tilley, 2006) / 30 years = 8.96E+10 sej/m^2/year

---

[pp] Campbell and Tilley (2014b) used this value as a transformity for rock, sand, and gravel.

Benefits

13. Primary Production

   The emergy yielded by bioretention primary production was assumed to equal the emergy of evapotranspiration.

14. Urban Heat Island

   UHI emergy = Annual ET ^{qq} × Density of water × Latent heat of vaporization × Transformity of global latent heat

   ET emergy = 7812.2 mm/year × 1m/1000mm × 1000 kg/m^3 x 2264.76 kJ/kg × 1000J/kJ × 12.6 sej/J (Odum et al., 2000) = 2.23E+11 sej/m^2/year

15. Stormwater Retention

   To quantify stormwater retention across storm events (>5 mm), the soil depletion method was applied— refer to section 3.3.2 for a detailed description of how retention was determined. Storm events were defined as the time precipitation began until the precipitation ceased. Independent storm events consisted of events separated by six or more hours. In the event runoff was still occurring 6h after the first event, the two events were combined (Getter et al., 2007). Retention volumes per month were calculated then averaged across the two-year study period.

	Retention (m^3/month)
January	9.90
February	3.71
March	6.14
April	2.86
May	5.92
June	11.9
July	2.20
August	7.41
September	2.70
October	4.20
November	5.76
December	6.08
Total	68.8 (m^3/year)

Table F-3 Total retention of the bioretention area per month was averaged across the two-year study period, then summed over the year.

---

^{qq} See step 2 for evapotranspiration calculation methodology.

Stormwater emergy = Retention volume x Density of Water × Gibbs chemical energy of water × Transformity of rain water / Bioretention area

Stormwater emergy = 68.8 m^3/year × 1000 kg/m^3 × 4,949J/kg × 3.06 E+04 sej/J (Odum, 1996) / 32.6 m^2 = 3.20E+11 sej/m^2/year

16. Wastewater Treatment Energy Savings

Indirect energy savings was modeled based on the assumption that a typical medium sized wastewater treatment (WWTP) plant in the U.S. consumes 1200 kilowatt hours (kWh) per million gallons (MG) of wastewater (Flynn and Traver, 2013).

Emergy of WWTP energy savings = Retention volume × 1200 kWh/MG × Transformity of electricity / Bioretention area

Emergy of WWTP energy savings= 68.8 m^3/year [rr] × 1 MG / 3785.4 m^3 × 1200 kWh/MG × 3.6E+06 J/kWh × 2.69E+05 sej/J (Odum, 1996) / 32.6 m^2 = 6.47E+11 sej/m^2/year

Wastewater Treatment Emissions Avoided

Emergy carbon dioxide avoided = Retention volume [ss] × 1200 kWh/MG × Emission factor [tt] × Transformity of pollutant / Bioretention area

17. Carbon Dioxide

Emergy carbon dioxide avoided = 68.8 m^3/year × 1 MG / 3785.4 m^3 × 1200 kWh/MG × 454.4 g/kWh (EPA, 2014) × 5.80E+08 sej/g (Campbell and Tilley, 2014a) / 8.68 m^2 = 1.76E+11 sej/m^2/year

18. Nitrogen Dioxide

Emergy of nitrogen dioxide avoided = 68.8 m^3/year × 1 MG / 3785.4 m^3 × 1200 kWh/MG × 0.007 g/kWh (EPA, 2014) × 6.84E+09 sej/g (Campbell and Tilley, 2014a) / 8.68 m^2 = 3.20E+07 sej/m^2/year

19. Methane

Emergy of methane avoided = 68.8 m^3/year × 1 MG / 3785.4 m^3 × 1200 kWh/MG × 0.012 g/kWh (EPA, 2014) × 5.55E+04 J/g [uu] × 4.35E+04 sej/J (Bastianoni et al., 2009) / 8.68 m^2 = 1.94E+7 sej/m^2/year

---

[rr] See step 15 for stormwater reduction methodology.
[ss] See step 15 for stormwater reduction methodology.
[tt] An emission factor is defined as the annual amount of air pollutant emission by the annual amount of electricity production at local power stations (Peng and Jim, 2015).
[uu] Energy content of methane is 55.5 MJ/kg.

20. Biophilia

Biophilia was modeled from a study that attempted to quantify an important yet not scientifically proven assumption concerning the biophilic relationship between views of nature and daylighting in the workplace and their impacts on sick leave of office workers. Researchers found that someone working in an office with the best view would be expected to use, on average, about 57 hours of sick leave (a little more than 7 days), but someone with no view at all would be expected to use almost 68 hours (11 hours or close to one and one-half days more per year) (Elzeyadi, 2011).

Emergy of biophilia = Sick hours saved × Hourly wage × Number of inhabitants × Emergy Money-Dollar Ratio / *WaterShed* site area

Emergy of biophilia = 11 hr/person/year × 2 persons [vv] × 28 \$/hr [ww] × 8.32E+11 sej/\$ (Tilley, 2006) / 464.5 m^2 = 1.10E+12 sej/m^2/year

---

[vv] *WaterShed* was designed for two persons.
[ww] According to the state of Maryland, average personal income in 2016 was \$57,936 or approximately \$28/hr.

Appendix G Emergy Diversity Index Calculations

Equation G-1 $\text{Emergy diversity (ED)} = -\sum \text{EIV}_i \log[\text{EIV}_i]$

Equation G-2 $\text{EIV}_i = \dfrac{\text{NP}_i \times \tau_i}{\sum \text{NP}_i \times \tau_i}$

Where EIV_i is the emergy importance value,

NP_i is the net production (e.g. J/year),

τ_i is the computed transformity of component i (e.g. sej/J)

Table G-1 Green roof emergy diversity calculations (note, a log base of two was used for calculations).

			$\text{NP}_i \times \tau_i$ (sej/year/ m²)	EIV_i	$\text{EIV}_i \log_2[\text{EIV}_i]$	B inputs
Renewable						
	1	Sun	3.12E+09	0.00	-0.00244049	
	2	Evapotranspiration	1.95E+10	0.00	-0.01197024	
Purchased						
	3	Polypropylene module	7.51E+11	0.05	-0.20941643	
		Engineered Soil				
	4	*Expanded shale*	9.40E+12	0.60	-0.44389532	
	5	*Sand*	1.82E+11	0.01	-0.07452006	
	6	*Compost*	1.76E+11	0.01	-0.07241148	
	7	Sedum cuttings	2.60E+12	0.17	-0.42952152	
	8	Snow guard	2.63E+11	0.02	-0.09873585	
	9	Roof edge	3.55E+11	0.02	-0.12336038	
Purchased services						
	10	Labor	1.49E+12	0.09	-0.32238146	
	11	Transportation	4.85E+11	0.03	-0.1548348	
			1.57E+13			**1.94**

Benefits		$NP_i \times \tau_i$ (sej/year/ m²)	EIV_i	$EIV_i \log_2[EIV_i]$	B_{benefits}
	Energy savings				
12	*Heating*	4.28E+11	0.06	-0.24382925	
13	*Cooling*	3.87E+12	0.54	-0.47815677	
14	Primary production	1.95E+10	0.00	-0.02332478	
15	Urban heat island	3.67E+09	0.00	-0.00563852	
16	Stormwater reduction	4.37E+10	0.01	-0.04509787	
17	Habitat birds	1.47E+08	0.00	-0.00032168	
18	Habitat insects	4.83EE+09	0.00	-0.00713869	
	Air pollution				
19	*Ozone*	2.75E+11	0.04	-0.18154074	
20	*Nitrogen dioxide*	1.57E+10	0.00	-0.01946505	
21	*Particulate matter*	2.43E+10	0.00	-0.02795637	
22	*sulfur dioxide*	3.13E+10	0.00	-0.03443004	
23	Carbon sequestration	7.25E+09	0.00	-0.0101253	
	Energy savings emissions avoided				
24	*Carbon dioxide*	1.17E+12	0.16	-0.428162	
25	*Nitrogen dioxide*	2.11E+08	0.00	-0.00044615	
26	*Methane*	1.32E+08	0.00	-0.00029068	
	Water quality				
27	*Ammonia nitrogen*	3.11E+09	0.00	-0.00487552	
28	*Lead*	5.28E+09	0.00	-0.0077134	
29	*Zinc*	1.80E+09	0.00	-0.00302225	
30	Wastewater energy savings	8.85E+10	0.01	-0.07869147	
	Wastewater emissions avoided				
31	*Carbon dioxide*	2.41E+10	0.00	-0.027784	
32	*Nitrogen dioxide*	4.35E+06	0.00	-1.2613e-05	
33	*Methane*	2.71E+06	0.00	-8.1211e-06	
34	Biophilia	1.10E+12	0.16	-0.41694173	
		7.12E+12			**2.04**

Table G-2 Constructed wetland emergy diversity calculations (note, a log base of two was used for calculations).

		$NP_i \times \tau_i$ (sej/year/ m^2)	EIV_i	$EIV_i \log_2[EIV_i]$	B inputs
Renewable					
1	Sun	3.12E+09	0.00	-0.000262863	
2	Evapotranspiration	7.28E+11	0.00	-0.030935406	
Purchased					
3	Concrete	2.99E+13	0.16	-0.421036003	
4	PVC pipes	8.99E+11	0.00	-0.036746623	
5	Waterproofing spray	1.25E+11	0.00	-0.006993414	
	Vegetation				
6	*Nursery pots*	1.13E+14	0.60	-0.442231347	
7	*Soil*	4.48E+12	0.02	-0.128191538	
8	*Cattail plants*	2.74E+13	0.15	-0.40402205	
9	Gravel	1.12E+13	0.06	-0.241305484	
10	Land value	5.17E+11	0.00	-0.023326025	
11	Labor	3.22E+11	0.00	-0.015699921	
		1.89E+14			**1.75**

		$NP_i \times \tau_i$ (sej/year/ m^2)	EIV_i	$EIV_i \log_2[EIV_i]$	B benefits
Benefits					
12	Primary production	7.28E+11	0.07	-0.260769727	
13	Urban heat island	1.37E+11	0.01	-0.079442585	
14	Stormwater reduction	2.58E+11	0.02	-0.127913973	
	Water quality				
15	*Sediment*	7.86E+12	0.72	-0.33988903	
16	*Phosphorus*	1.44E+11	0.01	-0.082535922	
17	Wastewater energy savings	5.23E+11	0.05	-0.210238985	
	Wastewater Emissions avoided				
18	*Carbon dioxide*	1.42E+11	0.01	-0.081783257	
19	*Nitrogen dioxide*	2.59E+07	0.00	-4.43619E-05	
20	*Methane*	1.57E+07	0.00	-2.78836E-05	
21	Biophilia	1.10E+12	0.10	-0.334556879	
		1.09E+13			**1.52**

Table G-3 Bioretention emergy diversity calculations (note, a log base of two was used for calculations).

		$NP_i \times \tau_i$ (sej/year/ m²)	EIV_i	$EIV_i \log_2[EIV_i]$	B_{inputs}
Renewable					
1	Sun	3.12E+09	0.00	-0.000666502	
2	Evapotranspiration	1.18E+12	0.02	-0.102327229	
Purchased					
3	3" Mulch layer	2.49E+11	0.00	-0.029802723	
4	21" Planting media	2.27E+13	0.34	-0.528815719	
5	6" Sand bed	1.37E+13	0.20	-0.466748295	
6	9" Stone layer	1.97E+13	0.29	-0.518551224	
7	Perforated PVC pipes	1.79E+11	0.00	-0.022761665	
	Vegetation				
8	*Nursery Pots*	8.89E+12	0.13	-0.385285691	
9	*Soil*	9.37E+10	0.00	-0.013189737	
10	*Switchgrass*	1.52E+11	0.00	-0.019868203	
11	Land Value	5.17E+11	0.01	-0.053865722	
12	Labor	8.96E+10	0.00	-0.012690681	
		6.74E+13			**2.15**

Benefits		$NP_i \times \tau_i$ (sej/year/ m²)	EIV_i	$EIV_i \log_2[EIV_i]$	$B_{benefits}$
13	Primary production	1.18E+12	0.32	-0.526787701	
14	Urban heat island	2.23E+11	0.06	-0.246232308	
15	Stormwater reduction	3.20E+11	0.09	-0.307485632	
16	Wastewater energy savings	6.47E+11	0.18	-0.442393142	
	Wastewater emissions avoided				
17	*Carbon dioxide*	1.76E+11	0.05	-0.211049373	
18	*Nitrogen dioxide*	3.20E+07	0.00	-0.000147295	
19	*Methane*	1.94E+07	0.00	-0.000092970	
20	Biophilia	1.10E+12	0.30	-0.521692417	
		3.65E+12			**2.26**

Glossary

Albedo (solar reflectance or reflection coefficient): the ratio of reflected radiation from a surface to the amount of solar radiation that hits it (α = Shortwave reflected/ Incoming Shortwave).

Antecedent (pre-event) water content: average water content 1 hour prior to a storm event.

Bioretention (rain gardens or biofilters): bioretention systems are generally depressional areas constructed by placing a porous soil medium in shallow trenches or basins and planting various types of vegetation. It is largely being adopted in urban and suburban areas to reduce stormwater flow rate, flow volume, pollutant concentrations and to facilitate groundwater recharge.

Constructed wetland (CW): also known as constructed stormwater wetlands, or reed beds– CWs are natural wastewater treatment systems, capable of modifying, removing or transforming a variety of water pollutants by a combination of biological, chemical and physical processes, whilst, depending on their area, are also able to provide the wildlife and recreational benefits commonly associated with natural wetland systems.

Cool roof (white roof): generally defined as a roof system with a coating characterized by high solar reflectance and high thermal emissivity. These thermal properties limit the rise in roof surface temperatures under the sun and reduce the heat transfer to the built environment by reflecting incident solar radiation away from the building and radiating heat away at night compared to conventional building materials.

Crassulacean acid metabolism (CAM): under water stress conditions, CAM plants only open their stomata to metabolize at night when temperatures are cooler. ET loss is therefore lower than from C3 or C4 plants that evapotranspire soil–water during warm daylight conditions.

Emergy: an accounting method used to evaluate the sustainability of ecological-economic systems by evaluating direct and indirect environmental inputs of system flows relative to outputs (calculated in solar energy joules or solar emjoules). Solar energy joules (sej) account for the amount of "free" environmental work done by nature to generate flows.

Emergy diversity index (system-level diversity index or ED): an emergy-based index of complexity derived from the Shannon information formula; it provides a quantitative assessment of the diversity of sources/flows in a system.

Emergy importance value (EIV): the relative contribution of each component to the total emergy flow through all biotic components (EIV=emergy of component/emergy of all components).

Emergy Yield Ratio (EYR = Y/F): is obtained by dividing the emergy output (Y) divided by the emergy of all inputs coming from the human economy (F).

Environmental Loading Ratio (ELR = F/R): is the emergy of purchased and non-renewable resources divided by the emergy of renewable inputs. This indicates the pressure of a system on the surrounding environment.

Evapotranspiration (ET): the movement of water vapor from the surface of the green roof substrate, either directly (by evaporation), or through plants (by transpiration).

Event frequency (time between events): was the time (days) between the end one of one storm event and the beginning of the next.

Event intensity: this refers to the rate of precipitation falling over time (mm/min). This was calculated as total amount of stormwater received (event size) over the length of the storm event.

Event size: was classified as the total amount of stormwater (mm) received by a system during a storm event.

FAO-56 Penman Monteith: the updated Penman Monteith equation recommended by FAO (Food and Agricultural Organization of the UN) and the World Meteorological Organization to estimate reference potential ET from a grass surface.

Green infrastructure: natural and constructed green spaces that utilize vegetation, soil, and other components to replicate natural processes that provide benefits for human populations in the urban setting.

Green roof: also termed vegetated, eco or living roofs are essentially roofs planted with vegetation on top of a growing medium (substrate or soil layer).

K_C (crop coefficient): an adjustment that can be made to the FAO-56 to account for physiological attributes of different plant species; a crop coefficient approach calculates ET for a specific crop (ET_C) while accounting for all the physical and physiological differences between the specific and reference crop.

K_S (water stress coefficient): An adjustment that can be made to the FAO-56 to account for the available water.

Leaf area index (LAI): a measure of canopy density— a count was done for the number of leaves touching a 1 m^2 object inserted through the green roof media. This number was then divided by the measured area of the quadrant (1 m^2) to yield the zone LAI (number of leaves per area).

Percent cover: was defined as the percentage of the green roof's ground surface covered by vegetation.

Resilience: as applied to integrated systems of people and the natural environment, has three interrelated characteristics: (1) the amount of change the system can undergo and still retain the same controls on function and structure; (2) the degree to which the system is capable of self-organization; and (3) the ability to build and increase the capacity for learning and adaptation. In the resilience discourse, management of diversity per se is considered to be a key attribute for building resilience in complex adaptive systems.

Solar transformity or unit emergy value (UEV): is a key concept in the emergy evaluation process. Solar transformity values convert flows (e.g., grams, joules, dollars) to solar energy joules– in other words, it represents the amount of emergy required to produce one unit of an output or benefit.

Soil depletion method: was used to calculate retention and evapotranspiration; it determines changes in substrate storage between fifteen-minute sensor readings ($\pm\Delta S = S_{t15}$-S_{t0}), where, +ΔS signifies retention, and –ΔS signifies water loss due to substrate drainage or ET.

Storm event (rain event): the time precipitation began until the precipitation ceased – independent storm events consisted of events separated by six or more hours. In the event runoff was still occurring 6h after the first event, the two events were combined. We defined the start and stop times of storm events based on rain gauge data from the onsite weather station.

Stormwater: is defined as precipitation that falls on non-soil surfaces and which does not infiltrate as would occur in an agricultural or ecological environment.

Stormwater retention: the amount of water (mm) retained by a system during a storm event.

Substrate water content: refers to the level of water (mm) retained by a system at any given time. Substrate water content was also present in terms of volume (m^3/m^3).

U-value (thermal conductance or heat transfer coefficient): it is a measure of the flow of heat through a material— the lower the U-value, the better the insulating ability of the material. It is also the inverse of an R-value (thermal resistance).

Urban heat island (UHI): the phenomena where urban air temperatures are significantly warmer than surrounding rural areas. This primarily occurs due to the removal of natural vegetation and its replacement with buildings and paved surfaces.

References

Ahiablame, L.M., Engel, B.A., Chaubey, I., 2012. Effectiveness of low impact development practices: Literature review and suggestions for future research. Water. Air. Soil Pollut. 223, 4253–4273. https://doi.org/10.1007/s11270-012-1189-2

Al-Busaidi, A., Yamamoto, T., Tanak, S., Moritani, S., 2013. Evapotranspiration of Succulent Plant (Sedum aizoonvar.floibundum). Evapotranspiration - An Overv. https://doi.org/10.5772/53213

Al-Rubaei, A.M., Engström, M., Viklander, M., Blecken, G.T., 2016. Long-term hydraulic and treatment performance of a 19-year old constructed stormwater wetland—Finally maturated or in need of maintenance? Ecol. Eng. 95, 73–82. https://doi.org/10.1016/j.ecoleng.2016.06.031

Allen, R.G., Pereira, L.S., Raes, D., Smith, M., 1998. Crop evapotranspiration - Guidelines for computing crop water requirements, FAO - Food and Agriculture Organization of the United Nations. Rome.

Bass, B., Baskaran, B., 2001. Evaluating Rooftop and Vertical Gardens as an Adaptation Strategy for Urban Areas. Natl. Res. Counc. Canada 111. https://doi.org/NRCC-46737

Bastianoni, S., Campbell, D.E., Ridolfi, R., Pulselli, F.M., 2009. The solar transformity of petroleum fuels. Ecol. Modell. 220, 40–50. https://doi.org/10.1016/j.ecolmodel.2008.09.003

Bean, Z.B. (North C.S.U., 2005. A Field Study to Evaluate Permeable Pavement Surface Infiltration Rates, Runoff Quantity, Runoff Quality, and Exfiltrate Quality. North Carolina State University.

Berardi, U., GhaffarianHoseini, A., GhaffarianHoseini, A., 2014. State-of-the-art analysis of the environmental benefits of green roofs. Appl. Energy 115, 411–428. https://doi.org/10.1016/j.apenergy.2013.10.047

Berretta, C., Poë, S., Stovin, V., Poë¨, S., Stovin, V., 2014. Moisture content behaviour in extensive green roofs during dry periods: The influence of vegetation and substrate characteristics. J. Hydrol. 516, 37–49. https://doi.org/10.1016/j.jhydrol.2014.04.001

Besir, A.B., Cuce, E., 2018. Green roofs and facades: A comprehensive review. Renew. Sustain. Energy Rev. 82, 915–939. https://doi.org/10.1016/j.rser.2017.09.106

Bevilacqua, P., Mazzeo, D., Bruno, R., Arcuri, N., 2017. Surface temperature analysis of

an extensive green roof for the mitigation of urban heat island in southern mediterranean climate. Energy Build. 150, 318–327. https://doi.org/10.1016/j.enbuild.2017.05.081

Bevilacqua, P., Mazzeo, D., Bruno, R., Arcuri, N., 2016. Experimental investigation of the thermal performances of an extensive green roof in the Mediterranean area. Energy Build. 122, 63–79. https://doi.org/10.1016/j.enbuild.2016.03.062

Bianchini, F., Hewage, K., 2012a. How "green" are the green roofs? Lifecycle analysis of green roof materials. Build. Environ. 48, 57–65. https://doi.org/10.1016/j.buildenv.2011.08.019

Bianchini, F., Hewage, K., 2012b. Probabilistic social cost-benefit analysis for green roofs: A lifecycle approach. Build. Environ. 58, 152–162. https://doi.org/10.1016/j.buildenv.2012.07.005

Borchers, B., Chow, C., Doelp, M., Ent, L., Hakes, R., Heo, C., Hunsley, K., Sinha, S., Whittaker, A., 2015. Evaluating the Feasibility of Implementing a Green Roof Retrofit on Pitched Residential Roofs. University of Maryland.

Borgström, S.T., Elmqvist, T., Angelstam, P., Alfsen-Norodom, C., 2006. Scale mismatches in management of urban landscapes. Ecol. Soc. 11. https://doi.org/10.1097/MCC.0b013e32807f2aa5

Bozonnet, E., Doya, M., Allard, F., 2011. Cool roofs impact on building thermal response: A French case study. Energy Build. 43, 3006–3012. https://doi.org/10.1016/j.enbuild.2011.07.017

Bozorg Chenani, S., Lehvävirta, S., Häkkinen, T., 2015. Life cycle assessment of layers of green roofs. J. Clean. Prod. 90, 153–162. https://doi.org/10.1016/j.jclepro.2014.11.070

Brandt-Williams, S.L., 2002. Folio # 4 (2nd printing) Emergy of Florida Agriculture, in: Handbook of Emergy Evaluation: A Compendium of Data for Emergy Computation Issued in a Series of Folios. p. 40.

Brandt-Williams, S.L., 1999. Evaluation of Watershed Control of Two Central Florida. University of Florida.

Brown, M.T., Cohen, M.J., Bardi, E., Ingwersen, W.W., 2006. Species diversity in the Florida Everglades, USA: A systems approach to calculating biodiversity. Aquat. Sci. 68, 254–277. https://doi.org/10.1007/s00027-006-0854-1

Brown, R.A., Line, D.E., Hunt, W.F., 2012. LID Treatment Train: Pervious Concrete with Subsurface Storage in Series with Bioretention and Care with Seasonal High Water Tables. J. Environ. Eng. 138, 689–697. https://doi.org/10.1061/(ASCE)EE.1943-7870.0000506

Brudler, S., Arnbjerg-Nielsen, K., Hauschild, M.Z., Rygaard, M., 2016. Life cycle assessment of stormwater management in the context of climate change adaptation. Water Res. 106, 394–404. https://doi.org/10.1016/j.watres.2016.10.024

Buranakarm, V., Brown, M.T., 2000. Emergy Evaluation of Material Cycles and Recycle, in: Emergy Synthesis: Theory and Applications of the Emergy Methodology. pp. 81–99.

Buranakarn, V., 1998. Evaluation of Recycling and Reuse of Building Materials using the Emergy Analysis Method 33, 83–92. https://doi.org/10.1108/eb050773

Campbell, D.E., Ohrt, A., 2009. Environmental Accounting Using Emergy: Evaluation of Minnesota.

Campbell, E.T., Brown, M.T., 2012. Environmental accounting of natural capital and ecosystem services for the US National Forest System. Environ. Dev. Sustain. 14, 691–724. https://doi.org/10.1007/s10668-012-9348-6

Campbell, E.T., Tilley, D.R., 2014a. Valuing ecosystem services from Maryland forests using environmental accounting. Ecosyst. Serv. 7, 141–151.

Campbell, E.T., Tilley, D.R., 2014b. How environmental emergy equates to currency. Ecosyst. Serv. 7, 128–140.

Carson, T.B., Marasco, D.E., Culligan, P.J., McGillis, W.R., 2013. Hydrological performance of extensive green roofs in New York City: Observations and multi-year modeling of three full-scale systems. Environ. Res. Lett. 8. https://doi.org/10.1088/1748-9326/8/2/024036

Carter, T., Keeler, A., 2008. Life-cycle cost-benefit analysis of extensive vegetated roof systems. J. Environ. Manage. 87, 350–363. https://doi.org/10.1016/j.jenvman.2007.01.024

Castleton, H.F., Stovin, V., Beck, S.B.M., Davison, J.B., 2010. Green roofs; building energy savings and the potential for retrofit. Energy Build. 42, 1582–1591. https://doi.org/10.1016/j.enbuild.2010.05.004

Chapman, C., Horner, R., 2010. Performance assessment of a street-drainage bioretention

system. Water Environ. Res. 82, 109–119.

Cheung, H.K.W., 2011. An urban heat island study for building and urban design Henry Kei Wang Cheung. The University of Manchester.

Chui, T.F.M., Liu, X., Zhan, W., 2016. Assessing cost-effectiveness of specific LID practice designs in response to large storm events. J. Hydrol. 533, 353–364. https://doi.org/10.1016/j.jhydrol.2015.12.011

Clark, C., Adriaens, P., Talbot, F.B., 2008. Green roof valuation: a probabilistic economic analysis of environmental benefits. Environ. Sci. Technol. 42, 2155–61. https://doi.org/10.1021/es0706652

Coffman, R., 2007. Vegetated Roof Systems: Design, Productivity, Retention, Habitat, and Sustainability in Green Roof And Ecoroof Technology. Ohio State University.

Cohen, M., Brown, M.T., Sweeney, S., 2007. puting the Unit Emergy Value of Crustal Elements. EMERGY Synth. 4 Theory Appl. Emergy Methodol.

Colding, J., Barthel, S., 2013. The potential of "Urban Green Commons" in the resilience building of cities. Ecol. Econ. 86, 156–166. https://doi.org/10.1016/j.ecolecon.2012.10.016

Coutts, A.M., Daly, E., Beringer, J., Tapper, N.J., 2013. Assessing practical measures to reduce urban heat: Green and cool roofs. Build. Environ. 70, 266–276. https://doi.org/10.1016/j.buildenv.2013.08.021

Cox, B.K., 2010. The Influence of Ambient Temperature on Green Roof R-values.

Czemiel Berndtsson, J., 2010. Green roof performance towards management of runoff water quantity and quality: A review. Ecol. Eng. 36, 351–360. https://doi.org/10.1016/j.ecoleng.2009.12.014

Dale, E., Nobe, M.C., Clevenger, C., Cross, J., 2013. Life Cycle Analysis of a St. Louis Flat Roof Residential Retrofit for Improved Energy Efficiency. ICSDEC 818–825. https://doi.org/10.1061/9780784412688.108

Davis, A.P., 2008. Field Performance of Bioretention: Hydrology Impacts. J. Hydrol. Eng. 13, 90–95. https://doi.org/10.1061/(ASCE)1084-0699(2008)13:2(90)

Davis, S.C., Williams, S.E., Boundy, R.G., 2016. Transportation Energy Data Book, 35th ed.

Droguett, B.R., 2011. Sustainability Assessment of Green Infrastructure Practices For Stormwater Management: A Comparative Emergy Analysis. State University of New York.

Eksi, M., Rowe, D.B., 2016. Green roof substrates: Effect of recycled crushed porcelain and foamed glass on plant growth and water retention. Urban For. Urban Green. 20, 81–88. https://doi.org/10.1016/j.ufug.2016.08.008

Elzeyadi, I., 2011. Daylighting-Bias and Biophilia: Quantifying the Impact of Daylighting on Occupants Health. Greenbuild 2011 1–9.

EPA, 2014. Emission factors for greenhouse gas inventories. U.S. EPA Cent. Corp. Clim. Leadersh. 1–5. https://doi.org/10.1177/0160017615614897

Feng, C., Meng, Q., Zhang, Y., 2010. Theoretical and experimental analysis of the energy balance of extensive green roofs. Energy Build. 42, 959–965. https://doi.org/10.1016/j.enbuild.2009.12.014

Fernandez-Canero, R., Gonzalez-Redondo, P., 2010. Green roofs as a habitat for birds: A review. J. Anim. Vet. Adv. https://doi.org/10.3923/javaa.2010.2041.2052

Fletcher, T.D., Andrieu, H., Hamel, P., 2013. Understanding, management and modelling of urban hydrology and its consequences for receiving waters: A state of the art. Adv. Water Resour. 51, 261–279. https://doi.org/10.1016/j.advwatres.2012.09.001

Flynn, K.M., Traver, R.G., 2013. Green infrastructure life cycle assessment: A bio-infiltration case study. Ecol. Eng. 55, 9–22. https://doi.org/10.1016/j.ecoleng.2013.01.004

Gaffin, S., Rosenzweig, C., Parshall, L., Beattie, D.J., Berghage, R.D., O'Keeffe, G., Braman, D., S Gaffin, N., 2005. Energy balance modeling applied to a comparison of white and green roof cooling efficiency. Third Annu. Green. Rooftops Sustain. Communities Conf. 1–11.

Gaffin, S.R., Imhoff, M., Rosenzweig, C., Khanbilvardi, R., Pasqualini, A., Kong, A.Y.Y., Grillo, D., Freed, A., Hillel, D., Hartung, E., 2012. Bright is the new blackmulti-year performance of high-albedo roofs in an urban climate. Environ. Res. Lett. 7. https://doi.org/10.1088/1748-9326/7/1/014029

Gaffin, S.R., Khanbilvardi, R., Rosenzweig, C., 2009. Development of a Green Roof Environmental Monitoring and Meteorological Network in New York City 2647–2660. https://doi.org/10.3390/s90402647

Ganguly, A., Chowdhury, D., Neogi, S., 2015. Performance of Building Roofs on Energy Efficiency - A Review. Energy Procedia 90, 200–208. https://doi.org/10.1016/j.egypro.2016.11.186

Getter, K.L., Rowe, D.B., Andresen, J.A., Wichman, I.S., 2011. Seasonal heat flux properties of an extensive green roof in a Midwestern U.S. climate. Energy Build. 43, 3548–3557. https://doi.org/10.1016/j.enbuild.2011.09.018

Getter, K.L., Rowe, D.B., Andresen, J. a., 2007. Quantifying the effect of slope on extensive green roof stormwater retention. Ecol. Eng. 31, 225–231. https://doi.org/10.1016/j.ecoleng.2007.06.004

Greenway, M., 2015. Stormwater wetlands for the enhancement of environmental ecosystem services: case studies for two retrofit wetlands in Brisbane, Australia. J. Clean. Prod. https://doi.org/10.1016/j.jclepro.2015.12.081

Gregoire, B.G., Clausen, J.C., 2011. Effect of a modular extensive green roof on stormwater runoff and water quality. Ecol. Eng. 37, 963–969. https://doi.org/10.1016/j.ecoleng.2011.02.004

Griffin, W.N., 2014. EXTENSIVE GREEN ROOF SUBSTRATE COMPOSITION: EFFECTS OF PHYSICAL PROPERTIES ON MATRIC POTENTIAL, HYDRAULIC CONDUCTIVITY, PLANT GROWTH, AND STORMWATER RETENTION IN THE MID-ATLANTIC.

Hashemi, S.S.G., Mahmud, H. Bin, Ashraf, M.A., 2015. Performance of green roofs with respect to water quality and reduction of energy consumption in tropics: A review. Renew. Sustain. Energy Rev. 52, 669–679. https://doi.org/10.1016/j.rser.2015.07.163

Hatt, B.E., Fletcher, T.D., Deletic, A., 2009. Hydrologic and pollutant removal performance of stormwater biofiltration systems at the field scale. J. Hydrol. 365, 310–321. https://doi.org/10.1016/j.jhydrol.2008.12.001

He, H., Jim, C.Y., 2010. Simulation of thermodynamic transmission in green roof ecosystem. Ecol. Modell. 221, 2949–2958. https://doi.org/10.1016/j.ecolmodel.2010.09.002

He, Y., Yu, H., Dong, N., Ye, H., 2016. Thermal and energy performance assessment of extensive green roof in summer: A case study of a lightweight building in Shanghai. Energy Build. 127, 762–773. https://doi.org/10.1016/j.enbuild.2016.06.016

He, Y., Yu, H., Ozaki, A., Dong, N., Zheng, S., 2017. Influence of plant and soil layer on energy balance and thermal performance of green roof system. Energy 141, 1285–

1299. https://doi.org/10.1016/j.energy.2017.08.064

Hilten, R.N., 2005. An Alaysis of the Energetics and Stormwater Mediation Potential of Green Roofs. University of Georgia.

Hunt, W.F., Jarrett, A.R., Smith, J.T., Sharkey, L.J., 2006. Evaluating Bioretention Hydrology and Nutrient Removal at Three Field Sites in North Carolina. J. Irrig. Drain. Eng. 132, 600–608. https://doi.org/10.1061/(ASCE)0733-9437(2006)132:6(600)

Jia, H., Wang, X., Ti, C., Zhai, Y., Field, R., Tafuri, A.N., Cai, H., Yu, S.L., 2015. Field monitoring of a LID-BMP treatment train system in China. Environ. Monit. Assess. 187. https://doi.org/10.1007/s10661-015-4595-2

Jim, C.Y., 2012. Effect of vegetation biomass structure on thermal performance of tropical green roof. Landsc. Ecol. Eng. 8, 173–187. https://doi.org/10.1007/s11355-011-0161-4

Jim, C.Y., Peng, L.L.H., 2012. Substrate moisture effect on water balance and thermal regime of a tropical extensive green roof. Ecol. Eng. 47, 9–23. https://doi.org/10.1016/j.ecoleng.2012.06.020

Johannesson, K.M., Kynkäänniemi, P., Ulén, B., Weisner, S.E.B., Tonderski, K.S., 2015. Phosphorus and particle retention in constructed wetlands—A catchment comparison. Ecol. Eng. 80, 20–31. https://doi.org/10.1016/j.ecoleng.2014.08.014

Joksimovic, D., Alam, Z., 2014. Cost efficiency of Low Impact Development (LID) stormwater management practices. Procedia Eng. 89, 734–741. https://doi.org/10.1016/j.proeng.2014.11.501

Kim, J., Hong, T., Jeong, J., Koo, C., Jeong, K., 2016. An optimization model for selecting the optimal green systems by considering the thermal comfort and energy consumption. Appl. Energy 169, 682–695. https://doi.org/10.1016/j.apenergy.2016.02.032

Kolokotroni, M., Gowreesunker, B.L., Giridharan, R., 2013. Cool roof technology in London: An experimental and modelling study. Energy Build. 67, 658–667. https://doi.org/10.1016/j.enbuild.2011.07.011

Kosareo, L., Ries, R., 2007. Comparative environmental life cycle assessment of green roofs. Build. Environ. 42, 2606–2613. https://doi.org/10.1016/j.buildenv.2006.06.019

Kotsiris, G., Androutsopoulos, A., Polychroni, E., Nektarios, P.A., 2012. Dynamic U-value

estimation and energy simulation for green roofs. Energy Build. 45, 240–249. https://doi.org/10.1016/j.enbuild.2011.11.005

La Roche, P., Berardi, U., 2014. Comfort and energy savings with active green roofs. Energy Build. 82, 492–504. https://doi.org/10.1016/j.enbuild.2014.07.055

Lanham, J.K., 2007. Thermal Properties of Green Roofs in Cold Climates.

Larson, W., 2015. New Estimates of Value of Land of the United States. https://doi.org/10.1177/0042098014557208

Law, E.P., Diemont, S.A.W., Toland, T.R., 2017. A sustainability comparison of green infrastructure interventions using emergy evaluation. J. Clean. Prod. 145, 374–385. https://doi.org/10.1016/j.jclepro.2016.12.039

Lazzarin, R.M., Castellotti, F., Busato, F., 2005. Experimental measurements and numerical modelling of a green roof. Energy Build. 37, 1260–1267. https://doi.org/10.1016/j.enbuild.2005.02.001

Lee, J.Y., Moon, H.J., Kim, T.I., Kim, H.W., Han, M.Y., 2013. Quantitative analysis on the urban flood mitigation effect by the extensive green roof system. Environ. Pollut. 181, 257–61. https://doi.org/10.1016/j.envpol.2013.06.039

Lenhart, H.A., Hunt, W.F., 2011. Evaluating Four Storm-Water Performance Metrics with a North Carolina Coastal Plain Storm-Water Wetland 137, 155–162.

Li, D., Bou-zeid, E., Oppenheimer, M., 2014. The effectiveness of cool and green roofs as urban heat island mitigation strategies. https://doi.org/10.1088/1748-9326/9/5/055002

Lin, Y.J., Lin, H.T., 2011. Thermal performance of different planting substrates and irrigation frequencies in extensive tropical rooftop greeneries. Build. Environ. 46, 345–355. https://doi.org/10.1016/j.buildenv.2010.07.027

Line, D.E., Brown, R. a, Hunt, W.F., Asce, M., Lord, W.G., 2012. Effectiveness of LID for Commercial Development in North Carolina. J. Environ. Eng. 138, 680–689. https://doi.org/10.1061/(ASCE)EE.1943-7870.0000515.

Liu, J., Sample, D., Bell, C., Guan, Y., 2014. Review and Research Needs of Bioretention Used for the Treatment of Urban Stormwater. Water 6, 1069–1099. https://doi.org/10.3390/w6041069

Liu, K., Baskaran, B., 2003. Thermal performance of green roofs through field evaluation.

Proc. First Annu. Int. Green Roofs Conf. Green. Rooftops Sustain. Comunities. 10.

Liu, K.K.Y., Minor, J., 2005. Performance Evaluation of an Extensive Green Roof. Green. Rooftops Sustain. Communities 1–11. https://doi.org/10.1109/ICEOE.2011.6013104

LiveRoof, L., 2009. LiveRoof LITE System Specifications 49456, 49456.

Lucke, T., Nichols, P.W.B., 2015. The pollution removal and stormwater reduction performance of street-side bioretention basins after ten years in operation. Sci. Total Environ. 536, 784–92. https://doi.org/10.1016/j.scitotenv.2015.07.142

MacIvor, J.S., Lundholm, J., 2011. Insect species composition and diversity on intensive green roofs and adjacent level-ground habitats. Urban Ecosyst. 14, 225–241. https://doi.org/10.1007/s11252-010-0149-0

Makarieva, A.M., Gorshkov, V.G., Li, B.-L., Chown, S.L., Gavrilov, V.M., Reich, P.B., 2008. Mean Mass-Specific Metabolic Rates Are Strikingly Similar across Life's Major Domains: Evidence for Life's Metabolic Optimum. PNAS 105, 16994–16999. https://doi.org/10.1073/pnas.080

Manso, M., Castro-Gomes, J., Paulo, B., Bentes, I., Teixeira, C.A.C.A., 2018. Life cycle analysis of a new modular greening system. Sci. Total Environ. 627, 1146–1153. https://doi.org/10.1016/j.scitotenv.2018.01.198

Marasco, D.E., Culligan, P.J., McGillis, W.R., 2015. Evaluation of common evapotranspiration models based on measurements from two extensive green roofs in New York City. Ecol. Eng. 84, 451–462. https://doi.org/10.1016/j.ecoleng.2015.09.001

Mastrapostoli, E., Karlessi, T., Pantazaras, A., Kolokotsa, D., Gobakis, K., Santamouris, M., 2014. On the cooling potential of cool roofs in cold climates : Use of cool fluorocarbon coatings to enhance the optical properties and the energy performance of industrial buildings. Energy Build. 69, 417–425. https://doi.org/10.1016/j.enbuild.2013.10.024

Matlock, J.M., Rowe, D.B., 2016. The suitability of crushed porcelain and foamed glass as alternatives to heat-expanded shale in green roof substrates: An assessment of plant growth, substrate moisture, and thermal regulation. Ecol. Eng. 94, 244–254. https://doi.org/10.1016/j.ecoleng.2016.05.044

Mayer, A.L., Shuster, W.D., Beaulieu, J.J., Hopton, M.E., Rhea, L.K., Roy, A.H., Thurston, H.W., 2012. Building Green Infrastructure via Citizen Participation: A Six-Year Study in the Shepherd Creek (Ohio). Environ. Pract. 14, 57–67.

McNab, B.K., 2009. Ecological factors affect the level and scaling of avian BMR. Comp. Biochem. Physiol. - A Mol. Integr. Physiol. 152, 22–45. https://doi.org/10.1016/j.cbpa.2008.08.021

MDE, 2009. Appendix A: Landscaping Guidance for Stormwater BMPs, in: Maryland Stormwater Design Manual , Volumes I and II. p. A.1-A.50.

Montalto, F., Behr, C., Alfredo, K., Wolf, M., Arye, M., Walsh, M., 2007. Rapid assessment of the cost-effectiveness of low impact development for CSO control. Landsc. Urban Plan. 82, 117–131. https://doi.org/10.1016/j.landurbplan.2007.02.004

Moody, S.S., Sailor, D.J., 2013. Development and application of a building energy performance metric for green roof systems. Energy Build. 60, 262–269. https://doi.org/10.1016/j.enbuild.2013.02.002

Morau, D., Libelle, T., Garde, F., 2012. Performance evaluation of green roof for thermal protection of buildings in reunion Island. Energy Procedia 14, 1008–1016. https://doi.org/10.1016/j.egypro.2011.12.1047

Nardini, A., Andri, S., Crasso, M., 2011. Influence of substrate depth and vegetation type on temperature and water runoff mitigation by extensive green roofs: shrubs versus herbaceous plants. Urban Ecosyst. 15, 697–708. https://doi.org/10.1007/s11252-011-0220-5

Nawaz, R., McDonald, A., Postoyko, S., 2015. Hydrological performance of a full-scale extensive green roof located in a temperate climate. Ecol. Eng. 82, 66–80. https://doi.org/10.1016/j.ecoleng.2014.11.061

Nelson, M., Odum, H.T., Brown, M.T., Alling, A., 2001. "Living off the land": Resource efficiency of Wetland wastewater treatment. Adv. Sp. Res. 27, 1547–1556. https://doi.org/10.1016/S0273-1177(01)00246-0

Niachou, A., Papakonstantinou, K., Santamouris, M., Tsangrassoulis, A., Mihalakakou, G., 2001. Analysis of the green roof thermal properties and investigation of its energy performance. Energy Build. 33, 719–729. https://doi.org/10.1016/S0378-7788(01)00062-7

NIU, H.A.O., Clark, C., ZHOU, J., Adriaens, P., 2010. Scaling of economic benefits from green roof implementation in Washington, DC. Environ. Sci. Technol. 44, 4302–4308. https://doi.org/10.1021/es902456x

Odum, H.T., 1996. Environmental Accounting: Emergy and Environmental Decision-Making. John Wiley & Sons, New York.

Odum, H.T., Brown, M.T., Brandt-Williams, S., 2000. Handbook of emergy evaluation Folio 1: Introduction and global budget. Univ. Florida, Gainesv.

Onmura, S., Matsumoto, M., Hokoi, S., 2001. Study on evaporative cooling effect of roof lawn gardens. Energy Build. 33, 653–666. https://doi.org/10.1016/S0378-7788(00)00134-1

Orrell, J.J., 1998. Cross scale comparison of plant and production diversity. University of Florida, Gainesville.

Ouldboukhitine, S.E., Spolek, G., Belarbi, R., 2014. Impact of plants transpiration, grey and clean water irrigation on the thermal resistance of green roofs. Ecol. Eng. 67, 60–66. https://doi.org/10.1016/j.ecoleng.2014.03.052

Palomo Del Barrio, E., 1998. Analysis of the green roofs cooling potential in buildings. Energy Build. 27, 179–193. https://doi.org/10.1016/S0378-7788(97)00029-7

Paus, K.H., Muthanna, T.M., Braskerud, B.C., 2015. The hydrological performance of bioretention cells in regions with cold climates: seasonal variation and implications for design. Hydrol. Res. nh2015084. https://doi.org/10.2166/nh.2015.084

Pearlmutter, D., Rosenfeld, S., 2008. Performance analysis of a simple roof cooling system with irrigated soil and two shading alternatives. Energy Build. 40, 855–864. https://doi.org/10.1016/j.enbuild.2007.06.004

Peng, L.L.H., Jim, C.Y., 2015. Economic evaluation of green-roof environmental benefits in the context of climate change: The case of Hong Kong. Urban For. Urban Green. 14, 554–561. https://doi.org/10.1016/j.ufug.2015.05.006

Pennino, M.J., McDonald, R.I., Jaffe, P.R., 2016. Watershed-scale impacts of stormwater green infrastructure on hydrology, nutrient fluxes, and combined sewer overflows in the mid-Atlantic region. Sci. Total Environ. 565, 1044–53. https://doi.org/10.1016/j.scitotenv.2016.05.101

Pennsylvania Stormwater Best Management Practices Manual, 2006. . pp. 151–162.

Pérez, G., Vila, A., Rincón, L., Solé, C., Cabeza, L.F., 2012. Use of rubber crumbs as drainage layer in green roofs as potential energy improvement material. Appl. Energy 97, 347–354. https://doi.org/10.1016/j.apenergy.2011.11.051

Perini, K., Rosasco, P., 2016. Is greening the building envelope economically sustainable? An analysis to evaluate the advantages of economy of scope of vertical greening systems and green roofs. Urban For. Urban Green. 20, 328–337.

https://doi.org/10.1016/j.ufug.2016.08.002

Poë, S., Stovin, V., Berretta, C., 2015. Parameters influencing the regeneration of a green roof's retention capacity via evapotranspiration. J. Hydrol. 523, 356–367. https://doi.org/10.1016/j.jhydrol.2015.02.002

Price, J., 2010. Green Facade Energetics. University of Maryland.

Pulselli, R.M., Pulselli, F.M., Mazzali, U., Peron, F., Bastianoni, S., 2014. Emergy based evaluation of environmental performances of Living Wall and Grass Wall systems. Energy Build. 73, 200–211. https://doi.org/10.1016/j.enbuild.2014.01.034

Qin, X., Wu, X., Chiew, Y.-M., Li, Y., 2012. A green roof test bed for stormwater management and reduction of urban heat island effect in Singapore. Br. J. Environ. Clim. Chang. 2, 410–420. https://doi.org/10.9734/BJECC/2012/2704

Raji, B., Tenpierik, M.J., Van Den Dobbelsteen, A., 2015. The impact of greening systems on building energy performance: A literature review. Renew. Sustain. Energy Rev. 45, 610–623. https://doi.org/10.1016/j.rser.2015.02.011

Raugei, M., Rugani, B., Benetto, E., Ingwersen, W.W., 2014. Integrating emergy into LCA: Potential added value and lingering obstacles. Ecol. Modell. 271, 4–9. https://doi.org/10.1016/j.ecolmodel.2012.11.025

Reza, B., 2013. Emergy-based life cycle assessment (Em-LCA) for sustainability appraisal of built environment.

Reza, B., Sadiq, R., Hewage, K., 2014. Emergy-based life cycle assessment (Em-LCA) of multi-unit and single-family residential buildings in Canada. Int. J. Sustain. Built Environ. 3, 207–224. https://doi.org/10.1016/j.ijsbe.2014.09.001

Richards, P.J., Farrell, C., Tom, M., Williams, N.S.G., Fletcher, T.D., 2015. Vegetable raingardens can produce food and reduce stormwater runoff. Urban For. Urban Green. 14, 646–654. https://doi.org/10.1016/j.ufug.2015.06.007

Rincón, L., Coma, J., Pérez, G., Castell, A., Boer, D., Cabeza, L.F., 2014. Environmental performance of recycled rubber as drainage layer in extensive green roofs. A comparative Life Cycle Assessment. Build. Environ. 74, 22–30. https://doi.org/10.1016/j.buildenv.2014.01.001

Riposo, D., Kangas, P., 2009. Wildlife and Wind Energy: An Emergy Analysis of Bird and Bat Impacts at Maple Ridge Wind Farm, in: EMERGY SYNTHESIS 5: Theory and Applications of the Emergy Methodology.

Romeo, C., Zinzi, M., 2013. Impact of a cool roof application on the energy and comfort performance in an existing non-residential building. A Sicilian case study. Energy Build. 67, 647–657. https://doi.org/10.1016/j.enbuild.2011.07.023

Rosenzweig, C., Gaffin, S., Parshall, L., 2006. Green Roofs in the New York Metropolitan Region: Research Report, Columbia University Center for Climate Systems Research and NASA Goddard Institute for Space Studies.

Rosenzweig, C., Solecki, W.D., Parshall, L., Chopping, M., Pope, G., Goldberg, R., 2005. Characterizing the urban heat island in current and future climates in New Jersey. Environ. Hazards 6, 51–62. https://doi.org/10.1016/j.hazards.2004.12.001

Rowe, D.B., 2011. Green roofs as a means of pollution abatement. Environ. Pollut. 159, 2100–10. https://doi.org/10.1016/j.envpol.2010.10.029

Rushton, B., 2001. Low-Impact Parking Lot Design Reduces Runoff and Pollutant Loads. Water Resour. Plan. Manag. 127, 172–179.

Rustagi, N., Tilley, D., Schramski, J., 2009. Total Energy Requirements of a Living Extensive Green Roof, in: Fifth Biennial Emergy Conference.

Saadatian, O., Sopian, K., Salleh, E., Lim, C.H., Riffat, S., Saadatian, E., Toudeshki, A., Sulaiman, M.Y., 2013. A review of energy aspects of green roofs. Renew. Sustain. Energy Rev. 23, 155–168. https://doi.org/10.1016/j.rser.2013.02.022

Santamouris, M., 2014. Cooling the cities - A review of reflective and green roof mitigation technologies to fight heat island and improve comfort in urban environments. Sol. Energy 103, 682–703. https://doi.org/10.1016/j.solener.2012.07.003

Scharf, B., Pitha, U., Trimmel, H., 2012. Thermal Performance of Green Roofs, in: World Green Roof Congress, Copenhagen. pp. 23–29.

Scharf, B., Zluwa, I., 2017. Case study investigation of the building physical properties of seven different green roof systems. Energy Build. 151, 564–573. https://doi.org/10.1016/j.enbuild.2017.06.050

Scholes, L., Shutes, R.B.E., Revitt, D.M., Forshaw, M., Purchase, D., 1998. The treatment of metals in urban runoff by constructed wetlands 211–219.

Schramski, J.R., Tilley, D.R., Carter, T.L., 2009. Comparative Embodied Energy Analysis to Assess Green Roof Sustainability, in: Greening Rooftops for Sustainable Communities. pp. 1–13.

Schweitzer, O., Erell, E., 2014. Evaluation of the energy performance and irrigation requirements of extensive green roofs in a water-scarce Mediterranean climate. Energy Build. 68, 25–32. https://doi.org/10.1016/j.enbuild.2013.09.012

Scientific, C., 2014. CS650 & CS655 Soil Water Content Reflectometers.

Scientific, C., 2010. Submersible Pressure Transducer 2010.

Simmons, M.T., Gardiner, B., Windhager, S., Tinsley, J., 2008. Green roofs are not created equal: The hydrologic and thermal performance of six different extensive green roofs and reflective and non-reflective roofs in a sub-tropical climate. Urban Ecosyst. 11, 339–348. https://doi.org/10.1007/s11252-008-0069-4

Sonne, J., 2006. Evaluating Green Roof Energy Performance. ASHRE 48, 2005–2007.

Spatari, S., Yu, Z., Montalto, F.A., 2011. Life cycle implications of urban green infrastructure. Environ. Pollut. 159, 2174–9. https://doi.org/10.1016/j.envpol.2011.01.015

Speak, A.F., Rothwell, J.J., Lindley, S.J., Smith, C.L., 2013. Reduction of the urban cooling effects of an intensive green roof due to vegetation damage. Urban Clim. 3, 40–55. https://doi.org/10.1016/j.uclim.2013.01.001

Sproul, J., Wan, M.P., Mandel, B.H., Rosenfeld, A.H., 2014. Economic comparison of white, green, and black flat roofs in the United States. Energy Build. 71, 20–27. https://doi.org/10.1016/j.enbuild.2013.11.058

Starry, O., 2013. The Comparative Effects of Three Sedum Species on Green Roof Stormwater Retention. University of Maryland, College Park.

Starry, O., Lea-Cox, J.D.D., Kim, J., van Iersel, M.W.W., 2014. Photosynthesis and water use by two Sedum species in green roof substrate. Environ. Exp. Bot. 107, 105–112. https://doi.org/10.1016/j.envexpbot.2014.05.014

Stovin, V., Poë, S., Berretta, C., 2013. A modelling study of long term green roof retention performance. J. Environ. Manage. 131, 206–15. https://doi.org/10.1016/j.jenvman.2013.09.026

Sumner, D.M., Jacobs, J.M., 2005. Utility of Penman-Monteith, Priestley-Taylor, reference evapotranspiration, and pan evaporation methods to estimate pasture evapotranspiration. J. Hydrol. 308, 81–104. https://doi.org/10.1016/j.jhydrol.2004.10.023

Sun, T., Bou-Zeid, E., Ni, G.-H., 2014. To irrigate or not to irrigate: Analysis of green roof performance via a vertically-resolved hygrothermal model. Build. Environ. 73, 127–137. https://doi.org/10.1016/j.buildenv.2013.12.004

Susca, T., Gaffin, S.R., Dell'osso, G.R., 2011. Positive effects of vegetation: Urban heat island and green roofs. Environ. Pollut. 159, 2119–2126. https://doi.org/10.1016/j.envpol.2011.03.007

Synnefa, A., Santamouris, M., Akbari, H., 2007. Estimating the effect of using cool coatings on energy loads and thermal comfort in residential buildings in various climatic conditions 39, 1167–1174. https://doi.org/10.1016/j.enbuild.2007.01.004

Tabares-Velasco, P.C., Srebric, J., 2011. Experimental quantification of heat and mass transfer process through vegetated roof samples in a new laboratory setup. Int. J. Heat Mass Transf. 54, 5149–5162. https://doi.org/10.1016/j.ijheatmasstransfer.2011.08.034

Takebayashi, H., Moriyama, M., 2007. Surface heat budget on green roof and high reflection roof for mitigation of urban heat island. Build. Environ. 42, 2971–2979. https://doi.org/10.1016/j.buildenv.2006.06.017

Tan, C.L., Tan, P.Y., Wong, N.H., Takasuna, H., Kudo, T., Takemasa, Y., Lim, C.V.J., Chua, H.X.V., 2017. Impact of soil and water retention characteristics on green roof thermal performance. Energy Build. 152, 830–842. https://doi.org/10.1016/j.enbuild.2017.01.011

Teemusk, A., Mander, Ü., 2010. Temperature regime of planted roofs compared with conventional roofing systems. Ecol. Eng. 36, 91–95. https://doi.org/10.1016/j.ecoleng.2009.09.009

Teemusk, A., Mander, Ü., 2009. Greenroof potential to reduce temperature fluctuations of a roof membrane: A case study from Estonia. Build. Environ. 44, 643–650. https://doi.org/10.1016/j.buildenv.2008.05.011

Testa, J., Krarti, M., 2017. A review of benefits and limitations of static and switchable cool roof systems. Renew. Sustain. Energy Rev. 77, 451–460. https://doi.org/10.1016/j.rser.2017.04.030

Theodosiou, T., Aravantinos, D., Tsikaloudaki, K., 2014. Thermal behaviour of a green vs. a conventional roof under Mediterranean climate conditions. Int. J. Sustain. Energy 33, 227–241. https://doi.org/10.1080/14786451.2013.772616

Tilley, D.R., 2006. National metabolism and communications technology development in

the United States, 1790-2000. Environ. Hist. Camb. 12, 165–190. https://doi.org/10.3197/096734006776680227

Tjaden, S., 2014. Energy Balance, Water Balance, and Plant Dynamics of a Sloped, Thin Extensive Green Roof Installed In The Mid-Atlantic Region of The United States.

Tjaden, S., 2013. Integrated Water & Energy Monitoring of the Living Technologies of WaterShed ; the 2011 Solar Decathlon Winning Sustainable Home 1–21.

Ulgiati, S., Ascione, M., Zucaro, a., Campanella, L., 2011. Emergy-based complexity measures in natural and social systems. Ecol. Indic. 11, 1185–1190. https://doi.org/10.1016/j.ecolind.2010.12.021

United Nations, 2016. The World's Cities in 2016: Data Booklet. Econ. Soc. Aff. 29. https://doi.org/10.18356/8519891f-en

United States General Services Administration, 2011. The Benefits and Challenges of Green Roofs on Public and Commercial Buildings: A Report of the United States General Services Administration.

Ürge-Vorsatz, D., Eyre, N., Graham, P., Harvey, D., Hertwich, E., Jiang, Y., Kornevall, C., Majumdar, M., McMahon, J.E., Mirasgedis, S., Murakami, S., Novikova, A., 2012. Energy End-Use: Buildings, in: In Global Energy Assessment - Toward a Sustainable Future. pp. 649–760.

VanWoert, N.D., Rowe, D.B., Andresen, J. a, Rugh, C.L., Fernandez, R.T., Xiao, L., 2005. Green roof stormwater retention: effects of roof surface, slope, and media depth. J. Environ. Qual. 34, 1036–44. https://doi.org/10.2134/jeq2004.0364

Vijayaraghavan, K., 2016. Green roofs: A critical review on the role of components, benefits, limitations and trends. Renew. Sustain. Energy Rev. 57, 740–752. https://doi.org/10.1016/j.rser.2015.12.119

Volder, A., Dvorak, B., 2014. Event size, substrate water content and vegetation affect storm water retention efficiency of an un-irrigated extensive green roof system in Central Texas. Sustain. Cities Soc. 10, 59–64. https://doi.org/10.1016/j.scs.2013.05.005

Voyde, E.A., 2011. Quantifying the Complete Hydrologic Budget for an Extensive Living Roof. The University of Aukland.

Wang, Y., Bakker, F., de Groot, R., Wörtche, H., 2014. Effect of ecosystem services provided by urban green infrastructure on indoor environment: A literature review.

Build. Environ. 77, 88–100. https://doi.org/10.1016/j.buildenv.2014.03.021

Wilson, C.E., Hunt, W.F., Winston, R.J., Smith, P., 2015. Comparison of Runoff Quality and Quantity from a Commercial Low-Impact and Conventional Development in Raleigh, North Carolina. J. Environ. Eng. 141, 5014005. https://doi.org/10.1061/(ASCE)EE.1943-7870.0000842

Winfrey, B.K., 2012. Material and Emergy Cycling in Natural and Human-Dominated Systems.

Winooski Natural Resources Conservation District, 2007. The Vermont Rain Garden Manual 20.

Winston, R.J., Dorsey, J.D., Hunt, W.F., 2016. Quantifying volume reduction and peak flow mitigation for three bioretention cells in clay soils in northeast Ohio. Sci. Total Environ. 553, 83–95. https://doi.org/10.1016/j.scitotenv.2016.02.081

Wong, N.H., Chen, Y., Ong, C.L., Sia, A., 2003. Investigation of thermal benefits of rooftop garden in the tropical environment. Build. Environ. 38, 261–270. https://doi.org/10.1016/S0360-1323(02)00066-5

Wong, N.H., Cheong, D.K.W., Yan, H., Soh, J., Ong, C.L., Sia, A., 2003. The effects of rooftop garden on energy consumption of a commercial building in Singapore. Energy Build. 35, 353–364. https://doi.org/10.1016/S0378-7788(02)00108-1

Xu, T., Sathaye, J., Akbari, H., Garg, V., Tetali, S., 2012. Quantifying the direct benefits of cool roofs in an urban setting: Reduced cooling energy use and lowered greenhouse gas emissions. Build. Environ. 48, 1–6. https://doi.org/10.1016/j.buildenv.2011.08.011

Yang, H., Dick, W.A., McCoy, E.L., Phelan, P.L., Grewal, P.S., 2013. Field evaluation of a new biphasic rain garden for stormwater flow management and pollutant removal. Ecol. Eng. 54, 22–31. https://doi.org/10.1016/j.ecoleng.2013.01.005

Yang, R., Cui, B., 2012. Framework of Integrated Stormwater Management of Jinan City, China. Procedia Environ. Sci. 13, 2346–2352. https://doi.org/10.1016/j.proenv.2012.01.223

Zhan, W., Chui, T.F.M., 2016. Evaluating the life cycle net benefit of low impact development in a city. Urban For. Urban Green. 20, 295–304. https://doi.org/10.1016/j.ufug.2016.09.006

Zhang, Q., Miao, L., Wang, X., Liu, D., Zhu, L., Zhou, B., Sun, J., Liu, J., 2015. The

capacity of greening roof to reduce stormwater runoff and pollution. Landsc. Urban Plan. 144, 142–150. https://doi.org/10.1016/j.landurbplan.2015.08.017

Zhao, M., Srebric, J., Berghage, R.D., Dressler, K.A., 2015. Accumulated snow layer influence on the heat transfer process through green roof assemblies. Build. Environ. 87, 82–91. https://doi.org/10.1016/j.buildenv.2014.12.018

Zinzi, M., Agnoli, S., 2012. Cool and green roofs. An energy and comfort comparison between passive cooling and mitigation urban heat island techniques for residential buildings in the Mediterranean region. Energy Build. 55, 66–76. https://doi.org/10.1016/j.enbuild.2011.09.024

Zinzi, M., Fasano, G., 2009. Properties and performance of advanced reflective paints to reduce the cooling loads in buildings and mitigate the heat island effect in urban areas. Int. J. Sustain. Energy 28, 123–139. https://doi.org/10.1080/14786450802453314

Zotarelli, L., Dukes, M., 2010. Step by step calculation of the Penman-Monteith Evapotranspiration (FAO-56 Method), Institute of Food and Agricultural Sciences, University of Florida.